

**UNIVERSITY OF GAZIANTEP
GRADUATE SCHOOL OF
NATURAL & APPLIED SCIENCES**

**MODELLING AND IDENTIFICATION OF
AN INTERNAL COMBUSTION ENGINE
TO PROVIDE SIMULATOR FOR
CONTROL PURPOSES**

**Ph.D THESIS
IN
MECHANICAL ENGINEERING**

**BY
NECLA KARA TOĞUN
SEPTEMBER 2010**

**Modelling and Identification of an Internal
Combustion Engine to Provide Simulator for Control
Purposes**

**PhD Thesis
in
Mechanical Engineering
University of Gaziantep**

**Supervisor
Prof. Dr. Sedat BAYSEÇ**

**by
Necla KARA TOĞUN**

September 2010

T.C.
UNIVERSITY OF GAZİANTEP
GRADUATE SCHOOL OF
NATURAL & APPLIED SCIENCES
NAME OF THE DEPARTMENT

Name of the thesis : Modelling and identification of an internal combustion engine to provide simulator for control purposes

Name of the student: Necla KARA TOĞUN

Exam date : 03.09.2010

Approval of the Graduate School of Natural and Applied Sciences

Prof. Dr. Ramazan KOÇ

I certify that this thesis satisfies all the requirements as a thesis for the degree of Doctor of Philosophy.

Prof. Dr. L. Canan DÜLGER
Head of Department

This is to certify that we have read this thesis and that in our opinion it is fully adequate, in scope and quality, as a thesis for the degree of Doctor of Philosophy.

Prof. Dr. Sedat BAYSEÇ
Supervisor

Examining Committee Members

signature

Prof. Dr. İbrahim Deniz AKÇALI

Prof. Dr. Sedat BAYSEÇ

Prof. Dr. İbrahim Halil GÜZELBEY

Prof. Dr. L. Canan DÜLGER

Assoc. Prof. Dr. İlyas EKER

ABSTRACT

MODELLING AND IDENTIFICATION OF AN INTERNAL COMBUSTION ENGINE TO PROVIDE SIMULATOR FOR CONTROL PURPOSES

TOĞUN, Necla KARA

Ph.D. in Mechanical Engineering.

Supervisor: Prof. Dr. Sedat BAYSEÇ

August 2010, 222 pages

Field of “System Identification” has become an important discipline. Identification is basically the process of developing a mathematical representation of a physical system using experimental data. The identification of nonlinear dynamical systems is a substantial part of the control science and therefore appropriate models should be developed to control nonlinear dynamic systems. The main idea that lies under the procedure is to obtain a regular and mathematically tractable model of the system of interest. Automotive internal combustion engine (ICE) control is one of the most complex control problems for control system engineers and researchers. Among all the engine control variables, the engine torque is one of the most important performance variables of an ICE and, for this reason, a technique based on optimizing the engine torque control can improve substantially the performance of the overall vehicle. There are two objective of this work. First one is to develop a steady-state model of a gasoline engine torque and brake specific fuel consumption by using *neural network* and *genetic programming* and second one is to develop an accurate and robust model of a spark ignition (SI) engine torque by using the most common nonlinear black-box parametric models namely *Hammerstein model*, *nonlinear auto-regressive with exogenous inputs (NARX) model* and *neural network model* that is including *multilayer feedforward neural network (FFNN) model*, *radial basis function (RBF) neural network model* and *Elman type recurrent neural network model*. These developed methods are implemented to an existing 1400 cc, four cylinder Fiat SI engine. The artificial neural network (ANN) is a newly developed technique among the other identification methods. There are various methods used for training of ANN. Two of them are included in this study. These are, namely, the *backpropagation method* and the *Levenberg-Marquardt algorithm*. The different nonlinear identification approaches are used in this thesis. The neural network based model has captured the dynamics very well and the method has been found suitable for modeling the SI engine torque. However all the nonlinear identification methods identified the SI engine torque dynamics at acceptable levels of accuracy.

Key Words: SI engine, engine torque identification, nonlinear modeling, nonlinear identification, Hammerstein model, NARX model, neural networks, genetic programming

ÖZET

İÇTEN YANMALI BİR MOTORUN KONTROL AMAÇLI SİMULATORÜNÜN SAĞLANMASI İÇİN MODELLENMESİ VE TANIMLANMASI

TOĞUN, Necla KARA
Doktora Tezi, Makina Müh. Bölümü
Tez Yöneticisi: Prof. Dr. Sedat BAYSEÇ
Ağustos 2010, 222 sayfa

Sistem tanımlanması alanı önemli disiplin haline gelmiştir. Tanımlama temelde fiziksel bir sistemi deneysel verileri kullanarak matematiksel olarak modelinin geliştirilmesidir. Doğrusal olmayan dinamik sistemlerin tanımlanması kontrol için önemli bir bölümdür. Bu nedenle, uygun modeller doğrusal olmayan dinamik sistemleri kontrol etmek için geliştirilmelidir. Prosedürün altında yatan ana düşünce ilgilenilen sisteme ilişkin düzenli ve matematiksel olarak kolay işlenebilir bir modelin elde edilmesidir. Otomotiv içten yanmalı motor kontrolü, kontrol sistem mühendisleri ve araştırmacılar için en karmaşık kontrol sorunlarından biridir. Tüm motor kontrol değişkenleri arasında motor torku bir motorun en önemli performans değişkenlerinden biridir. Bu nedenle, bir tork kontrol sistemi tüm aracın büyük ölçüde performansını artırabilir. Bu çalışmanın iki amacı vardır. Birincisi, benzinli bir motor torkunu ve özgül yakıt tüketimini *yapay sinir ağları* ve *genetik programlama* kullanarak kararlı hal modelini geliştirmektir. İkincisi, benzinli bir motorun torkunun en yaygın doğrusal olmayan *Hammerstein* and *NARX* parametrik modeli kullanılarak oluşturulması ve *ileri beslemeli*, *radyal tabanlı* ve *Elman tipi yinelenen yapay sinir ağı* modelinin doğru ve kesin olarak geliştirilmesidir. Bu geliştirilen metotlar 1400 hacimli 4 silindirli fiat marka benzinli bir motora uygulanmıştır. Yapay sinir ağları (YSA) tanımlama yöntemleri arasında yeni geliştirilmiş bir tekniktir. Yapay sinir ağlarının eğitiminde birçok yöntem kullanılmaktadır. Bu çalışmada iki yöntem ele alınmıştır: *hata geriye yayma yöntemi* ve *Levenberg-Marquardt* algoritmasıdır. Bu tezde farklı doğrusal olmayan tanımlama yaklaşımları kullanılmıştır. Bunlar arasından yapay sinir ağları tabanlı model sistem dinamiklerini çok iyi yakalamıştır ve bu model benzinli bir motor torkunu modellemek için uygundur. Ancak, tüm doğrusal olmayan tanımlama metotları doğruluğu kabul edilebilir düzeyde bir motor tork dinamiğini tanımlamıştır.

Anahtar Kelimeler: Benzinli motor, motor tork tanımlama, doğrusal olmayan modelleme, doğrusal olmayan tanımlama, Hammerstein model, NARX model, sinir ağları, genetik programlama

ACKNOWLEDGEMENTS

First of all, I would like to express my sincere gratitude to Prof. Dr. Sedat BAYSEÇ without whose guidance, encouragement and advice, this thesis would not have been a reality. He motivated me to pursue my studies in all stages of the thesis.

I would also like to thank the other members of my PhD committee who monitored my work and took effort in reading and providing me valuable comments on earlier versions of this thesis: Prof. Dr. İbrahim Deniz AKÇALI and Prof. Dr. L. Canan DÜLGER. I sincerely thank Prof. Dr. İbrahim GÜZELBEY for his valuable advices.

I would like to express my deepest gratitude to Dr. Orhan ARPA from Department of Mechanical Engineering Dicle University for his support. I would like to thank Dr. Tolgay KARA for his support.

I would like to emphasize my love and encomium to my mother and my father, my dear husband İsmail, my lovely daughter Elif Nisa, my sister and my brothers and my friends in mechanical engineering department for their continuous encouragement in idiomorphic time. My efforts would have been fruitless without their zeal to support me throughout this study.

CONTENTS

ABSTRACT	iii
ÖZET	iv
ACKNOWLEDGEMENTS	v
CONTENTS	vi
LIST OF FIGURES	x
LIST OF TABLES.....	xiii
LIST OF SYMBOLS	xiv
CHAPTER 1: INTRODUCTION.....	1
1.1 Motivation of the Thesis.....	1
1.2 The Purpose and Contribution of the Thesis	4
1.3 Layout of the Thesis	5
CHAPTER 2: LITERATURE SURVEY	7
2.1 Introduction.....	7
2.2 Classical Nonlinear Identification of the Engine	7
2.3 Artificial Neural Network Approach for Nonlinear Identification of Engine	16
2.4 Genetic Programming Approach for Nonlinear Identification of Engine ..	31
2.5 Conclusions.....	36
CHAPTER 3: DYNAMIC MODELING OF RECIPROCATING ENGINE	38
3.1 Introduction.....	38
3.2 Equation of Motion for a Slider-Crank Mechanism.....	38
3.3 Kinematic Analysis	47
3.4 Dynamic Model Results	47
3.5 Conclusions.....	50
CHAPTER 4: SYSTEM IDENTIFICATION.....	51
4.1 Introduction.....	51
4.2 Nonlinear System Identification	53
4.2.1 Nonlinear System Representation	53

4.2.1.1	Volterra Series Model	55
4.2.1.2	Wiener Model	55
4.2.1.3	Hammerstein Model.....	56
4.2.1.4	NARMAX Model	58
4.3	Identification of Hammerstein Model	59
4.4	Conclusions.....	62
CHAPTER 5: ARTIFICIAL NEURAL NETWORK.....		63
5.1	Introduction.....	63
5.2	History of Neural Networks.....	64
5.3	Biological and Artificial Neurons	65
5.4	Types of Activation Function	67
5.5	Neural Network Architectures	68
5.5.1	Multilayer Perceptron Feedforward Neural Network.....	68
5.5.2	Radial Basis Function Neural Network	70
5.5.3	Recurrent Neural Network	72
5.5.3.1	Elman Recurrent Neural Network	74
5.6	Learning Algorithm	76
5.6.1	Backpropagation Algorithm.....	77
5.6.2	Levenberg-Marquardt Algorithm	78
5.7	Neural Networks for Identification of Nonlinear Dynamic Systems.....	80
5.7.1	External Dynamics	82
5.7.2	Internal Dynamics	83
5.7.3	Training Feedforward and Recurrent Structures.....	83
5.7.4	Choosing a Model.....	84
5.8	Conclusions.....	85
CHAPTER 6: MEAN VALUE MODEL OF A SPARK IGNITION ENGINE		86
6.1	Introduction.....	86
6.2	Intake Manifold Filling Dynamics	89
6.2.1	Throttle Body Flow	89
6.2.2	Cylinder Flow.....	91
6.3	Fueling Dynamics	91
6.4	Crankshaft Speed Dynamics	93
6.4.1	Indicated Combustion Torque.....	93
6.4.2	Friction and Pumping Losses	94

6.5	Conclusions.....	95
CHAPTER 7: EXPERIMENTAL SET-UP AND MEASUREMENT DEVICES.....		96
7.1	Introduction.....	96
7.2	The Experimental Set-up	96
7.2.1	Torque Measurement	98
7.2.2	Mass Fuel Flow Rate Measurement	101
7.2.3	Servo Motor	101
7.2.4	Data Acquisition.....	102
7.2.5	Matlab Toolbox	104
7.3	Experimental Procedure for Steady-State Condition	104
7.4	Experimental Procedure for Dynamic Condition.....	105
7.5	Uncertainty Analysis	105
CHAPTER 8: CASE STUDIES		110
8.1	Introduction.....	110
8.2	Case Studies	111
8.2.1	Prediction of torque and specific fuel consumption of a gasoline engine by using artificial neural networks	111
8.2.1.1	Introduction	111
8.2.1.2	Artificial Neural Network Model and Parameters.....	113
8.2.1.3	Analysis Results	114
8.2.1.4	Conclusions	119
8.2.2	Genetic programming approach to predict torque and brake specific fuel consumption of a gasoline engine	120
8.2.2.1	Introduction	120
8.2.2.2	Overview of Genetic Expression Programming (GEP).....	123
8.2.2.3	Modeling with GP.....	125
8.2.2.4	Results and Discussion.....	127
8.2.2.5	GP vs Neural Network (NN).....	131
8.2.2.6	Conclusions	132
8.2.3	Nonlinear modeling and identification of a spark ignition engine torque using Hammerstein model	133
8.2.3.1	Introduction	133
8.2.3.2	Simplified Mean-value SI Engine Model	136
8.2.3.3	Nonlinear System Identification.....	139

8.2.3.4	Hammerstein Model of Nonlinear SI Engine Dynamics	143
8.2.3.5	Identification Results	144
8.2.3.6	Model Validation	147
8.2.3.7	Conclusions	148
8.2.4	Nonlinear modeling and identification of a spark ignition engine torque using NARX model	149
8.2.4.1	Introduction	149
8.2.4.2	NARX Model	150
8.2.4.3	Identification Results	152
8.2.4.4	NARX Model Validation	156
8.2.4.5	Conclusions	158
8.2.5	A comparative study of neural network structures in identification of gasoline engine torque	159
8.2.5.1	Introduction	159
8.2.5.2	Neural Network System Identification	161
8.2.5.2.1	Feed Forward Neural Networks (FFNN) for System Identification	163
8.2.5.2.2	Radial Basis Function (RBF) Neural Networks for System Identification	169
8.2.5.2.3	Recurrent Neural Networks (RNN) for System Identification	174
8.2.5.3	Comparison of the Three Approaches	179
8.2.5.4	Conclusions	180
CHAPTER 9: CONCLUSIONS		182
9.1	Recommendations for Future Work	186
REFERENCES		188
APPENDIX 1: IDENTIFICATION OF THE GENERAL NARMAX MODEL.....		215
APPENDIX 2: SPECIFICATIONS OF THE DYNAMOMETER		217
APPENDIX 3: SPECIFICATIONS OF THE PRESURE TRANSDUCER		218
APPENDIX 4: TECHNICAL SPECIFICATIONS OF THE SERVO MOTOR		219
APPENDIX 5: SPECIFICATIONS OF THE DATA ACQUISITON CARD.....		220
CURRICULUM VITAE		221

LIST OF FIGURES

Figure 3.1 Slider-crank mechanism	39
Figure 3.2 A four-cylinder in-line engine	46
Figure 3.3 Numerical results of a slider crank mechanism for a) angle θ b) angular velocity $\dot{\theta}$ c) the angular acceleration $\ddot{\theta}$ of the crank	48
Figure 3.4 Numerical results of a slider crank mechanism for a) displacement b) speed and c) acceleration of a slider	49
Figure 3.5 Kinetic, potential and total energy of a slider-crank mechanism	50
Figure 4.1 A dynamic system with input $u(t)$, output $y(t)$ and disturbance $v(t)$, where t denotes time [27]	51
Figure 4.2 Schematic flowchart of system identification [27]	52
Figure 4.3 Overview of system identification methods [78].....	54
Figure 4.4 Nonlinear system with additive noise	55
Figure 4.5 General Wiener model structure	55
Figure 4.6 Hammerstein model structure.....	57
Figure 4.7 General NARMAX system structure [152].....	58
Figure 5.1 A simplified model of a biological neuron [156]	65
Figure 5.2 A simplified model of an artificial neuron [156].....	66
Figure 5.3 Basic elements of an artificial neuron.....	66
Figure 5.4 Multilayer perceptron neural network structure	69
Figure 5.5 Radial basis function neural network structure	71
Figure 5.6 Recurrent neural network structure.....	73
Figure 5.7 Elman recurrent neural network structure	74
Figure 5.8 a) Series-parallel model b) parallel model	81
Figure 6.1 Main system's input/output signals in a COM of an SI engine.....	87
Figure 6.2 Mean-value SI engine structure [172].....	87
Figure 6.3 Cause and effect diagram of an SI engine system [172]	88
Figure 6.4 Throttle body flow	90
Figure 7.1 Schematics of test engine and setup.....	97

Figure 7.2 Photograph of the SI test engine	97
Figure 7.3 Schematic representations of water brake dynamometer and measurement devices. 1) Dynamometer body, 2) jam nut, 3) end push rod, 4) hydraulic load cell, 5) digital voltmeter, 6) electrical power supply, 7) transducer	100
Figure 7.4 Go Power System DA 516 model water brake dynamometer.....	100
Figure 7.5 Schematic representations of throttle valve position control and control unit on it. 1) throttle valve, 2) servo motor, 3) control panel, 4) data logger 5) computer.....	102
Figure 7.6 Photograph of the throttle valve position control	102
Figure 7.7 DT 304 Data Acquisition Card [180].....	103
Figure 7.8 Data Translation STP 300 Screw Terminal Panel and EP305 Cable [180]	103
Figure 8.1 Architecture of proposed NN model.....	114
Figure 8.2 Prediction of NN and actual values for training sets (a) T (b) BSFC	115
Figure 8.3 Prediction of NN and actual values for testing sets (a) T (b) BSFC.....	116
Figure 8.4 Percentage error of training set (a) T (b) BSFC	116
Figure 8.5 Percentage error of testing set (a) T (b) BSFC	117
Figure 8.6 Genetic Programming Flowchart [206]	124
Figure 8.7 Expression tree (ET)	125
Figure 8.8 Expression tree for engine torque	129
Figure 8.9 Expression tree for brake specific fuel consumption	130
Figure 8.10 GP vs test results for (a) torque and (b) BSFC	131
Figure 8.11 Simplified mean-value schematic SI engine diagram.....	137
Figure 8.12 Simplified conceptual throttle model.....	138
Figure 8.13 Simplified conceptual torque generation model	139
Figure 8.14 Hammerstein system structure.....	140
Figure 8.15 Hammerstein model for torque generation.....	143
Figure 8.16 Hammerstein model of SI engine dynamics.....	144
Figure 8.17 Results of the identification experiment. Torque response of the SI engine is given in solid line, and estimated torque recorded through recursions is given in dotted line	145
Figure 8.18 Validation of identification results. Torque response of the SI engine to a PRBS input is given in solid line, and simulated response of the obtained Hammerstein model is given in dotted line.....	146

Figure 8.19 Validation of identification results by a different set of data. Torque response of the SI engine to a square wave input is given in solid line, and simulated response of the obtained Hammerstein model is given in dotted line	147
Figure 8.20 NARX model structure.....	151
Figure 8.21 PRBS of the throttle valve position (bottom) and measured values of torque (top).....	155
Figure 8.22 Results of the identification experiment. Torque response of the SI engine is given in solid line, and NARX model estimated torque is given in dotted line	156
Figure 8.23 Validation of identification results. Torque response of the SI engine to PRBS input is given in solid line, and simulated response of the obtained NARX model is given in dotted line	157
Figure 8.24 Series- parallel model for neural network identification.....	162
Figure 8.25 FFNN architecture.....	167
Figure 8.26 Modeling results of the FFNN model with identification experiment	168
Figure 8.27 Modeling results of the FFNN model with validation of identification results	168
Figure 8.28 RBF neural network structure.....	172
Figure 8.29 Modeling results of the RBF neural network model with identification experiment.....	173
Figure 8.30 Modeling results of the RBF neural network model with validation of identification results.....	174
Figure 8.31 Structure of Elman neural network	175
Figure 8.32 Modeling results of the Elman NN model with identification experiment	178
Figure 8.33 Modeling results of the Elman NN model with validation of identification results.....	178

LIST OF TABLES

Table 3.1 Fiat Tofaş 131 motor parameters	39
Table 5.1 Types of activation function	67
Table 7.1 Test engine specifications.....	98
Table 7.2 Uncertainty values for measurements	109
Table 8.1 Range of input-output parameters in training-testing phase and normalization values	115
Table 8.2 Statistical parameters of train and test sets	115
Table 8.3 Variables used in model construction	126
Table 8.4 Parameters of the GP model	126
Table 8.5 Statistical results of GP and NN models for training and testing sets.....	132
Table 8.6 Estimates of Hammerstein model parameters	145
Table 8.7 MSE values for nonlinear identification experiments.....	148
Table 8.8 MSE values and nonlinear parameters for nonlinear identification with different polynomial orders.....	148
Table 8.9 Parameters of SISO NARX models	153
Table 8.10 MSE values for nonlinear identification experiments.....	158
Table 8.11 Performance comparison for neural models	166
Table 8.12 Performance comparison for Elman neural network model.....	176
Table 8.13 Statistical performance of three approaches	180

LIST OF SYMBOLS

b_i	constant term (bias)
F_E	external disturbance force
F_B	friction force
g	gravitational acceleration (m/s^2)
I_c	the centroidal mass moment of inertia ($kg.m^2$)
J	Jacobian matrix for Levenberg-Marquardt algorithm
l_2	connecting rod length (mm)
L	Lagrange function
m	mass (kg)
\dot{m}	mass flow rate (kg/sec)
r_1	crankshaft radius (mm)
t	time
T	the kinetic energy of a slider-crank mechanism
u_i	weighted average obtained by combining all input numerical information from upstream nodes
$u(t)$	input variables
$v(t)$	disturbances
$y(t)$	output variables
V	the potential energy of a slider-crank mechanism
x_j	activation for each node
w_{ij}	weight values
∂x	virtual displacement
$\partial \theta$	virtual angle
∂W^A	virtual work
\dot{m}_{at}	air mass flow rate past through throttle plate

\dot{m}_{ap}	air mass flow rate into the intake port
P	pressure (pa or bar)
R	ideal gas constant (J/kg K)
T	temperature (C)
V	volume (m ³)
c_d	discharge coefficient
A	area (m ²)
ω	speed (rad/sec)
θ	the angle position of the crank (rad)

Abbreviations

AFR	Air-fuel ratio
AI	Artificial Intelligence
ANFIS	Neuro-fuzzy inference systems
ANN	Artificial neural network
ARMA	Autoregressive moving average
ARMAX	Autoregressive moving average with exogenous input
ARX	Auto-regressive with exogenous inputs
BP	Back-propagation
BSFC	Brake specific fuel consumption
CA	Crank angle
COM	Control oriented models
EGR	Exhaust gas recirculation
ETs	Expression trees
FFNN	Feedforward neural network
GA	Genetic algorithm
GEP	Gene-Expression programming
GP	Genetic programming
HCCI	Homogenous charge compression ignition engine
ICE	Internal combustion engine
IPS	Induction-to-power-stroke
LM	Levenberg-Marquardt

LMS	Least mean square
LPG	Liquefied petroleum gas
MATLAB	Matrix laboratory
MAE	Mean absolute error
MAPE	Mean absolute percentage error
MIMO	Multi input multi output
MLP	Multilayer perceptron
MLPFF	Multilayer perceptron feedforward
MSE	Mean squared error
MVEM	Mean-value engine model
NARMAX	Nonlinear autoregressive moving average with exogenous input
NARX	Nonlinear auto-regressive with exogenous inputs
N	Engine speed
NN	Neural network
NOE	Nonlinear output error
PRBS	Pseudo-random-binary-signal
R	Correlation coefficient
RAS	Random amplitude signals
RBF	Radial basis function
RGS	Random Gaussian signals
RLS	Recursive least square
RNN	Recurrent neural network
SA	Spark advance
SI	Spark ignition
SISO	single input single output
T	Torque
TDNN	Time delay neural network
TP	Throttle position

Subscripts

α, a, β	the air or ambient
m	the manifold or mean values
φ, ψ, f	the fuel
ζ	the timing (ignition, injection,...)
ε	exhaust gas recirculation
e	the engine
d	displacement of the engine cylinder
c	the crankshaft
cr	the connecting rod
p	the piston

Greek Letters

γ_n	phase difference between the angular position of the first and n th cylinder
β_n	the phase difference between the firing angle of engine cylinders
τ	the applied torque
∇	the gradient operator
η_{vol}	the volumetric efficiency
λ	forgetting factor

CHAPTER 1

1. INTRODUCTION

1.1 Motivation of the Thesis

Automotive internal combustion engine (ICE) control is one of the most complex control problems for control system engineers and researchers. Due to increasing requirements of governments and customers, car manufacturers always strive to reduce substantially, emissions and fuel consumption while maintaining the best engine performance. To satisfy these requirements, a variety of variables need to be controlled, such as engine speed, engine torque, spark ignition timing, fuel injection timing, air intake, air-fuel ratio (AFR) and so on. These variables are complicatedly related to each other. Moreover, car engines have several different operating modes including start up, idle, running and braking. Engine dynamics is highly nonlinear and multivariable because of these factors [1-5].

Among all the engine control variables, the engine torque has important applications in the automotive industry: for example, automatically setting gears, optimizing engine performance, reducing emissions and designing drivelines [6]. For these reasons; a good torque control system can improve substantially the performance of the overall vehicle [7, 8]. Torque models can be classified according to their inputs. Most are directly based on engine inputs such as the air and fuel mass flow rates, intake and exhaust pressures, ignition timing, injection timing, engine speed and throttle angle have been widely used for torque model and control application [6, 9]. Torque modeling efforts have been based on an experimental method of system identification that captures the nonlinear engine torque characteristics [10].

Exact mathematical models of mechanical systems are derivable by Lagrange, Hamilton and Newton-Euler formulations or by energy methods. This requires all the

system parameters such as masses, mass moments of inertia, stiffnesses, damping coefficients and physical dimensions explicitly. The system generally needs to be dismantled into its main components where each parameter of the system is lumped for measurement. In applications where this is not possible, system identification becomes very useful, generating an empirical mathematical model for the response of the system [11].

System modeling plays a fundamental role in modern engineering, as it is typically the first step in a design cycle. However, it is also one of the more complicated tasks in engineering, as it is more closely connected with reality (in contrast with the tasks of analysis and design, which are usually performed on mathematical models). In some cases, one can build a so called “white-box” model based on first principles (Newton’s law, Kirchhoff’s laws, laws of thermodynamics, etc.), but in many cases such models will be overly complex and perhaps even impossible to obtain in reasonable time due to complex nature of many systems and processes. A much more common approach is therefore to start from measurements of the behavior of the system and the external influences (inputs to the system) and try to determine a mathematical relation between them without going into the details of what is actually happening inside the system. This approach is called *system identification* [12].

Most systems encountered in the real world are nonlinear in nature, and since linear models can not capture the rich dynamic behavior of limit cycles, bifurcations, etc. associated with nonlinear systems, it is imperative to have identification techniques which are specific for nonlinear systems [13]. System identification has become an important area of study because of the increasing need to estimate the behavior of a system with partially known dynamics. Especially in the areas of control, pattern recognition and even in the realm of stock markets, the system of interest needs to be known to some extent [14, 15].

In engineering dynamics, control engineering and many other areas, *auto-regressive with exogenous inputs* (ARX) models are widely utilized for describing dynamic data regimes for linear and nonlinear systems [16]. And also, the *Hammerstein model* is probably the most widely known and applied nonlinear dynamic modeling approach.

It assumes a separation between the nonlinearity and the dynamics of the process [17].

In classical polynomial approaches for nonlinear system identification, *Nonlinear auto-regressive with exogenous input* (NARX) model, *Hammerstein model*, *Wiener model* are suitable only restricted classes of processes [17]. However, even when there exists some structural process/model mismatch these simplified models may be sufficiently accurate for many applications, and thus some of them, in particular the Hammerstein structure, are widely utilized in practice. [17].

Artificial neural network (ANN) has opened a new horizon in identification and control of highly nonlinear and complex structured systems. These networks are implemented using massive connections among the neurons with variable strengths. Moreover, their parallel, distributed and fault tolerant processing properties make them powerful tools for both identification and control of nonlinear dynamical systems. Especially learning capabilities of these networks enable them to process the information adaptively [18, 19].

Neural networks (NN) have been proved to be effective in modeling complex nonlinear systems. They are natural candidates to approximate a nonlinear process due to their inherent nonlinearity and computational simplicity. There are many kinds of neural networks that can be used for nonlinear function approximation. For example, multilayer feedforward neural network (FFNN), radial basis function (RBF) neural network, recurrent neural network (RNN) is just a few examples [1].

The use of artificial neural network (ANN) in system identification has been gaining more and more attention in recent years. Neural networks (NN) have good general approximation capabilities for reasonable nonlinear systems [20, 21]. Nerendra and Parthasaraty [22] have demonstrated that ANN could be used successfully for the identification and control of nonlinear dynamic systems. A series of works performed by Chen and Billings and their coworkers have developed the foundation of using neural networks as a tool for nonlinear system identification [23-25].

1.2 The Purpose and Contribution of the Thesis

The objective of this work has been to develop an accurate and robust model of a spark ignition (SI) engine torque by using the most common nonlinear black-box parametric models, namely Hammerstein model and Nonlinear auto-regressive with Exogenous inputs (NARX) model and neural network model that is including multilayer feedforward neural network (FFNN) model, radial basis function (RBF) neural network model and Elman type recurrent neural network model. These developed methods are implemented to an existing 1400 cc, four cylinder Fiat SI engine.

When the physical system structure and parameters are not available or dependent on time or operating conditions, a mathematical model representing the system behavior may be very difficult to obtain. For such a case, the system parameters should be obtained using a system identification procedure [26, 27]. Identification of linear systems is rather an old field of study, and many methods are available in literature [26, 27]. However, identification of nonlinear systems is respectively a new topic of interest [26-28]. In internal combustion engines (ICE), identification is an occasionally employed method for examination and detection of the system parameters. The nonlinear identification of ICE has also been of interest in recent years.

To satisfy the intended objective, the following scope of works was carried out.

1. A comprehensive literature review has been carried out on identification and modeling of the internal combustion engine (ICE).
2. Steady-state experiments were carried out in a spark ignition (SI) engine to model the SI engine torque and brake specific fuel consumption (bsfc) using soft computing techniques.
3. Dynamic experiments were carried out in a SI engine to identify and model the SI engine.

4. Development of artificial neural network (ANN) and Gene-Expression Programming (GEP) model of SI engine torque and brake specific fuel consumption at steady-state conditions and comparison with ANN model and GEP model.
5. Development of Hammerstein model and NARX model for identifying and modeling of SI engine torque for control purposes and their comparison.
6. Development of various kinds of neural network structure for modeling and identification of SI engine torque for control purposes and comparison of the neural network structures.
7. For the modeling and identification of SI engine, an attempt has been made to develop a computer program using Matlab based on system identification toolbox and artificial neural network toolbox of Matlab.

The results of this PhD thesis came up very promising. The proposed models came up far more accurate than all the work published, when compared to real test engine output.

1.3 Layout of the Thesis

The presentation of the work done in this thesis is organized as follows:

In Chapter 2, a comprehensive literature review on identification and modeling of the internal combustion engine (ICE) is presented. The survey is presented under three titles: classical nonlinear identification, neural network nonlinear identification and genetic programming nonlinear identification.

In Chapter 3, the dynamic formulations of a piston-crank mechanism have been done with only one independent variable using Lagrange equation. And also, more complex sets of equations of motion are derived for multi-cylinder engines.

In Chapter 4, a general view of nonlinear system modeling and identification with a parametric approach is given. Identification of Hammerstein model is presented in this chapter.

In Chapter 5, background information on neural network and neural network structures is given. Neural networks for identification of nonlinear dynamic systems are explained in this chapter.

In Chapter 6, the mean value engine model (MVEM) which is generally accepted as the modeling paradigm in engine control is extensively described.

In Chapter 7, a detailed description of the spark ignition (SI) engine experimental set-up and the measuring devices on it are presented. The experimental set up details are provided with the specifications of the measuring instruments. The experimental procedure for steady-state condition and the experimental procedure for dynamic condition are given in this chapter. The uncertainty analysis has been carried out to calculate the percentage of measurement errors in this chapter.

In Chapter 8, steady-state modeling of the gasoline engine torque and brake specific fuel consumption is investigated by means of a number of case studies. These case studies can be categorized under two headings with respect to the used methods namely the *neural network* and the *genetic programming* approach. Nonlinear identification and modeling of a gasoline engine torque is investigated by means of a number of case studies. These case studies which can be categorized under three headings with respect to the used methods namely the *Hammerstein model*, *NARX model* and the *Neural Network models*, are presented also in this chapter.

In Chapter 9, conclusions drawn from the study are pointed out and further recommendations for study are provided.

CHAPTER 2

2. LITERATURE SURVEY

2.1 Introduction

In this chapter, a comprehensive literature survey on identification and modeling of the internal combustion engine (ICE) is presented. The survey is presented under three headings: classical nonlinear identification, neural network nonlinear identification and genetic programming nonlinear identification. The survey provides a historical view and various methodologies developed over the years.

2.2 Classical Nonlinear Identification of the Engine

In order to control nonlinear dynamic systems, appropriate models should be developed. A discrete time nonlinear dynamic system can be described by a nonlinear autoregressive with exogenous input (NARX) model, nonlinear autoregressive moving average with exogenous input (NARMAX) model, Hammerstein model and Wiener model [29].

System modeling and identification refers to a systematic method to determine and improve the mathematical models for the proper representation of dynamic systems [30]. Many articles were published in order to control and identify the internal combustion engine. Majors of these are given below.

Pérez et al. [31] have proposed a new approach to control the air management process of a Diesel engine. Identification and control schemes based on model predictive control and Wiener and Hammerstein models have been proposed. Proposed algorithms were implemented on a real world engine. In the end, useful hints are given, offering an improvement in the application, were proposed.

Nicolao et al. [32-34] have presented an application of the identification procedure for nonlinear autoregressive with exogenous input (NARX) models and control of ICEs in idle speed conditions. The inputs of the nonlinear identification model were the position of the idle speed air actuation system and the spark advance, while outputs were the pressure inside the intake manifold and the crankshaft speed. The estimated model was then used to synthesize an idle speed controller with the linear quadratic technique. Some identification and control results obtained by applying this method to a 1200 cm³ engine [32], a 1400 cm³ engine [33] and two more commercial engines namely a 1200 and 1600 cm³ [34] were reported to witness the effectiveness of the proposed approach.

Hrovat and Sun [35] have surveyed different ICE models and controller design methodologies for idle speed control applications. Linear engine models used for control system synthesis and analysis, as well as nonlinear models for computer simulation and control design validation are discussed. The survey includes both classical designs and those based on advanced control theory.

Rachid et al. [36] have studied the nonlinear identification of a turbocharged Diesel engine. A combined use of nonlinear autoregressive moving average with exogenous input (NARMAX) models and group method data handling method was proposed in an attempt to provide a systematic approach to identify nonlinear systems using relatively simple models well suited to computer handling.

Glass and Frankchek [37] have presented in a detail their study of a single input single output (SISO) nonlinear modeling and robust controller design methodology experimentally on an ICE. The methodology begins with the identification of a NARMAX model that captures the nonlinear dynamics relating the input to the output of a system. This model is converted to a describing function representation for the purpose of robust feedback controller design. For the engine idle speed control application of this study, a SISO NARMAX model of the engine was developed between the by-pass idle air valve and engine speed. The controller performance is then validated through numerical simulations and experimental verification.

Pfeiffer et al. [38] have investigated the potential of the use of inlet air temperature as a means of control for ignition actuation. This study describes a method for system identification of the homogenous charge compression ignition engine process, and development of an effective linear quadratic Gaussian controller for the combustion process, Matlab and Simulink being used in computations and simulations.

Jones et al. [39] have explored the use of adaptive control as a means of precise control of the AFR. A control-oriented, physics based engine model, in which the sampling rate is based on crank angle instead of time, has been utilized to construct a feedforward/feedback control scheme to regulate AFR. A nonlinear least squares identification technique is used to accurately determine the model parameters using normal engine operating data. These parameter values are then employed in the design of an estimator based controller for a single cylinder engine.

Souder and Hedrick [40] have used a simplified model of an ICE to derive a sliding mode control law. Adaptive update laws are derived for two fueling parameters that describe fuel flow into cylinders, and a third parameter that describes air flow. The performance of sliding mode adaptive controllers have been found encouraging and described as an effective method of achieving accurate AFR control.

Arsie et al. [41] have presented a procedure for the identification of emission models for the design of an optimal controller for a SI engine. A two step scheme has been built: in the first step the available physical models, based on a multi-zone thermodynamic model with emission sub-models, are parameterized and an intermediate model, based on Taylor approximation, is derived in order to describe the nonlinear influences exerted by the physical parameters; in the second step the physical parameters are modeled by means of nonlinear regression, taking into account the effect of operating engine variables, and the optimal parameters obtained via stepwise approach.

Luh and Rizzoni [42] have presented the application of advanced modeling techniques to construct engine models for the detection and isolation of incipient faults. A nonlinear black-box engine model is derived using the NARMAX models. A forward-regression estimator is applied to identify the model parameters.

Experimental validation is performed using data from a production engine. They have pointed out that the agreement between the estimated and measured values of all the variables have been excellent except for the load torque. Further, they have stated that this kind of a model was adequate for diagnostic purposes.

Falcone et al. [43] have proposed a combustion model of direct injection diesel engine to calculate the in-cylinder pressure and a slider-crank mechanism model to calculate instantaneous indicated torque. The crankshaft is modeled as a rigid body. The parameters of both models are identified via nonlinear least square optimization algorithm. The model is generated using pressure data collected from an engine test bed, equipped with a BMW four cylinder diesel engine. The obtained model was intended to be the benchmark to develop and test another model which would be able to estimate the produced torque and to be implemented on commercial vehicles simply.

Ingram et al. [10] have presented a robust feedback controller design procedure to regulate the torque of a SI engine equipped with an electronic throttle mass air flow controller. A Ford 4.6 L V8 SI engine torque production system level model was experimentally determined. In addition, an H_∞ controller was designed to control engine torque. It was observed that the torque disturbances may be reduced using the same controller design methodology outlined in this paper by taking into account spark timing and exhaust gas recirculation.

Khier et al. [44] have estimated the combustion torque of an ICE with the only measurement available on a mass production car. Two estimators have been developed based on two different unknown input observers: a high gain and a second order sliding mode. The main advantage of these designs is the systematic aspect of the method to deal with a large class of ICE. The method has been applied to a three cylinder-turbocharged gasoline engine. The results showed the efficiency of the proposed method.

Rakotomamonjy et al. [6] have compared the torque estimation problem using four methods: linear least squares, linear and nonlinear neural networks and support vector machines. It has been found that a nonlinear model structure is necessary for

accurate torque estimation. The most efficient torque model built came up to be a nonlinear neural network that achieves about 2% test normalized mean square error in nominal conditions.

Franco et al. [45] have presented a real time engine brake torque estimation model whose input is the instantaneous engine speed. This model is separated into steady-state and transient torque estimations. The steady-state portion of the model is developed using orthogonal least squares estimation, where as the transient portion is identified using a time domain identification method. This study had shown that the engine speed and mean engine speed were sufficient to estimate the engine brake torque. Validation of the engine brake torque model is provided using a computational engine model for a 6 cylinder heavy duty diesel engine.

Vong et al. [46] have determined the approximated power and torque model of a vehicle engine by training the sample data acquired from the dynamometer with least square support vector machines. The vehicle engine is run on the dynamometer to show the actual engine output torque and power. In this paper, the construction, validation and accuracy of the functions are discussed. The study has shown that the predicted results using the estimated model from least squares support vector machines are in good agreement with the actual test results. Also, the study conducted in Ref. [56] illustrated the significance of the least squares support vector machines methodology, in predicting automotive engine power and torque by comparing the results with that regressed using multilayer feed forward neural networks. From the perspective of automotive engineering, the construction of modern automotive gasoline engine power and torque functions using proposed method, least squares support vector machines, is a new attempt and this methodology can also be applied to different kinds of vehicle engines.

Ali and Blath [47] have proposed a nonlinear state space controller for the optimal torque of a SI engine. The controller design is based on feedback linearization in combustion with pole placement. The resulting controller basically compensates the intake manifold filling dynamics and thus improves tracking performance of torque demand changes generated by the driver. The tracking performance is superior to the performance of the original controller supplied by the ECU manufacturer.

Ali and Blath [9] have investigated the application of three modern design techniques to the torque control problem of a SI direct injection engine. The system to be controlled is a highly nonlinear system characterized mainly by the intake manifold dynamics. Control laws based on feedback linearization in order to achieve a linear and uniform system behavior over the whole range of operation, nonlinear model predictive control in order to optimize the control law over a finite time horizon taking the input and state constraints into account during optimization and gain scheduled LQ optimal control in order to describe the system in state-space form are derived for the highly nonlinear automotive engine. A comparative study of these schemes with the help of computer simulation is presented. The schemes have shown that all of these schemes are capable of achieving a high performance of the control loop. Nonlinear model predictive control outperforms other two schemes in the sense of uniformity of the loop response.

Falcone et al. [7] have presented an engine torque estimator. The results reported that a good performance of the estimator and validate the design criteria. This feature makes it suitable for applications in which a good estimation of engine torque is required.

Connolly and Yagle [48] have presented a new model relating cylinder combustion pressure to crankshaft angular velocity in an ICE. There are three aspects to this model. First, by changing the independent variable from time to crankshaft angle, second, parametrising the pressure by the sample modulating sequence, third, the inverse problem of reconstructing pressure from noisy angular velocity measurements. Simulation result show that the parameterized pressure can be deconvolved at low noise levels, and combustion misfires detected, in all real time. The second part of their study [49] have presented and discussed the experimental results that confirm this model, at least at the relatively low-speed, low-to-moderate load operating conditions analyzed. They have shown that cyclic combustion pressure variation is fairly well modelled and may be directly estimated from angular velocity measurements. The experimental data are taken from an actual V-6 automobile engine.

Billings et al. [50] have described the identification of both linear and nonlinear models of a Leyland TL11 turbocharged, direct injection diesel engine. Two sets of data are used in the identification and in both cases the input is fuel rack position and the output is engine speed. A hydraulic (position) actuator acts directly onto the fuel rack of the injection pump. The fuel rack was perturbed by a pseudo-random-binary-signal (PRBS). An input-output model is a means for representing the input-output relationship of a system and therefore a NARMAX model is chosen. The objective of the study was to demonstrate that parsimonious nonlinear models can be used to predict engine response. It has been shown that the combined procedure of orthogonal and prediction-error estimation coupled with correlation and chi-squared model validity tests provides a powerful interactive toolkit for fitting parsimonious models to practical systems.

Rizzoni and Zhang [51] have discussed a method for the identification of a nonlinear model of the dynamics relating combustion pressure to crankshaft angular velocity. Such a model can be useful in the implementation of control strategies that require an estimate of individual cylinder indicated torque or pressure. The method demonstrated in this paper utilizes a known model structure and employs nonlinear programming for the identification of relevant model parameters. The technique is applied to single cylinder research engine, and successfully validated with experimental data. Finally, the model thus derived is used to design an input observer for the estimation of indicated torque. The accuracy achieved is sufficient to permit the design of indicated torque estimators, with potential application to diagnostic and control tasks. The diagnostic application of this modeling technique included as end-of assembly tests, misfire detection, detection of abnormal piston and ring friction, poor compression, and the diagnosis of other malfunctions related to the combustion process and the reciprocating and rotating dynamics of the engine.

Polóni et al. [52] have proposed a nonlinear modeling of AFR dynamics of gasoline engines during transient operations. In advanced control methods the model plays the most important role. The purpose of the study is to identify a suitable model for nonlinear model based control strategy and verify its ability to deal with nonlinear parameter varying AFR dynamics. They have discussed an open loop identification procedure of AFR on a 2.8 liter engine. Specifically, composite local linear ARX

models with weighted validity are identified to model AFR nonlinear dynamics. The global AFR model is then validated against the measured data. The estimation of local ARX model parameters is performed using the data from engine which are measured with an exhaust gas oxygen sensor and with the air mass flow sensor as a reference sensor. To excite the air path dynamics they have applied PRBS to the throttle and have recorded the AFR signal. All signals were sampled with a frequency of 10 Hz. It has been found that the studied global model has the ability to approximate nonlinear effects and varying dynamics of AFR.

Brahma et al. [53] have investigated a system approach to modeling the response of brake torque and NO_x emissions of a high speed common rail diesel engine. A multivariate mean value model is proposed, identified and validated. They proposed a linear grey-box approach to modeling the torque and NO_x dynamics in response to combined fuel quantity-timing excitation. Brake torque was measured using the dynamometer load cell and NO_x was measured using a Horiba emissions bench. Observers are presented for the physically based model and it is shown that torque and NO_x can be predicted using existing measurements of manifold pressure and air mass flow.

Bengtsson et al. [54] have estimated dynamic models of homogenous charge compression ignition engine (HCCI), both SISO and MIMO models. Two different actuator approaches (dual fuel and variable valve actuation) were used and models for both approaches were estimated. Model based control synthesis requiring dynamic models of low complexity and HCCI combustion models were estimated by system identification and by physical modeling. The models identified by system identification were used to design model predictive control with several desirable features and today applicable very fast systems. Whereas satisfactory results were obtained for both approaches, the dynamics were different among the models. Finally, system identification and model predictive control provide effective and pragmatic means to control system.

Cook and Powell [55] have presented the development of a basic nonlinear representation of an engine dynamic system. The model contains descriptions for the induction process and engine power system as well as characterization of the fuel

system. In addition, a linear model has been developed for a particular six cylinder engine and a time response of the system is presented.

Jankovic [56] has shown how the disturbance decoupling results and the notation of relative degree introduced by the geometric theory of nonlinear control can be used to design a controller that coordinates the throttle and the variable cam timing actuator to achieve the desired transient performance. This study also illustrated the design aspects relevant to experimental implementation of the control law. Due to its nonlinear, multivariable nature, engine control systems can benefit from application of advanced nonlinear control techniques.

Fritzsche and Dünow [8] have discussed a control approach for torque control of a gasoline engines. The torque controller can be designed on base of linear models. An appropriate standard control concept for the superordinate torque controller is the model predictive control principle. The control approach described in this study demonstrated that modern control approaches have considerable potential to improve the performance of embedded control systems.

Zito and Landau [57] have applied a nonlinear system identification procedure, based on polynomial NARMAX representation, to a variable geometry turbocharged diesel engine. The relation between the variable geometry turbine command and the intake manifold air pressure is described by a nonlinear model, directly identified by raw data. The intent of the study is to explore the advantages of such a modeling procedure in automotive applications in terms of efficiency and complexity, in view of the related controller design and tuning problem. Simulation results on a diesel engine model illustrate the whole procedure.

Weeks and Moskwa [58] have presented an automotive engine model designed for real-time control applications in the context of a Simulink engine and control system model. Subsystems within the model were briefly described with some additional detail related to the air and fuel dynamics portion of the intake manifold subsystem. Example simulations were presented to show some of the potential uses of the model. In general, they are stated that the model may be used in five different ways: 1. as a nonreal-time engine model for testing engine control algorithms, 2. as a real-

time engine model for hardware-in-the-loop testing, 3. as an embedded model within a control algorithm or observer, 4. as a system model for evaluating engine sensor and actuator models, 5. as a subsystem in a powertrain or vehicle dynamics model. Although developed and validated for a specific engine, the model is generic enough to be used for a wide range of SI engines.

Larimore and Javaherian [59] have presented to extend and refine the nonlinear canonical variate analysis methods for system identification and monitoring of automotive engines. In the nonlinear case, departures from optimality are investigated, but the procedure is shown to still work quite effectively for detecting and identifying system faults and changes.

Ohata et al. [60] have proposed the identification approach for a nonlinear stable system by the nonlinear ARX model. The identification of ARX coefficients is done around the selected level of input and/or output. The dependence of the parameters on the levels of input and output is easily represented by the nonlinear functions like polynomials. The propose approach may be used for the practical study of the industrial processes like automotive engine. The proposed method gives an approach to identify and to represent a nonlinear system which may be used to design a controller.

2.3 Artificial Neural Network Approach for Nonlinear Identification of Engine

The use of artificial neural networks (ANN) in system identification has been gaining more and more attention in recent years. Recently, neural networks have become an attractive tool in the construction of models of complex nonlinear processes. This is because neural networks have an inherent ability to learn and approximate nonlinear functions arbitrarily well, and a large number of identification and control structures based on neural networks have been proposed [22, 23, 61-68].

The ability of neural networks to approximate large classes of nonlinear function sufficiently accurately makes them an important candidate for use in dynamic model representation of nonlinear systems [69, 70]. One of the most common neural networks in the area of system identification and control is the multilayer

feedforward neural network and recurrent neural network [63]. Feedforward neural networks with backpropagation learning algorithm have been successfully utilized to identify nonlinear dynamical systems [71]. In neural network system identification algorithms, the process model is usually described as continuous-time [72, 73] model or discrete-time model. In nonlinear system identification, the Hopfield neural network is used a new dynamic neural network model [74].

After pioneering works mentioned above, many prominent researches contributed to the further development of neural networks and system identification and the dissemination of its application. Work in this area is continuing. Among the works of the rich literature of the neural network concept, the major works related internal combustion engine are taken below.

Arsie et al. [75] have studied the identification of recurrent neural network (RNN) for simulating the air-fuel ratio (AFR) dynamics into the intake manifold of a spark ignition (SI) engine. Considering the manifold as an MISO system, the basic input variables are the manifold pressure, the engine speed and the injected fuel flow rate, while the model output is the AFR. The main contribution of this work was the development of a procedure that allows identifying a RNN based AFR simulator with high generalization and limiting data set. The procedure tested by comparing RNN simulations with AFR transients generated using a nonlinear dynamic engine model. In this paper, a second order method based on the Levenberg-Marquardt training algorithm was considered. A dynamic model of SI engine powertrain has been used to generate AFR transients for training and testing the RNN. The model, developed by the authors is run in Matlab-Simulink environment. The results showed how training the network making use of inputs that are uncorrelated and distributed over the entire engine operating domain allows improving model generalization and reducing the experimental burden. The three following steps have to be accomplished to design a neural network (NN) model: (1) choose the proper learning procedure to find the weights of the neurons connections; (2) define the network structure with the minimum number of layers and nodes; (3) generate training data set extended enough to guarantee acceptable generalization of the knowledge retained in the training examples.

Arsie et al. [76] have focused on the experimental identification and validation of RNN models for AFR estimation and control in SI engines. Suited training procedures and experimental tests are proposed to improve the RNN precision and generalization in predicting AFR transients for a wide range of operating scenarios. The simulations performed on test-sets show that the ability of the RNN to reproduce the target patterns with satisfactory accuracy.

Tan and Saif [1] have presented a procedure for using neural networks to identify the nonlinear dynamic models for the manifold pressure and the mass air flow process in an automotive engine. A dynamic neural network called external RNN, was used for dynamic mapping and model construction. Dynamic Levenberg-Marquardt algorithm was then applied to the weight-estimation problem. In this paper, measured input/output data is employed to construct neural network model of the manifold dynamics. Experimental results in this paper indicated that the NN based models have more precise, a rather simple structure and generalized in performance than the first principles based models. In this models can be used for control system design, or in a model based fault detection and diagnosis strategy.

Wang et al. [2-4] have presented an application of adaptive neural network modeling and model based predictive control for modeling the crankshaft speed, intake manifold pressure, manifold temperature [2], air fuel ratio [3] and engine speed [4]. A radial basis function (RBF) neural network was utilized for them. This studies shown that adaptive model based predictive control was superior over the fixed parameter model based control. In these papers investigated the effectiveness of the adaptive neural network model in modeling parameter uncertainties and severe nonlinearities of SI engines, as well as the feasibility of the adaptive model based model predictive control for air-fuel ratio control. The adaptive RBF neural network trained by recursive least squares method with fixed centers is proved to be more appropriate for modeling the air-fuel ratio dynamics of a SI engine. In these studies concluded that the adaptive neural network model based model predictive control is a potential control scheme to replace the PI control for controlling air-fuel ratio.

Zhai and Yu [77] have applied an adaptive RBF model based model predictive control to the AFR control of automotive engines. The constructed model was

adapted in on-line mode to cope with system uncertainty and time varying effects. Thus, the control performance is more accurate and robust compared with non adaptive model based methods. The simulation results demonstrated that the effectiveness of the developed method.

Beham and Yu [78] have compared different neural networks like multilayer perceptron (MLP), pseudo linear radial basis function and local linear model tree networks for modeling a variable valve timing SI engine torque, HC, NO_x, CO₂ and CO. Five MISO models were developed with each modeling model of the engine outputs. Different model orders and a number of hidden layer nodes were tested in the model training and validation to find the most appropriate model structure for the nonlinear dynamic behavior of the process. Real data were collected when the engine was under different operating conditions and these data were used in training and validation of the developed neural models. The obtained models were finally tested in a real time online model configuration on the test bench. The model outputs were compared with process output and compared among different models. These models performed well and can be used in the model based engine control and optimization. Comparison between different types of network model has been done. It was revealed that the local linear model tree networks and pseudo linear radial basis function network models performed better than MLP. The best models for the HC have been achieved using the pseudo linear radial basis function network, while for NO_x, CO₂ and CO the best models were achieved using the local linear model tree networks. They used the different neural network methods to model the torque of a variable valve timing SI engine in Ref. [79]. The best models for the torque have been achieved using the pseudo linear radial basis function network models.

Wang and Yu [80] have proposed to develop adaptive RBF neural network method to estimate two control parameters in on-line mode, so as to compensate for the model uncertainty and engine time varying dynamics. The adaptive law of the neural network is derived using the Lyapunov method, so that the stability of the whole system and the convergence of the networks are guaranteed. Computer simulations based on a mean value engine model demonstrate the effectiveness of the technique. The simulation results indicated that a significant improvement in AFR when the engine is subjected to a sudden change of throttle angle with 25% uncertainty.

Nicolao et al. [5] have modeled the volumetric efficiency of internal combustion engine (ICE). The volumetric efficiency represents a measure of the effectiveness of an air pumping system, and is one of the most commonly used parameters in the characterization and control of four-stroke ICE. Physical models of volumetric efficiency require the knowledge of some quantities usually not available in normal operating conditions. Hence, a purely black-box approach is often used to determine the dependence of volumetric efficiency upon the main engine variables, like the crankshaft speed and intake manifold pressure. In this work, various black-box approaches for the estimation of volumetric efficiency are reviewed, varying from parametric (polynomial-type) models, to non-parametric and neural network techniques, like additive models, radial basis function neural network and multi-layer perceptrons. The benefits and limitations of these approaches were examined and compared. The problem considered here can be viewed as a realistic benchmark for different estimation techniques. The performance of the different identification methods, as measured by the sum of square of residuals on the validation data set and the corresponding standard deviation of residuals were presented.

Zhang et al. [81] have presented recurrent neural network (RNN) model for air-fuel ratio (AFR) estimation in SI engine. AFR estimation is difficult due to the nonlinearity and dynamic behavior in SI engine. Additionally, delays in engine dynamics limit the performance of engine controller. RNN is trained using data from engine simulations in Matlab/Simulink environment. Uncorrelated signals were generated for training and validation. It has been shown that RNN can predict engine simulations with reasonably good accuracy. These predictions were found to be quite accurate as estimation errors are within ± 0.02 for approximately 95% of the transient. This estimation model can be used for indirect control of AFR.

Yin and Ge [82] have applied neural network identification approach to establish the dynamic model of torque and fuel consumption of Santana 2000 EFI engine through the learning of a great deal of test data. A multi layer feed forward neural network was applied in this study. The result of their studies showed that the obtained model compared with the model built by traditional identification method, the dynamic model based on neural network has higher precision and generalizing capability.

Efe and Kaynak [14, 15] have investigated the identification of nonlinear systems by utilizing soft computing approaches. As the identification methods, feedforward neural networks, radial basis function neural networks, Runge-Kutta neural networks, and adaptive neuro-fuzzy inference systems (ANFIS) based identification mechanisms were studied and their performances are comparatively evaluated on a three degrees of freedom anthropomorphic robotic manipulator [14] and a two degrees of freedom direct drive robotic manipulator [15]. The results presented in both studies have indicated that ANFIS structure is a good candidate for identification purposes.

Hafner et al. [83] have presented the application of fast neural network models for engine control design purposes. Advanced engine control systems require accurate dynamic models of the combustion process, which are substantially nonlinear. In this work the special local linear radial basis function network is initially introduced followed by a description of the process of building adequate dynamic engine model. These neuro-models are then integrated into upper-level emission optimization tool, which calculates a cost function for exhaust versus consumption/torque and determines optimal engine settings. According to the authors, the system allows a fast application of the optimization tool at the engine test stand. Hafner et al. [84] presented a fast neural network of local linear model tree type models for model based control of diesel engine exhaust.

Isermann and Muller [85] have applied a dynamic local linear neural network approach for modeling the NO_x emission characteristics of a 1.9 direct injection diesel engine. The obtained dynamic model for the NO_x emissions can be used for off-line or on-line optimization of exhaust gas emissions, and has been implemented on a rapid control prototyping system as explained in this paper. The structure of rapid control prototyping system was explained, which allows fast measurement signal evaluation, and rapid prototyping of advanced engine control algorithm.

Zweiri [86] has presented an artificial neural networks approach to estimate the indicated torque of a single-cylinder diesel engine from crankshaft angular position and velocity measurements. The estimator may be useful in the implementation of the control or diagnostic strategies that require cylinder indicated torque. The

approach is to design indicated torque estimators using feedback and an ANN model as feedforward. Such an approach can offer the advantage of being amenable to real time implementation. The estimated results of the engine indicated torque are presented, which compare with experimental data indicate a good agreement.

Zweiri et al. [87] have presented three different dynamic models for a single cylinder diesel engine. The models have been implemented in Matlab/Simulink. The models describe the dynamic relationship between indicated pressure and engine speed. The first model is a detailed analytical nonlinear dynamic model, including dynamometer dynamics, instantaneous friction components, viscosity variations with temperature and inertia variations with piston pin offset. In cycle calculations are performed at each crank angle. The second model is a nonlinear dynamic model which includes a mean friction model for the engine components and dynamometer dynamics, but does not include the piston pin offset as well as the inertia variations. The third model is obtained by an identification procedure to find a low order linear transfer function between the engine input and output. The three models are used to predict the behavior of a diesel engine. The models are compared using experimentally measured engine speed, under steady state and transient operating conditions. The paper discusses the suitability of the models for various control applications such as engine simulation, fueling control system design and fault diagnostics.

Chamaillard et al. [88] have presented a simple method for designing a robust controller which can be used on uncertain and nonlinear systems. The method has been illustrated on an SI engine torque control. In terms of control, the engine torque has a single input system: the throttle angle. A very precise model is used to simulate the engine. A PRBS was designed for throttle angle position to obtain a representative set of input-output data. Two controllers have been defined: a PI controller and an LQ controller. The best results have been obtained for a PI controller. In all cases, robust stability is guaranteed in the whole range of engine torque control.

Ayoubi [89] has described and compared two approaches to the experimental identification of dynamic nonlinear processes: the dynamic multi layered perceptron and the generalized Hammerstein model. The performance comparison was based on

the identification of the charging process in diesel engines. The charging process is mainly determined by the resulting loading pressure. The experimental identification based on the neural network needed no a priori assumptions about the process structures, which highlights flexibility and universality of the model. The application of the Hammerstein model, in contrast, was based on the assumption that the process nonlinearity has to be static in nature, and involved in the process inputs as well. Such a priori assumptions require a physical insight into the process and are restrictive, since good results can only be obtained if the model structure matches the process structure.

Yazdanpanah and Kalhor [90] have presented an efficient method in AFR for SI engines using a controller based on a neural network and an estimator. This study shown that by combining two separate methods, a useful control strategy may be generated. Simulation results revealed the superiority of this method. Also the robustness of this method because of using neural network is high against the error estimation of parameters.

Hou et al. [91] have provided a method of identifying AFR of a HL495Q gasoline engine based on elman neural network. AFR is a key index affecting power performance and fuel economy and exhaust emissions of the gasoline engine whose accurate model is the foundation of accuracy AFR control. They choose sigmoid function as the activation function of elman neural network structure. This study shown that the AFR model based on elman neural network has simple structure and can accurately approximate AFR transient process and average relative error is less than 1%. And also shown that AFR based on elman neural network is better than AFR model based on back propagation NN.

Ouladsine et al. [92] have described a neural approach for modeling and control of a turbocharged diesel engine. A neural model was built for the engine speed, intake manifold pressure and exhaust gas opacity. The objective of the study was to build a model to be used to control the diesel engine. Multilayer perceptron (MLP) neural network architectures with one hidden layer of sigmoid function and linear activation function for the output unit was used in this study. Training was performed by minimizing the mean squared error (MSE) function, with a Levenberg-Marquardt

algorithm. Neural networks, which are flexible and parsimonious nonlinear black-box models, with universal approximation capabilities, can accurately describe or control complex nonlinear systems, with little a priori theoretical knowledge. The results highlight the interest of using neural networks both for engine modeling and control, despite strong dynamics and nonlinearities. Preliminary results show that neural networks can be used as embedded models for engine control, to satisfy the more and more restricting pollutant emission legislation. Particularly, they are able to model nonlinear dynamics and outperform during transients the control schemes based on static mappings.

Colin et al. [93] have performed the airpath control of SI engines using neural network. An efficient control of the air actuators: intake throttle, turbine wastegate and variable camshaft timing presented. Artificial neural networks have been the focus of a great deal of attention due to their capabilities to solve nonlinear problems by learning from data. As physical models are too complex, black-box solutions as NNs become attractive techniques for engine modeling and control. The control scheme proposed here a nonlinear model based control scheme which combines separate, but coordinated, control modules for the different actuators. These modules are based on different model based control strategies: internal model control, model predictive control and optimal control. It was shown how neural models can be used at different levels and included in the control modules.

Sangha et al. [94] have investigated fault detection and isolation in dynamic data from an automotive engine air path using ANN. A generic SI mean value engine model is used for experimentation. RBF neural networks are trained to detect and diagnose the faults. Three dynamic cases of fault occurrence were considered with increasing generality of engine operation. The approach shown the results are successful in each case.

Cui [95] has presented a neural network approach to control exhaust gas recirculation (EGR) in a liquefied petroleum gas (LPG) engine. RBF neural network and on-line adaptation strategy are applied in this paper. EGR system is introduced to achieve a significant reduction of NO_x emissions. Neural networks are suitable for the identification and control of nonlinear dynamic systems. Neural networks for the

EGR control have been developed on a 1.46 liter 4 cylinder SI LGG engine. The experimental result shown that the EGR system can achieve satisfied control effect.

Li and Yu [96] have proposed continuous time recurrent multilayer perceptrons to identify nonlinear systems. The system outputs are manifold pressure and engine speed, whereas control inputs are throttle angle and spark advance. Using the function approximation theorem for multilayer perceptrons, they concluded that recurrent multilayer perceptron can approximate any dynamic system in any degree of accuracy.

Ayeb et al. [97] have proposed a procedure to derive global dynamic models based on dynamic neural networks. The abilities of neural networks as universal approximation tools of nonlinear functional relationships as well as identification tools for nonlinear dynamic systems have been recognized and used successfully in many application areas like modeling, control and diagnosis of systems. In this paper RNN model with Levenberg-Marquardt training algorithm was used. The procedure can be used to derive robust models ensuring a minimized parameters variance. The application described shows the ability of dynamic neural networks to present complex behavior such as the dependencies between engine torque and engine states and control parameters.

Isermann and Muller [98] have introduced the identification of nonlinear process with grid based look-up tables and a special local linear radial basis function network, a comparison is made with regard to computation effort, storage requirements and convergence speed. A PRBS signals were used because it is often very suitable as process inputs because they excite the process at a wide range of amplitudes and frequencies. Application examples and experimental results are shown for multidimensional nonlinear model of NO_x emissions of a diesel engine, and for the adaptive feedforward control of the ignition angle of a SI engine.

Hafner et al. [99] have presented a new approach towards a model based optimization of ICE control on dynamometers. The proposed methodology comprises advanced measurement strategies for a fast dynamic measurement of engine characteristics on dynamometers, a model based offline optimization of

feedforward control maps, and the optimization of dynamic transitions of turbocharged engines with exhaust gas recirculation. This study shortly reviews the design of measurement, the identification of the engine and the optimization of the static and dynamic engine behavior.

Czarnigowski [100] has presented an algorithm of idle speed stabilization in the SI engine by means of spark advance control. The used algorithm is based on a well known approach of a model based adaptive control and uses ANN. The control algorithm is based on a NN model observer of the additional effective torque. The algorithm was experimentally compared with PID and adaptive algorithms. The experiments were conducted in a steady state. The effective torque model was constructed on the basis of a MLP BP neural network.

Biao et al. [101] have built the dynamic model of the 16 cylinders locomotive diesel engine with neural network. The diesel engine system identification with neural network belongs to the experiments modeling, which has strong information integrate capability and can deal with large numbers of different inputs at the same time. The neural network also can solve the redundancy and the inconsistency of the input information, so it is suitable to the diesel engine modeling. In this study used NARMAX as the main structure and used Levenberg-Marquardt algorithm to train the network. Comparison between the train results and the measured results show that the dynamic model has the good real-time performances and little output error. So the model can meet the need of the system character analysis and technology application.

Alippi et al. [102] have suggested a neural network based solution to the AFR control in fuel injection systems. An indirect control approach has been considered which requires a preliminary modeling of the engine dynamics. The model for the engine and the final controller are based on RNN with external feedbacks. Requirements for feasible control actions and the static precision of control have been integrated in the controller design to guide learning toward an effective control solution. In this study, they considered a fuel injection system composed of a SI engine with a catalytic converter and a linear oxygen sensor on the exhaust manifold to measure the AFR

after the combustion process. The case study was applied to an Alfa Romeo 1.31 engine.

Alippi et al. [103] have presented an application where neural techniques can be effectively used in the automotive field: the control of AFR to keep minimum value the exhaust car engine emissions. They focused the attention on SI engines characterized by a catalytic converter and a linear oxygen sensor at the output of the exhaust manifold which measures the features of the combustion. The neural controller has been obtained with an indirect control scheme, based on a neural model of the process. It was designed to optimize performance and limit the necessary control actions. Encouraging results were obtained and validated on simulations and transients coming from a real engine.

Frith et al. [104] have investigated the application ANNs for adaptive AFR control in gasoline engines. Multiple ANN architecture has been designed and implemented to accommodate the variable time constant, gain and time delay aspects of the engine process. The paper discussed the rationale behind the multiple network design, the problems encountered in developing an ANN model of a process already under control, and a possible technique for online adaption of that model. They pointed out that ANNs offer the capability to model the process nonlinearities, clearing the way for nonlinear ANN model based predictive engine control.

Saraswati and Chand [105] have used RNN for AFR identification in SI engine. AFR identification is difficult due to nonlinear and dynamic behavior of SI engines. Delays present in the engine dynamics limits the performance of engine controller. Identifying AFR few steps in advance can help engine controller to take care of these. RNN is trained using data from engine simulations in Matlab/Simulink environment. Uncorrelated signals were generated for training and generalization and it has been shown that RNN can predict engine simulations with reasonable good accuracy.

Wu et al. [106] have described an ICE fault diagnosis system using the manifold pressure of the intake system. The manifold pressure of the engine intake system always demonstrates the engine condition and affects the volumetric efficiency, fuel

consumption and performance of ICE. In this study, a system consisted of manifold pressure signal feature extraction using discrete wavelet transform and fault recognition using the neural network technique is proposed. To verify the effect of the proposed system for identification, both the RBF and generalized regression neural network are used and compared in this study. The experimental results indicated that the proposed system using manifold pressure signal as data input is effective for engine fault diagnosis in the experimental engine platform.

Thompson et al. [107] have shown the application of a neural network to model the output torque and exhaust emissions from a modern heavy duty diesel engine [Navistar T444E). They predicted the continuous torque and exhaust emissions from a heavy duty diesel engine for the Federal heavy duty engine transient test procedure cycle and two random cycles to within 5 percent of their measured values after only 100 minute of transient dynamometer training. Neural network based engine modeling offers the potential for a multidimensional, adaptive, learning control system that does not require knowledge of the governing equations for engine performance or the combustion kinetics of emission formation that a conventional map based engine model requires. Applications of such a neural network model include emissions virtual sensing, on-board diagnostics and engine control optimization.

García-Nieto et al. [108] have proposed a new approach to control the air management process of a diesel engine. This study can be concluded as follows: 1) predictive control and model identification schemes for local model network models shown. Proposed algorithms are easily implemented in a real engine, 2) a test platform is developed, including complex nonlinear behavior and real hardware data acquisition, 3) practical application based on local model networks modeling and explicit model predictive control, 4) results from applying the proposed control schemes, offering an improvement in the system behavior, are shown.

Worden et al. [109] have provided an overview of a number of nonlinear system identification methods as applied to the analysis of nonlinear automotive dampers. Three different approaches are presented as follows: 1) the restoring force surface method, which is capable of forming a nonparametric visualization of the nonlinear

characteristics of the absorber, 2) the versatile nonlinear identification by feedback of outputs approach, which is capable of fitting parametric models where the parameters actually encode frequency dependence, 3) the discussion returns to the time domain for a method motivated by a neural network analogy that fits a parametric model assuming a hyperbolic tangent form for the damping force of the absorber. The approaches are demonstrated on both synthetic data and data obtained from testing of real dampers.

Turin and Geering [110] have deduced convenient models of the significant dynamic processes, i.e., intake manifold, wall-wetting and oxygen sensor dynamics. They separated the analysis in terms of an air and a fuel path. In the case of linear dynamics they aim to achieve a linear regression form whereas in the case of nonlinear dynamics, they will augment the system state and apply extended Kalman filter theory. They showed that the proposed Kalman filtering methods provide highly effective means to solve the present classes of identification problems.

Franchek et al. [111] have presented a feedforward fueling controller identification methodology for the transient fueling control of a SI engines. The feedforward fueling control of SI engines can be separated into steady state and transient phenomena and that the majority of the nonlinear behavior associated with engine fueling can be captured with nonlinear steady state models. The proposed transient controller identification process is built from standard nonparametric identification techniques followed by parametric model recovery. Crank angle serves as the independent variable for these models. Two separate system identification problems are solved to identify the air path dynamics and fueling path dynamics. The transient feedforward controller is then calculated as the ratio of the air path over the fueling path dynamics thereby coordinating the engine fueling with the air path dynamics. It is shown that a linear transient feedforward fueling controller operating in tandem with a nonlinear steady state fueling controller can achieve AFR regulation comparable to the production fueling controller without the extensive controller calibration process. The engine used in this investigation is a 1999 Ford 4.6 L V8 fuel injected engine.

Stroh et al. [112] have presented an adaptive, model based, transient and steady-state fueling control system for SI engines. Since the fueling control system is model based, the engine maps currently used in engine fueling control are eliminated. Models are developed using an input-output approach with only measurable parameters which concisely represent the static and dynamic behavior of the AFR loop. The steady state fueling compensation utilizes a feedforward controller which determines the necessary fuel pulsewidth after a throttle transient to achieve stoichiometric. This feedforward controller is comprised of two nonlinear models capturing the steady state characteristics of the fueling process. These models are identified from an input-output testing procedure where the inputs are fuel pulsewidth and mass air flow signal and the output is AFR. The transient fueling compensation also utilizes a feedforward controller that captures the essential dynamic characteristics of the transient fueling operation. This controller is measured using a frequency domain system identification approach. This proposed fueling control system is demonstrated on a Ford 4.6 L V-8 fuel injected engine.

Ye [113] has presented a thorough review of various dynamic control technologies which have been successfully applied to idle speed control systems. Automotive idle speed control is one of the most challenging aspects in engine control fields. Essentially it is a highly nonlinear, time-varying, complicated and uncertain dynamic control problem. In particular, practical implementations on a variety of different engine types are provided, which cover broad areas of control, including classical control, modern control and intelligent control. Over 90 selected papers are reviewed and then summarized from a control point of view.

Ortner and del Re [114] have presented the model based control of the air path of diesel engines in terms of an optimal control problem. A multilinear model identified from data and a switched controller design is used to cope with the nonlinearity of the engine. Experimental results on a production engine confirm that the proposed control method strongly improves the dynamics of the air path and enormously reduces the parameterization work if compared with the conventional approach.

2.4 Genetic Programming Approach for Nonlinear Identification of Engine

A variety of system identification techniques are applied to the modeling of process dynamics. Identification of nonlinear system suffers many problems including determination of the structure and parameters of the system. Many methods of system identification are based on parameter estimation, and mainly rely on least squares method. Recently, soft computing based system identification approaches have been proposed, mainly fuzzy systems, artificial neural network, and evolutionary computation methods [115].

GP is an evolutionary method which may be applied to the identification of the nonlinear structure of a dynamic model from experimental data [116, 117]. Several publications describe the usage of GP for nonlinear process modeling [118-120]. The nonlinear system identification method based on genetic expression programming (GEP) can find the accurate mode on the condition that there is less or none information about the system [121, 122].

Recently, the identification of nonlinear systems by genetic programming (GP) approaches has been successfully applied in many applications. However a GP based identification and modeling of ICE, to the best knowledge of the authors, has not yet existed in the literature. In this section major studies of the genetic programming identification in the literature are given with important applications of system identification.

Coelho and Pessôa [115] have applied the nonlinear system identification procedure, based on NARX representation and GP to empirical case study of an experimental ball-and-tube system. The result demonstrated that the GP with orthogonal least squares is a promising technique for NARX modeling.

Rodríguez-Vázquez and Fleming [123] have applied successfully multiobjective GP-NARMAX approach to the identification of gas turbine engine. In order to identify a model capable of representing the engine at all operating points, they used multiobjective GP approach on the same data and allocated weights to various objectives, to assess their significance in the structure selection of NARMAX models

of the engine. A simple NARX model was identified which was able to represent both the small and large signal dynamics of the engine. They demonstrated that a practical application of this technique to obtain a model of the relationship between the fuel feed and the shaft speed dynamics of a gas turbine engine. Rodríguez-Vázquez and Fleming [124] have shown that a multiobjective evolutionary identification method produce a similar and even better performance in nonlinear system identification than conventional techniques.

Evans et al. [125] have improved the efficiency and cost-effectiveness of system identification techniques. Three system identification approaches were outlined in their study. They are based upon: multisine testing and frequency domain identification, time varying models estimated using extended least squares with optimal smoothing, and multiobjective genetic programming to select model structure. They provide significant insights into alternative identification strategies. They concentrated on the dynamic relationship between the measured input fuel flow and the high pressure and low pressure shaft speeds. Arkov et al. [126] outlined four system identification techniques. Only one method added to the study of [126] namely identification using ambient noise only data.

Ruano et al. [127] have presented identification results for the shaft speed dynamics of an aircraft gas turbine under normal operation. They considered two different approaches: NARX models, and NN models, namely multilayer perceptrons, RBF networks and B-spline networks. They gave a special attention to GP, in a multiobjective fashion, to determine the structure of NARMAX and B-spline models.

Rodríguez-Vázquez et al. [128] has presented a method for identifying the structure of nonlinear polynomial dynamic models. This approach uses a GP in a multiobjective fashion to generate global models which describe the dynamic behavior of the nonlinear system under investigation. The validation stage of system identification is simultaneously evaluated using the multiobjective tool, in order to direct the identification process to a set of global models of the system.

Kiguchi et al. [129] have proposed an effective identification method using soft computing techniques (combination of GP and NN) in order to identify robot

manipulators. The back-propagated error is used for finding the important subtrees in each NN. The experimental results with two degree of freedom robot manipulator showed that the effectiveness of the proposed identification method.

Kronberger et al. [130] have used linear regression, support vector regression, and GP to create linear and nonlinear models describing different aspects of the blast furnace process: the melting rate, the required specific amount of oxygen and the carbon content in the hot metal.

Han et al. [131] have proposed a new method for chaotic system identification based on polynomial NARMAX representation and multiobjective GP. NARMAX model representation is used for the basis of the hierarchical tree encoding in GP. The simulation results show that the proposed technique provides an efficient method to get the optimum NARMAX difference equation model of chaotic systems.

Beligiannis et al. [132] have proposed an effective GP based technique for system identification of complex biomedical data. The method combines the ability of GP to explore automatically and effectively the whole set of candidate model structures and the robustness of evolutionally multimodel partitioning filters. Simulation results show that the algorithm identifies the true model and the true values of the unknown parameters for each different model structure, thus assisting the GP technique to converge more quickly to the near optimal structure.

Yang et al. [133] have presented a GP based method for the identification of unknown excitation force of dynamic systems. The numerical examples show that the GP system is able to identify the excitation force of a single-degree, a three-degree and more complex frame dynamic systems. Comparison between the measured and the estimated force have validated the proposed GP based method.

Hussian et al. [134] have presented a new method for modeling the dynamics of a winding process using GP and compare it with traditional modeling approaches. They used three methods for modeling a wire winding machine. These models include moving average, ARMA models and GP models. They used data sets collected from an actual industrial process throughout the experiments. It is

concluded that GP for modeling nonlinear systems are promising, and with the proper evaluation function and tuning of the GP system, they can get better results.

Winkler et al. [135] have described research that was done for the project ‘specification, design and implementation of a GP approach for identifying nonlinear models of mechatronic systems’. The goal of the project is to find model for mechatronic system. Their task was to examine whether the methods of GP are suitable for determining the structures of physical systems by analyzing a system’s measured behavior or not.

Willis et al. [136] have used a GP algorithm to developed empirical models chemical process systems. Initially, steady-state model development using GP algorithm considered, next the methodology is extended to the development of dynamic input-output models. Two examples were used to highlight the utility of this approach: a vacuum distillation column and a twin screw cooking extruder. The results revealed that in each case the GP algorithm can generate an accurate model based solely on observed data. McKay et al. [137] have demonstrated the usefulness of the GP technique by the development of steady-state models for two typical processes, a vacuum distillation column and a chemical reactor system.

Grosman and Lewin [138] have described an improved GP to facilitate the generation of steady-state nonlinear empirical models for process system engineering applications. The key feature of the method is its ability to adjust the complexity of the required model to accurately predict the true process behavior. The improved GP code incorporates a novel fitness calculation, the optimal creation of new generations, and parameter allocation. The advantages of these modifications are tested against the more commonly used approaches.

Hinchliffe and Willis [139] have used GP to evolve discrete time models of dynamic systems. GP algorithm is its ability to automatically discover the appropriate time history of model terms required to build an accurate model. Two case studies were used to compare the performance of the GP algorithm with that of filter based neural networks. A test system is with a time delay and an industrial cooking extruder. They

show that a major benefit of the GP approach is that additional model performance criteria can be included during the model development process.

Witczak et al. [140] have provided a new system identification framework based on a GP technique. System identification is one of the most important research directions. It is a diverse field which can be employed in many different areas. One of them is the model based fault diagnosis. Thus, the problems of system identification and fault diagnosis are closely related. Unfortunately, in both cases, the research is strongly oriented towards linear systems, while the problem of identification and fault diagnosis of nonlinear dynamic systems still remains open. A fault diagnosis scheme for nonlinear systems was proposed. In particular, a new fault detection observer was presented, and the Lyapunov approach was used to show that the proposed observer is convergent under certain conditions. It is also shown how to use the GP technique to increase the convergence rate of the observer. The final part of this study contains numerical examples concerning identification of chosen parts of the evaporation station at the Lublin Sugar Factory, as well as state estimation and fault diagnosis of an induction motor.

Lew et al. [141] have extended the class of possible models considerably by carrying out a general symbolic regression using a GP approach. The approach is demonstrated on both univariate and multivariate problems with both computational and experimental data. The results also showed that GP could identify the most influential design variables with respect to output.

Yuan et al. [142] have defined two levels of crossover operation. A linear time-invariant system, a nonlinear time invariant and a time varying system were identified by the improved GP algorithm, good models of object systems were achieved with accurate and simultaneous identification of both structures and parameters. This study shows that GP is good at handling different kinds of dynamic system identification problems and is better than other artificial intelligence algorithms like neural network or fuzzy logic which only model systems as complete black boxes.

Grosman and Lewin [143] have described the use of GP to generate empirical dynamic model of a process, and its use in a nonlinear, model predictive control strategy. GP derives both a model structure and its parameter values in such a way that the process trajectory is predicted accurately. Consequently, the performance of the nonlinear model predictive control strategy are described, and demonstrated by simulation on two simulated processes: (a) a mixing vessel fed by streams of salt and fresh water, in which the control objectives are to be maintain a desired fluid level and a salt concentration in the tank, and (b) a Karr liquid-liquid extraction column, which has been verified against experimental data. They demonstrated that the GP based nonlinear model predictive control strategy leads to good closed-loop performance in both cases.

2.5 Conclusions

The extended overview has provided in this chapter indicates that there are a large number studies on nonlinear identification and modeling of ICE in literature. A good fraction of these studies have considered NARX and NARMAX models when identifying and modeling the nonlinear systems. This thesis differs from the previously conducted studies as follows:

a) The presented study is on the nonlinear identification and modeling of gasoline engine. The thesis is original in this scope and content and there is no such study in the open literature, to the best of the author's knowledge and it is the main motivation behind this study.

b) In literature, a small number of studies consider gasoline engine torque modeling and identification. The analysis in the literature studies are mostly related to nonlinear identification and modeling of AFR of ICE.

c) Identification of linear systems is a rather old field of study, and many methods are available in literature. However, identification of nonlinear systems is a respectively new topic of interest. The nonlinear identification of internal combustion engines have also been of interest in recent years.

d) However, ICE modeling is still an open field of research due to the antithetical needs of describing a very complex, nonlinear system and driving simple model structures suitable for the control synthesis or diagnosis phase.

CHAPTER 3

3. DYNAMIC MODELING OF RECIPROCATING ENGINE

3.1 Introduction

Exact mathematical models of mechanical systems are derivable by Lagrange, Hamilton and Newton-Euler formulations or by energy methods. This requires all the system parameters such as masses, mass moments of inertia, stiffnesses, damping coefficients and physical dimensions explicitly. The system generally needs to be dismantled into its main components where each parameter of the system is lumped for measurement. In applications where this is not possible, system identification becomes very useful, generating empirical mathematical model for the response of the system [11].

3.2 Equation of Motion for a Slider-Crank Mechanism

A slider-crank mechanism is widely used in gasoline and diesel engines, and has been studied extensively in the past three decades [144]. Slider-crank mechanism converts the translational motion of piston to rotary motion of crank. Driving effect of slider-crank mechanism is obtained by a gas pressure arising from combustion of mixture consisting of fuel and air. The force corresponds to this pressure causes the piston to translate along the vertical axis and this action is transmitted to crank through connecting rod [145].

The dynamic formulation is expressed by only one independent variable of rotation angle. A slider-crank mechanism is a single-looped mechanism with a very simple construction shown in Figure 3.1. Lagrange equation and geometric constraints are employed to formulate the differential equation of motion for a slider-crank mechanism. Euler-Lagrange equation is used to derive the dynamic modeling

of mechanism and the dynamic equation obtained in terms of only one independent variable θ . The main parameters of a slider-crank mechanism of a four cylinder 1.6 injection Ford Escort motor are given in Table 3.1.

Table 3.1 Fiat Tofaş 131 motor parameters

Crankshaft weight (m_c)	2.61 kg	(for a single slider-crank mechanisms only)
Connecting rod weight (m_{cr})	0.560 kg	(including bearings at both ends and assembly bolts and washers)
Piston weight (m_p)	0.278 kg	(standard 76 mm diameter piston, including piston pin and 3 piston rings)
Crankshaft radius (r_1)	35.75 mm	(location of the mass center of the crank is 1.917 mm offset from the crankshaft axis, on the symmetry line, towards the counterbalance weights)
Connecting rod length (l_2)	107.25 mm	(location of the mass center of the connecting rod from crank bearing center, on the symmetry axis is 35.75 mm towards the piston end)
Crankshaft inertia (I_c)	0.00781 kgm ²	(for a single slider-crank mechanisms only)
Connecting rod inertia (I_{cr})	0.00236 kgm ²	(including bearings at both ends and assembly bolts and washers)

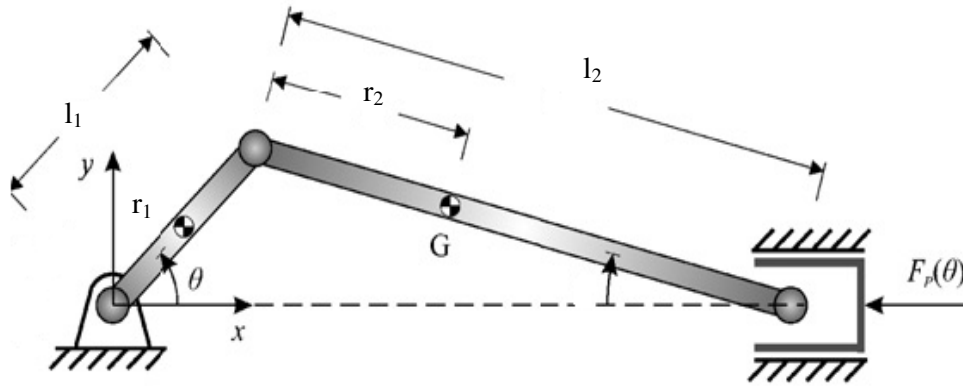


Figure 3.1 Slider-crank mechanism

Due to the complexity of the system examined, its equations of motion will be derived by applying Lagrange's equations. For this reason, the kinetic energy of the engine model is considered first. In particular, this quantity is split in the form

$$T = T_c + T_{cr} + T_p \quad (3.1)$$

where the three terms on the right-hand side represent the kinetic energy of the crank, the connecting rod and piston, respectively. Since the crankshaft performs plane motion, its kinetic energy is expressed in the form

$$T_c = \frac{1}{2}I_c \dot{\theta}^2 + \frac{1}{2}m_c (\dot{x}_c^2 + \dot{y}_c^2) \quad (3.2)$$

where I_c is the centroidal mass moment of inertia and m_c is the mass of the crankshaft. Moreover, the couple (x_c, y_c) identifies the position of the crank center of mass. From elementary kinematics it can be immediately be seen from Figure 3.1 that

$$x_c = r_1 \cos \theta \quad \text{and} \quad y_c = r_1 \sin \theta \quad (3.3)$$

which after differentiation yield the velocity components of the crank center of mass in the form

$$\dot{x}_c = -r_1 \dot{\theta} \sin \theta \quad \text{and} \quad \dot{y}_c = r_1 \dot{\theta} \cos \theta \quad (3.4)$$

then, substitution in Equation 3.2 and performance of some algebraic manipulations yields eventually the kinetic energy of the crank in the form

$$T_c = \frac{1}{2}I_c \dot{\theta}^2 + \frac{1}{2}m_c (r_1^2 \dot{\theta}^2 \sin^2 \theta + r_1^2 \dot{\theta}^2 \cos^2 \theta) \quad (3.5)$$

$$T_c = \frac{1}{2}I_c \dot{\theta}^2 + \frac{1}{2}m_c r_1^2 \dot{\theta}^2$$

Likewise, taking into account that the connecting rod undergoes a plane motion also, its kinetic energy is expressed in the form

$$T_{cr} = \frac{1}{2}I_{cr} \dot{\beta}^2 + \frac{1}{2}m_{cr} (\dot{x}_{cr}^2 + \dot{y}_{cr}^2) \quad (3.6)$$

the geometric positions of gravity centers of the connecting rod are as follows:

$$x_{cr} = l_1 \cos \theta + r_2 \cos \beta \quad \text{and} \quad y_{cr} = (l_2 - r_2) \sin \beta \quad (3.7)$$

The mechanism has a constrained condition as follows:

$$l_1 \sin \theta = l_2 \sin \beta \quad (3.8)$$

$$\sin \beta = \frac{l_1}{l_2} \sin \theta \quad \text{and} \quad \cos \beta = \sqrt{1 - \frac{l_1^2}{l_2^2} \sin^2 \theta} \quad (3.9)$$

After differentiation a constrained equation with respect to time yield the angular velocity of connecting rod in the form

$$l_1 \dot{\theta} \cos \theta = l_2 \dot{\beta} \cos \beta \quad (3.10)$$

$$\dot{\beta} = \frac{l_1 \dot{\theta} \cos \theta}{\sqrt{l_2^2 - l_1^2 \sin^2 \theta}}$$

which after differentiation yield the velocity components of the connecting rod center of mass in the form

$$\dot{x}_{cr} = -l_1 \dot{\theta} \sin \theta - r_2 \dot{\beta} \sin \beta \quad \text{and} \quad \dot{y}_{cr} = (l_2 - r_2) \dot{\beta} \cos \beta \quad (3.11)$$

Then, substitution in Equations 3.9 and 3.10 into Equation 3.11

$$\dot{x}_{cr} = -l_1 \dot{\theta} \sin \theta - r_2 \frac{l_1 \dot{\theta} \cos \theta}{\sqrt{l_2^2 - l_1^2 \sin^2 \theta}} \frac{l_1}{l_2} \sin \theta \quad (3.12)$$

$$c = \sqrt{l_2^2 - l_1^2 \sin^2 \theta} \quad (3.13)$$

So, rearranging Equation 3.12

$$\dot{x}_{cr} = -l_1 \dot{\theta} \sin \theta - \frac{l_1^2 r_2 \dot{\theta} \cos \theta \sin \theta}{l_2 c} \quad (3.14)$$

$$\dot{y}_{cr} = (l_2 - r_2) \frac{l_1 \dot{\theta} \cos \theta}{\sqrt{l_2^2 - l_1^2 \sin^2 \theta}} \sqrt{l_2^2 - l_1^2 \sin^2 \theta} \frac{1}{l_2} \quad (3.15)$$

$$\dot{y}_{cr} = \frac{(l_2 - r_2) l_1 \dot{\theta} \cos \theta}{l_2}$$

Then, substitution in Equation 3.6 and performance of some algebraic manipulations yields eventually the kinetic energy of the connecting rod in the form of

$$T_{cr} = \frac{1}{2} I_{cr} \frac{l_1^2 \dot{\theta}^2 \cos^2 \theta}{c^2} + \frac{1}{2} m_{cr} \left\{ l_1^2 \dot{\theta}^2 \sin^2 \theta + \frac{l_1^4 \dot{\theta}^2 r_2^2 \cos^2 \theta \sin^2 \theta}{l_2^2 c^2} + \frac{2l_1^3 r_2 \dot{\theta}^2 \sin^2 \theta \cos \theta}{l_2 c} + \frac{(l_2 - r_2)^2 l_1^2 \dot{\theta}^2 \cos^2 \theta}{l_2^2} \right\} \quad (3.16)$$

Finally, kinetic energy of the piston can be written as,

$$T_p = \frac{1}{2} m_p (\dot{x}_p^2 + \dot{y}_p^2) \quad (3.17)$$

while the piston is translating along the axis x only, with displacement

$$x_p = l_1 \cos \theta + l_2 \cos \beta \quad \text{and} \quad y_p = 0 \quad (3.18)$$

After differentiation of Equation 3.18 with respect to time yield the velocity components of the piston in the form of,

$$\dot{x}_p = -l_1 \dot{\theta} \sin \theta - l_2 \dot{\beta} \sin \beta$$

$$\dot{x}_p = -l_1 \dot{\theta} \sin \theta - l_2 \frac{l_1 \dot{\theta} \cos \theta}{c} \frac{l_1}{l_2} \sin \theta \quad (3.19)$$

$$\dot{x}_p = -l_1 \dot{\theta} \sin \theta - \frac{l_1^2 \dot{\theta} \cos \theta \sin \theta}{c}$$

Then, substitution into Equation 3.17 and performance of some algebraic manipulations yields eventually the kinetic energy of the piston in the form of,

$$T_p = \frac{1}{2} m_p \left\{ l_1^2 \dot{\theta}^2 \sin^2 \theta + \frac{l_1^4 \dot{\theta}^2 \cos^2 \theta \sin^2 \theta}{c^2} + \frac{2l_1^3 \dot{\theta}^2 \sin^2 \theta \cos \theta}{c} \right\} \quad (3.20)$$

Finally total kinetic energy of the slider-crank mechanism is

$$\begin{aligned} T_{\text{total}} = & \frac{1}{2} I_c \dot{\theta}^2 + \frac{1}{2} m_c r_1^2 \dot{\theta}^2 + \frac{1}{2} I_{cr} \frac{l_1^2 \dot{\theta}^2 \cos^2 \theta}{c^2} + \frac{1}{2} m_{cr} \{ l_1^2 \dot{\theta}^2 \sin^2 \theta \\ & + \frac{l_1^4 \dot{\theta}^2 r_2^2 \cos^2 \theta \sin^2 \theta}{l_2^2 c^2} + \frac{2l_1^3 r_2 \dot{\theta}^2 \sin^2 \theta \cos \theta}{l_2 c} + \frac{(l_2 - r_2)^2 l_1^2 \dot{\theta}^2 \cos^2 \theta}{l_2^2} \} \\ & + \frac{1}{2} m_p \left\{ l_1^2 \dot{\theta}^2 \sin^2 \theta + \frac{l_1^4 \dot{\theta}^2 \cos^2 \theta \sin^2 \theta}{c^2} + \frac{2l_1^3 \dot{\theta}^2 \sin^2 \theta \cos \theta}{c} \right\} \end{aligned} \quad (3.21)$$

The gravitational potential energy of the crank, connected rod and piston is written respectively

$$\begin{aligned} V &= V_c + V_{cr} + V_p \\ V_c &= m_c g r_1 \sin \theta \\ V_{cr} &= m_{cr} g (l_2 - r_2) \frac{l_1}{l_2} \sin \theta \\ V_p &= 0 \end{aligned} \quad (3.22)$$

$$V_{\text{total}} = m_c g r_1 \sin \theta + m_{cr} g (l_2 - r_2) \frac{l_1}{l_2} \sin \theta \quad (3.23)$$

The Lagrange function L is obtained as follows:

$$L = T - V$$

$$\begin{aligned}
L = & \frac{1}{2} I_c \dot{\theta}^2 + \frac{1}{2} m_c r_1^2 \dot{\theta}^2 + \frac{1}{2} I_{cr} \frac{l_1^2 \dot{\theta}^2 \cos^2 \theta}{c^2} + \frac{1}{2} m_{cr} \{l_1^2 \dot{\theta}^2 \sin^2 \theta \\
& + \frac{l_1^4 \dot{\theta}^2 r_2^2 \cos^2 \theta \sin^2 \theta}{l_2^2 c^2} + \frac{2l_1^3 r_2 \dot{\theta}^2 \sin^2 \theta \cos \theta}{l_2 c} + \frac{(l_2 - r_2)^2 l_1^2 \dot{\theta}^2 \cos^2 \theta}{l_2^2} \} \\
& + \frac{1}{2} m_p \{l_1^2 \dot{\theta}^2 \sin^2 \theta + \frac{l_1^4 \dot{\theta}^2 \cos^2 \theta \sin^2 \theta}{c^2} + \frac{2l_1^3 \dot{\theta}^2 \sin^2 \theta \cos \theta}{c} \} \\
& - m_c g r_1 \sin \theta - m_{cr} g (l_2 - r_2) \frac{l_1}{l_2} \sin \theta
\end{aligned} \tag{3.24}$$

The virtual works ∂W^A done by the external disturbance force F_E and friction force F_B with the virtual displacement ∂x of the slider, and the applied torque τ with the virtual angle $\partial \theta$ are summed as

$$\begin{aligned}
\partial W^A &= \varpi \partial \theta + (F_E + F_B) \partial x \\
&= \varpi \partial \theta + (F_E + F_B) (-l_1 \sin \theta \partial \theta - l_2 \sin \beta \partial \beta) \\
&= \varpi \partial \theta + (F_E + F_B) (-l_1 \sin \theta \partial \theta - l_2 \frac{l_1}{l_2} \sin \theta \frac{l_1}{c} \cos \theta \partial \theta) \\
\partial W^A &= [\tau - (F_E + F_B) (1 + \frac{1}{c} l_1 \cos \theta) l_1 \sin \theta] \partial \theta
\end{aligned} \tag{3.25}$$

The Euler-Lagrange equation will be applied in the following form;

$$\frac{d}{dt} \left(\frac{\partial L}{\partial \dot{\theta}} \right) - \left(\frac{\partial L}{\partial \theta} \right) = Q^A \tag{3.26}$$

$$\begin{aligned}
\frac{\partial L}{\partial \dot{\theta}} = & I_c \dot{\theta} + m_c r_1^2 \dot{\theta} + \frac{I_{cr} l_1^2 \cos^2 \theta}{c^2} \dot{\theta} + m_{cr} l_1^2 \sin^2 \theta \dot{\theta} + \frac{m_{cr} l_1^4 r_2^2 \cos^2 \theta \sin^2 \theta}{l_2^2 c^2} \dot{\theta} \\
& + \frac{2m_{cr} l_1^3 r_2 \sin^2 \theta \cos \theta}{l_2 c} \dot{\theta} + \frac{m_{cr} (l_2 - r_2)^2 l_1^2 \cos^2 \theta}{l_2^2} \dot{\theta} + m_p l_1^2 \sin^2 \theta \dot{\theta} \\
& + \frac{m_p l_1^4 \cos^2 \theta \sin^2 \theta}{c^2} \dot{\theta} + \frac{2m_p l_1^3 \sin^2 \theta \cos \theta}{c} \dot{\theta}
\end{aligned}$$

$$\begin{aligned}
\frac{d}{dt} \left(\frac{\partial L}{\partial \dot{\theta}} \right) &= I_c \ddot{\theta} + m_c r_1^2 \ddot{\theta} + \frac{I_{cr} l_1^2 \cos^2 \theta}{c^2} \ddot{\theta} - \frac{2I_{cr} l_1^2 \cos \theta \sin \theta}{c^2} \dot{\theta}^2 + m_{cr} l_1^2 \sin^2 \theta \ddot{\theta} \\
&+ 2m_{cr} l_1^2 \sin \theta \cos \theta \dot{\theta}^2 + \frac{m_{cr} l_1^4 r_2^2 \cos^2 \theta \sin^2 \theta}{l_2^2 c^2} \ddot{\theta} - \frac{2m_{cr} l_1^4 r_2^2 \cos \theta \sin^3 \theta}{l_2^2 c^2} \dot{\theta}^2 \\
&+ \frac{2m_{cr} l_1^4 r_2^2 \cos^3 \theta \sin \theta}{l_2^2 c^2} \dot{\theta}^2 + \frac{2m_{cr} l_1^3 r_2 \sin^2 \theta \cos \theta}{l_2 c} \ddot{\theta} + \frac{4m_{cr} l_1^3 r_2 \sin \theta \cos^2 \theta}{l_2 c} \dot{\theta}^2 \\
&- \frac{2m_{cr} l_1^3 r_2 \sin^3 \theta}{l_2 c} \dot{\theta}^2 + \frac{m_{cr} (l_2 - r_2)^2 l_1^2 \cos^2 \theta}{l_2^2} \ddot{\theta} - \frac{2m_{cr} (l_2 - r_2)^2 l_1^2 \cos \theta \sin \theta}{l_2^2} \dot{\theta}^2 \\
&+ m_p l_1^2 \sin^2 \theta \ddot{\theta} + 2m_p l_1^2 \sin \theta \cos \theta \dot{\theta}^2 + \frac{m_p l_1^4 \cos^2 \theta \sin^2 \theta}{c^2} \ddot{\theta} - \frac{2m_p l_1^4 \cos \theta \sin^3 \theta}{c^2} \dot{\theta}^2 \\
&+ \frac{2m_p l_1^4 \cos^3 \theta \sin \theta}{c^2} \dot{\theta}^2 + \frac{2m_p l_1^3 \sin^2 \theta \cos \theta}{c} \ddot{\theta} + \frac{4m_p l_1^3 \sin \theta \cos^2 \theta}{c} \dot{\theta}^2 - \frac{2m_p l_1^3 \sin^3 \theta}{c} \dot{\theta}^2
\end{aligned}$$

$$\begin{aligned}
\frac{\partial L}{\partial \theta} &= -\frac{I_{cr} l_1^2 \cos \theta \sin \theta}{c^2} \dot{\theta}^2 + m_{cr} l_1^2 \sin \theta \cos \theta \dot{\theta}^2 - \frac{m_{cr} l_1^4 r_2^2 \cos \theta \sin^3 \theta}{l_2^2 c^2} \dot{\theta}^2 \\
&+ \frac{m_{cr} l_1^4 r_2^2 \cos^3 \theta \sin \theta}{l_2^2 c^2} \dot{\theta}^2 + \frac{2m_{cr} l_1^3 r_2 \sin \theta \cos^2 \theta}{l_2 c} \dot{\theta}^2 - \frac{m_{cr} l_1^3 r_2 \sin^3 \theta}{l_2 c} \dot{\theta}^2 \\
&- \frac{m_{cr} (l_2 - r_2)^2 l_1^2 \cos \theta \sin \theta}{l_2^2} \dot{\theta}^2 + m_p l_1^2 \sin \theta \cos \theta \dot{\theta}^2 - \frac{m_p l_1^4 \cos \theta \sin^3 \theta}{c^2} \dot{\theta}^2 \\
&+ \frac{m_p l_1^4 \cos^3 \theta \sin \theta}{c^2} \dot{\theta}^2 + \frac{2m_p l_1^3 \sin \theta \cos^2 \theta}{c} \dot{\theta}^2 - \frac{m_p l_1^3 \sin^3 \theta}{c} \dot{\theta}^2 - m_c g r_1 \cos \theta \\
&- m_{cr} g (l_2 - r_2) \frac{l_1}{l_2} \cos \theta
\end{aligned}$$

Finally Euler-Lagrange equation is obtained as follows:

$$\begin{aligned}
&\{I_c + m_c r_1^2 + l_1^2 \cos^2 \theta \left(\frac{I_{cr}}{c^2} + \frac{m_{cr} (l_2 - r_2)^2}{l_2^2} \right) + l_1^2 \sin^2 \theta (m_{cr} + m_p) \\
&+ \frac{l_1^3}{c} \sin^2 \theta \cos \theta \left(\frac{m_{cr} l_1 r_2^2}{l_2^2 c} \cos \theta + \frac{2m_{cr} r_2}{l_2} + \frac{m_p l_1}{c} \cos \theta + 2m_p \right) \} \ddot{\theta} \\
&+ \{ m_{cr} l_1^2 \sin \theta \cos \theta \left(-\frac{I_{cr}}{m_{cr} c^2} + 1 - \left(\frac{l_1 r_2}{l_2 c} \right)^2 \sin^2 \theta \right. \\
&+ \left. \left(\frac{l_1 r_2}{l_2 c} \right)^2 \cos^2 \theta + \frac{2l_1 r_2}{l_2 c} \cos \theta - \frac{(l_2 - r_2)^2}{l_2^2} \right) - \frac{m_{cr} l_1^3 r_2 \sin^3 \theta}{l_2 c} \\
&+ m_p l_1^2 \sin \theta \cos \theta \left(1 - \frac{l_1^2}{c^2} \sin^2 \theta + \frac{l_1^2}{c^2} \cos^2 \theta + \frac{2l_1}{c} \cos \theta \right) - \frac{m_p l_1^3 \sin^3 \theta}{c} \} \dot{\theta}^2 \\
&+ g \cos \theta (m_c r_1 + m_{cr} (l_2 - r_2) \frac{l_1}{l_2}) = -(F_E + F_B) \left(1 + \frac{1}{c} l_1 \cos \theta \right) l_1 \sin \theta
\end{aligned} \tag{3.27}$$

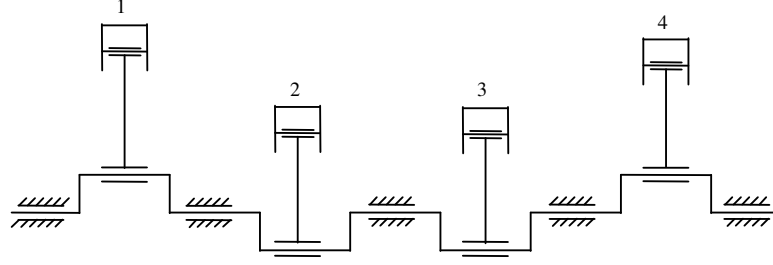


Figure 3.2 A four-cylinder in-line engine

Finally, more complex sets of equations of motion are derived for multi-cylinder engines, like the one shown in Figure 3.2, by application of similar methodologies. In particular, when the engine parts are considered to be rigid, the form of equations of motion remains the same as that of the single-cylinder engine. However, the equation of motion is determined by taking into account the engine set-up, including the relative position of the cylinders and their firing sequence [146]. For instance, the equation of motion for the system shown in Figure 3.2, with a four cylinder in-line engine, takes the form

$$\begin{aligned}
 & \left(\begin{aligned}
 & I_c + m_c r_1^2 + l_1^2 \cos^2(\theta - \gamma_n) \left(\frac{I_{cr}}{c^2} + \frac{m_{cr}(l_2 - r_2)^2}{l_2^2} \right) \\
 & + l_1^2 \sin^2(\theta - \gamma_n) (m_{cr} + m_p) + \frac{l_1^3}{c} \sin^2(\theta - \gamma_n) \cos(\theta - \gamma_n) \left(\frac{m_{cr} l_1 r_2^2}{l_2^2 c} \cos(\theta - \gamma_n) \right) \\
 & + \frac{2m_{cr} r_2}{l_2} + \frac{m_p l_1}{c} \cos(\theta - \gamma_n) + 2m_p
 \end{aligned} \right) \ddot{\theta} \\
 & \left(\begin{aligned}
 & m_{cr} l_1^2 \sin(\theta - \gamma_n) \cos(\theta - \gamma_n) \left(-\frac{I_{cr}}{m_{cr} c^2} + 1 - \left(\frac{l_1 r_2}{l_2 c} \right)^2 \sin^2(\theta - \gamma_n) \right) \\
 & + \left(\frac{l_1 r_2}{l_2 c} \right)^2 \cos^2(\theta - \gamma_n) + \frac{2l_1 r_2}{l_2 c} \cos(\theta - \gamma_n) - \frac{(l_2 - r_2)^2}{l_2^2} - \frac{m_{cr} l_1^3 r_2 \sin^3(\theta - \gamma_n)}{l_2 c} \\
 & + m_p l_1^2 \sin(\theta - \gamma_n) \cos(\theta - \gamma_n) \left(1 - \frac{l_1^2}{c^2} \sin^2(\theta - \gamma_n) + \frac{l_1^2}{c^2} \cos^2(\theta - \gamma_n) \right) \\
 & + \frac{2l_1}{c} \cos(\theta - \gamma_n) - \frac{m_p l_1^3 \sin^3(\theta - \gamma_n)}{c}
 \end{aligned} \right) \dot{\theta}^2 \\
 & + \sum_{n=1}^4 \left(g \cos(\theta - \gamma_n) (m_c r_1 + m_{cr} (l_2 - r_2) \frac{l_1}{l_2}) \right) \\
 & = \sum_{n=1}^4 \left(-(F_E + F_B) \left(1 + \frac{1}{c} l_1 \cos(\theta - \beta_n) \right) l_1 \sin(\theta - \beta_n) \right)
 \end{aligned} \tag{3.28}$$

γ_n is the phase difference between the angular position of the first and n th cylinder, so that $\gamma_1 = \gamma_4 = 0$ and $\gamma_2 = \gamma_3 = \pi$. Likewise, the angles β_n indicate the phase difference between the firing angle of engine cylinders, so that $\beta_1 = 0$, $\beta_2 = 3\pi$, $\beta_3 = \pi$ and $\beta_4 = 2\pi$ [146].

3.3 Kinematic Analysis

In the kinematic analysis, taking the first and second derivatives of the displacement of slider with respect to time, the speed and acceleration of slider are as follows:

$$x_B = l_1 \cos \theta + l_2 \cos \beta \quad (3.29)$$

$$\dot{x}_B = -l_1 \dot{\theta} \sin \theta - l_2 \dot{\beta} \sin \beta \quad (3.30)$$

$$\ddot{x}_B = -l_1 \ddot{\theta} \sin \theta - l_1 \dot{\theta}^2 \cos \theta - l_2 \ddot{\beta} \sin \beta - l_2 \dot{\beta}^2 \cos \beta \quad (3.31)$$

Similarly, angular velocity $\dot{\beta}$ and acceleration $\ddot{\beta}$ are obtained from Equation 3.8 as follows

$$l_1 \dot{\theta} \cos \theta = l_2 \dot{\beta} \cos \beta \quad (3.32)$$

$$\dot{\beta} = \frac{l_1 \dot{\theta} \cos \theta}{l_2 \cos \beta} \quad (3.33)$$

$$\ddot{\beta} = \frac{l_1 \ddot{\theta} \cos \theta \cos \beta + l_1 \dot{\theta} \dot{\beta} \cos \theta \sin \beta - l_1 \dot{\theta}^2 \sin \theta \cos \beta}{l_2 \cos^2 \beta} \quad (3.34)$$

3.4 Dynamic Model Results

Equation 3.27 is calculated by the Runge-Kutta method with time step $\Delta t = 0.001$ s from 0 to 2 s to obtain numerical solutions, which are used to dynamic equation results of a slider-crank mechanism, and shown in Figures 3.3 (a), (b) and (c) for the angle θ , the angular velocity $\dot{\theta}$ and the angular acceleration $\ddot{\theta}$ of the crank,

respectively. The displacement, velocity and acceleration of a slider are shown in Figures 3.4 (a), (b) and (c), respectively.

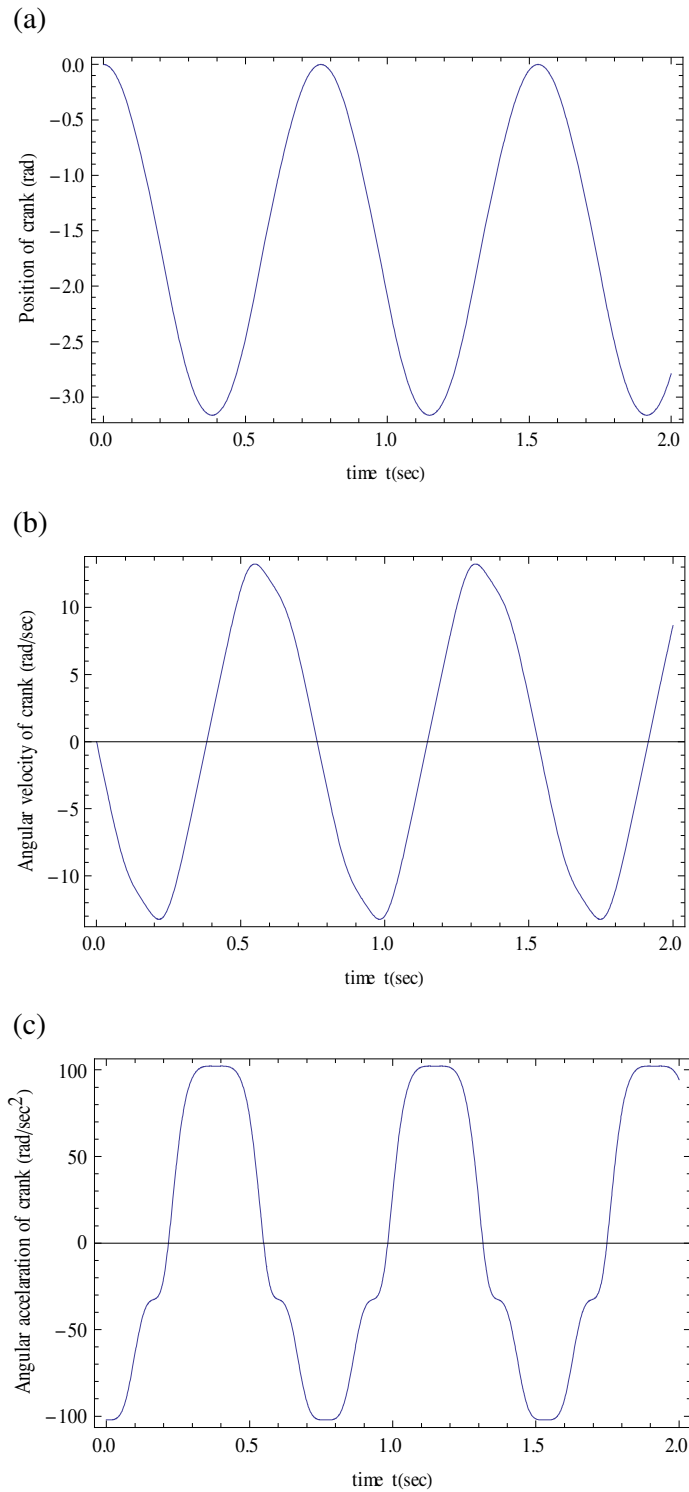


Figure 3.3 Numerical results of a slider crank mechanism for a) angle θ b) angular velocity $\dot{\theta}$ c) the angular acceleration $\ddot{\theta}$ of the crank

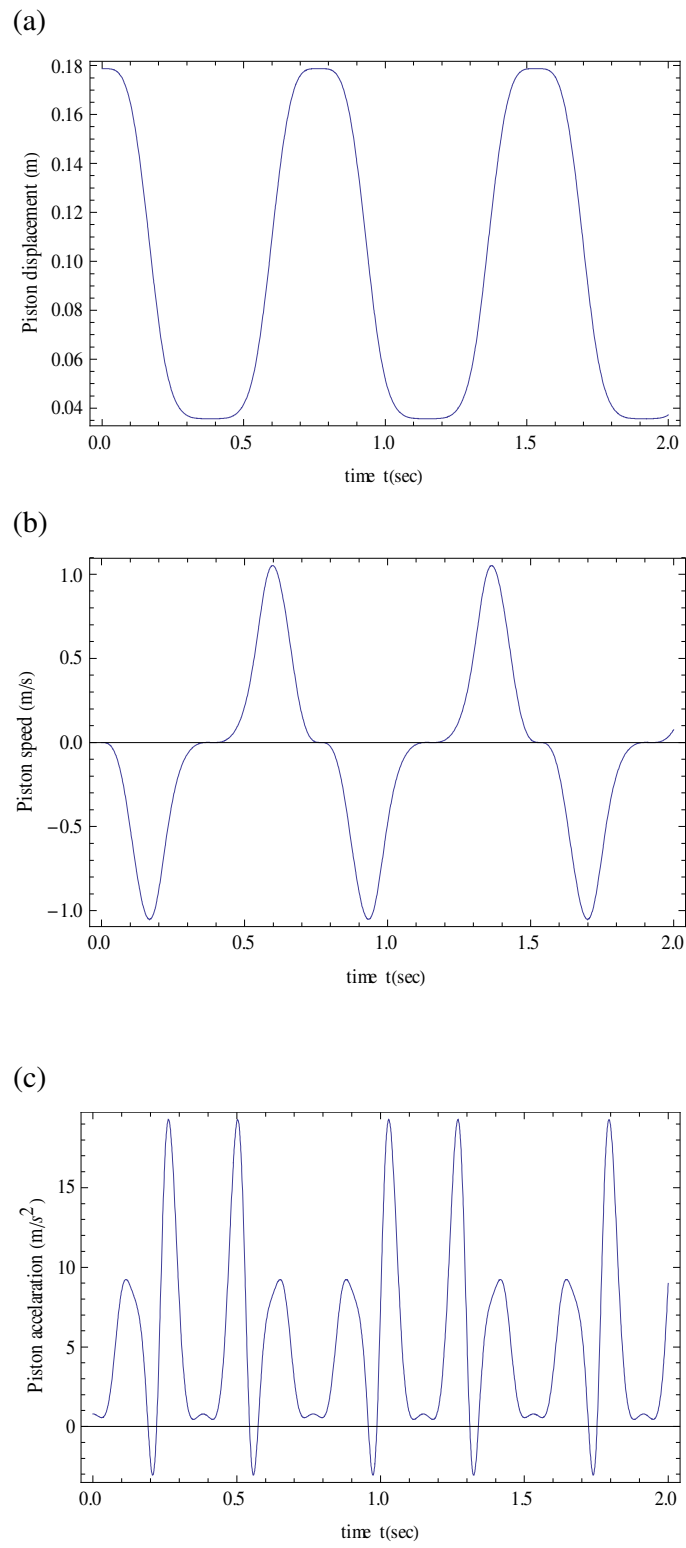


Figure 3.4 Numerical results of a slider crank mechanism for a) displacement b) speed and c) acceleration of a slider

It is seen that the responses $\theta, \dot{\theta}, \ddot{\theta}, x_B, \dot{x}_B$ and \ddot{x}_B numerical results are calculated by using Euler-Lagrange equation. Therefore, the simulation responses of a slider-crank mechanism are well predicted by the numerical results. But internal combustion engine mostly have nonlinear characteristics, so that to obtain dynamic equation very difficult and impossible. System identification becomes very useful, generating empirical mathematical model for the response of the system where the dynamic equations are not obtained.

The total kinetic energy and potential energy of a slider-crank mechanism can be obtained and their figures shown in Figure 3.5.

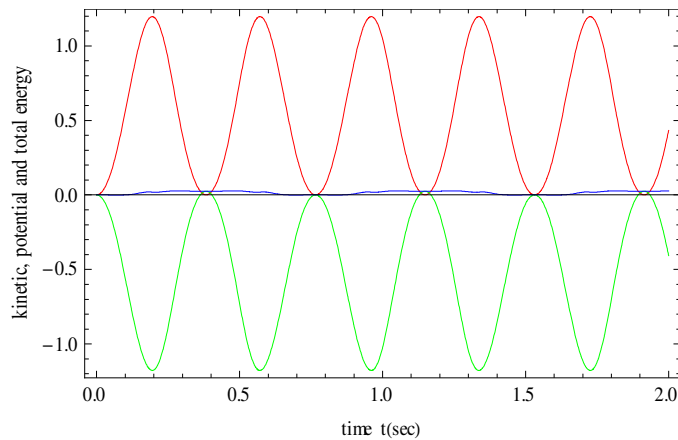


Figure 3.5 Kinetic, potential and total energy of a slider-crank mechanism

3.5 Conclusions

The dynamic formulations of a slider-crank mechanism have been successfully formulated with only one independent variable. Dynamic responses of the numerical simulations were obtained for the dynamic modeling. The dynamic formulation can give a good interpretation of a slider-crank mechanism by using numerical simulations.

CHAPTER 4

4. SYSTEM IDENTIFICATION

4.1 Introduction

System identification is the process of developing a mathematical model of a dynamic system based on the input and output data from the actual process [26]. This means it is possible to sample the input and output signals of a system and using this data generate a mathematical model. An important stage in control system design is the development of a mathematical model of the system to be controlled. In order to develop a controller, it must be possible to analyse the system to be controlled and this is done using a mathematical model. Another advantage of system identification is evident if the process is changed or modified. System identification allows the real system to be altered without having to calculate the dynamical equations and the model parameters again.

System identification is concerned with developing models [147]. A dynamic system can be conceptually described as in Figure 4.1. The system is driven by input variables $u(t)$ and disturbance $v(t)$. The user can control $u(t)$ but not $v(t)$. The output signals are variables which provide useful information about the system [27].

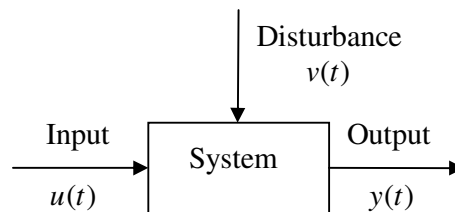


Figure 4.1 A dynamic system with input $u(t)$, output $y(t)$ and disturbance $v(t)$, where t denotes time [27]

Basically system identification is achieved by the adjusting the parameters of the model until the model output is similar to the output of the real system. Steps in

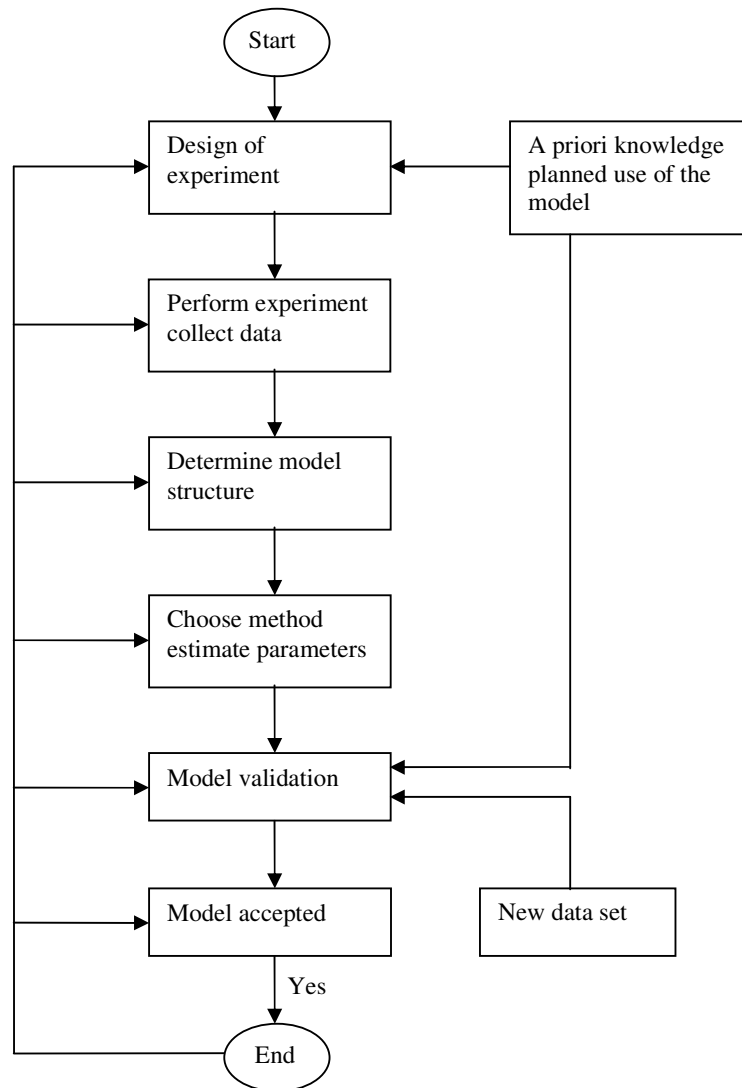


Figure 4.2 Schematic flowchart of system identification [27]

system identification are shown in Figure 4.2. The procedures for carrying out system identification can be divided into the following steps [148]:

- a. Specify and parameterize a class of mathematical models that represents the system to be identified.

- b. Apply an appropriately chosen test signal to the system and record the input-output data. If the system is in continuous operation data and a test signal is not permitted, then we must use the normal operating data for identification.
- c. Perform the parameter identification to select the model in the specified class that best fits the statistical data.
- d. Perform a validation test to see if the model chosen adequately represents the system with respect to final identification objectives.
- e. If the validation test is passed, the procedure ends. Otherwise, another class of models must be selected and steps (b) through (d) performed until a validation model is obtained.

In this chapter, system identification methods for nonlinear dynamic systems are presented. The methods are applicable to spark ignited engine.

4.2 Nonlinear System Identification

4.2.1 Nonlinear System Representation

A linear model is simple but is not always good enough to adequately approximate an inherent nonlinear process over its entire operating region [1]. Linearity has frequently been assumed in modeling input output characteristics of real systems and in developing the control rules. However, the input output characteristics of real systems contain nonlinearity and development of the nonlinear modeling approach seems to be very important in order to achieve highly precise prediction and control of nonlinear systems [149]. In addition, most systems encountered in the real world are nonlinear in nature, and since linear models can not capture the rich dynamic behaviour associated with nonlinear systems [13]. As a result, nonlinear system modeling and identification is necessary in control system science.

It is beneficial to first develop a model of the system to accurately control a system. The fundamental objective for the modeling and identification task is to obtain a good and reliable tool for analysis and control system development [150].

Almost all the systems in nature are inherently nonlinear over their operating range. Linearization of the models of these systems is in many cases possible only around a

specific operating point. However, in many cases we need to use nonlinear systems over the entire operating range and that is the main reason to think about nonlinear system modeling [64]. The theory and application of nonlinear system identification is as vast and varied as nonlinear systems themselves [151].

When the system is to be represented nonlinearly, the problem is far from being a simple order determination and parameter estimation problem. Unlike linear systems, there exists no straightforward way of expressing a general nonlinear system. This fact raises the need to decide in what form to represent the nonlinear system as a first step. In the last century, the studies on nonlinear system theory have evolved considerably, and many methods for representing nonlinear systems have been proposed [152]. As far as nonlinear system identification and control system design are concerned, the methods of premium concern are the Volterra series representation, the Hammerstein representation, the Wiener representation and the Wiener-Hammerstein or the nonlinear autoregressive moving average with exogenous input (NARMAX) representation [148].

Various system identification techniques that can be broadly classified as parametric and nonparametric techniques have been successfully applied in system identification. There are different kinds of identification methods for nonlinear dynamic systems, as can be seen in Figure 4.3.

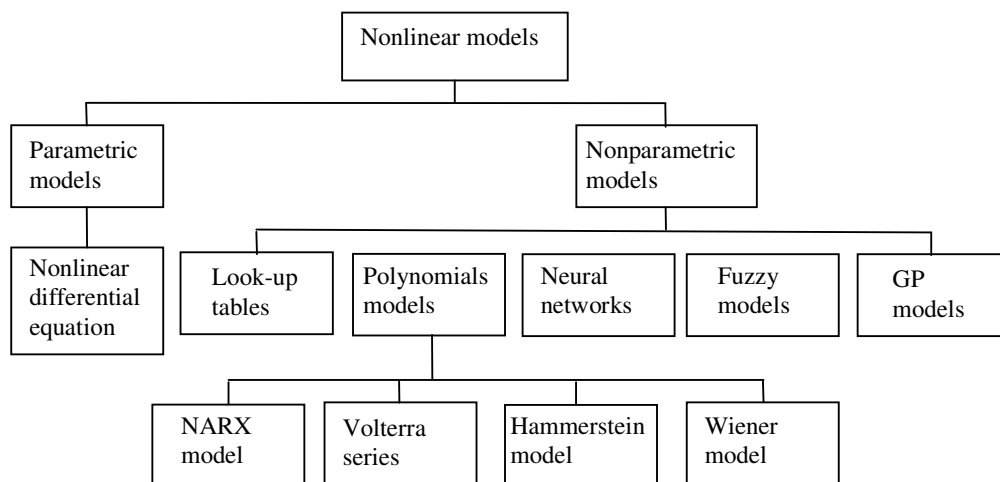


Figure 4.3 Overview of system identification methods [78]

4.2.1.1 Volterra Series Model

Most of the nonlinear systems can be represented by a Volterra series [148]. The single input single output (SISO) nonlinear system with additive noise shown in Figure 4.4.

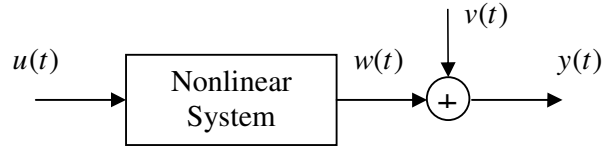


Figure 4.4 Nonlinear system with additive noise

The Volterra series explicitly expresses the input-output relationship of a nonlinear system as follows:

$$\begin{aligned}
 w(t) = & \int_{-\infty}^t g_1(\tau)u(t-\tau)d\tau + \int_{-\infty}^t \int_{-\infty}^t g_2(\tau_1, \tau_2)u(t-\tau_1)u(t-\tau_2)d\tau_1d\tau_2 + \dots \\
 & \dots + \int_{-\infty}^t \dots \int_{-\infty}^t g_n(\tau_1, \dots, \tau_n) \prod_{i=1}^n u(t-\tau_i)d\tau_i + \dots
 \end{aligned} \tag{4.1}$$

The n th order Volterra kernel $g_n(\tau_1, \dots, \tau_n)$ represents the weighting function of n th degree.

4.2.1.2 Wiener Model

The nonlinear Wiener models consist of a linear dynamic element followed in series by a static nonlinear element is schematically shown in Figure 4.5.

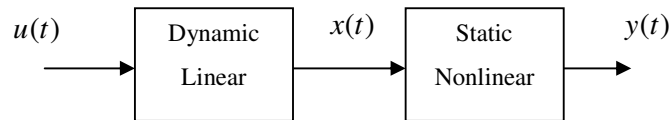


Figure 4.5 General Wiener model structure

An autoregressive exogenous (ARX) model is typically chosen to represent the linear dynamics of the model. This model is described by the following equation:

$$x(t) = b_1 u(t-1) + b_2 u(t-2) + \dots + b_{nb} u(t-nb) - a_1 x(t-1) - \dots - a_{na} x(t-na) \quad (4.2)$$

which is represented in operator form by

$$x(t) = \frac{B(q^{-1})}{A(q^{-1})} u(t) \quad (4.3)$$

where the operators $A(q^{-1})$ and $B(q^{-1})$ are

$$A(q^{-1}) = 1 + a_1 q^{-1} + a_2 q^{-2} + \dots + a_{na} q^{-na} \quad (4.4)$$

$$B(q^{-1}) = b_0 + b_1 q^{-1} + b_2 q^{-2} + \dots + b_{nb} q^{-nb} \quad (4.5)$$

Although any form of nonlinear function may be used as the static nonlinearity of the Wiener model, a polynomial model is usually employed. This is the most general form and has an inverse by means of its roots [153]. The complete Wiener model is represented by

$$x(t) = b_1 (u(t-1) + b_2 (u(t-2) + \dots + b_{nb} (u(t-nb) - a_1 (x(t-1) - \dots - a_{na} (x(t-na) \quad (4.6)$$

$$y(t) = \gamma_1 x(t) + \gamma_2 x^2(t) + \dots + \gamma_p x^p(t) \quad (4.7)$$

4.2.1.3 Hammerstein Model

As is well known, many real systems of very different physical nature can be modeled as a cascade interconnection of a static nonlinearity and a linear model; this interconnection is referred to as Hammerstien model of the real system [154].

Hammerstein model consists of a static nonlinear function followed by a linear dynamic function. This model is widely used to approximate many real world processes [148]. The Figure 4.6 represents this Hammerstein model:

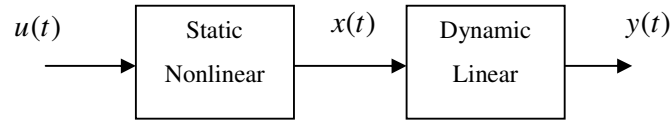


Figure 4.6 Hammerstein model structure

Let the static nonlinearity be represented by a nonlinear operator $F(\cdot)$. Then,

$$x(t) = F(u(t)) \quad (4.8)$$

The dynamical linear part in the Hammerstein model can be represented by an autoregressive with exogenous input (ARX) model. Then,

$$y(t) = \frac{B(q^{-1})}{A(q^{-1})} x(t) = \frac{B(q^{-1})}{A(q^{-1})} F(u(t)) \quad (4.9)$$

where q^{-1} is the backward time shift operator. The static nonlinear model $F(\cdot)$ is approximated by a power polynomial of order p ,

$$x(t) = F(u(t)) = \gamma_1 u(t) + \gamma_2 u^2(t) + \dots + \gamma_p u^p(t) \quad (4.10)$$

where $\gamma_j (j = 1, \dots, p)$ are the nonlinearity parameters, $\gamma_j \in R$.

Hammerstein models are popular in control engineering. It is easy to compensate the nonlinear process behavior by a controller that implements the inverse static nonlinearity $q^{-1}(\cdot)$ at its output. Another advantage of the distinction into nonlinear and linear blocks is that stability is determined solely by the linear part of the model, which can be easily checked. Thus, the Hammerstein model has many appealing features [17].

4.2.1.4 NARMAX Model

The Hammerstein and Wiener models for nonlinear systems are special cases of the general NARMAX representation of nonlinear systems [152]. Leontaritis and Billings [155] introduced the nonlinear autoregressive moving average with exogenous input (NARMAX) approach as a means of describing the input-output relationship of a nonlinear system. The model represents the extension of the well-known ARMAX model to the nonlinear case.

The NARMAX model structure with input nonlinearity $F_i(\cdot)$ and output nonlinearity $F_o(\cdot)$ is shown in Figure 4.7, where $\xi(k)$ is the white noise disturbance [152].

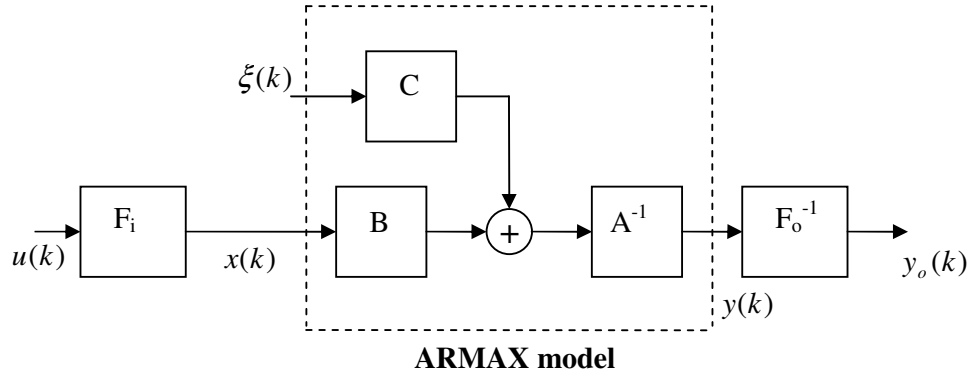


Figure 4.7 General NARMAX system structure [152]

The equation (4.12) which is commonly known as the ARMAX model is represented in operator form with input $x(k)$ and output $y(k)$ in the linear subsystem by

$$y(k) = \frac{B(q^{-1})}{A(q^{-1})}x(k) + \frac{C(q^{-1})}{A(q^{-1})}\xi(k) \quad (4.11)$$

The input nonlinearity has the following static characteristics:

$$x(k) = F_i(u(k)) = \gamma_{i1}u(k) + \gamma_{i2}u^2(k) + \dots + \gamma_{ip_i}u^{p_i}(k) \quad (4.12)$$

The output nonlinearity is given by

$$y(k) = F_o(y_o(k)) = \gamma_{o1}y_o(k) + \gamma_{o2}y_o^2(k) + \dots + \gamma_{op_o}y_o^{p_o}(k) \quad (4.13)$$

The relationship between the overall system output $y_o(t)$ and input $x(t)$ is as follows:

$$y_o(k) = F_o^{-1} \left(\frac{B(q^{-1})}{A(q^{-1})} F_i(u(k)) + \frac{C(q^{-1})}{A(q^{-1})} \xi(k) \right) \quad (4.14)$$

If the response of the system is dominated by nonlinear characteristics, it is often necessary to use a nonlinear model. The NARMAX representation gives a concise description for a large class of discrete time nonlinear systems [24]. NARMAX representation gives a more general nonlinear system model in comparison with the Hammerstein and the Wiener model [152]. Identification of systems represented by a NARMAX model can be found in Appendix 1.

4.3 Identification of Hammerstein Model

The Hammerstein model is probably the most widely known and applied nonlinear modeling approach. It assumes a separation between the linear dynamics and the nonlinear static part of the system [17]. The method to be used in Hammerstein system identification depends on the availability of a priori information. If sufficient amount of information is available, the system can be linearly parametrized and simple least square based identification algorithms can be built and applied [152].

The dynamical linear part in the Hammerstein model can be represented by an ARX model as for the linear system model [28]. The relationship between the linear part input $x(t)$ and output $y(t)$ can be given as:

$$A(q^{-1})y(t) = B(q^{-1})x(t) + e(t) \quad (4.15)$$

where $x(t)$ is the output of the nonlinearity, the polynomials in Equation 4.15 are given in Equations 4.4 and 4.5.

The static nonlinearity in the Hammerstein model is classically approximated by a polynomial of known order. The order of the polynomial is selected in accordance

with the hardness of the nonlinearity in the system. Consider the system in Figure 4.6. The static nonlinearity in the Hammerstein model can be approximated by a polynomial in input $u(t)$ of predetermined order p , as in Equation 4.10. The accuracy of this approximation depends on the suitable selection of the coefficients γ_i and the order p .

The additive noise $e(t)$ in Equation 4.15 is a random variable of zero mean. The problem of identification of the Hammerstein model reduces to estimating a_i , b_i , and γ_i using the data sequences $u(t)$ and $y(t)$, for predetermined values of p and n .

The combination of the linear and the nonlinear subsystems gives:

$$\begin{aligned} A(q^{-1})y(t) &= B(q^{-1})\left(\gamma_1 u(t) + \gamma_2 u^2(t) + \dots + \gamma_p u^p(t)\right) + e(t) \\ &= B(q^{-1})\sum_{i=1}^p \gamma_i u^i(t) + e(t) \end{aligned} \quad (4.16)$$

In Equation 4.16, the coefficients of $B(q^{-1})$ do not appear explicitly. Without loss of generality, the nonlinear part can be normalized with respect to γ_1 , and the Equation 4.16 can be rewritten with the assumption that $\gamma_1 = 1$ as follows:

$$A(q^{-1})y(t) = B(q^{-1})\left[u(t) + \sum_{i=2}^p \gamma_i u^i(t)\right] + e(t)$$

or

$$A(q^{-1})y(t) = B(q^{-1})u(t) + \sum_{i=2}^p \sum_{j=0}^n b_j \gamma_i q^{-j} u^i(t) + e(t) \quad (4.17)$$

Define a polynomial $S_i(q^{-1})$

$$S_i(q^{-1}) = \gamma_i B(q^{-1}) = s_{i0} + s_{i1} q^{-1} + \dots + s_{in} q^{-n} \quad (4.18)$$

where $s_{ij} = \gamma_i b_j$, $i = 1, \dots, p$, $j = 1, \dots, n$. Then, Equation 4.17 is improved to be

$$A(q^{-1})y(t) = B(q^{-1})u(t) + \sum_{i=2}^p S_i(q^{-1})u^i(t) + e(t) \quad (4.19)$$

Equation 4.19 can be put into linear regression forms as follows:

$$y(t) = \phi^T(t)\theta + e(t) \quad (4.20)$$

where

$$\phi(t) = \left(-y(t-1), -y(t-2), \dots, -y(t-n_a), u(t), u(t-1), \dots, u(t-n_b), \right. \\ \left. u^2(t), \dots, u^2(t-n_b), \dots, u^n(t), \dots, u^n(t-n_b) \right)^T \quad (4.21)$$

$$\theta = (a_1, a_2, \dots, a_{n_a}, b_0, b_1, \dots, b_{n_b}, s_{20}, \dots, s_{2n_b}, \dots, s_{n0}, \dots, s_{nn_b}) \quad (4.22)$$

The linear regression representation for the system given in Equation 4.20 permits direct application of the recursive least square (RLS) method. However, the vector of unknown parameters does not include the coefficients of the polynomial $B(q^{-1})$ explicitly. These coefficients are implicitly expressed in the form of products with the nonlinear subsystem parameters γ_j ($j = 1, \dots, n$). Consequently, the identification of the system parameters can not be performed at a single stage. The RLS method is, therefore, implemented in two steps. The first step of the algorithm gives the estimates of the parameters a_i and s_{jk} , and the second step estimates the parameters b_k and γ_j using the results of the first step, where $i = 1, \dots, n_a$, $j = 1, \dots, n$, $k = 1, \dots, n_b$. The nonlinear identification algorithm steps are summarized as follows:

- (i) Choose initial values for the covariance matrix P and forgetting factor λ .

(ii) Acquire the input and output of the system and form the data vector ϕ as given in Equation 4.21 for time instant t using the present and past values of the input u , output y and powers of u .

(iii) Solve for the parameter estimates $\hat{a}_i, \hat{b}_k, \hat{s}_{jk}$ using RLS estimates rule:

$$\varepsilon(t) = y(t) - \phi^T(t)\hat{\theta}(t-1)$$

$$P(t) = \frac{1}{\lambda} P(t-1) \left[I_p - \frac{\phi(t)\phi^T(t)P(t-1)}{\lambda + \phi^T(t)P(t-1)\phi(t)} \right]$$

$$\hat{\theta}(t) = \hat{\theta}(t-1) + P(t)\phi(t)\varepsilon(t)$$

(iv) (iv) Solve for the estimates $\hat{\gamma}_j, j = 1, \dots, n$ using the estimated values

\hat{b}_k, \hat{s}_{jk} by the formula :

$$\hat{\gamma}_j = \left(\sum_{k=1}^{n_b} \hat{b}_k^2 \right)^{-1} \sum_{k=1}^{n_b} \hat{b}_k \hat{s}_{jk} \quad j = 1, \dots, n.$$

(v) Update the time instant, $t = t + 1$. Return to step (ii)

4.4 Conclusions

In this chapter, a general view of nonlinear system modeling and identification with a parametric approach is given. Hammerstein, Volterra series, Wiener and NARMAX models are examined in detail. Identification of Hammerstein model is presented in this chapter. The model and identification method are applicable to all the nonlinear systems including gasoline engine.

CHAPTER 5

5. ARTIFICIAL NEURAL NETWORK

5.1 Introduction

Artificial Intelligence (AI) systems are widely accepted as a technology offering an alternative way to tackle complex and ill-defined problems. They can learn from examples, are fault tolerant in the sense that they are able to handle noisy and incomplete data, are able to deal with nonlinear problems, and once trained can perform prediction and generalization at high speed. They have been used in diverse applications in control, robotics, pattern recognition, forecasting, medicine, power systems, manufacturing, optimization, signal processing, and social/psychological sciences. They are particularly useful in system modeling such as in implementing complex mappings and system identification. AI systems comprise areas like, expert systems, artificial neural networks (ANN), genetic algorithm, fuzzy logic and various hybrid systems, which combine two or more techniques. [156].

ANNs mimic somewhat the learning process of a human brain. Instead of complex rules and mathematical routines, ANNs are able to learn the key information patterns within a multidimensional information domain. In addition, the inherently noisy data does not seem to present a problem, since they are neglected [157].

According to Haykin [158], a neural network is a massively parallel distributed processor that has a natural propensity for storing experiential knowledge and making it available for use. It resembles the human brain in two respects; the knowledge is acquired by the network through a learning process, and inter-neuron connection strengths known as synaptic weights are used to store the knowledge.

Neural network (NN) operates like a “black box” model, and does not require detailed information about the system. Instead, it learns the relationship between the input parameters and the controlled and uncontrolled variables by studying previously recorded data, in similar way that a nonlinear regression might be performed. Another advantage of using ANNs is their ability to handle large and complex systems with many interrelated parameters. They simply ignore excess input data that are of minimal significance and concentrate instead on the more important inputs [156].

ANN has emerged as a powerful learning technique to perform complex tasks in highly nonlinear dynamic environment. Some of the prime advantages of using ANN models are their ability to learn based on optimization of an appropriate error function and their excellent performance for approximation of nonlinear function [158]. Neural networks have good general approximation capabilities for reasonable nonlinear systems [20]. Nerandra and Parthasaraty [22] demonstrated that artificial neural networks could be used successfully for the identification and control of nonlinear dynamic systems. Chen and Billings [23] have reported nonlinear system modeling and identification using ANN structures.

5.2 History of Neural Networks

The modern era of NNs began with the pioneering work of Warren McCulloch, a neurophysiologist, and a young mathematician, Walter Pitts, wrote a paper on how neurons might work in 1943. They modeled a simple neural network with electrical circuit. The next major development in NNs came in 1949 with the publication of Hebb’s book *The Organization of Behavior*, in which an explicit statement of a physiological learning rule for synaptic modification was presented for the first time. After the publication of McCulloch and Pitt’s classic paper, a new approach to the pattern recognition problem was introduced by Rosenblatt (1958) in his work on the *perceptron*, a novel method of supervised learning. In 1959, Widrow and Hoff introduced the *least mean square* (LMS) algorithm and used it to formulate *Adaline* and *Madaline* which was the first NN to be applied to a real world problem. Minsky and Papert published the book in 1969 which used mathematics to demonstrate that there are fundamental limits on what single layer perceptrons can compute [158].

A more mathematical approach to NN started in the 1970s, but only gained success in the early 1980s. In 1982, Hopfield invented the Hopfield network whose dynamics were guaranteed to converge. After this invention, NN studies have raised again. In 1986, the development of the backpropagation algorithm was reported by Rumelhart, Hinton and Williams which has emerged as the most popular learning algorithm for the training of multilayer perceptrons [159].

5.3 Biological and Artificial Neurons

ANN is a system loosely modeled on the human brain. A biological neuron is shown in Figure 5.1. In brain, there is a flow of coded information from the synapses towards the axon. The axon of each neuron transmits information to a number of other neurons. The neuron receives information at the synapses from a large number of other neurons [156].

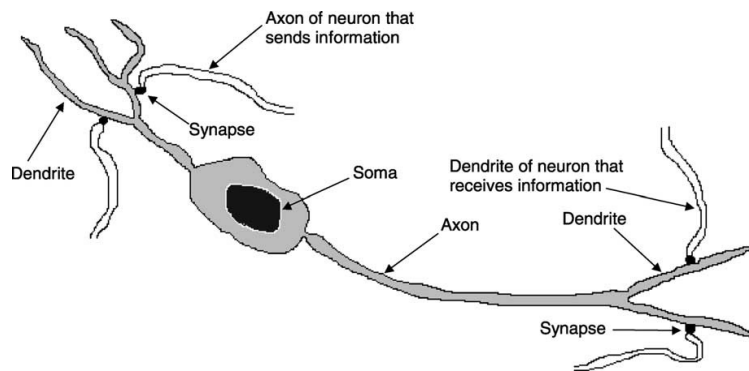


Figure 5.1 A simplified model of a biological neuron [156]

Figure 5.2 shows a highly simplified model of an artificial neuron, which may be used to stimulate some important aspects of the real biological neuron.

A neural network is composed of large numbers of highly interconnected processing elements known as neurons. The basic elements of an artificial neuron are shown in Figure 5.3. Artificial neuron consists of weight, bias and activation function mainly. Each neuron receives inputs x_1, x_2, \dots, x_n , attached with a weight ω_i which shows the connection strength for a particular input for each connection. Every input is then

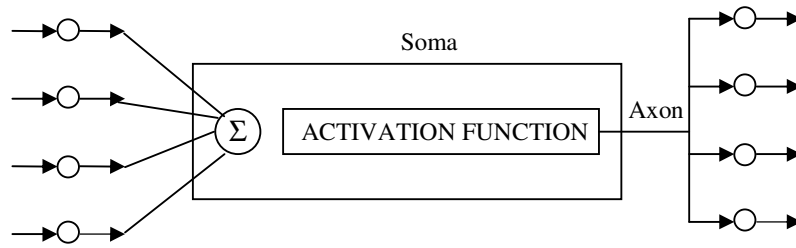


Figure 5.2 A simplified model of an artificial neuron [156]

multiplied by the corresponding weight of the neuron connection. A bias b_i can be defined as a type of connection weight with a constant nonzero value added to the summation of inputs and corresponding weights u , given in Equation 5.1.

$$u_i = \sum_{j=1}^n w_{ij} x_j + b_i. \quad (5.1)$$

The summation u_i is transferred using a scalar-to-scalar function called an “activation or transfer function”, $f(u_i)$, to yield a value called the unit’s “activation”, given in Equation 5.2.

$$y_i = f(u_i). \quad (5.2)$$

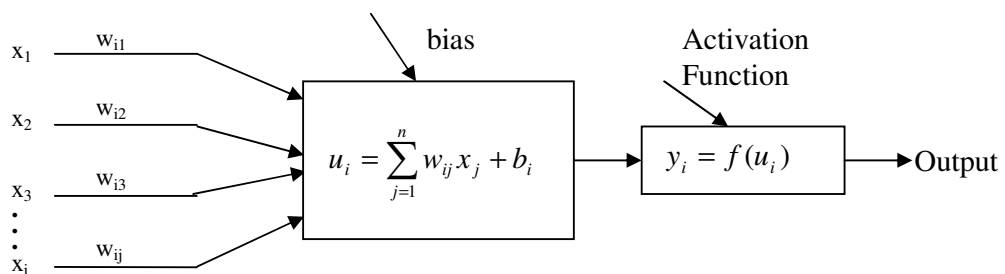


Figure 5.3 Basic elements of an artificial neuron

5.4 Types of Activation Function

Activation functions serve to introduce nonlinearity into neural networks which makes it more powerful than linear transformation. There are many forms of activation functions, which are selected to the specific problem. All the NN architectures employ the activation function [158]. Table 5.1 summarizes the basic types of activation functions. The most practical activation functions are the sigmoid and the hyperbolic tangent functions. This is because they are differentiable [160].

Table 5.1 Types of activation function

FUNCTION TYPE	MATHEMATICAL REPRESENTATION	FIGURE
Threshold	$y = f(v) = \begin{cases} 1, \dots v \geq 0 \\ 0, \dots v < 0 \end{cases}$	
Piecewise-linear	$y = f(v) = \begin{cases} 1, \dots v \geq +\frac{1}{2} \\ v, \dots +\frac{1}{2} > v > -\frac{1}{2} \\ 0, \dots v \leq -\frac{1}{2} \end{cases}$	
Sigmoid	$y = f(v) = \frac{1}{1 + \exp(-v)}$	
Hyperbolic tangent	$y = f(v) = \frac{1 - \exp(2v)}{1 + \exp(2v)}$	
Radial basis	$y = f(v) = \exp\left(\frac{-v^2}{2}\right)$	

5.5 Neural Network Architectures

Artificial neural network can be viewed as weighted directed graphs in which artificial neurons are nodes and directed edges (with weights) are connections between neuron outputs and neuron inputs [161]. Based on the connection pattern (architecture), ANNs can be grouped into two categories:

- feedforward networks (multilayer perceptron and radial basis function networks)
- recurrent or feedback networks (Elman and Hopfield networks)

In the most common family of feedforward networks, called multilayer perceptron, neurons are organized into layers that have unidirectional connections between them. Recurrent, or feedback, networks, on the other hand, are dynamic systems [63, 161].

5.5.1 Multilayer Perceptron Feedforward Neural Network

In the multilayer NN or multilayer perceptron, the input signal propagates through the network in a forward direction, on a layer-by-layer basis. This network has been successfully to solve some difficult and diverse problems by training in a supervised manner with a highly popular algorithm known as the error back-propagation algorithm [158].

Multilayer perceptron feedforward (MLPFF) computational structure is a nonlinear model able to perform a mapping between the input vector x and the output vector y . In Figure 4.4 a multi input multi output (MIMO) MLPFF is shown; the input data (i.e. the independent variables) are propagated from the input layer to the output one, through the hidden layers, to generate the corresponding output signal (i.e. the dependent variables). Each layer of the MLPFF is composed of several elementary processing units (neurons) that work in parallel and are connected each other to create a flow of information from input layer to output one. These elements can be considered as single output black-box computing units with multiple inputs, where outputs is obtained by processing the weighted sum of the inputs with a transfer function named activation function, which is usually a nonlinear function [75].

In Figure 5.4 $x_i(n)$ represents the input to the network, f_j and f_k represent the output of the two hidden layers and $y_i(n)$ represents the output layer of the NN. The connecting weights between the input to the first hidden layer, first to second hidden layer and second hidden layer to the output layers are represented by respectively.

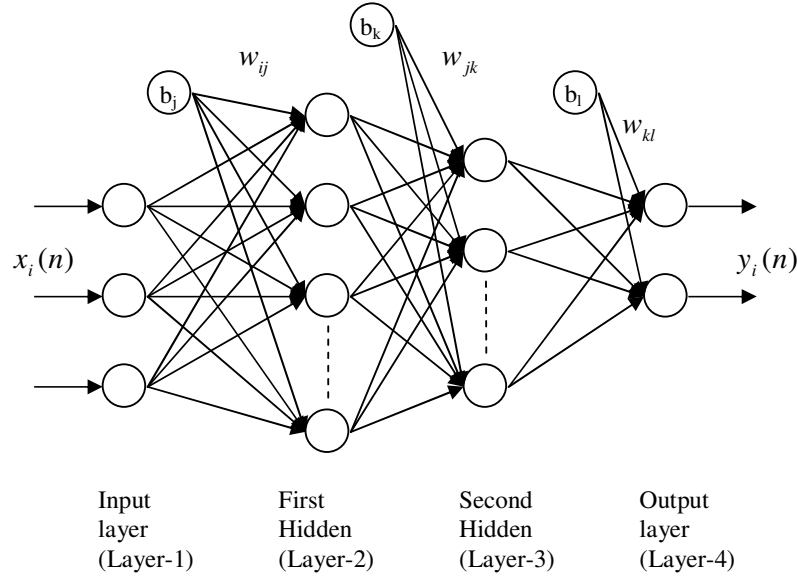


Figure 5.4 Multilayer perceptron neural network structure

If P_1 is the number of neurons in the first hidden layer, each element of the output vector of first hidden layer may be calculated as,

$$f_j = \varphi_j \left[\sum_{i=1}^N w_{ij} x_i(n) + b_j \right], \quad i = 1, 2, \dots, N, \quad j = 1, 2, \dots, P_1 \quad (5.3)$$

Where b_j is the bias to the neurons of the first hidden layer, N is the number of inputs and φ is the nonlinear activation function in the first hidden layer chosen from the Table 5.1. Let P_2 be the number of neurons in the first hidden layer. The output of this layer is represented as, f_k and may be written as,

$$f_k = \varphi_k \left[\sum_{j=1}^{P_1} w_{jk} f_j + b_k \right], \quad k = 1, 2, \dots, P_2 \quad (5.4)$$

where, b_k is the bias to the neurons of the second hidden layer. The output of the final output layer can be calculated as

$$y_l(n) = \varphi_l \left[\sum_{k=1}^{P_2} w_{kl} f_k + b_l \right], \quad l = 1, 2, \dots, P_3 \quad (5.5)$$

where, b_l is the bias to the neuron of the final layer and P_3 is the number of neurons in the output layer. The output of the MLP may be expressed as

$$y_l(n) = \varphi_l \left[\sum_{k=1}^{P_2} w_{kl} \left(\varphi_k \left[\sum_{j=1}^{P_1} w_{jk} \left(\varphi_j \left[\sum_{i=1}^N w_{ij} x_i(n) + b_j \right] \right) + \mathbf{b}_k \right] \right) + b_l \right] \quad (5.6)$$

5.5.2 Radial Basis Function Neural Network

Another popular layered feedforward network is the radial-basis function (RBF) network which has important universal approximation properties, and whose structure is shown in Figure 5.5 [158]. The alternative neural network architecture besides multilayer perceptron (MLP) is radial basis function [162].

RBF networks can be used to approximate any continuous nonlinear function. The weight can be linearly regulated. The learning speed and convergence is fast enough. The characteristics of RBF networks are suitable for many industrial fields such as system identification, control engineering and signal processing [95].

As shown in Figure 5.5, the RBF neural network has three layers: the input layer, the hidden layer and the output layer. The hidden layer consists of an array of computing units called hidden nodes. Each hidden node contains a centre c , which is a parameter vector, and calculates the Euclidean distance between the centre and the network input vector x defined by $\|x(t) - c_j(t)\|$ where $x(t)$ is the RBF neural network inputs, $c_j(t)$ is the j th centre.

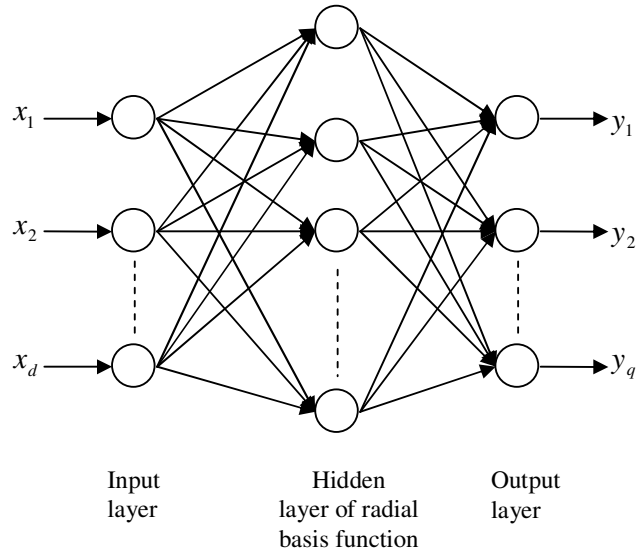


Figure 5.5 Radial basis function neural network structure

The results are then passed through a nonlinear activation function $\phi_j(t)$ to produce the output from the hidden nodes. A popular choice of activation function is the Gaussian basis function:

$$\phi_j(t) = \exp\left(-\frac{\|x(t) - c_j(t)\|^2}{\sigma_j^2}\right), \quad j = 1, 2, \dots, n_h \quad (5.7)$$

where σ_j is a positive scalar called a width and n_h is the number of centers. Since the output layer is essentially a linear combiner, then the i th output of the neural network model at time t is a weighted sum of the hidden node outputs:

$$y_i(t) = \sum_{j=1}^{n_h} \phi_j(t) w_{ji}, \quad i = 1, 2, \dots, q \quad (5.8)$$

Where w are the output layer weights and q is the number of outputs.

RBF networks are best suited for approximating continuous or piecewise continuous real valued mapping $f: R^n \rightarrow R^L$, where n is sufficiently small. These approximation problems include interpolation problems as a special case. From Equations 5.7 and 5.8, the RBF network can be viewed as approximating a desired function $f(x)$ by superposition of non-orthogonal, bell-shaped basis functions. The degree of accuracy of these RBF networks can be controlled by three parameters: the number of basis functions used, their location and their width [163].

5.5.3 Recurrent Neural Network

The recurrent neural network (RNN) that is a special type of the dynamic neural networks is derived from the MLPFF networks given in Figure 5.4 by considering feedback connections among the neurons. Thus, a dynamic effect is introduced into the computational system by a local memory process [75]. Moreover, by retaining the nonlinear mapping features of the MLPFF, the RNN are suitable for black-box nonlinear dynamic modeling [158].

Recurrent networks are the state of the art in nonlinear time series prediction, system identification, and temporal pattern classification. RNN are classified into local or global kind. The application of global feedback can take a variety of forms. The form of global feedback has feedback from the output neurons of the multilayer perceptron to the input layer given in Figure 5.6. Another possible form of global feedback is from the hidden neurons of the network to the input layer [158].

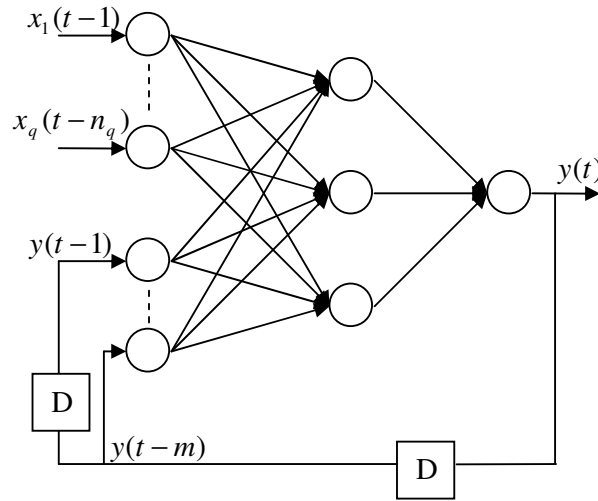


Figure 5.6 Recurrent neural network structure

The RNN with multi-input and single output shown in Figure 5.6 is of the form

$$y(t) = \sum_{i=1}^{HN} w_i s \left[\sum_{j=1}^n w_{ij} I_j(t) \right] \quad (5.9)$$

where $y(t)$ is the output of the neural model; w_i and w_{ij} are the synaptic weights which connect the hidden nodes with the output, and connect the inputs to the hidden nodes, respectively; HN is the number of hidden node; n is the number of total inputs; $I(t) = [y(t-1), \dots, y(t-m); x_1(t-1), \dots, x_1(t-m_1); x_q(t-1), \dots, x_q(t-n_q)]^T$ is the input vector where $\{y(t-1), \dots, y(t-m)\}$ are the recurrent terms which are the neural model output delayed in time. $s(\cdot)$ is the activation function listed in Table 5.1 [1].

Elman, Hopfield, self-organizing map can be given as an example of recurrent network. Elman network is the simplest structure and easiest to use. Some popular recurrent network architectures are the Elman recurrent network in which the hidden unit activation values are feedback to an extra set of input [164].

5.5.3.1 Elman Recurrent Neural Network

Elman neural network is a dynamic recurrent neural network with feedback layer which owns the dynamic characteristics and recurrent function [91]. The feedback connections in Elman recurrent neural network are from the outputs of neurons in the hidden layer to the context layer units that are called as context nodes. This part of input layer, namely, the context layer, plays a role in storing internal states in Elman neural networks [165]. Mathematical description of Elman type RNN can be given as follows:

The structure of an Elman RNN is illustrated in Figure 5.7. Here, X , Y , C , Z and z^{-1} and are input layer vector, hidden layer vector, context layer vector, output layer vector and unit delay element respectively [165].

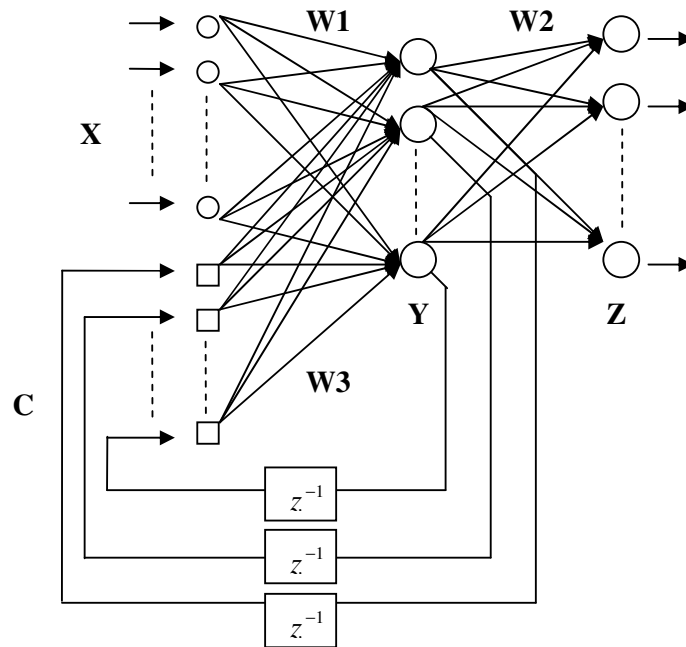


Figure 5.7 Elman recurrent neural network structure

Weight matrices are as follows: $W1$ is the weight matrix between input layer and hidden layer, $W3$ the weight matrix between context layer and hidden layer and $W2$ is the weight matrix between hidden layer and output layer [165].

At s th iteration, all vector components are as follows:

$$\begin{aligned} x_i^{(s)} &\in X, & i &= 1, \dots, n, \\ y_j^{(s)} &\in Y, & j &= 1, \dots, m, \\ z_k^{(s)} &\in Z, & k &= 1, \dots, l, \\ c_{i'}^{(s)} &= C, & i' &= j. \end{aligned}$$

Here, index i , j , k and i' indicate the number of input nodes, hidden nodes, output nodes and context layer nodes, respectively. And also, to compute the hidden node outputs, considering the activation function $f(\cdot)$ for j th hidden node output at s th iteration can be defined as

$$y_j^{(s)} = f(a_j^{(s)}), \quad (5.10)$$

where $a_j^{(s)}$ is linear output of hidden node j at s th iteration. Context layer input at s th iteration can also be given by

$$c_{i'}^{(s)} = y_j^{(s-1)} \quad (5.11)$$

For initial cases of Elman neural network, assuming

$$y_j^{(0)} = 0, \quad (j = 1, 2, \dots, m). \quad (5.12)$$

The context layer input at $s = 1$ leads to $c_i^{(1)} = 0$. In terms of weight matrix of the neural structure, each weight coefficient can be defined as an element of these matrices as $w1_{ij} \in W1$, $w3_{ij} \in W3$, $w2_{jk} \in W2$.

Hence, using the weight matrices, the outputs of the neurons in the hidden layer and output layer for s th iteration can be computed as

$$y_j^{(s)} = f\left(\sum_{i=1}^n w1_{ij} x_i^{(s)} + \sum_{j=1}^m w3_{ij} y_j^{(s-1)}\right), \quad (5.13)$$

and

$$z_k^{(s)} = f\left(\sum_{j=1}^m w2_{jk} y_j^{(s)}\right). \quad (5.14)$$

And also, updated weight coefficients can be given to minimize the approximation error E in the output layer by

$$w^{new} = w^{old} + \eta \Delta w, \quad (5.15)$$

where η is the learning rate. E is defined for all pattern vectors and output nodes with the following relationship:

$$E(w) = \frac{1}{2} \sum_{s=1}^p \sum_{k=1}^l [Z_k^{(s)} - z_k^{(s)}]^2, \quad (5.16)$$

where $Z_k^{(s)}$ is the target value at s th iteration.

Here, p is the length of the training sequence and weight coefficient matrices of $W1$ and $W3$, can be adjusted using the standard Back-Propagation algorithm, because this part of the network that takes place between the input and output layers, in the feedforward character [165].

5.6 Learning Algorithm

There are various types of algorithms for training the network. Basically, the purpose of every algorithm is to estimate the local error at each neuron and systematically update the network weights. In this thesis, the feedforward neural network was trained with the back propagation algorithm and Levenberg-Marquardt algorithm to estimate/assess their search efficiency and accuracy in this thesis. The details of the above algorithms are given in the following section.

5.6.1 Backpropagation Algorithm

A back propagation (BP) algorithm, which is the most widely used training algorithm for the multi layer perception, is a gradient descent technique to minimize the error for a particular training pattern and was popularized by Rumelhart and coworkers [159]. Accordingly, for a given input pattern, a flow of activation is forwarded from the input layer to the output layer via hidden layer(s). Then the errors in the output are initiated. BP algorithm is used to adjust the weights, a small amount at a time, in a way that reduces the error. The training of the network is accomplished by adjusting the weights and is carried out through a large number of training sets and training cycles (epochs). The goal of the learning procedure is to find the optimal set of weights, which in the ideal case would produce the right output for any input. The output of the network is compared with a desired response to produce an error. Once the ANN is adequately trained, it can generalize to similar cases, which it has never seen. The BP algorithm for a neural network works as follows.

Define the instantaneous overall network error at time t as

$$E(t) = \frac{1}{2} \sum_{j=1}^J [T_j(t) - z_j(t)]^2 \quad (5.17)$$

where $T_j(t)$ is the target value of neuron j at time t ; and $z_j(t)$ is the network output of neuron j at time t .

The energy function is obtained by summing $E(t)$ over all time T .

$$E_{\text{total}} = \sum_{i=1}^T E(t) \quad (5.18)$$

The weight change for any particular weight W_{ji} , which connects neuron j in this layer with neuron i in the previous layer, can thus be written as

$$\Delta W_{ji} = -\eta \frac{\partial E}{\partial W_{ji}} \quad (5.19)$$

where η is the learning rate parameter.

Using the chain rule for partial derivatives, the weight change can be generalized as

$$\Delta w_{ji}^n = \eta^n \delta_j^n z_j^{n-1} \quad (5.20)$$

where z_j^{n-1} represents the output value of neuron j in the $(n-1)$ th layer, $\delta_j^n = \left(\sum_{h=1} \delta_h^{n+1} w_{hj}^{n+1} \right) g'(v_j^n)$ for the hidden layers, and $g(\cdot)$ represents the first derivative of nonlinear activation function.

Further details on the BP algorithm can be found in Ref. [159].

5.6.2 Levenberg-Marquardt Algorithm

Levenberg-Marquardt method is an approximation to Newton's method [166]. The algorithm uses the second-order derivatives of the cost function so that a better convergence behavior is observed. In the ordinary gradient descent search, only the first-order derivatives are evaluated and the parameter change information contains solely the direction along which the cost is minimized, whereas the Levenberg-Marquardt technique extracts a better parameter change vector [166]. Newton's original approach assumes that a function $E(w)$ is minimized if the successive changes defined by Equation (5.21) are given to the parameter vector w .

$$\Delta w = -(\nabla^2 E(w))^{-1} \nabla E(w) \quad (5.21)$$

We assume the performance function is defined as follows;

$$E(w) = \frac{1}{2} \sum_{q=1}^Q (t_q - o_q)^T (t_q - o_q) \quad (5.22)$$

In Equation (5.22) q indexes the training pairs, and Q is the number of training pairs, t denotes the target output and o denotes the actual output of the network. If Equation (5.22) is rewritten with respect to the output error which depends on the weight vector, we obtain Equation (5.23).

$$E(w) = \frac{1}{2} \sum_{q=1}^Q e_q^T(w) e_q(w) \quad (5.23)$$

The objective is to minimize each individual multiplication in Equation (5.23). If Taylor series expansion is applied to $e_q(w)$ around w_0 ;

$$e_q(w) \approx \hat{e}_q(w) = e_q(w_0) + J^T(w - w_0) \quad (5.24)$$

In Equation (5.24) J is the Jacobian matrix and evaluated at w_0 . The entries of this matrix represent the derivative of the error evaluated at the i^{th} output with respect to the j^{th} parameter of the parameter vector. And, this statement obviously implies that the number of rows of the Jacobian matrix is equal to the multiplication of the number of network outputs and the number of the training pairs. Similarly, the parameter vector will have an entry for all weights and biases of the network [18].

$$J_{ij} = \frac{\partial e_{qi}(w)}{\partial w_j} \quad (5.25)$$

We define an approximate error component as described in Equation (5.26). Differentiating this equation with respect to parameter vector w and equating zero gives the usual “normal equation” of the linear least squares problem.

$$\varphi(w) = \hat{e}_q^T(w) \hat{e}_q(w) \quad (5.26)$$

$$J^T J(w - w_0) + J^T e_q(w) = 0 \quad (5.27)$$

From Equation (5.27), the change in parameter vector turns out to be Equation (5.28).

$$\Delta w = -(J^T J)^{-1} J^T e_q(w) \quad (5.28)$$

The terms appear in Equation (5.28) are explained as follows;

$$\nabla E(w) = J^T e_q(w) \quad (5.29)$$

$$\nabla^2 E(w) = J^T J \quad (5.30)$$

Equation (5.29) represents the first derivative of the performance function, Equation (5.30) represents the second derivative of the performance function and is called Hessian matrix. Levenberg and Marquardt Equation (5.28) by adding extra term to the Hessian matrix [18]. The resulting parameter update rule is then introduced to be;

$$\Delta w = -(J^T J + \mu I)^{-1} J^T e_q(w) \quad (5.31)$$

In fact, the reason for this modification is that this additional term compensates the approximation errors. Actually, the method seems to minimize Φ but this may not always imply that $E(w)$ is minimized. Therefore, a scaling is introduced to Hessian matrix evaluation part of the method. If a step reduces $E(w)$ then μ is decreased, otherwise μ is increased by some factor greater than one. Note that, if μ is large, the method becomes steepest descent because the modification dominates the term $J^T J$ term only the first order derivative information remains, on the other extreme, if μ is too small then the method becomes pure Gauss-Newton method. Therefore the method is considered as a trust region modification to Gauss-Newton [18].

5.7 Neural Networks for Identification of Nonlinear Dynamic Systems

In analogy to linear system identification, a nonlinear dynamic model can be used in two configurations: series-parallel and parallel models [17].

- Series-parallel model: the previous process inputs $u(k-i)$ and process outputs $y(k-i)$ are used as inputs to the model. This model can be considered as a feedforward. The model is said to have *external dynamics*.
- Parallel model: the previous process inputs $u(k-i)$ and the model outputs $\hat{y}(k-i)$ are used as inputs to the model. This model can be considered as a recurrent model. The model is said to have *internal dynamics*.

Figure 5.8 compares the model configuration for both models. In both cases the model is trained by minimizing a loss function dependent on the error $e(k)$.

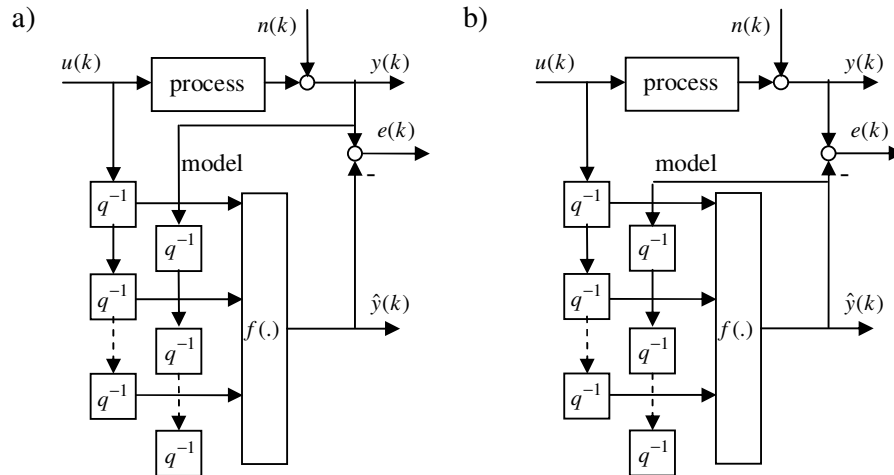


Figure 5.8 a) Series-parallel model b) parallel model

For dynamic systems and for controllers, the model must have some way to implement time lags. In other words: some memory function must be present in the model. In NN modeling this can be done twofold: either delayed inputs and outputs are used as extra external inputs, or some memory is included in the individual neurons [167].

5.7.1 External Dynamics

The external dynamics strategy is by far the most frequently applied nonlinear dynamic system modeling and identification approach. It is based on the nonlinear input/output model of a m th order in Equation 5.32 [17]

$$\hat{y}(k) = f(u(k-1), \dots, u(k-m), y(k-1), \dots, y(k-m)) \quad (5.32)$$

All nonlinear dynamic input/output models can be written in the form

$$\hat{y}(k) = f(\varphi(k)) \quad (5.33)$$

where the regression vector $\varphi(k)$ can contain previous and possibly current process inputs, previous process or model outputs, and previous prediction errors [17].

The three most common linear model structures are autoregressive with exogenous input (ARX), autoregressive moving average with exogenous input (ARMAX) and output error (OE) models. Their nonlinear counterparts possess the following regression vectors with $(e(k) = y(k) - \hat{y}(k))$:

Time delay neural network (TDNN) or NARX

$$\hat{y}(k) = f_{NN}(u(k-1), \dots, u(k-n_u), y(k-1), \dots, y(k-n_y)) \quad (5.34)$$

NARMAX

$$\hat{y}(k) = f_{NN}(u(k-1), \dots, u(k-n_u), y(k-1), \dots, y(k-n_y), e(k-1), \dots, e(k-n_e)) \quad (5.35)$$

NOE

$$\hat{y}(k) = f_{NN}(u(k-1), \dots, u(k-n_u), \hat{y}(k-1), \dots, \hat{y}(k-n_y)) \quad (5.36)$$

where n_y, n_u, n_e denoted the dynamic order of the model output, input and error respectively.

Thus, the NARX model is trained in series-parallel configuration (Figure 5.8a) and the NOE model is trained in parallel configuration. The NARMAX model requires both, process outputs $y(k-i)$ and model outputs $\hat{y}(k-i)$ contained in $e(k-i)$ [17].

Since for nonlinear problems the complexity usually increases strongly with the input space dimensionality, the application of lower dimensional NARX or NOE models is widespread. One drawback of models with output feedback is that the choice of the dynamic order is crucial for the performance and no really efficient methods for its determination are available. Often the user is left with a trial-and-error approach. Another disadvantage of output with feedback is that in general stability can not be proven for this kind of models [17].

In opposition to these drawbacks, models with output feedback compared with those without output feedback have the strong advantage of being a very compact description of the process [17].

5.7.2 Internal Dynamics

Models with internal dynamics are based on the extension of static models with internal memory. In contrast to models with external dynamics, the use of past inputs and past outputs at the model input is not necessary. Therefore, the application of internal dynamic models leads to a desirable reduction of the input space dimensionality. Since internal dynamic models possess no external feedback, only the parallel model approach in figure 5.8b can be applied. Consequently, these models are not well suited one-step prediction tasks.

5.7.3 Training Feedforward and Recurrent Structures

From the internal dynamic approach recurrent structures always arise. From the external dynamic approach NARX models are feedforward during training but NOE models are recurrent since they apply the parallel model configuration [17].

Training of feedforward structures is equivalent to the training of static models. However, training of recurrent structures is more complicated because the feedback has to be taken into account. In particular, training recurrent models is always a nonlinear optimization problem independent of whether the utilized static model architecture is linear or nonlinear in the parameters. This severe drawback is a further reason for the popularity of feedforward structures such as the NARX model. Therefore, in nonlinear system identification, the choice of the dynamic representation is highly interconnected with the choice of the model architecture [17].

5.7.4 Choosing a Model

Models with external dynamics can be seen as one-step predictors. Models with internal dynamics are best used for simulation purposes, as the model doesn't need the true plant outputs.

The criteria that determine the choice of the model are the following:

- Which information is available? It seems obvious that all possible information must be used for the model, i.e. the true outputs, the noise contributions, and the past inputs. The result is an increasing number of model parameters that need to be optimized. If only the exogenous input u is known, then the only models possible are NOE. If the plant outputs can be measured, a NARX model can be taken into consideration. In general it is not possible to know the process noise n , but it could be estimated for use with a NARMAX model.
- Can significant time lags be estimated? The determination of the values of n_y, n_u, n_e is still an open question. It seems obvious that large values allow for better prediction of the future state of the NN. However, large time lags also result in large parameters vector that need to be optimized.
- How many measurements are available for the optimization of the parameter vector? Models with a large number of parameters, don't match with a small measurement set.

- Is the model used for control of simulation purposes? For simulation purposes, only NOE or NFIR models fit the job, because they don't need the current plant outputs.
- Are transients an issue? Model with large time lags or with internal dynamics, can suffer from large transients when the system is brought into a new state.

Since it is the goal to have at least number of parameters, it makes sense to choose the simplest model available, and switch over to more complex models if this yields a significant improvement in performance [167].

5.8 Conclusions

In this chapter, the information about the neural network and neural network structures are provided. And also neural networks for identification of nonlinear dynamic systems explained. Neural network structures will be used in gasoline engine torque identification.

CHAPTER 6

6. MEAN VALUE MODEL OF A SPARK IGNITION ENGINE

6.1 Introduction

The engine model is referred to as the mean value engine model (MVEM) developed by Hendricks and coworkers [168-170] which is widely used benchmark for engine modeling and control. A mean value model (MVM) is a mathematical engine model which is intermediate between large cyclic simulation models and simplistic transfer function models. It predicts the mean values of major external engine variables like crankshaft speed and manifold pressure dynamically in time [171].

The main engine sub-models include the air system that defines how much air is inducted into the cylinder; the fuel system that defines how much fuel is inducted in to the cylinder; the torque generation system that defines how much torque is produced by the air and fuel in the cylinder as defined by the first two parts; the engine inertial system that defines the engine speed; the engine thermal system that defines the thermal behavior of the engine; the pollution formation system that models the engine out emission [172].

All these models are control oriented models (COM), i.e. they model the input-output behavior of the systems with reasonable precision but low computational complexity, and include explicitly, all relevant dynamic effects [172].

The SI engine has several input (command) signals, one main disturbance signal (the load torque) and several output signals as shown in Figure 6.1. The inputs are signals, i.e. quantities that can be arbitrarily chosen in order to allow full control of

engine, usually these will be electric signals. The outputs also are signals that can be used by controller without the system behavior being effected [172].

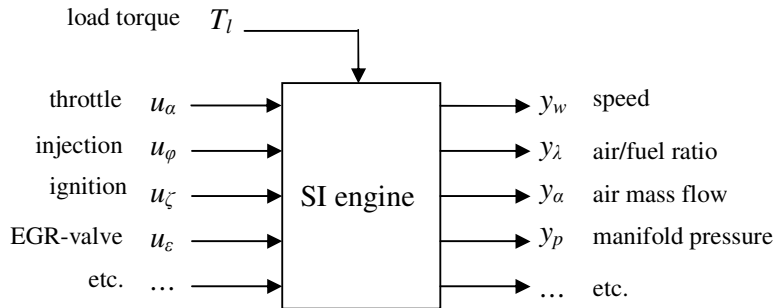


Figure 6.1 Main system's input/output signals in a COM of an SI engine

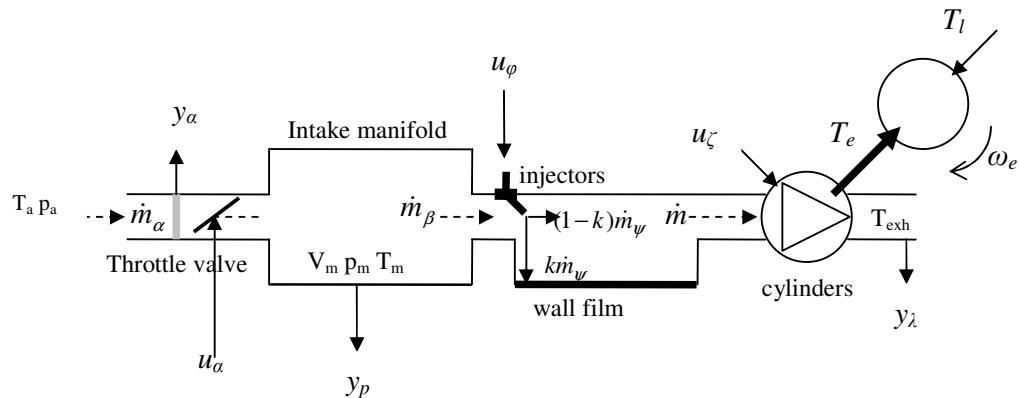


Figure 6.2 Mean-value SI engine structure [172]

Spark ignition (SI) engine system has the structure shown in Figure 6.2. In a mean value approach, the reciprocating behavior of the cylinders is replaced by a continuously working volumetric pump that produces exhaust gases and torque. The resulting main engine components are shown in Figure 6.2.

Figure 6.3 shows the resulting simplified cause and effect diagram of an SI engine. Both air and fuel paths affect the combustion through some delaying blocks while the ignition affects the combustion almost directly. The main output variables of the

combustion process are the engine torque T_e , the exhaust gas temperature T_{exh} and the air/fuel ratio λ_e .

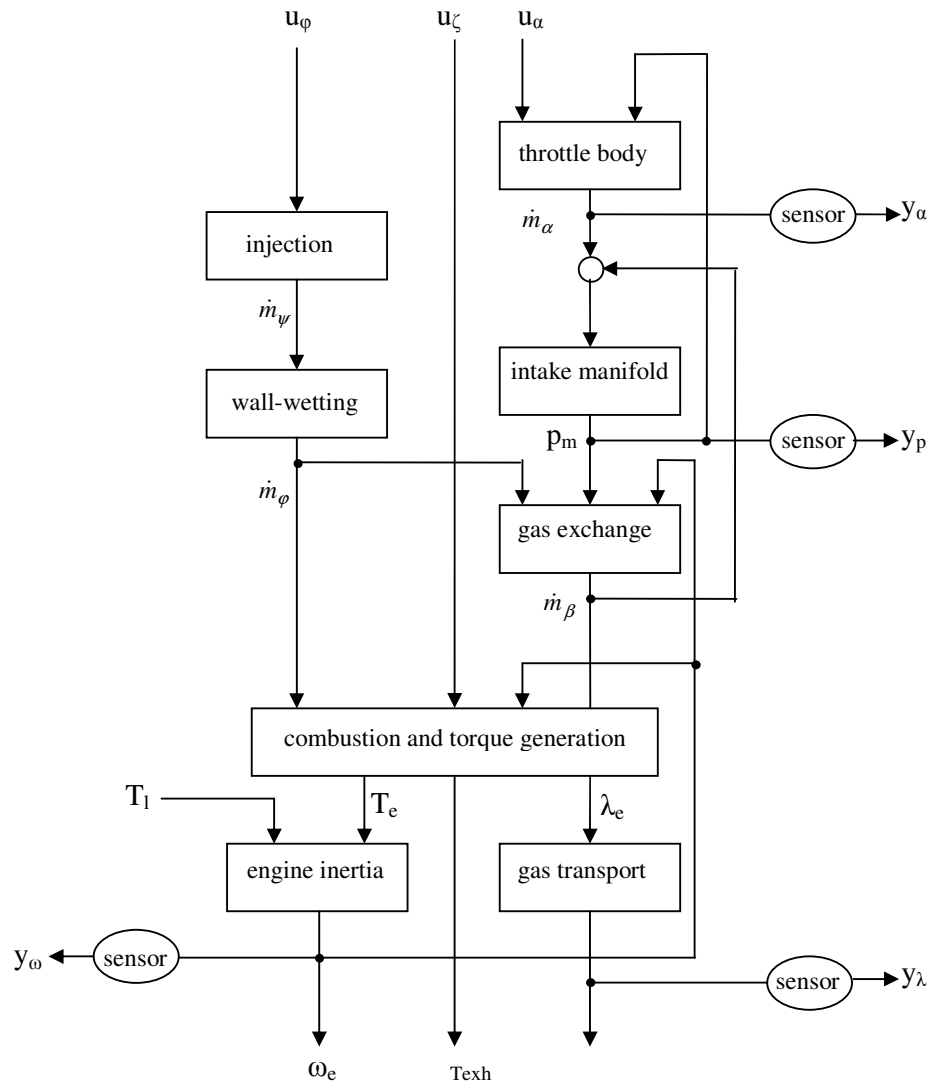


Figure 6.3 Cause and effect diagram of an SI engine system [172]

All gasoline fuelled SI MVEMs have basically three main subsystems: 1) the manifold air dynamics, 2) the fueling dynamics and 3) the crankshaft dynamics. Because of the nature of an SI engine, these subsystems are described by very different physical models which are more or less empirical [173].

6.2 Intake Manifold Filling Dynamics

The intake manifold of the engine is the volume between the throttle plate and the intake valves of the cylinder. The throttle controls the air flow into the intake manifold [171].

The intake manifold filling dynamics are analyzed from the viewpoint of the air mass conservation inside the intake manifold [170, 172].

$$\dot{m}_m = \dot{m}_{at} - \dot{m}_{ap} \quad (6.1)$$

where \dot{m}_{at} and \dot{m}_{ap} represents air mass flow rate past throttle plate and air mass flow rate into the intake port, respectively.

The pressure in the intake manifold p_m can be related to the mass of air in the manifold m_m using ideal gas equation [170-172]:

$$p_m V_m = m_m R T_m \quad (6.2)$$

where R is the ideal gas constant, T_m is the intake manifold temperature and V_m is the intake manifold volume.

Taking derivatives of equation 6.2 and substituting from equation 6.1, the intake manifold pressure equation is obtained as

$$\dot{p}_m = \frac{R T_m}{V_m} (\dot{m}_{at} - \dot{m}_{ap}) \quad (6.3)$$

6.2.1 Throttle Body Flow

Normally an engine has two mass flows: through the throttle valve and through the by-pass throttle valve. It is assumed that the by-pass is open only in the idle speed mode. However, nearly all available measurements are for other modes than the idle speed mode, so the by-pass air flow in the identification process is neglected. In fact,

the by-pass identification is included in the identification of the flow through the throttle valve [174].

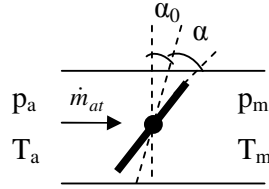


Figure 6.4 Throttle body flow

The throttle body consists of a cylindrical bore with a throttle plate to control the air flow to the engine shown in Figure 6.4. The throttle body model is based on the theory for one-dimensional, steady, isentropic, compressible flow of an ideal gas across an orifice [174]. The mass flow rate through the throttle body into the intake manifold can be calculated from the orifice equation for compressible fluid flow [168, 170]. The equation for the air mass flow entering the intake manifold through the throttle \dot{m}_{at} then becomes:

$$\dot{m}_{at} = c_d A(\alpha) \frac{p_a}{\sqrt{RT_a}} \Psi\left(\frac{p_a}{p_m}\right) \quad (6.4)$$

where c_d is the discharge coefficient and A is the opened area of throttle, depending on the angle (α) of the throttle plate [174].

$$A(\alpha) = \frac{\pi}{4} D^2 \left(1 - \frac{\cos(\alpha + \alpha_0)}{\cos(\alpha_0)}\right) \quad (6.5)$$

For many working fluids (e.g., intake air, exhaust gas at lower temperatures, etc.) with $\kappa \approx 1.4$ the flow function $\Psi(\cdot)$ is defined by [172]

$$\Psi\left(\frac{p_a}{p_m}\right) \approx \begin{cases} 1/\sqrt{2} & \text{for } p_m < \frac{1}{2} p_a \\ \sqrt{\frac{2p_m}{p_a} \left[1 - \frac{p_m}{p_a}\right]} & \text{for } p_m \geq \frac{1}{2} p_a \end{cases} \quad (6.6)$$

6.2.2 Cylinder Flow

The air mass flow \dot{m}_{ap} from the intake manifold into the cylinders follows from the so-called speed density formula [170]

$$\dot{m}_{ap} = \eta_{vol} \frac{\omega_e}{4\pi} V_d \frac{p_m}{RT_m} \quad (6.7)$$

where η_{vol} is the volumetric efficiency which is a complex function of many engine parameters and the variables p_m and ω_e , V_d is the displacement volume of the engine cylinders and $\frac{p_m}{RT_m}$ is the density of air in the intake manifold.

So, intake manifold pressure dynamic (Equation 6.3) can be written into the form

$$\dot{p}_m = \frac{RT_m}{V_m} \left(c_d A(\alpha) \frac{p_a}{\sqrt{RT_a}} \Psi \left(\frac{p_a}{p_m} \right) - \eta_{vol} \frac{\omega_e}{4\pi} V_d \frac{p_m}{RT_m} \right) \quad (6.8)$$

6.3 Fueling Dynamics

The fuel path which is the subsystem that provides the necessary fuel for the combustion process to the cylinder has its own dynamics. One of the most important dynamic effects in the fuel path is caused by the wall-wetting phenomena. The liquid fuel injected into the intake port only partially enters the cylinder in the next intake stroke. Some of it is stored in fuel puddles of the mass m_f at the intake port walls and at the back face of the intake valve. Of course, fuel also evaporates from these puddles such that a mass balance can be expressed as follows [172]:

$$\dot{m}_\varphi = (1 - \kappa(\omega_e, p_m, T_f, \dots)) \dot{m}_\psi + \frac{m_f}{\tau(\omega_e, p_m, T_f, \dots)} \quad (6.9)$$

and

$$\frac{d}{dt}m_f = \kappa(\omega_e, p_m, T_f, \dots)\dot{m}_\psi - \frac{m_f}{\tau(\omega_e, p_m, T_f, \dots)} \quad (6.10)$$

where \dot{m}_ψ is the fuel mass injected, \dot{m}_ϕ the fuel mass aspirated into the cylinder, and m_f the mass of fuel stored in the fuel film. The coefficients $\kappa(\cdot)$ and $\tau(\cdot)$ depend on the engine speed and load, and many other variables (mean fuel temperature T_f , etc.) [172].

The model applied in [175] is a simplified version of the model used in [172]. The fuel mass flow rate \dot{m}_ϕ is typically determined by a fuel injection control system which attempts to maintain stoichiometric air to fuel ratio in the cylinders. If it is assumed that a stoichiometric air fuel ratio is successfully maintained in the cylinders, then the fuel mass flow rate \dot{m}_ϕ is related to the outflow from the intake manifold into the cylinders of the engine as follows [175, 176]:

$$\dot{m}_\phi = \frac{\dot{m}_{ap}}{\lambda L_{th}} \quad (6.11)$$

where \dot{m}_{ap} is the air mass flow rate out of the intake manifold an into the cylinder, L_{th} is the stoichiometric air/fuel mass ratio for gasoline (fuel) and λ is the air/fuel equivalence ratio. Here, $\lambda=1$ and $L_{th}=14.67$ [175].

According to Hendricks's identification experiments with SI engine, the fuel flow dynamics could be described as following equations [177]:

$$\dot{m}_{ff} = \frac{1}{\tau_f}(-\dot{m}_{ff} + X_f \dot{m}_{fi}) \quad (6.12)$$

$$\dot{m}_{fv} = (1 - X_f)\dot{m}_{fi} \quad (6.13)$$

$$\dot{m}_\phi = \dot{m}_{fv} + \dot{m}_{ff} \quad (6.14)$$

where the model is based on keeping track of the fuel mass flow. The parameters in the model are the time constant for fuel evaporation, τ_f , and the proportion X_f of the fuel which is deposited on the intake manifold, \dot{m}_{ff} , or close to the intake valves, \dot{m}_{fv} . These parameters are operating point dependent and thus the model is non-linear in spite of its linear form.

6.4 Crankshaft Speed Dynamics

The primary objective of an engine is to produce mechanical power. The torque generation phase, which consists of the cylinders that convert the chemical energy in air fuel mixture inflow into mechanical engine torque, is governed by a nonlinear dynamic equation of dependent variables including air/fuel ratio, fuel mass in cylinders, engine speed, ignition and injection timing, and several others. The mean-value engine torque is therefore expressed as a nonlinear function of these variables and time [172].

The crankshaft rotational dynamics can be represented by [171]

$$I_e \dot{\omega}_e = T_{ind} - T_{load} + T_f \quad (6.15)$$

where I_e is the moment of inertia of the engine flywheel, crankshaft, connecting rod, piston and valve train assembly. T_{load} is the external load torque. Under road conditions, this torque is mainly due to rolling resistance, aerodynamic drag of the vehicle and the friction in the driveline, etc. Also torques to drive engine accessories (power-steering, fan and air conditioner) can contribute to T_{load} . Under testing conditions, T_{load} equals the brake torque applied by the dynamometer (measured). T_f is the torque due to friction and pumping losses in the engine. T_{ind} represents the indicated combustion torque [174].

6.4.1 Indicated Combustion Torque

The indicated torque, T_{ind} , is generated by combustion and can be represented by [170]:

$$T_{ind} = \frac{H_u \eta_i \dot{m}_\phi}{\omega_e} \quad (6.16)$$

where H_u is the fuel heating value of gasoline ($H_u=45.10^6$ J/kg), η_i is the thermal efficiency multiplier and accounts for the cooling and exhaust system losses, and \dot{m}_ϕ represents the fuel mass flow rate into the cylinders given in Equation 6.11.

In reality, the indicated and friction torques vary as the engine rotates through the thermodynamic cycle. In a mean value engine model however, the dynamics of rotation are averaged over time [171].

6.4.2 Friction and Pumping Losses

The term T_f in the rotational engine dynamic equation 6.15 represents the hydrodynamic and pumping friction losses represented in terms of a loss torque [171].

The fundamental component of mechanical friction losses in an engine is hydrodynamic or fluid-film friction. A reasonable choice of polynomial expression for these friction losses in terms of engine speed ω_e rad/s is [178]:

$$F_{loss} = a_0 \omega_e^2 + a_1 \omega_e + a_2 \quad (6.17)$$

In this expression, the constant term a_2 represents boundary friction, the linear term $a_1 \omega_e$ accounts for hydrodynamic or viscous friction and $a_0 \omega_e^2$ accounts for turbulent dissipation. Turbulent dissipation is found to be proportional to ω_e^2 and constant of proportionality depends on the geometry of the flow-path [178].

The pumping losses are found to be proportional to the pumping mean effective pressure and the operational speed [170]. The pumping mean effective pressure is defined to be the difference between exhaust pressure and manifold pressure, $p_{exh} - p_m$. Therefore the pumping losses can be modeled as [170, 171]:

$$P_{loss} = b_0 \omega_e p_m + b_1 p_m \quad (6.18)$$

since the exhaust pressure is nearly constant and is equal to the atmospheric pressure.

Total friction and pumping losses in an engine can thus be expressed as polynomials in the engine speed and manifold pressure as follows [170, 175]:

$$T_f = a_0 \omega_e^2 + a_1 \omega_e + a_2 + b_0 \omega_e p_m + b_1 p_m \quad (6.19)$$

where a_0, a_1, a_2, b_0, b_1 are parameters dependent on the specific engine.

Finally, the crankshaft speed is derived based on the conservation of the rotational energy on the crankshaft.

$$\begin{aligned} \dot{\omega}_e = & -\frac{1}{I} (F_{loss}(\omega_e) + P_{loss}(p_m, \omega_e) + T_{load}(\omega_e)) \\ & + \frac{1}{I} H_u \eta_i(p_m, \omega_e, \lambda) \dot{m}_\varphi(t - \Delta\tau_d). \end{aligned} \quad (6.20)$$

where I is the scaled moment of inertia of the engine and its load and mean injection torque time delay has been taken into account with variable $\Delta\tau_d$ [94].

6.5 Conclusions

Mean value engine models (MVEM) are generally accepted as the modeling paradigm for engine control, and are extensively described in the literature. It allows modeling the mean value behavior of some engine parameters. This kind of model represents the global dynamic of the engine and can be easily identified using the common measurements available on production vehicles.

CHAPTER 7

7. EXPERIMENTAL SET-UP AND MEASUREMENT DEVICES

7.1 Introduction

Internal combustion engines have been major power source throughout the history of ground vehicles. The purpose of internal combustion engines is the production of mechanical power from the chemical energy contained in the fuel [178].

In this chapter, we present a detailed description of spark ignition (SI) engine experimental set-up and measuring devices on it. The experimental set up details is provided in section 7.2 along with the specifications of measuring instruments. The experimental procedure for steady-state condition is given in section 7.3. Finally, the experimental procedure for dynamic condition is given in section 7.4. The accuracy of the measuring instruments will affect the calculated results. Hence the uncertainty analysis has to be carried out to calculate the percentage of errors in measurements is given in section 7.5.

7.2 The Experimental Set-up

The engine used in the study has specifications of four-stroke and four cylinders, water cooled cooling system, fueled with carburetor and naturally aspirated. Each cylinder has a bore of 76 mm and a stroke of 71.5 mm. Figure 7.1 shows the schematic representation of the experimental set-up and also measuring devices on it, Figure 7.2 shows the photograph of the SI engine.

The maximum power output of the engine was 52.2 kW at 5500 rpm. The engine is produced by the Fiat Company. Besides the engine itself, flywheel, starting motor, alternator, fuel pump, fuel tank, dashboard and exhaust assemblies are mounted

to the proper places. Specifications of the engine are shown in Table 7.1 in detail. The parts of the system were given in the following sections.

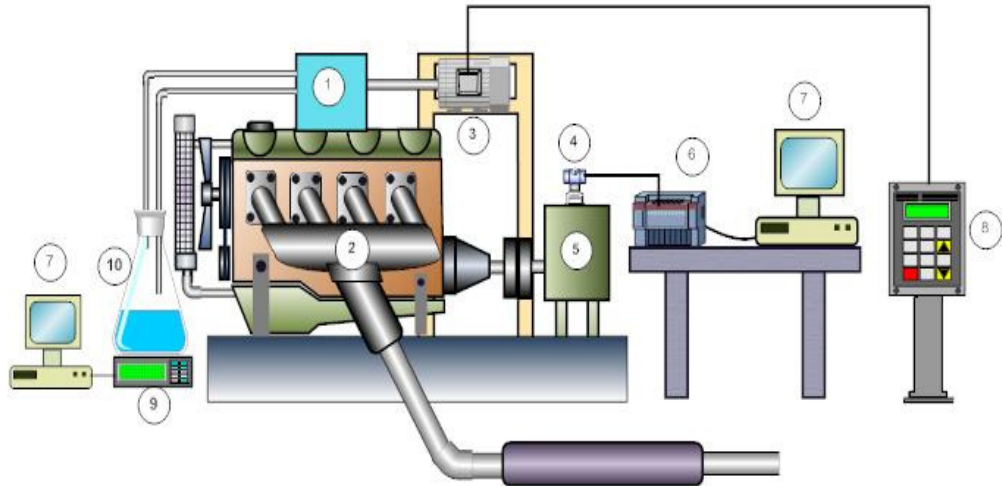


Figure 7.1 Schematics of test engine and setup

1) carburetor, 2) exhaust manifold, 3) servo motor, 4) transducer, 5) dynamometer, 6) data logger, 7) computer, 8) control panel, 9) weighing device, 10) fuel container



Figure 7.2 Photograph of the SI test engine

Table 7.1 Test engine specifications

Type	Fiat Tofaş 131
Engine type	Four-stroke
Fuel type	Gasoline
Swept volume (cm ³)	1297
Cylinder bore (mm)	76
Cylinder stroke (mm)	71.5
Compression ratio	7.8:1
Number of cylinders	4
Cooling type	Water cooled in closed circuit
Fuel supply system	Naturally aspirated carburetor
Maximum torque	12.5 kgm at 3000 rpm
Maximum power	52.2/70 kW/HP at 5500 rpm
Engine position	Vertical

7.2.1 Torque Measurement

Dynamometers are used to measure torque and power over the engine operating ranges of speed and load. They do this by using various methods to absorb the energy output of the engine, all of which eventually ends up as in the form of heat. Some dynamometers absorb energy in a mechanical friction brake (prony brake). These are the simplest dynamometers but are not as flexible and accurate as others at high energy levels. Fluid or hydraulic dynamometers absorb engine energy in water or oil which are pumped through orifices or dissipated with viscous losses in a rotor-stator combination. Large amounts of energy can be absorbed in this manner, making this an attractive type of dynamometer for the largest engines. Eddy current dynamometers use a disk, driven by engine being tested, rotating in a magnetic field of controlled strength. One of the best types of dynamometer is the electric dynamometer, which absorb energy with electrical output from a connected generator [179].

The water brake dynamometer converts the rotating torque of the engine to stationary torque that can be exactly measured and calculated. Simply stated, as the amount of

water within the dynamometer is increased, the load or resistance on the engine is also increased. The resistance made up by dynamometer increases with the speed of the engine. The power made up by the engine is absorbed by the dynamometer, converted into heat energy and transferred into the water flowing out of the absorption unit. The water might enter about at 15 °C and leave at 50 °C.

When the force is applied to the hydraulic load cell piston the pressure induced in the load cell is transferred to pressure transducer. Schematic diagram and picture of water brake engine dynamometer are shown in Figures 7.3 and 7.4, respectively. Equipments used in the experimental study such as water brake dynamometer and hydraulic system, transducer for torque measurement, electrical power supply and voltmeter were schematically shown in Figure 7.3. Torque has obtained in dynamometer when load was applied to engine by dynamometer and thus this causes pressure increase in hydraulic cylinder (4 in Figure 7.3). Then the pressure is measured by transducer volts. The specifications of the dynamometer used in this study were given in Appendix 2.

Dynamometer is calibrated by controlling air in hydraulic system before the experiment started. Engine is run under unloaded conditions as idle after taking air out from hydraulic system. During this process jam nuts (2 in Figure 7.3) are loosened for controlling pressure in hydraulic cylinders (2 in Figure 7.3). Therefore system is set-up for 0.5 volt value of voltage in digital voltmeter. After setup procedure, nuts (2 in Figure 6.6) are fastened. Transducer gives 0.5-5.5 volt in 0-250 psi pressure value linear for pressure measurement. The properties of pressure transducer which is used to measure torque were given in Appendix 3.

Electrical voltage in voltmeter translated to torque by equation 7.1.

$$T = V \cdot \frac{250}{5} \text{ (ft.lb)} \quad (7.1)$$

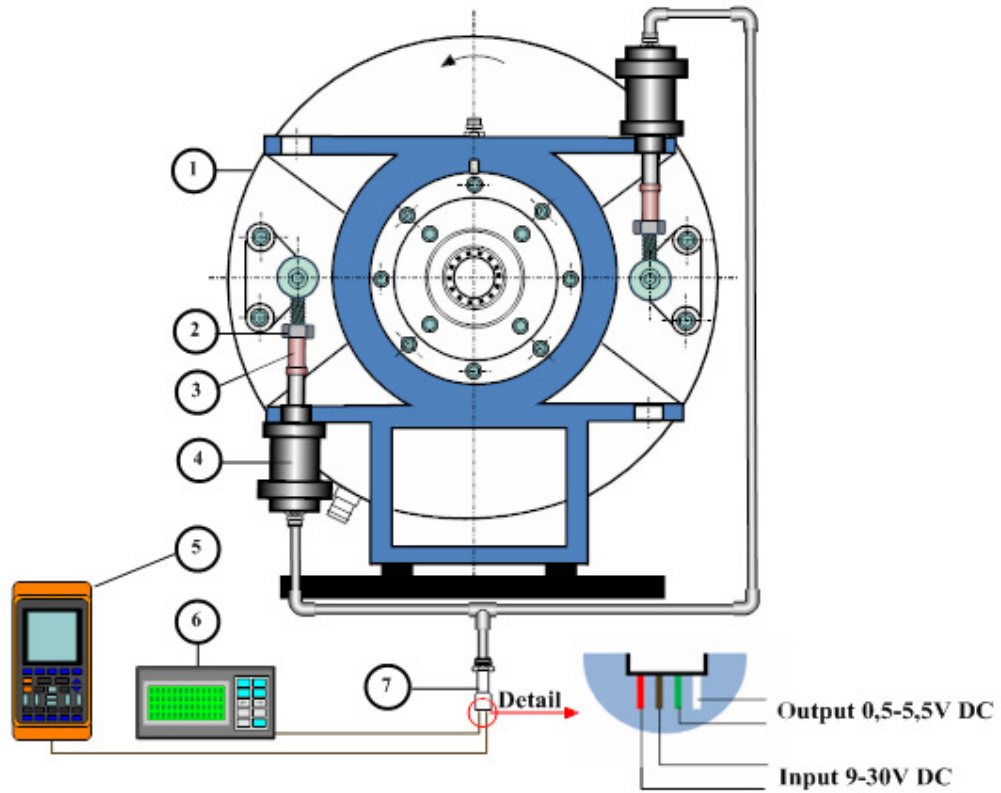


Figure 7.3 Schematic representations of water brake dynamometer and measurement devices. 1) Dynamometer body, 2) jam nut, 3) end push rod, 4) hydraulic load cell, 5) digital voltmeter, 6) electrical power supply, 7) transducer

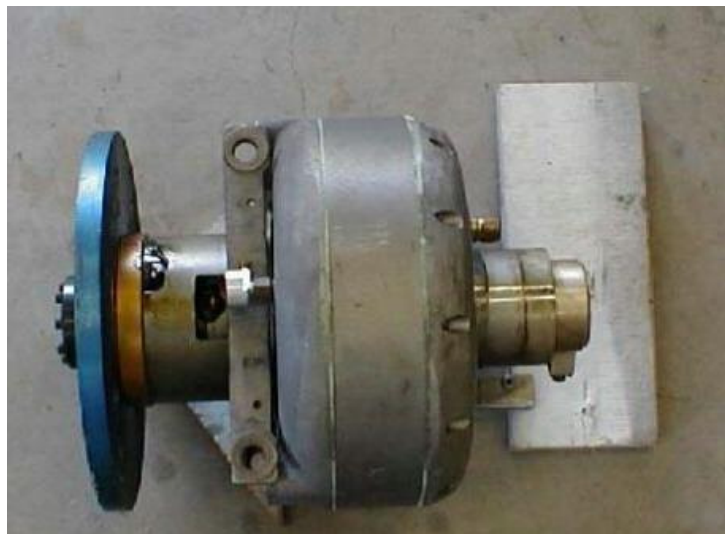


Figure 7.4 Go Power System DA 516 model water brake dynamometer

7.2.2 Mass Fuel Flow Rate Measurement

The electronic scales with 0.1 g resolution were used for the measurement of fuel mass flow rate. The measurements were displayed and stored by computer. For fuel measuring a weight measuring electronic signal output system was used.

In order to calculate the indicated specific fuel consumption, it is necessary to determine accurately the mass of fuel that is consumed by the engine per unit time under given operating conditions. To accomplish this, the engine fuel was supplied with fuel from a small tank. The tank rests on a digital scale that was calibrated in grams. This allows the mass of fuel used by the engine over a given length of time to be measured, so the mass fuel consumption per unit time can be calculated. One of the most important features of the fuel monitoring system is the fuel line support stand. This stand is tripod structure that straddles the scale supporting the fuel line so that it does not rest on the beaker, which would cause an error in the fuel mass measurements. This digital scale was mounted the computer by using RS-232 port. Home-made software was used for reading and saving the outputs of the digital scale.

7.2.3 Servo Motor

Throttle valve is a valve used in vehicles to control the air flow into the engine combustion system. Throttle valve assembly having a servo motor and servo drive to control the opening and closing of the throttle valve in the range of from 0° to about 80°. In automotive engine throttle valve opening is control by the driver actuating the gas pedal. Schematic diagram and picture of servo motor and control unit are shown in Figures 7.5 and 7.6, respectively.

Servo motor is connected on the throttle valve and converts the electrical signal into a throttle valve angle. Throttle valve position is controlled by servo motor which has a 0.75 kW and 3000 rpm. The experimental apparatus consists of a personal computer connected to a servo motor to send an input signal for input-output data measurement. The specifications of the servo motor used in this study were given in Appendix 4.

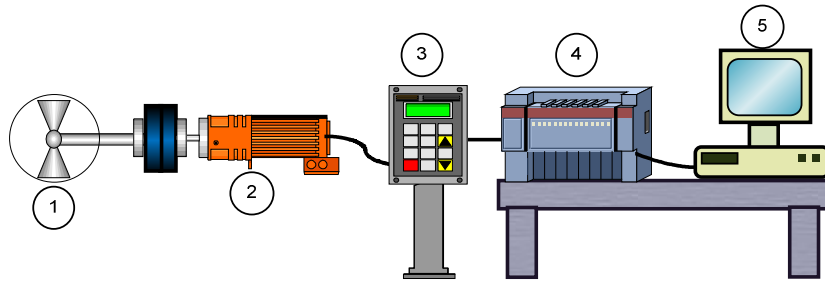


Figure 7.5 Schematic representations of throttle valve position control and control unit on it. 1) throttle valve, 2) servo motor, 3) control panel, 4) data logger 5) computer.

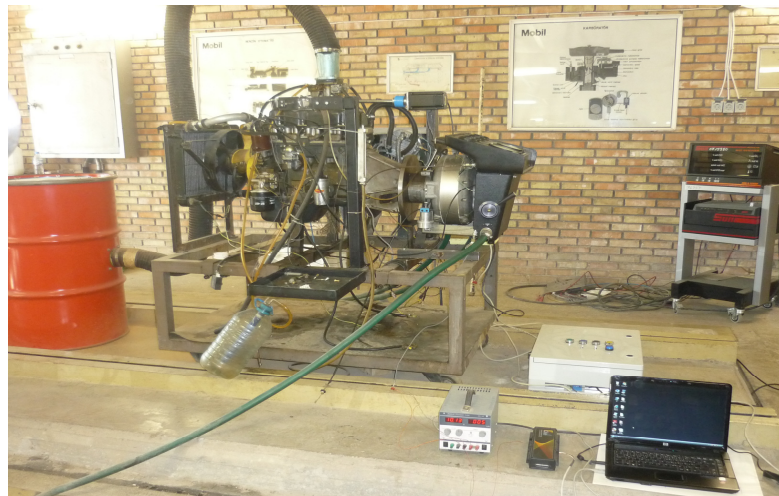


Figure 7.6 Photograph of the throttle valve position control

7.2.4 Data Acquisition

To read and record the data by computer, an interface is necessary between computer and transducers. In our SI engine Data Translation DT 304 DAQ (Data Acquisition Card) is used for that purposes. DT 304 is a family of low cost multi function data acquisition board and is connected at PCI bus of computer. DT 304 board contains 2 analog output channels, 16 single-ended or 8 differential analog input channels and 23 digital input-output channels. Analog channels of the board can acquire or send signal at 12 bit resolution and 400 kS/s (i.e. kHz) sampling rate. Analog output channels are able to generate voltage between -10 DCV to +10 DCV for controlling the position of throttle valve and analog input channels are able to measure between -

10 DCV to +10 DCV for measuring SI engine output torque via pressure transducer. Figure 7.7 shows the general appearance of DT 304 Data acquisition card. Specifications of the DT 304 Data Acquisition Card are given in Appendix 5.

The entire data acquisition cards need a screw terminal panel and connection cable to acquire or to send signals between card and equipments. In our application, Data Translation EP305 68-pin, 2 meter, shielded cable and Data Translation STP300 screw terminal panel are used and general appearance of the cable and screw terminal panel can be seen in Figure 7.8.



Figure 7.7 DT 304 Data Acquisition Card [180]



Figure 7.8 Data Translation STP 300 Screw Terminal Panel and EP305 Cable [180]

7.2.5 Matlab Toolbox

Matlab is a mathematic analysis package produced by Mathworks. This program enables immediate access to high numerical computing and extended with interactive graphical capability. The entire identification and modeling task was performed using Matlab Version R2007a. This software provides Data Acquisition Toolbox for making measurements with a data acquisition system, System Identification Toolbox for fitting nonlinear mathematical models to input and output data from dynamic systems and Neural Network Toolbox for ANN model development with different types of network structure such as feedforward, recurrent, Elman, Radial Basis as well as others.

7.3 Experimental Procedure for Steady-State Condition

Calibration checks of the devices were made two times, one before and one after each successive test. To transfer data into a computer, data logger systems were used. All measurements were conducted under steady-state condition. The measurement was not started until engine runs faultless. Since there were many measurement points, three different PC data logger combinations were used to reduce error resulting from the measurements. The functions of computers, measuring equipments and method of measurement are briefly explained as follows to obtain mass flow rate of air, fuel entering the combustion chamber and engine speed.

The experimental work in this investigation was performed at various spark advance, throttle position and engine speed conditions. Before starting the engine, the spark advance has been adjusted to 10° crank angle (CA), which is a predefined design value of the engine. To start with, our computer-controlled gasoline engine, which is connected to a hydraulic dynamometer, has been loaded, with the 50% throttle position. The engine has been tested in the ranges of 3500- 1500 rpm at intervals of 250 rpm. Torque, fuel flow rate, air flow rate and specific fuel consumption have been recorded. Similarly, these measurements have been repeated for the throttle positions of 75% and 100%.

After the measurements, the engine has been left to cool. Then the ignition time has been adjusted to successively 5 and 0° CA respectively and the above procedure has been repeated.

7.4 Experimental Procedure for Dynamic Condition

Throttle valve position is controlled by servo motor which has a 0.75 kW and 3000 rpm. The torque output was measured by a dynamometer. The experimental apparatus consists of a personal computer connected to a servo motor and torque output, to some input-output measurement. The measured input-output data are transferred with the computer (Pentium III 733 Mhz in speed with 256 MB of RAM) by a data acquisition card (Data Translation DT300 series, 400 kHz in speed, 12 bit high speed A/D converter with a conversion time of 2.5 μ s). The data acquisition card permits user defined programs interfaced with Matlab.

System identification is done using the input-output test data. The test data must incorporate all the properties of the system. So the way system identification experiment is performed is very crucial. In this experiment, considering the engine as an SISO system, the basic input variable is throttle valve position, while the model output engine torque. In engine data collection, the input-output data must be representative of engine behavior in order to identify the engine. This means that input and output signals should adequately cover the region in which the system is going to be modeled. A set of Pseudo Random Binary Signal (PRBS) signals are often very suitable as process inputs because they excite the process at a wide range of amplitudes and frequencies [61, 83, 98]. To create the disturbances needed to perform identification of the process, PRBS were used [38, 52]. A PRBS was designed for throttle angle position to obtain a representative set of input-output data. A set of data samples, including throttle valve position and the torque was collected for the system identification. Each set contains 2000 data samples.

7.5 Uncertainty Analysis

Any experimental result involves some level of uncertainty that may originate from causes such as the lack of accuracy in measurement equipment and approximations

in data reduction relations. These individual inaccuracies eventually translate into uncertainty in the final results.

The uncertainty in calculated results is related to the primary uncertainty for each independent variable. This is based on the method of Kline and McClintock (1953) which state:

$$R = f(x_1, x_2, \dots, x_n) \quad (7.2)$$

Equation 7.2 is the general form of a calculated result R , a function of n variables x_1, x_2, \dots, x_n . We want to estimate the uncertainty in this calculated result based on the uncertainties of the individual variables.

w_R = estimate of the uncertainty in the calculated result R .

w_{x_i} = estimate of the uncertainty in the variable x_i .

$\frac{\partial R}{\partial x_i}$ = sensitivity coefficient for the variable x_i .

$$w_R = \sum_{i=1}^n w_{x_i} \frac{\partial R}{\partial x_i} \quad (7.3)$$

Equation 7.3 is a logical but inappropriate estimate of total uncertainty. It seems like you could just multiply the uncertainty in each term by its sensitivity coefficient, and add them all together to get the total uncertainty. Because of the partials might be negative, and this would cancel some of the error, equation 7.3 shouldn't be used.

$$w_R = \sum_{i=1}^n \left| w_{x_i} \frac{\partial R}{\partial x_i} \right| \quad (7.4)$$

Equation 7.4 corrects the potential problems with negative errors, but tends to overestimate the actual uncertainty. Therefore Equation 7.4 can not be used.

$$w_R = \left(\sum_{i=1}^n \left[w_{x_i} \frac{\partial R}{\partial x_i} \right]^2 \right)^{1/2} \quad (7.5)$$

Equation 7.5 is the one we want. It is referred to as the root of the sum of the squares form, and it not only corrects the sign problem, it has another useful characteristic. Equation 7.5 inherits the same level of confidence as the individual terms. For example, if you established a 95% confidence level for each of the w_{x_i} values, then w_R will also have a 95% confidence level. Equation 7.5 can be used. Note that the partial derivatives will contain values of the variables themselves. The mean value for that variable should be used.

The open form of Equation 7.5 can be written as following

$$w_R = \left[\left(\frac{\partial R}{\partial x_1} w_1 \right)^2 + \left(\frac{\partial R}{\partial x_2} w_2 \right)^2 + \dots + \left(\frac{\partial R}{\partial x_n} w_n \right)^2 \right]^{1/2} \quad (7.6)$$

Cole Parmer C-68075-50 type pressure transducer was used to torque measurement in this study. The specifications of used transducer have been given in Table A.2 in Appendix 3. According to Table B.1 the accuracy of transducer is $\pm 0.25\%$ full-scale. For this reason w_T in Equation 7.5 was selected as 0.0025.

Electrical voltage is given by transducer translated to torque by using following equation.

$$T = V \cdot \frac{250}{5} \cdot 1.356 \quad (7.7)$$

Equation 7.7 only depends on voltage (V) variable, thus $\frac{\partial R}{\partial x_1} = \frac{\partial T}{\partial V}$ can be written.

$$\frac{\partial T}{\partial V} = 50 * 1.356$$

Substituting w_T and $\frac{\partial T}{\partial V}$ in Equation 7.5 gives the uncertainty for torque measurement

$$W_T = \left[\left(\frac{\partial T}{\partial V} w_T \right)^2 \right]^{1/2} = [(50 * 1.356 * 0.0025)^2]^{1/2} \cong \pm 0.17 \text{ (Nm)}$$

The brake power delivered by the engine and absorbed by the dynamometer is the product of torque and engine speed, which is given in the Equation 7.8 by

$$P_b = \frac{n \cdot T}{9554.1401} \quad (7.8)$$

To calculate uncertainty of power:

$$W_{P_b} = \left[\left(\frac{\partial P_b}{\partial T} w_T \right)^2 + \left(\frac{\partial P_b}{\partial n} w_n \right)^2 \right]^{1/2} \quad (7.9)$$

The uncertainty w_n of the tachometer which was used to measure the revolution of engine is 0.5.

$$W_{P_b} = \left[\left(\frac{n}{9554.1401} w_T \right)^2 + \left(\frac{T}{9554.1401} w_n \right)^2 \right]^{1/2} \quad (7.10)$$

If Equation 7.10 is divided by Equation 7.8, the following relation can be obtained.

$$W_{P_b} = \left[\left(\frac{w_T}{T} \right)^2 + \left(\frac{w_n}{n} \right)^2 \right]^{1/2} = [(0.17)^2 + (0.5)^2]^{1/2} \cong \pm 0.53 \text{ kW}$$

was obtained as uncertainty of power.

Brake specific fuel consumption was given in Equation 7.11. The weighing machine with sensitivity of ± 0.1 g was used to determine fuel consumption of engine.

$$Bsf_c = \frac{\dot{m}_f}{P_b} \cdot 10^3 \quad (7.11)$$

The uncertainty of brake specific fuel consumption can be written as

$$W_{Bspc} = \left[\left(\frac{\partial B_{spc}}{\partial \dot{m}_f} w_m \right)^2 + \left(\frac{\partial B_{spc}}{\partial P_b} w_{P_b} \right)^2 \right]^{1/2} \quad (7.12)$$

$$W_{Bspc} = \left[\left(\frac{10^3}{P_b} w_m \right)^2 + \left(-\frac{10^3 \dot{m}_f}{P_b^2} w_{P_b} \right)^2 \right]^{1/2} \quad (7.13)$$

If Equation 7.13 is divided by Equation 7.11, the uncertainty of brake fuel consumption is

$$W_{Bspc} = \left[\left(\frac{w_m}{\dot{m}_f} \right)^2 + \left(-\frac{w_{P_b}}{P_b} \right)^2 \right]^{1/2} = \left[(0.1)^2 + (-0.53)^2 \right]^{1/2} \cong \pm 0.54 \text{ (g/kWh)}$$

The uncertainties in calculated characteristics with respect to measured parameters are shown in Table 7.2.

Table 7.2 Uncertainty values for measurements

	Uncertainty (\pm)
Torque (Nm)	0.17
Bsfc (g/kWh)	0.54

CHAPTER 8

8. CASE STUDIES

8.1 Introduction

In this chapter, steady-state modeling of gasoline engine torque and brake specific fuel consumption is investigated by means of a number of case studies. These case studies can be categorized under 2 headings with respect to the used methods namely neural network and genetic programming approach. And nonlinear identification and modeling of a gasoline engine torque is investigated by means of a number of case studies. These case studies can be categorized under 3 headings with respect to the used methods namely Hammerstein model, NARX model and neural network models.

- a) Steady-state modeling of gasoline engine torque and brake specific fuel consumption
- b) Nonlinear modeling and identification of gasoline engine torque

The experimental based case studies consist of different types of modeling and identification techniques.

- a) Steady-state modeling of gasoline engine torque and brake specific fuel consumption
 - Prediction of torque and specific fuel consumption of a gasoline engine by using artificial neural networks
 - Genetic programming approach to predict torque and brake specific fuel consumption of a gasoline engine

b) Nonlinear modeling and identification of gasoline engine torque

- Nonlinear modeling and identification of a spark ignition engine torque using Hammerstein model.
- Nonlinear modeling and identification of a spark ignition engine torque using NARX model.
- A comparative study of neural network structures in identification of gasoline engine torque.

8.2 Case Studies

8.2.1 Prediction of torque and specific fuel consumption of a gasoline engine by using artificial neural networks

8.2.1.1 Introduction

An engineering phenomenon may embed complicated physical, chemical or electrical theory and may require very complicated arithmetic to describe them, yet, arithmetic emerged may not be solvable in closed form. Artificial neural network (ANN) is an alternative technique for providing a relationship between the variable quantities of interest. ANN requires only a set of experimental results, numerical in nature and describes the relation by analyzing them. In other words, it only needs solution examples concerning the problem. ANN techniques require a lot of arithmetic basically of trial-and-error nature, involving numerical differentiation and integration, noise rejection etc, and are never feasible without fast computation facilities. Advent of digital computers providing high speed arithmetic and vast amounts of data storage has given rise to the application of ANN techniques to many engineering problems. In recent years, this method has been applied to various disciplines including automotive engineering, in the forecasting of engine characteristics for different working conditions.

The relationship between the temperature of the exhaust gases and fuel consumption of an internal combustion engine has been studied in [181]. ANN approach has been used in another study, to analyze the effect of cetane number on exhaust emissions from the engine [182], and also in [183], to model diesel particulate

emission. [184] and [185] are remarkable studies where ANN is used to forecast gasoline consumption and the effect of intake valve timing on engine performance and fuel economy respectively. Similarly in [1], the effect of throttling is studied, taking the intake manifold geometry into consideration.

Numerous studies have been undertaken to predict the performance and exhaust emission characteristics of internal combustion engines by using ANNs [122, 186-189]. Studies done by neural networks and genetic algorithms have been used to predict and reduce diesel engine emissions [190].

Neural networks have been found to be the domain for numerous successful applications of prediction tasks, in modeling and prediction of energy-engineering systems [191], prediction of the energy consumption of passive solar buildings [157], and modeling a burner heated catalytic converter during cold start in a four stroke, spark ignition engine [192]. And also artificial neural network techniques have been applied to control the air fuel ratio of the engine [3, 90] and exhaust gas recirculation control [95].

In this study, a neural network approach was developed to model the torque and brake specific fuel consumption of a gasoline engine at steady-state conditions in terms of the spark advance, the throttle position and the engine speed. Experimental studies were completed to obtain training and testing data. The experimental data from totally 81 test runs was used to train and test the ANN model for predicting torque and brake specific fuel consumption. Inputs for the network were the spark advance, the throttle position and the engine speed, while the outputs were the torque and the brake specific fuel consumption. The experimental study to determine the torque and the fuel consumption characteristics in a gasoline engine is complex, time consuming and costly. It also requires specific instrumentation. To overcome these difficulties, an ANN can be used for the prediction of performance in a gasoline engine. The proposed ANN approach is quite accurate, fast and practical.

8.2.1.2 Artificial Neural Network Model and Parameters

The main focus of this study is modeling of torque (T) and brake specific fuel consumption (BSFC) of a gasoline engine at steady-state conditions using ANN based on experimental results described in Chapter 7.3. The spark advance, the throttle position and the engine speed have been used as input-layer components, while the T and BSFC were used separately as output-layer components of the ANNs. In the ANN model, the experimental data set includes 81 values, of which 63 values were used for training the network and 18 values were selected randomly to test the performance of the trained network.

In this study, a computer program has been developed and performed under Matlab. The back-propagation learning algorithm has been used in feedforward with one hidden-layer. The input layer neurons receive information from the outside environment and transmit them to the neurons of the hidden layer without performing any calculation. The hidden layer neurons then process the incoming information and extract useful features to reconstruct the mapping from the input space. The neighboring layers are fully interconnected by weights. Finally, the output layer neurons produce the network prediction to the outside world.

One of the most important tasks in ANN studies is to determine the optimal network architecture which is related to the number of hidden layers and neurons in it. Generally, the *trial and error* approach is used. In this study, the best architecture of the network was obtained by trying different number of hidden layers and neurons. The trial started on hidden layer with seven neurons, and the performance of each network was checked by correlation coefficient (R). The goal is to maximize correlation coefficient to obtain a network with the best generalization. Many different network models were tried and their R values were calculated. The highest correlation coefficient for both T and BSFC was obtained at a network. Based on this analysis, the optimal architecture of the ANN was constructed as 3-13-1 NN architecture for T and 3-15-1 NN architecture for BSFC representing the number of inputs, neurons in hidden layers, and outputs, respectively. The proposed ANN model is given in Figure 8.1. The learning algorithm used in the study is Levenberg-

Marquardt (LM), activation function is logistic sigmoid (logsig) transfer functions and number of epochs is 10000.

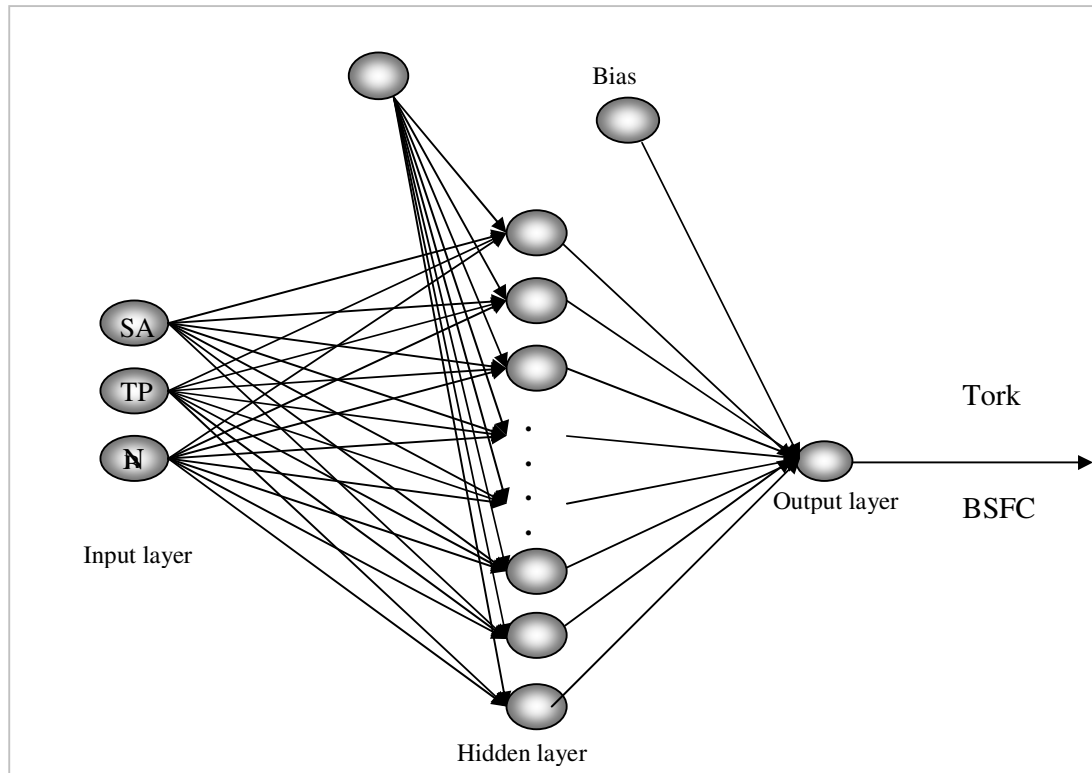


Figure 8.1 Architecture of proposed NN model

8.2.1.3 Analysis Results

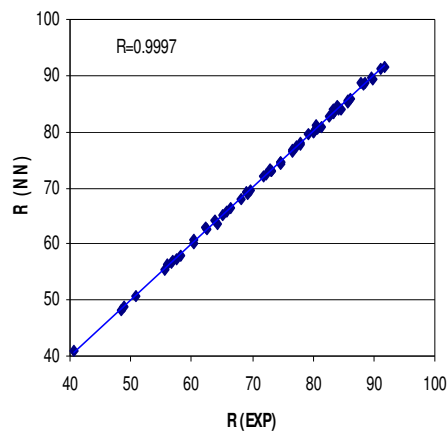
The ANN approach developed in this study is used to model the T and BSFC based on the spark advance, throttle position and engine speed. A total of 63 samples were used for training the network and other 18 (chosen randomly) were used as a test set. Data set was normalized using a simple normalization method. The range of the samples and normalization values are given in Table 8.1. The performance of the proposed ANN model was plotted in Figures 8.2 and 8.3 for both T and BSFC, respectively. It was observed that a high prediction capability was achieved for both training and testing data sets of T and BSFC. Therefore, the ANN appears to have a high generalization capability. The statistical values for both T and BSFC in training and test sets are given in Table 8.2. As seen in Table 8.2, a high correlation coefficient (R) and a low mean absolute percentage error (MAPE) were obtained for

Table 8.1 Range of input-output parameters in training-testing phase and normalization values

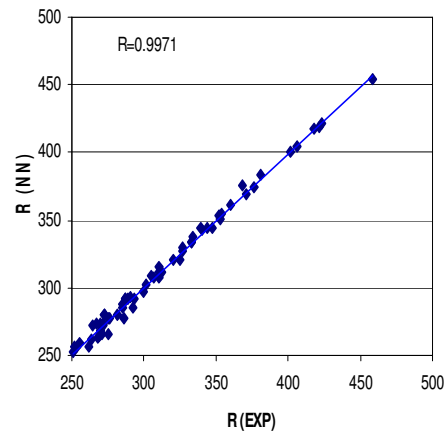
Parameters	Range of values		Normalization value
	Min	Max	
SA	0	10	10
TP (%)	50	100	100
N (rpm)	1500	3500	3500
T (Nm)	40.7	92.8	30
BSFC (g/kWhr)	248.41	458.49	500

Table 8.2 Statistical parameters of train and test sets

		MSE	MAPE	Corr. Coff. R
Torque (T)	Test set	0.002	1.74	0.99505
	Train set	0.0001	0.2912	0.9997
Brake specific fuel consumption (BSFC)	Test set	0.0005	2.7588	0.98331
	Train set	0.0001	1.0186	0.9971

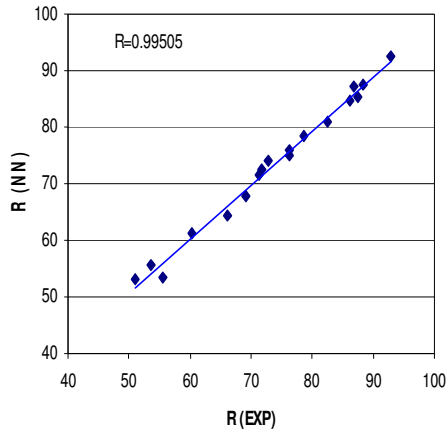


(a)

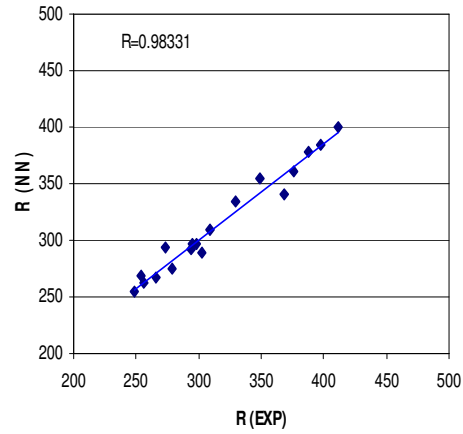


(b)

Figure 8.2 Prediction of NN and actual values for training sets (a) T (b) BSFC



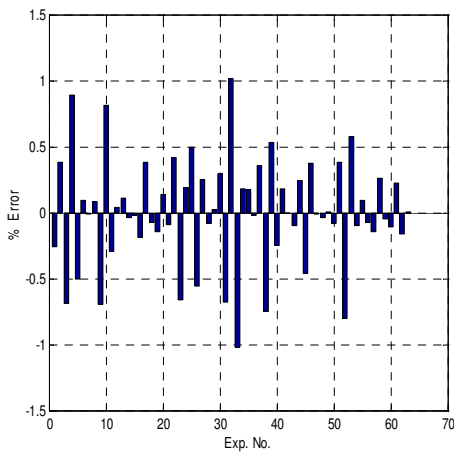
(a)



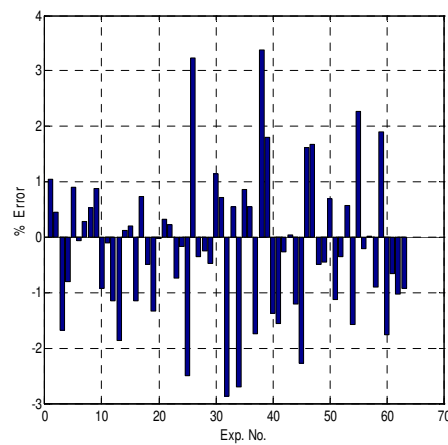
(b)

Figure 8.3 Prediction of NN and actual values for testing sets (a) T (b) BSFC

the training and testing data sets for both T and BSFC. The proposed ANN model for T and BSFC prediction had correlation coefficients of 0.9997 and 0.9971 respectively, for training data sets, 0.99505 and 0.98331, respectively, for testing data sets. Moreover, MAPE of the T prediction was about 0.2912 and 1.74 for the training and testing set, respectively. Similarly, MAPE of the BSFC prediction was about 1.0186 and 2.7588 for the training and testing set, respectively. As it is seen these MAPE are fairly reasonable. Figures 8.2 and 8.3 also demonstrated that the ANN was quite successful in learning the relationship between the different input parameters and the outputs (T and BSFC). The result of testing phase in Figures 8.2

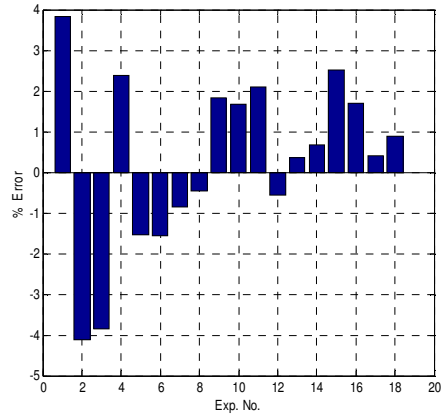


(a)

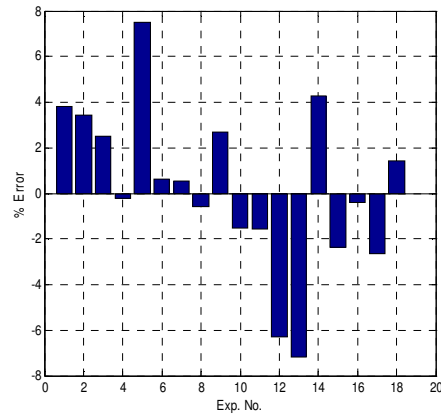


(b)

Figure 8.4 Percentage error of training set (a) T (b) BSFC



(a)



(b)

Figure 8.5 Percentage error of testing set (a) T (b) BSFC

and 8.3 has shown that the ANN was capable of generalizing between input variables and output reasonably well. Figures 8.4 and 8.5 demonstrate the percentage errors of training and testing sets for the predicted T and BSFC.

ANN applications are treated as black-box applications in literature. However this study opens this black box and introduces the ANN application in a closed form solution. This study aims to present the closed form solution of T and BSFC based on the trained ANN parameters (weights and biases) as a function spark advance (SA), throttle position (TP) and engine speed (N). Using weights and biases of trained ANN model, engine torque can be given as follows:

$$T = f(SA, TP, N)$$

$$T = 30 * \left(\frac{1}{1 + e^{-w}} \right)$$

Where

$$\begin{aligned}
W = & (0.7479) * \left(\frac{1}{1 + e^{-U_1}} \right) + (0.6726) * \left(\frac{1}{1 + e^{-U_2}} \right) + (3.0776) * \left(\frac{1}{1 + e^{-U_3}} \right) \\
& + (0.7687) * \left(\frac{1}{1 + e^{-U_4}} \right) + (0.6354) * \left(\frac{1}{1 + e^{-U_5}} \right) + (-1.5951) * \left(\frac{1}{1 + e^{-U_6}} \right) \\
& + (-0.3399) * \left(\frac{1}{1 + e^{-U_7}} \right) + (0.5024) * \left(\frac{1}{1 + e^{-U_8}} \right) + (-0.2028) * \left(\frac{1}{1 + e^{-U_9}} \right) \\
& + (1.9807) * \left(\frac{1}{1 + e^{-U_{10}}} \right) + (-3.1996) * \left(\frac{1}{1 + e^{-U_{11}}} \right) + (-0.1289) * \left(\frac{1}{1 + e^{-U_{12}}} \right) \\
& + (0.1742) * \left(\frac{1}{1 + e^{-U_{13}}} \right) + (-0.3153)
\end{aligned}$$

$$\begin{aligned}
U_1 = & -1.2725 * SA + 0.1925 * TP - 0.0034 * N + 11.8911 \\
U_2 = & -1.741 * SA - 0.1166 * TP - 0.00064 * N + 27.5182 \\
U_3 = & 0.0061 * SA - 0.0932 * TP + 0.0023 * N + 3.597 \\
U_4 = & 1.64 * SA - 0.0867 * TP + 0.001 * N - 4.9378 \\
U_5 = & -0.343 * SA + 0.2451 * TP + 0.002 * N - 15.8767 \\
U_6 = & 0.0533 * SA - 0.1257 * TP + 0.002 * N - 0.4814 \\
U_7 = & -0.8738 * SA + 0.4051 * TP - 0.0049 * N - 5.5608 \\
U_8 = & 2.4591 * SA - 0.1951 * TP + 0.0032 * N + 5.0804 \\
U_9 = & -0.6457 * SA + 0.2505 * TP + 0.0032 * N - 28.016 \\
U_{10} = & -0.0365 * SA - 0.2125 * TP - 0.0033 * N + 30.006 \\
U_{11} = & 0.013 * SA - 0.1984 * TP + 0.0015 * N + 12.8857 \\
U_{12} = & 0.7099 * SA - 0.1447 * TP - 0.0069 * N + 24.1371 \\
U_{13} = & 0.1032 * SA + 0.0824 * TP - 0.0052 * N + 9.4364
\end{aligned}$$

Similarly, BSFC can be found as follows:

$$BSFC = 500 * \left(\frac{1}{1 + e^{-W}} \right)$$

where

$$\begin{aligned}
W = & (-0.0417) * \left(\frac{1}{1 + e^{-U_1}} \right) + (-0.0597) * \left(\frac{1}{1 + e^{-U_2}} \right) + (0.0831) * \left(\frac{1}{1 + e^{-U_3}} \right) \\
& + (-0.1335) * \left(\frac{1}{1 + e^{-U_4}} \right) + (0.1716) * \left(\frac{1}{1 + e^{-U_5}} \right) + (-0.1525) * \left(\frac{1}{1 + e^{-U_6}} \right) \\
& + (0.0784) * \left(\frac{1}{1 + e^{-U_7}} \right) + (0.0279) * \left(\frac{1}{1 + e^{-U_8}} \right) + (0.0659) * \left(\frac{1}{1 + e^{-U_9}} \right) \\
& + (0.1134) * \left(\frac{1}{1 + e^{-U_{10}}} \right) + (-0.0224) * \left(\frac{1}{1 + e^{-U_{11}}} \right) + (-0.1295) * \left(\frac{1}{1 + e^{-U_{12}}} \right) \\
& + (-0.3636) * \left(\frac{1}{1 + e^{-U_{13}}} \right) + (0.2162) * \left(\frac{1}{1 + e^{-U_{14}}} \right) + (0.3334) * \left(\frac{1}{1 + e^{-U_{15}}} \right) \\
& + (0.7102)
\end{aligned}$$

$$\begin{aligned}
U_1 &= 0.1653 * SA + 0.1768 * TP - 0.005 * N - 9.222 \\
U_2 &= -0.3659 * SA + 0.1835 * TP + 0.0057 * N - 18.5103 \\
U_3 &= -0.7941 * SA + 0.2073 * TP + 0.0018 * N - 13.0825 \\
U_4 &= -0.2102 * SA + 0.0125 * TP + 0.0063 * N - 11.3466 \\
U_5 &= -1.4948 * SA + 0.0218 * TP + 0.005 * N - 2.7369 \\
U_6 &= -0.857 * SA + 0.0686 * TP + 0.0049 * N - 12.0769 \\
U_7 &= 1.1732 * SA - 0.1451 * TP + 0.003 * N - 5.6508 \\
U_8 &= 0.6916 * SA + 0.0152 * TP + 0.0053 * N - 19.3996 \\
U_9 &= 0.9153 * SA + 0.144 * TP + 0.0042 * N - 24.4002 \\
U_{10} &= 1.3535 * SA + 0.1177 * TP + 0.0027 * N - 13.664 \\
U_{11} &= -0.2564 * SA + 0.1639 * TP - 0.0054 * N + 7.3443 \\
U_{12} &= 0.534 * SA + 0.071 * TP - 0.0053 * N + 10.0671 \\
U_{13} &= 0.7501 * SA + 0.0331 * TP + 0.0041 * N - 13.0804 \\
U_{14} &= 1.1861 * SA - 0.1221 * TP - 0.0012 * N + 12.5888 \\
U_{15} &= -0.8518 * SA + 0.0531 * TP + 0.0041 * N - 15.8735
\end{aligned}$$

It should be noted that the proposed explicit formulation of the NN model presented above is valid for the ranges of training set.

8.2.1.4 Conclusions

This study presents a new and efficient approach for the modeling of torque and brake specific fuel consumption of a gasoline engine at steady-state conditions using ANNs. The database used for NN training is based on experimental results. It used 63 results as data sets to train the network, while 18 results were used as test data

from the total of 81 experimental results. To train the network, the spark advance, the engine speed, and the throttle positions are used as the input layer, while outputs are the engine torque and the brake specific fuel consumption. Back-propagation NNs are used for the training process. The proposed NN model shows perfect agreement with experimental results.

The proposed ANN model for torque and brake specific fuel consumption had correlation coefficients of 0.9997, 0.9971 respectively, for training data sets, 0.99505 and 0.98331, respectively, for testing data sets. Moreover, MAPE of the T prediction was about 0.2912 and 1.74 for the training and testing set, respectively. Similarly, MAPE of the BSFC prediction was about 1.0186 and 2.7588 for the training and testing set, respectively which may easily consider within the acceptable range. The explicit formulation of torque and brake specific fuel consumption based on the proposed NN model is also obtained and presented. As a result the proposed NN model has strong potential as feasible tools for prediction of torque and brake specific fuel consumption. And also the engine torque and brake specific fuel consumption can be determined using models with ANN methodology.

8.2.2 Genetic programming approach to predict torque and brake specific fuel consumption of a gasoline engine

8.2.2.1 Introduction

Experimental investigations to measure the performance of a gasoline engine are complex, time consuming, and costly. To predict the performance parameters from the engines, one approach is to use mathematical models. However, their accuracies may not be sufficiently high [193]. The alternative to a mathematical model is the experiment-based approach.

Genetic Algorithm (GA), which is based on solutions of fixed-length chromosomes, usually consisting of binary genes, organized into sequences, often termed schema is the most commonly used evolutionary-computation algorithm [194]. Mimicking nature, the algorithm starts its search from an initial population of solutions, in which the performance of each individual is evaluated using a fitness function, with the

most efficient chromosomes having a higher probability to reproduce. In synthetic evolution, biological reproduction is mimicked by operators like crossover (pairing) and mutation, thus creating a generation of offspring solutions. Crossover generates new features in the solution space by combining genetic information, while mutation does this by adding random perturbations. Fitness-proportional selection, combined with these genetic operators produce generation after generation of offspring solutions. Since the more appropriate solutions are given higher probabilities to reproduce, one would expect a growing improvement of the solutions over generations.

GA as an optimization technique is widely used for optimization of engineering problems. Many engineering design problems are very complex and therefore difficult to solve with conventional optimization techniques [195]. Numerous studies have been undertaken by using GA for optimization of engine characteristics, neural networks and genetic algorithms have been used to predict and reduce diesel engine emissions [190], genetic algorithm and artificial neural network for engine optimization of efficiency and NO_x emission [196], a group method of data handling type neural network and evolutionary algorithms for modeling the effects of intake valve timing and engine speed of a spark ignition engine on both engine torque and fuel consumption [197], genetic algorithms for hydrogen-fueled engine optimization of power, economy, emission performance and operating parameters [198], multi-objective optimization of diesel engine emissions and fuel economy using genetic algorithms [199], performance prediction and optimization of liquid rocket engine nozzle using genetic algorithm [200], genetic algorithm and its application to diesel engine optimization [201], optimization of system parameters for the gas-generator engines using multi-objective methods [202].

GA is employed by [203] to optimize the capacity and operation strategy of CCHP system on the basis of energy flow. Fuel consumption of a gasoline engine can be minimized through dynamic optimization [204]. Neuro-fuzzy interface system (ANFIS) to study the effect of boost pressure on the engine performance parameters of a single cylinder diesel engine has been studied in [205].

However, they are unsuitable for generating empirical model structures, since they manipulate populations of solutions of fixed-length chromosomes, while the optimal complexity of empirical models is unknown in advance. Because of this perceived need for more intelligent construction of empirical models, a new family of evolutionary computation methods has emerged, based on established GA ideas. These new algorithms, referred to as genetic programming (GP), rely on tree-like building blocks, and therefore support populations of model structures of varying length and complexity. Activity in genetic programming was introduced by Koza [206], who demonstrated their applications in fields such as robotics, games, control, and symbolic regression.

Numerous studies have been undertaken by using GP, a member of the evolutionary computation field, to a nonlinear identification of aircraft gas turbine engine [125-127], nonlinear model structure identification [116], identification of a dynamic system [128, 142], gas turbine engine identification [123], mechanical system identification [115], dynamic system modeling [139] and steady-state process modeling [138]. [207] used an intelligent approach by using GP to construct mathematical model for diagnosing the engine valve faults correctly and quickly.

Kalogirou [156] reviewed Artificial intelligence for the modeling and control of combustion processes. A number of AI techniques have been described in this paper. An explicit neural network formulation that predicts the torque and brake specific fuel consumption of a gasoline engine as a function of experimental parameters; spark advance, throttle position and engine speed, has recently been performed by Togun and Baysec [208]. However a GP based explicit formulation for gasoline engine performance parameters, to the best knowledge of the authors, has not yet existed in the literature. Therefore, the purpose of this study is to develop a GP based mathematical model for the prediction of gasoline engine torque and brake specific fuel consumption in terms of spark advance, throttle position and engine speed. The performance of the proposed models was compared to neural networks model developed by Togun and Baysec [208]. The data taken from experimental study were utilized in training and testing the developed models. An important advantage of the proposed GP approach is the simplicity of the modeling and its wide range of

applicability to empirical modeling of various engineering problems where sufficient experimental results exist.

8.2.2.2 Overview of Genetic Expression Programming (GEP)

Koza [206] proposed genetic programming (GP) technique which is an extension to Genetic Algorithms. In genetic programming, populations of hundreds or thousands of computer programs are genetically bred. This breeding is done using the Darwinian principle of survival and reproduction of the fittest along with a genetic recombination (crossover) operation appropriate for mating computer programs [206]. GP breeds computer programs to solve problems by executing the following three steps (Figure 8.6):

(1) Generate an initial population of random computer programs composed of the primitive functions and terminals of the problem.

(2) Iteratively perform the following sub-steps until the termination criterion is satisfied:

(a) Execute each problem in the population so that a fitness measure indicating how well the program solves the problem can be computed for the program.

(b) Create a new population of programs by selecting programs in the population with a probability based on fitness and then applying the following primary operations:

(i) Reproduction: Copy an existing program to the new population.

(ii) Crossover: Create new computer programs by crossover.

(iii) Mutation: Create new computer programs by mutation.

(iv) Choose an architecture-altering operation to one selected program.

(3) The single best computer program in the population produced during the run (best solution so far) is designated as the result of genetic programming [206].

Gene expression programming (GEP) software is an extension to GP that evolves computer programs encoded in linear chromosomes of fixed length. The structure of

GEP chromosomes allows the easy implementation of multiple genes, each encoding a data set [209, 210]. In addition, the structural and functional organization of the linear chromosomes allows the unconstrained operation of important genetic operators such as mutation, transposition, and recombination. One strength of the GEP approach is that the creation of genetic diversity is extremely simplified as genetic operators work at the chromosome level. Another strength of GEP consists of its unique, multigenic nature which allows the evolution of more complex programs composed of several sub-programs. As a result GEP surpasses the old GP system by a factor of 100–10,000 times [210].

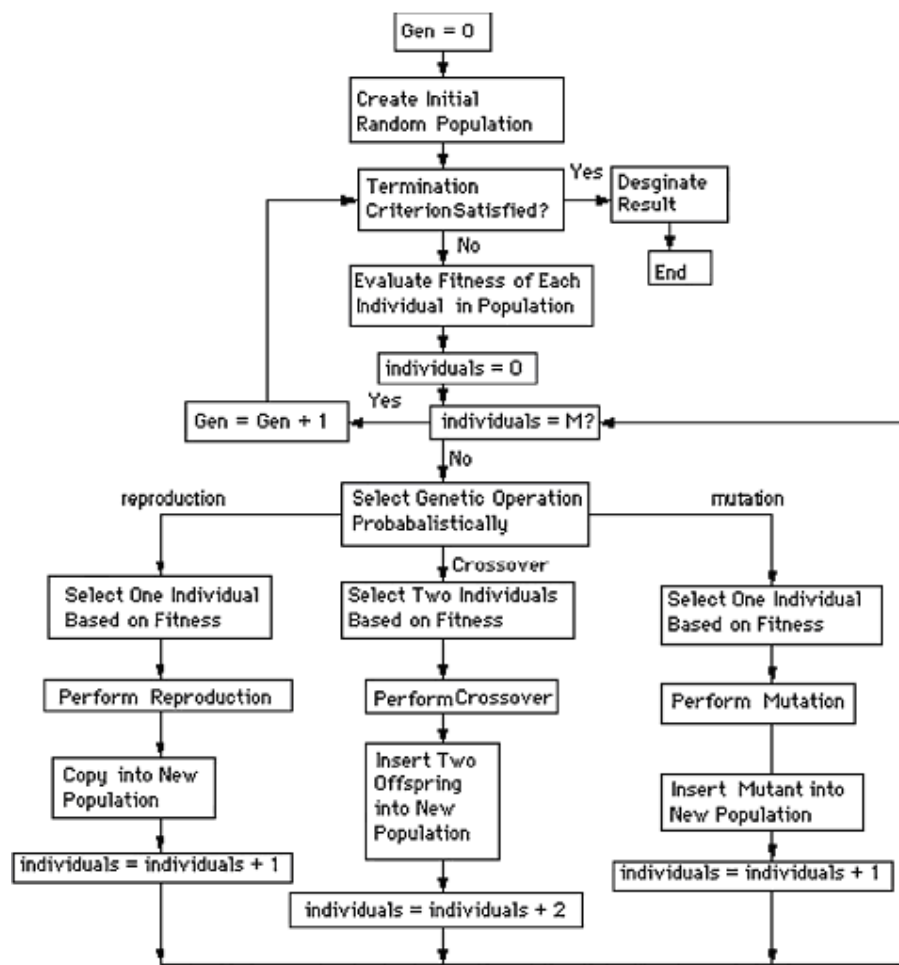


Figure 8.6 Genetic Programming Flowchart [206]

The main difference between GA, GP and GEP resides in the nature of the individuals: in GAs the individuals are symbolic strings of fixed length

(chromosomes); in GP the individuals are nonlinear entities of different sizes and shapes (parse trees); and in GEP the individuals are encoded as symbolic strings of fixed length (chromosomes) which are then expressed as nonlinear entities of different sizes and shapes (expression trees). The main parameters in GEP are the chromosomes and expression trees (ETs). The process of information decoding (from the chromosomes to the ETs) is called translation which implies obviously a kind of code and a set of rules. The genetic code is very simple: a one-to-one relationship between the symbols of the chromosome and the functions or terminals they represent. The rules that are also very simple determine the spatial organization of the functions and terminals in the ETs and the type of interaction between sub-ETs [209, 210].

In GEP there are two languages: the language of genes and the language of ETs and knowing the sequence or structure of one, is knowing the other. In nature, despite being possible to infer the sequence of proteins given the sequence of genes and vice versa this is called as Karva language. Consider, for example, the algebraic expression $(d0 - d4 - d2 + d1 + (d0/d4))$ can be represented by a diagram which is the expression tree as shown in Figure 8.7.

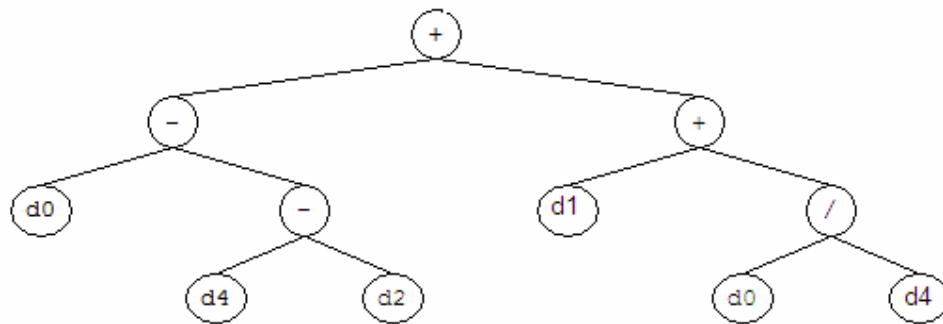


Figure 8.7 Expression tree (ET)

8.2.2.3 Modeling with GP

The main aim of this study is to obtain a model for torque (T) and brake specific fuel consumption (bsfc) of gasoline engine at steady-state conditions using genetic programming based on experimental results. Details of the experimental procedure have been explained in Section 7.3.

The details of the experimental database including the parameters and their range are presented in Table 8.3. To achieve generalization capacity for the formulations, the experimental database is divided into two sets as training and test sets. The formulations are based on training sets and are further tested by test set values to measure their generalization capability. In the literature, this type of studies includes test sets as 20-30% of the training set. The patterns used in testing and training sets are selected randomly. Among the experimental data, 63 sets were used for GP training and 18 sets for GP testing. It should be noted that the proposed GP formulation is valid for the ranges of training set given in Table 8.3. Parameters of the GP models are presented in Table 8.4.

Table 8.3 Variables used in model construction

Code	Input variable	Range	Output variable	Range
d0	Ignition time	0-10	Torque (Nm)	40.7-92.8
d1	Throttle position	50-100	Bsfc (g/kWhr)	248.41-458.49
d2	Speed (rpm)	1500-3500		

Table 8.4 Parameters of the GP model

P1	Number of generation	Between 3000 and 20000
P2	Function set	+, -, *, /, power, exp, ln(x), log, $\sqrt{\quad}$, X^2 , X^3 , (1/X).
P3	Chromosomes	30-55
P4	Number of genes	3, 4, 5, 6, 7, 8
P5	Head size	8, 10, 15
P6	Linking function	Addition, multiplication
P7	Mutation rate	0,044
P8	Inversion rate	0,1
P9	One-point recombination rate	0,3
P10	Two-point recombination rate	0,3
P11	Gene recombination rate	0,1
P12	Gene transposition rate	0,1

The purpose of this case study is to obtain a model for the torque and the brake specific fuel consumption (bsfc) of a gasoline engine as a function of spark advance (SA), the throttle position (TP) and the engine speed (n). Explicit formulations based on GP for torque and bsfc were obtained as a function of experimental parameters as

$$\text{Torque and bsfc} = f(SA, TP, n)$$

Figure 8.8 and Figure 8.9 show the expression of GP models, whose explicit formulations are:

$$\begin{aligned} \text{Torque} = & \left[4.93(1 + \sin(2SA^2 * TP - 40.85)) \right] + \left[8.48 * \sin(2.99n) + \frac{(2SA + 8.48)}{\sin(8.48)} \right] \\ & + \left[TP * \sin\left(\sin\left(TP + \frac{SA}{n} + 1.057\right)\right) \right] \end{aligned} \quad (8.1)$$

$$\begin{aligned} \text{bsfc} = & \left[\cos\left(TP + \frac{2SA}{n}\right) * (9.9516 + \cos(-17.8228)) \right] \\ & * [\cos(\cos(TP)) - (\log(\log(TP)) - 3.62n)] + 4.7926 \\ & * [\cos(SA + 0.6181 * \cos(nSA) + 7.6941)] + 7.6941 \end{aligned} \quad (8.2)$$

It should be noted that proposed GP formulations in Equations (8.1) and (8.2) is valid for the ranges of training set given in Table 8.3.

8.2.2.4 Results and Discussion

Data (81 tests in total), taken from the experimental study were used as training and testing sets for the GP architecture. Among these, 18 were randomly reserved for the test and the remaining data were used for the training. The overall performances of both sets were evaluated by the correlation coefficient (R) and mean squared error (MSE) given by:

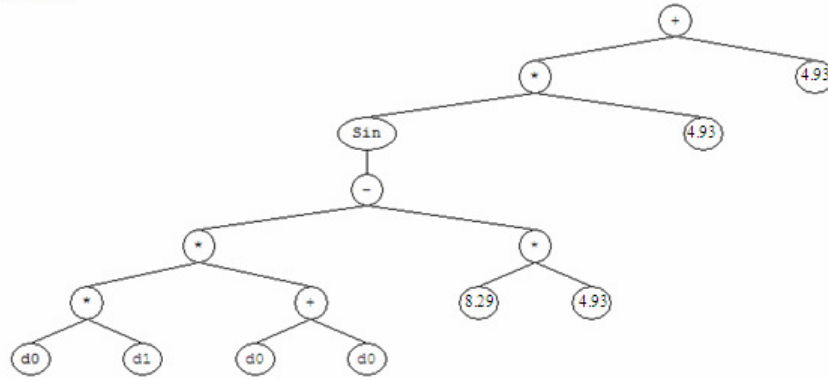
$$R = \frac{\sum_{i=1}^N (d_i - d')(y_i - y')}{\sqrt{\sum (d_i - d')^2 \sum (y_i - y')^2}} \quad (8.3)$$

$$MSE = \frac{\sum_{i=1}^N (d_i - y_i)^2}{N} \quad (8.4)$$

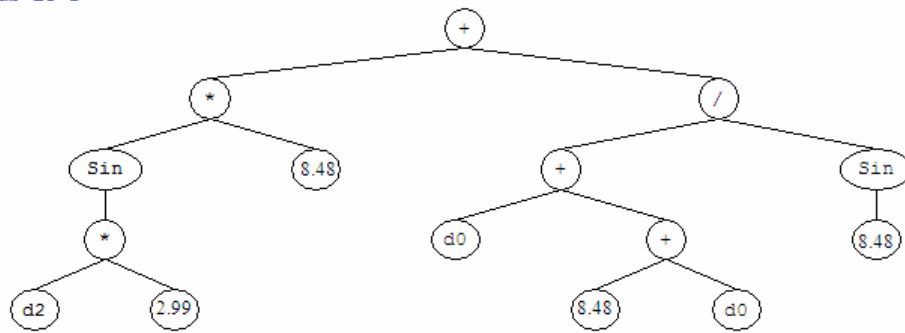
where y' are the mean values of d_i and y_i and N is the number of total number of data.

The GP estimates are compared to the experimental data for training and testing sets. The training results proved that the proposed GP models have impressively learned well the nonlinear relationship between the input and output variables with high correlation ($R=0.9878$ for torque and $R=0.9744$ for bsfc) and relatively low error ($MSE=3.5719$ for torque and $MSE= 148.441$ for bsfc) values.

Sub-ET 1



Sub-ET 2



Sub-ET 3

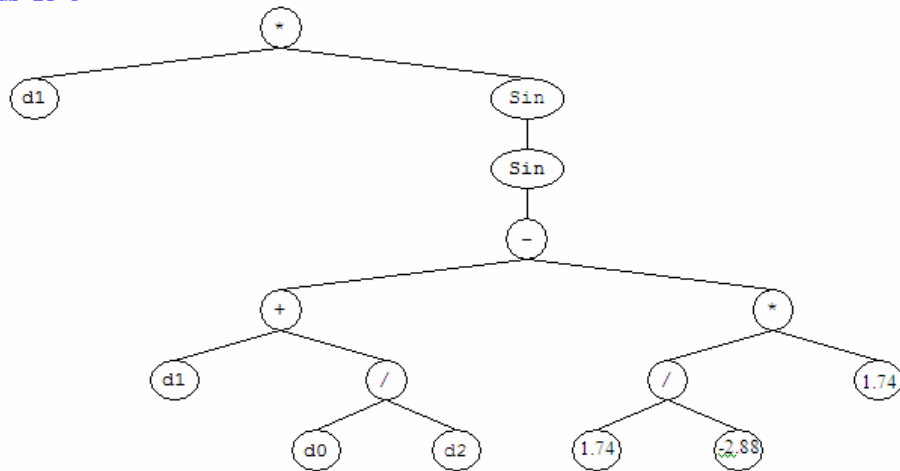
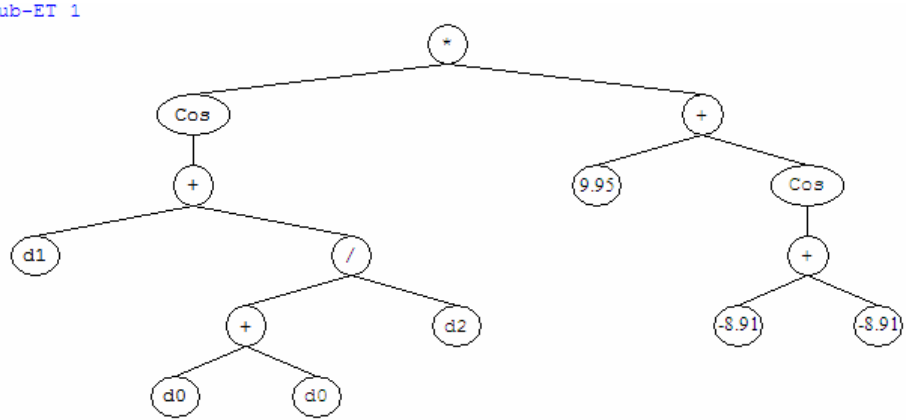
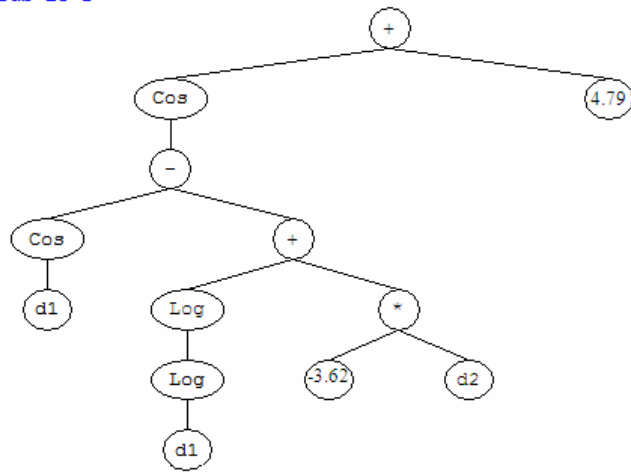


Figure 8.8 Expression tree for engine torque

Sub-ET 1



Sub-ET 2



Sub-ET 3

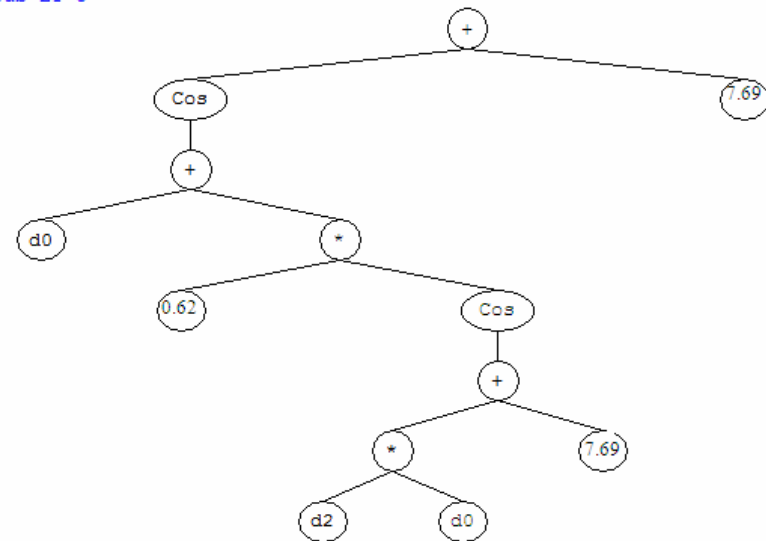


Figure 8.9 Expression tree for brake specific fuel consumption

Comparing the GP predictions with the experimental data for the test stage (see Figure 8.10) demonstrates a high generalization capacity of the proposed model ($R=0.9869$ for torque and $R=0.9855$ for bsfc) and relatively low error ($MSE=4.1878$ for torque and $MSE=167.985$ for bsfc) values. All these findings show a successful performance of the GP model for estimating torque and bsfc both in training and testing stages.

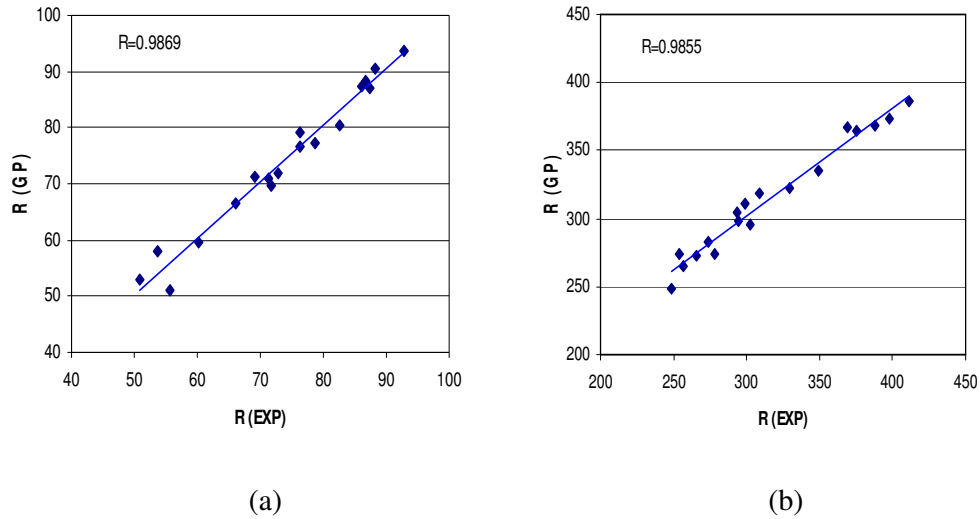


Figure 8.10 GP vs test results for (a) torque and (b) BSFC

8.2.2.5 GP vs Neural Network (NN)

Proposed GP based models of torque and bsfc were compared with neural network (NN) model that has been presented by Togun and Baysec [208]. The same training and testing data were utilized in both studies. The statistical performance of both methods in testing and training stage is given in Table 8.5. It can be deduced from the table that both methods performed well in simulating torque and bsfc relatively small mean absolute error (MAE) and high correlation (R). The mean absolute error is given by:

$$MAE = \left| \frac{d_i - y_i}{d_i} \right| / N \quad (8.5)$$

Table 8.5 Statistical results of GP and NN models for training and testing sets

Parameter	Set	Model	MSE	MAE	Corr. Coff. R	R_{GP}/R_{NN}
Torque (T)	Train	GP	3.5719	1.5749	0.9878	0.988
		NN	0.0001	0.2912	0.9997	
Brake specific fuel consumption (bsfc)	Train	GP	148.441	9.6672	0.9744	0.977
		NN	0.0001	1.0186	0.9971	
Torque	Test	GP	4.1878	1.6592	0.9869	0.992
		NN	0.002	1.74	0.99505	
Brake specific fuel consumption (bsfc)	Test	GP	167.985	10.838	0.9855	1.00
		NN	0.0005	2.7588	0.98331	

In fact, NN performed slightly better performance than GP in prediction of torque and bsfc. The prediction of the proposed GP formulation vs NN formulation (R_{GP}/R_{NN}) is also given in Table 8.5.

8.2.2.6 Conclusions

This study presents a new and efficient approach for the modeling of engine performance parameters at steady-state conditions using GP. This is done for the first time. The objective of the study is to develop an alternative robust formulations based on experimental data and to verify the use of GP for generating the formulations for gasoline engine torque and brake specific fuel consumption. The proposed GP formulations are empirical formulations based on experimental results collected from a test engine. The proposed GP formulations show very good agreement with the experimental results. The performance of accuracies of proposed GP models are quite satisfactory ($R^2 = 0.9878$ for gasoline engine torque and $R^2 = 0.9744$ for gasoline engine brake specific fuel consumption). The results of the proposed GP formulations are compared to the neural network model developed by Togun and Baysec [208] with which the results are found to be in excellent

agreement. The outcomes of the study are very promising. This study proves that GP can be effectively used to obtain formulations for high nonlinear function approximation problems in general.

8.2.3 Nonlinear modeling and identification of a spark ignition engine torque using Hammerstein model

8.2.3.1 Introduction

System identification is the process of creating models of dynamic process from input-output signal. System identification is the art and methodology of making mathematical models from dynamic systems base on the input-output data [211]. System modeling and identification refers to a systematic way to determine and improve the mathematical models for proper representation of dynamic systems [30]. A large body of work on the topic is available in the literature [26, 27].

Most systems encountered in the real word are nonlinear in nature, and since linear models can not capture the rich dynamic behavior of limit cycles, bifurcations, etc. associated with nonlinear systems, it is imperative to have identification techniques which are specific for nonlinear systems [13]. System identification has become an important area of study because of the increasing need to estimate the behavior of a system with partially known dynamics. Especially in the areas of control, pattern recognition and even in the realm of stock markets, the system of interest needs to be known to some extent [14].

Theory of system identification plays a significant role in many fields of science and engineering including simulation, automatic control, fault tolerant analysis, prediction, etc [12, 26, 37]. Several techniques have been proposed for identification of nonlinear systems. Among the various linear in the parameter structures available, nonlinear autoregressive exogenous model (NARX)/NARMAX (Nonlinear Autoregressive Moving Average with Exogenous input) is one of the earliest and perhaps most widely used model types, with many successful industrial applications reported. For example, it has been used in the modeling and control of power systems, such as internal combustion engine (ICE) [37], automotive diesel engine

[50], dynamic modeling of three way catalysts [212]. Ref. [36] deals with the nonlinear identification of a turbocharged diesel engine. A combined use of NARMAX models and group method data handling method is proposed in an attempt to provide a systematic approach to identify nonlinear systems using relatively simple models well suited to computer handling. A nonlinear system identification procedure, based on a polynomial NARMAX representation, is applied to a variable geometry turbocharged diesel engine [57]. A nonlinear black box engine model is derived using the NARMAX models proposed. Input-output models allow the identification of black-box models derived purely from experimental data, both online and offline [42].

An identification procedure for NARX models describing the pressure inside the intake manifold and the crankshaft speed of ICE have been handled in [32-34]. A number of methodologies for idle speed control design have been presented in literature [34, 35].

A new approach to control air management process of a diesel engine has been proposed. Predictive control and model identification schemes for Wiener and Hammerstein models have been shown [31]. Ref. [89] has described and compared two approaches to the experimental identification of dynamic nonlinear processes: the dynamic multi layer perceptron and the generalized Hammerstein model. A large number of research studies have indicated the superior capability and effectiveness of Wiener models in nonlinear dynamic system identification and control [29].

Tan and Saif have proposed a recurrent neural network for modeling the nonlinear dynamics of the intake manifold pressure for onboard diagnosis application [1]. Dynamic of air manifold and fuel injection of spark ignited (SI) engines are very fast, severely nonlinear and with constraints imposed on the states and inputs [1, 5]. To model volumetric efficiency of internal combustion by using parametric, nonparametric and neural network techniques is studied [5].

Advanced research on engine control often relies on model based control strategies. Model based engine diagnostics also is another area that relies on an engine model. Therefore, the development of simplified models of automotive engines appropriate

for control/diagnostic system research and design is an important subject for research and development [1]. Ref. [88] deals with methods based on engine model linearization in order to apply linear control theory. Jones et al. [39] implemented a nonlinear least squares state estimator for an adaptive control schema. Least square support vector machines have been handled regression problems [46]. NARX models have already been used in engine modeling for control and diagnosis purposes [42]. Dynamic models in ICE have been applied to design, optimization or diagnosis [48, 49], using geometric and dynamic engine characteristics. Several different methods have been proposed and investigated for pressure reconstruction, mathematical engine models [48, 213]. A procedure for the identification of emission models for the design of optimal control of SI engine is presented [41].

Automotive engine control is one of the most complex control problems for control system engineers and researches. Due to the increasing requirements of governments and customers, car manufacturers always strive to reduce substantially emissions and fuel consumption while maintaining the best engine performance. To satisfy these requirements, a variety of variables need to be controlled, such as engine speed, engine torque, spark ignition timing, fuel injection timing, air intake, air/fuel ratio (AFR) and so on. These variables are complicatedly related to each other. Engine dynamics are highly nonlinear and multivariable because of these factors [1, 2]. Among all the engine control variables, engine torque estimation has important applications in the automotive industry: for example, automatically setting gears, optimizing engine performance, reducing emissions and designing drivelines [6]. The coordinated overall torque reference value is realized by the manipulation of variables like throttle position, ignition timing, injection timing and others [9].

A number of such control strategies has been reported in the literature during the current decade. Most of these control schemes deal with manifold pressure control, AFR control and idle speed control [47]. The article deals with nonlinear modeling of AFR dynamics of gasoline engines during transient operation [52]. The influence identification scheme developed in Ref. [214] is applied to the system for the determination of the inputs that affect exhaust oxygen content and the appropriate time delays that the system imposes on each variable. Ref. [215] included the effect of exhaust gas recirculation in a nonlinear model to investigate engine dynamics. In

another application, a finite difference model is used to represent engine nonlinear inverse dynamics between engine speeds and throttle duty cycle signals [216]. A detailed physically motivated simulation model is derived in [217]. An adaptive (online) identification algorithm, developed recently in [218] for continuous time Single-Input-Single-Output (SISO) linear time delay system with uncertain time-invariant parameters, is tested in an experimental study of the transient fuel parameter identification in a port fuel injected ICE.

The engine torque is one of the most important performance variables of an ICE and, for this reason; a torque control system can improve substantially the performance of the overall vehicle [7, 8]. Their modeling efforts were focused on an experimental method of system identification that captures the nonlinear engine torque characteristics for a large range of operating conditions [10]. In recent years considerable interest has been placed on the estimation of ICE torque both for control and diagnostic applications. Ref. [51] discusses a method for the identification of a nonlinear model of the dynamics relating combustion pressure to crankshaft angular velocity. A linear gray box approach to modeling the torque and NO_x dynamics in response to combined fuel quantity/timing excitations has been handled in [53].

This study basically focuses on nonlinear modeling and identification of SI engine torque. In this case study section, a procedure to provide the nonlinear model of the dynamics between the throttle valve command and torque in a gasoline engine directly from raw data is presented. The nonlinear system model is built and a nonlinear Hammerstein model structure is used for the identification procedure.

8.2.3.2 Simplified Mean-value SI Engine Model

Automotive engines are multivariable system with severe nonlinear dynamics, and their modeling and control are challenging tasks for control engineers. Mean value engine models (MVEM) are generally accepted as the modeling paradigm for engine control, and are extensively described in the literature [170, 172, 173]. It allows modeling the mean value behavior of some engine parameters. This kind of model represents the global dynamic of the engine and can be easily identified using the common measurements available on production vehicles. The engine model adopted

in this paper is referred to as the MVEM developed by Guzzella and Onder [172], which is widely used benchmark for engine modeling and control.

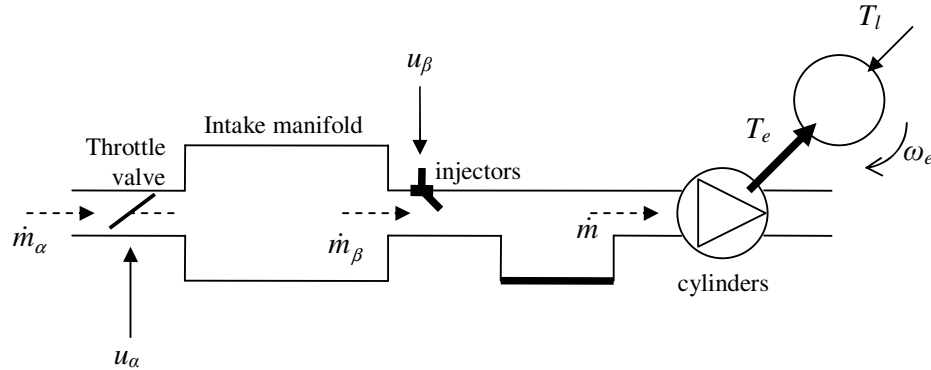


Figure 8.11 Simplified mean-value schematic SI engine diagram

Mean-value models developed for SI engines include nonlinear dynamic equations and time varying terms like induction-to-power-stroke (IPS) delay. A simplified schematic diagram of the SI engine process is given in Figure 8.11. The torque generation phase, which consists of the cylinders that convert the chemical energy in air fuel mixture inflow into mechanical engine torque, is governed by a nonlinear dynamic equation of dependent variables including air/fuel ratio, fuel mass in cylinders, engine speed, ignition and injection timing, and several others. The mean-value engine torque is therefore expressed as a nonlinear function of these variables and time [172]. For control and identification purposes, nonlinear dynamic and time-varying terms create difficulties, which can be overcome by developing simplified approximate models. The Hammerstein model of nonlinear system dynamics is a simplified model that contains the dynamics and nonlinearity separately in cascaded form, resulting in a more complete model compared to linear approximations, and superior power to apply conventional identification techniques compared to nonlinear dynamic models [28].

a) Throttle Model

The throttle input is the throttle valve angle in radians, and the output is the air-fuel mixture mass flow rate in kilograms per second. It is assumed that the valve angle and the air mass flow rate are proportionally related [178]. The air-fuel-ratio (AFR) is taken to be 6.8 per cent, which is typical to gasoline engines under stoichiometric

conditions [178]. The conceptual block diagram of the combined throttle model is given in Figure 8.12, where

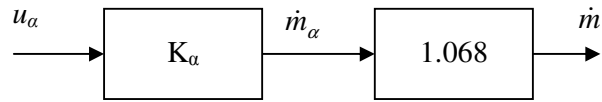


Figure 8.12 Simplified conceptual throttle model

- u_α : throttle valve angle (rad.)
- \dot{m}_α : air mass flow rate through the intake manifold (kg/sec)
- \dot{m} : total mixture flow rate into the cylinders (kg/sec)
- K_α : valve constant.

In the model, spark advance (SA) input is disregarded, and transport delay along the intake manifold is negligibly small. The frictional losses are also neglected. Thus, the throttle valve output mass flow rate is taken to be the input of the torque generation sub process.

b) Torque Generation Model

The torque generation sub process is a process with nonlinear dynamics and variable time delay. The time delay is a result of the fact that the torque generated by the engine does not respond immediately to an increase in the manifold pressure, but after a certain amount of time called the induction-to-power-stroke (IPS) delay approximately given in terms of the engine speed by:

$$\tau_{IPS} \approx \frac{2\pi}{\omega_e}$$

The engine speed takes a minimum value of 600 rpm in idle speed condition, which corresponds to an angular speed of $\omega_e = 20\pi$ rad/sec. Consequently, the maximum possible delay is found to be 0.1 seconds, which can be neglected in the process

dynamics. The model then reduces to a time-invariant single-input-single-output nonlinear dynamic model, which is given in Figure 8.13.

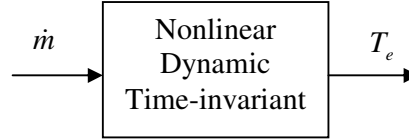


Figure 8.13 Simplified conceptual torque generation model

8.2.3.3 Nonlinear System Identification

Ljung [26] and Soderstrom and Stoica [27] published a comprehensive book detailing many system identification algorithms, nonrecursive and recursive, such as least squares, recursive least squares, instrumentation methods, and recursive prediction error methods. Their work is considered as a cornerstone reference guide.

The identification process consists of estimating the unknown parameters of the system dynamics [26]. Consequently, determination of the assumed system structure is of great importance in the process of system identification [27].

The recursive least squares (RLS) method has been recommended for the identification process for easy implementation and application to real systems [26, 27]. For the linear identification process, a discrete time ARX model for the mechatronic system has been used. This model structure is, in some sense, a linear regression form and permits easy implementation of the linear regression based identification [26]. The ARX model for the linear system is given as in Ref. [27]:

$$A(q^{-1})y(t) = B(q^{-1})u(t) + e(t) \quad (8.6)$$

Where

$$A(q^{-1}) = 1 + a_1q^{-1} + a_2q^{-2} + \dots + a_{na}q^{-na},$$

$$B(q^{-1}) = b_0 + b_1q^{-1} + b_2q^{-2} + \dots + a_{nb}q^{-nb}$$

and the symbol q^{-1} denotes the backward shift operator, $(y(t-1) = q^{-1}y(t))$, $u(t)$ and $y(t)$ are the symbol input and output, respectively, $e(t)$ is assumed to be an immeasurable, statistically independent noise sequence with $E\{e(t)\} = 0$ of variance σ_e^2 . The parameters a_i and b_i are the real coefficients, $a_i, b_i \in R$, and n_a and n_b are the orders of the polynomials $A(q^{-1})$ and $B(q^{-1})$, respectively, where $n_a \geq n_b$. It is also assumed that the polynomial $1 + \sum_{i=1}^N a_i q^{-i}$ never becomes zero in $|z| \geq 1$, and the model parameters a_i and b_i do not become zero simultaneously.

Identification of nonlinear systems can be achieved in a number of ways. Several methods for nonlinear system representation and identification have been proposed [26, 27]. Nonparametric methods of nonlinear system identification do not require parametric expressions for the system nonlinearities. In addition, these methods have the advantage of applicability to nonlinear systems with dynamic nonlinearities [28]. However, these methods take the system as a whole and do not permit separate analysis and identification of the linear dynamics. With the assumption that the nonlinearities in the system are static, in other words, the system dynamics can be expressed in linear terms only, the parametric identification methods can be employed. This assumption leads to nonlinear system structures called the Hammerstein model, the Wiener model and the general NARMAX model [28]. The nonlinear Hammerstein model structure, given in Figure 8.14, has several advantages, such as the nonlinear system identification problem can be put into linear regression form, methods of linear system identification can be applied and it can describe a nonlinearity of a dynamical system efficiently [28]. In addition, this structure covers wide range of nonlinear systems despite its simplicity [28, 219].

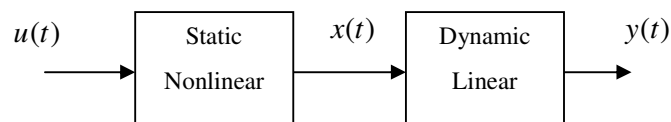


Figure 8.14 Hammerstein system structure

The dynamical linear part in the Hammerstein model can be represented by an ARX model as for the linear system model [28]. The relationship between the linear part input $x(t)$ and the output $y(t)$ can be given as:

$$\tilde{A}(q^{-1})y(t) = \tilde{B}(q^{-1})x(t) + e(t) \quad (8.7)$$

where $x(t)$ is the output of the nonlinearity.

The nonlinear part in the Hammerstein model is generally chosen to be polynomial of known order. The order of the polynomial is selected in accordance with the hardness of the nonlinearity in the system. The nonlinearity function $x(t)$ is given by [28]:

$$x(t) = \gamma_1 u(t) + \gamma_2 u^2(t) + \dots + \gamma_n u^n(t) \quad (8.8)$$

where γ_j ($j=1, \dots, n$) are the nonlinearity parameters, $\gamma_j \in R$. The nonlinear equation, Eq. (3), is re-arranged to be [28]:

$$\tilde{A}(q^{-1})y(t) = \tilde{B}(q^{-1}) \sum_{j=1}^n \gamma_j u^j(t) + e(t) \quad (8.9)$$

In Equation (8.9), the coefficients of $\tilde{B}(q^{-1})$ do not appear explicitly. Without loss of generality, the nonlinear part can be normalized with respect to γ_1 , and Equation (8.9) can be rewritten with the assumption that $\gamma_1 = 1$ as follows:

$$\tilde{A}(q^{-1})y(t) = \tilde{B}(q^{-1})u(t) + \sum_{j=2}^n \sum_{k=0}^{n_b} \tilde{b}_k \gamma_j q^{-k} u^j(t) + e(t) \quad (8.10)$$

define a polynomial $S_j(q^{-1})$

$$S_j(q^{-1}) = \gamma_j \tilde{B}(q^{-1}) = s_{j0} + s_{j1} q^{-1} + \dots + s_{jn_b} q^{-n_b} \quad (8.11)$$

where $s_{jk} = \gamma_j \tilde{b}_k$, $j = 1, \dots, n$, $k = 0, \dots, n_b$. Then, Equation (8.10) is improved to be

$$\tilde{A}(q^{-1})y(t) = \tilde{B}(q^{-1})u(t) + \sum_{j=2}^n S_j(q^{-1})u^j(t) + e(t) \quad (8.12)$$

Equation (8.12) can be put into linear regression form as follows:

$$y(t) = \phi^T(t)\theta + e(t) \quad (8.13)$$

where

$$\phi(t) = (-y(t-1), -y(t-2), \dots, -y(t-n_a), u(t), u(t-1), \dots, u(t-n_b), \quad (8.14)$$

$$u^2(t), \dots, u^2(t-n_b), \dots, u^n(t), \dots, u^n(t-n_b))^T$$

$$\theta = (\tilde{a}_1, \tilde{a}_2, \dots, \tilde{a}_{n_a}, \tilde{b}_0, \tilde{b}_1, \dots, \tilde{b}_{n_b}, s_{20}, \dots, s_{2n_b}, \dots, s_{n0}, \dots, s_{nn_b}) \quad (8.15)$$

The linear regression representation for the system given in Equation (8.13) permits direct application of the RLS method. However, the vector of unknown parameters does not include the coefficients of the polynomial $\tilde{B}(q^{-1})$ explicitly. These coefficients are implicitly expressed in the form of products with the nonlinear subsystem parameters γ_j ($j = 1, \dots, n$). Consequently, the identification of the system parameters can not be performed at a single stage. The RLS method is, therefore, implemented in two steps. The first step of the algorithm gives the estimates of the parameters a_i and s_{jk} , and the second step estimates the parameters b_k and γ_j using the results of the first step, where $i = 1, \dots, n_a$, $j = 1, \dots, n$, $k = 1, \dots, n_b$. The nonlinear identification algorithm steps are summarized as follows:

- (vi) Choose initial values for the covariance matrix P and forgetting factor λ .
- (vii) Acquire the input and output of the system and form the data vector ϕ as given in Equation (8.14) for time instant t using the present and past values of the input u , output y and powers of u .

(viii) Solve for the parameter estimates $\hat{a}_i, \hat{b}_k, \hat{s}_{jk}$ using RLS estimates rule:

$$\varepsilon(t) = y(t) - \phi^T(t)\hat{\theta}(t-1)$$

$$P(t) = \frac{1}{\lambda} P(t-1) \left[I_p - \frac{\phi(t)\phi^T(t)P(t-1)}{\lambda + \phi^T(t)P(t-1)\phi(t)} \right]$$

$$\hat{\theta}(t) = \hat{\theta}(t-1) + P(t)\phi(t)\varepsilon(t)$$

(ix) (iv) Solve for the estimates $\hat{\gamma}_j, j = 1, \dots, n$ using the estimated values

\hat{b}_k, \hat{s}_{jk} by the formula :

$$\hat{\gamma}_j = \left(\sum_{k=1}^{n_b} \hat{b}_k^2 \right)^{-1} \sum_{k=1}^{n_b} \hat{b}_k \hat{s}_{jk} \quad j = 1, \dots, n.$$

(x) Update the time instant, $t = t + 1$. Return to step (ii).

8.2.3.4 Hammerstein Model of Nonlinear SI Engine Dynamics

It is possible to decompose the nonlinear torque generation dynamics given in Figure 8.13 into its nonlinear static and linear dynamic parts, which constitute a Hammerstein type structure. This model relies on the assumption that the nonlinearity in the process, which is a result of thermodynamics and mechanics of the gas in the cylinders, and mechanics of piston motion, is approximately static, and the dynamics of system behavior are approximately linear [28]. With this assumption, the torque generation conceptual diagram is given in Figure 8.15, where $g(\cdot)$ is a static nonlinear function, and $H(q^{-1})$ is a linear transfer function in terms of the discrete delay operator q^{-1} . For the sake of simplicity and ease of calculation, the nonlinearity in the model is given as a polynomial of known order with constant coefficients.

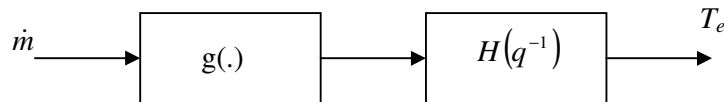


Figure 8.15 Hammerstein model for torque generation

The combination of the throttle model and torque generation model is obtained by integrating the throttle sensitivity given by $1.068K_0$, and its powers up to order n into the nonlinear function. Without loss of generality, the nonlinear polynomial coefficients can be normalized with respect to the constant term that is the zeroth order term of the polynomial. The combined Hammerstein system structure is given in Figure 8.16.

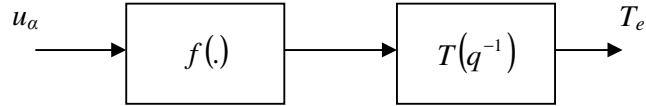


Figure 8.16 Hammerstein model of SI engine dynamics

With the introduction of the combined Hammerstein model in Figure 8.15, the problem of nonlinear system identification reduces to the problem of estimation of model parameters given by γ_i , b_j , and a_k ($i=2, \dots, n$; $j=0, \dots, n_b$; $k=1, \dots, n_a$).

8.2.3.5 Identification Results

Spark ignition engine identification experiments were performed using the set-up described in section 7.4. Nonlinear parameter estimation procedure for Hammerstein system structure was used following the steps in section 8.2.3.3. Nonlinear polynomial order, maximum output delay, and maximum input delay are selected respectively as: $n=2$, $n_a=4$, $n_b=3$. The parameter estimation algorithm, coded and run in Matlab environment, converged to the values tabulated in Table 8.6. Figure 8.17 gives the recorded response of the experimental set-up to the PRBS test signal together with the estimated response recorded during the recursive identification process. Since RLS relies on the minimization of the cost function, which requires the minimization of the error of recursive estimation, the two signals are close as expected. However, convergence of the estimated response to the real system output in a recursive identification algorithm does not guarantee the convergence of the parameter estimates to the true values. Consequently, minimizing the least squares error alone is not enough to show the success of the identification procedure.

Obtained model should be validated using the estimated parameters to generate a new set of output data by simulation of the identified model.

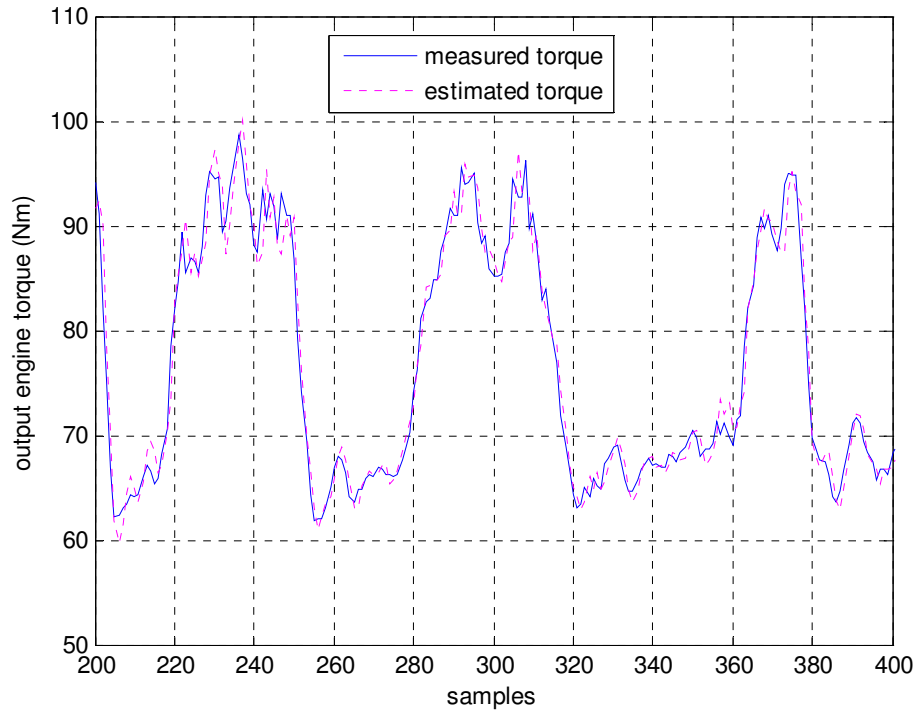


Figure 8.17 Results of the identification experiment. Torque response of the SI engine is given in solid line, and estimated torque recorded through recursions is given in dotted line

Table 8.6 Estimates of Hammerstein model parameters

a_1	a_2	a_3	a_4	b_0	b_1	b_2	b_3	γ_2
-1.1935	0.1138	0.0635	-0.0791	0.0708	0.0707	0.0707	0.0708	$-12.4 \cdot 10^{-3}$

The Hammerstein model obtained by identification of the engine is tested by simulating the model with two input data sets. First set belongs to the PRBS input signal applied to the process for identification. The simulated response is given in Figure 8.18 together with the real system response obtained by experiment. Secondly, in order to generate an independent set of data, a square wave is applied to

the engine and response is recorded. This input signal is applied to the identified Hammerstein model as well, of which response is recorded as a result of digital simulation. Results are given in Figure 8.19.

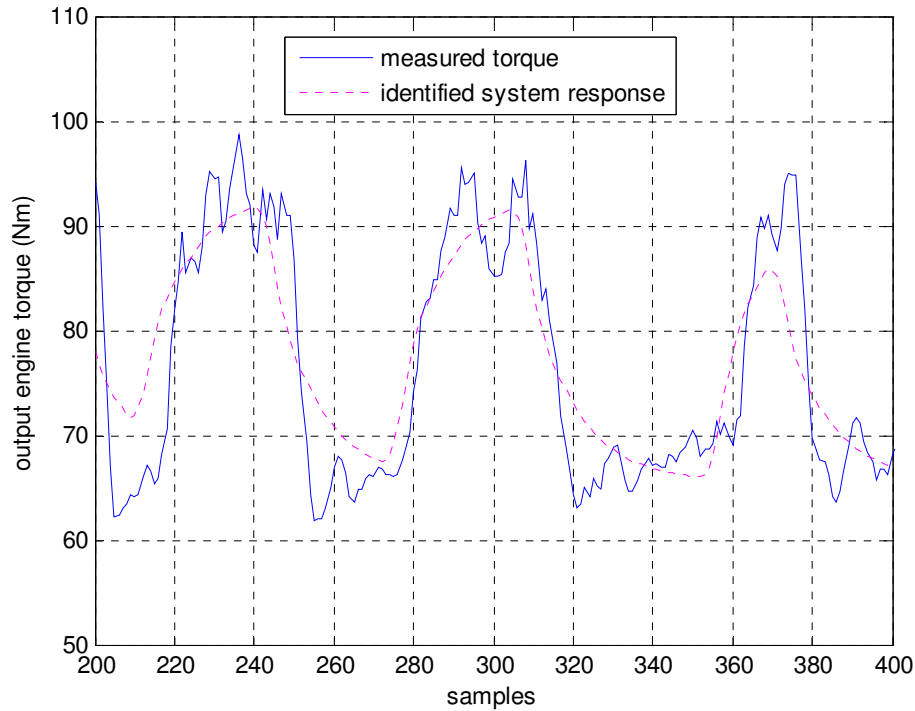


Figure 8.18 Validation of identification results. Torque response of the SI engine to a PRBS input is given in solid line, and simulated response of the obtained Hammerstein model is given in dotted line

Inspection of the identification results in Figure 8.17 reveals that the identification procedure generates a highly accurate estimated response to input variations even in fast transient phases and high frequency load effects. Although it does not guarantee that the identified model accurately represents the process behavior, this result gives useful information for online applications of control. Figures 8.18 and 8.19 give plots of the model validation experiments. The identified model is tested using the set of data used in identification, and results in Figure 8.18 reveal the performance of the model in response to the PRBS test signal. Identified model is also tested using a square wave input to get the results of an independent model validation experiment. The model obtained consists of a second order polynomial cascaded to a fourth order linear system. Despite the fact that this model is too simple to represent the highly

nonlinear and complex thermodynamics, gas dynamics, and mechanics in the engine, the identified model response follows the true torque measurement with an acceptable degree of accuracy. However, it should be noted that the model is insufficient in representing the high frequency components that result from effects like measurement noise and mechanical vibrations in the process.

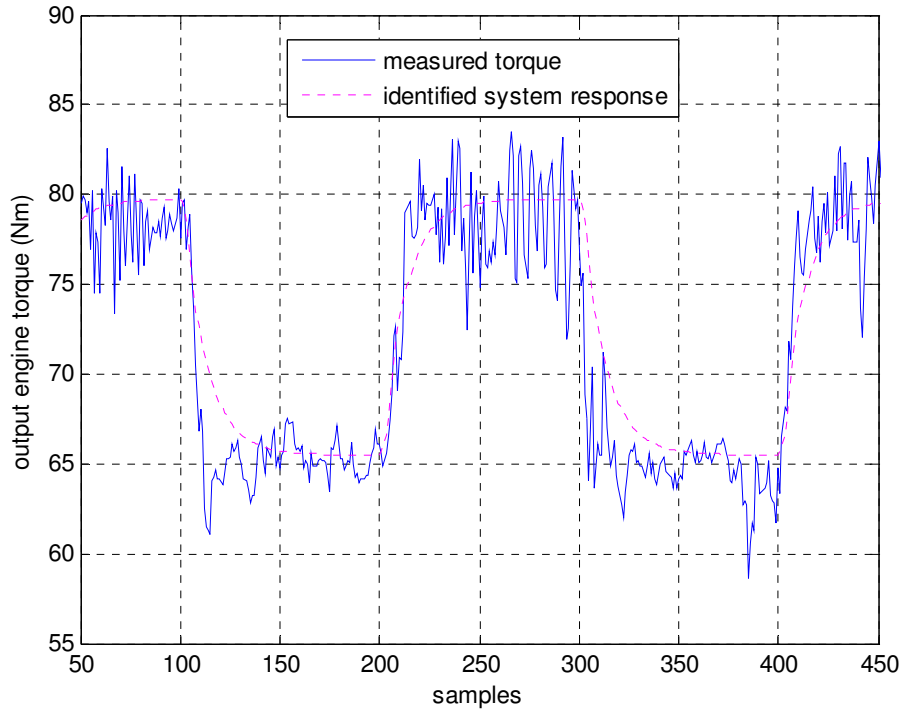


Figure 8.19 Validation of identification results by a different set of data. Torque response of the SI engine to a square wave input is given in solid line, and simulated response of the obtained Hammerstein model is given in dotted line

8.2.3.6 Model Validation

The mean square error (MSE) method is the most commonly used one for model testing purposes [28, 219].

$$MSE = \frac{1}{N} \sum (y(t) - \hat{y}(t))^2 \quad (8.16)$$

where $\hat{y}(t)$ is the predicted output and N is the number of samples used in the identification process. The MSE values for the nonlinear identification experiments were calculated for different model orders, and the results are tabulated in Table 8.7.

During the nonlinear identification, the order of the nonlinear polynomial was kept constant at two. The linear identification experiments result in the selection of the fourth or fifth order model for representing the present system. The nonlinear identification results, however, reveal definitely that the fourth order model gives the best result as far as the identification error is concerned. Further increase in the model order brought no significant improvement in the performance of the predicted models. The MSE values for different orders of the nonlinear polynomial were calculated and tabulated with the linear part of order fourth. The results presented in Table 8.8 reveal clearly that the selection of the second order nonlinearity in the nonlinear identification experiments gives the best result.

Table 8.7 MSE values for nonlinear identification experiments

Model order	1	2	3	4	5	6	7
MSE	151.312	129.072	31.28	17.782	20.127	22.939	23.124

Table 8.8 MSE values and nonlinear parameters for nonlinear identification with different polynomial orders

order	2	3	4
MSE	17.782	5.891×10^{-3}	6.908×10^{-15}
γ_2	-0.0124	-0.0853	22.6186
γ_3	-	0.0014	-1.664
γ_4	-	-	0.0269

8.2.3.7 Conclusions

This case study deals with the problem of identifying of a spark ignition engine torque from input-output data. Nonlinear model was developed for the system. A nonlinear representation and identification approach using the nonlinear

Hammerstein system structure was used for the present system. A suitable experimental setup was built and tested using RLS identification algorithm for the nonlinear case. The measured data obtained experimental setup is used by a software program that runs in Matlab environment to identify unknown system parameters. The nonlinear system identification with fourth order linear dynamics gives the best result. And also selection of the second order nonlinearity gives the best result. The results are numerically and graphically demonstrated. Inspection of the identification results reveals that the identification procedure generates a highly accurate estimated response to input variations even in fast transient phases and high frequency load effects. The results of the present study are meant to constitute a starting point for on going studies on identification of gasoline engine system by other nonlinear methods and adaptive control applications for nonlinear systems.

8.2.4 Nonlinear modeling and identification of a spark ignition engine torque using NARX model

8.2.4.1 Introduction

System identification, as a subject of control engineering, refers to the procedure of building a mathematical description of the dynamic behavior of a system/process from measured data so as to provide accurate prediction of the future behavior for given inputs [26, 27, 220]. The key problem in system identification is to find a suitable model structure, within which a good model is to be found [21]. Development of nonlinear model is the critical step in the application of nonlinear model based control strategies. Nonlinear behavior is the rule, rather than the exception, in the dynamic behavior of physical systems. Most physical systems have nonlinear characteristics outside a limited linear range [221, 222]. The development of simplified models of automotive engines appropriate for control/diagnostic system research and design is an important subject for research and development [3].

In engineering dynamics, control engineering and many other areas, auto-regressive with exogenous inputs (ARX) models are widely utilized for describing dynamic data regimes for linear and nonlinear systems [16]. However, the performance of these linear models for prediction and control has been limited. In particular, the

nonlinear nature and strong directionality of the process present problems during identification. NARX model has been considered as alternatives to linear models in a number of ICE applications such as describing the pressure inside the intake manifold and the crankshaft speed of ICE [32, 34], identification and control of ICE in idle-speed conditions [33]. NARX model from input-output data are used by [60] to identify a nonlinear system.

The engine torque is one of the most important performance variables of an ICE and, for this reason; a torque control system can improve substantially the performance of the overall vehicle [7, 8]. Their modeling efforts were focused on an experimental method of system identification that captures the nonlinear engine torque characteristics for a large range of operating conditions [10]. The objective of this case study is to obtain a nonlinear model of SI engine torque. In this case study, a procedure to provide the nonlinear model of the dynamics between the throttle valve command and torque in a gasoline engine directly from raw data is presented. The nonlinear system model is built and a sigmoid based nonlinear ARX model is developed using input and output regressors.

8.2.4.2 NARX Model

Nonlinear ARX models extend the linear ARX models to the nonlinear case and have this structure:

$$y(t) = f(y(t-1), \dots, y(t-na), u(t-nk), \dots, u(t-nk-nb+1)) \quad (8.17)$$

where the function f depends on a finite number of previous inputs u and outputs y . na is the number of past output terms used to predict the current output. nb is the number of past input terms used to predict current output. nk is the delay from the input to the output.

The nonlinear ARX structure models dynamic systems using a parallel combination of nonlinear and linear blocks, as shown in the Figure 8.20.

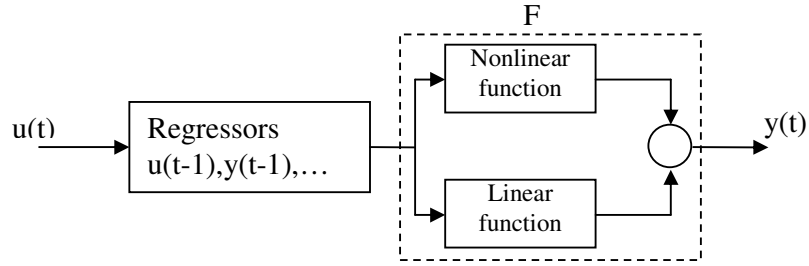


Figure 8.20 NARX model structure

The nonlinear and linear functions are expressed in terms of variables called regressors, which are functions of measured input-output data. The predicted output $\hat{y}(t)$ of a nonlinear model at time t is given by the following general equation.

$$\hat{y}(t) = F(x(t)) \quad (8.18)$$

where, $x(t)$ represents the regressors. F is a nonlinear regression function, which is approximated by the nonlinearity estimators. The function F can include both linear and nonlinear functions of $x(t)$, as show in Figure 8.20.

The sigmoidnet based nonlinear is used to capture the nonlinearity of the NARX model. The function $F(x)$ is given by the following expression:

$$F(x) = (x-r)PL + a_1 f((x-r)Qb_1c_1) + a_2 f((x-r)Qb_2c_2) + \dots + a_n f((x-r)Qb_n c_n) + d \quad (8.19)$$

The sigmoid function f in the above equation is given by

$$f(z) = 1/(\exp(-z) + 1) \quad (8.20)$$

where

P is a nonlinear subspace matrix

Q is a linear subspace matrix

r is a regressor mean vector
 L is a linear coefficients vector
 b_n is a dilation matrix
 a_n is an output coefficients vector
 c_n is a translation vector
 d is an output offset scalar

The parameters of sigmoidnet based NARX models were estimated using the ident function system identification toolbox version 7.0 in Matlab. The iterative prediction-error minimization method discussed in Ljung [26] was used to calculate the model parameters.

8.2.4.3 Identification Results

SI engine identification experiments were performed using the set-up described in section 7.4. SISO NARX model is developed in this case study to model the nonlinear dynamics of the SI engine. The SISO NARX model is used throttle valve position as inputs and engine torque as output.

The position of a throttle valve is controlled by a servo motor. The air flow rate in the intake manifold is controlled by the size of the valve opening through which the air flows into the manifold. The output engine torque is then a function of the throttle valve position. Figure 8.21 shows measured values of the throttle valve size u and the output engine torque y , which are input and output signals respectively. As seen in the output engine torque, we have a very oscillative settling period after a change of the throttle valve size. These oscillations are caused by highly nonlinear and complex thermodynamics, gas dynamics, and mechanics in the engine. The parameter estimation algorithm, coded and run in Matlab environment, converged to the values tabulated in Table 8.9.

In the SISO NARX model used this work, sigmoidnet function is used as nonlinear regressor function containing five past output regressors ($n_a=5$) and minimum of a one-sample input delay ($n_k=1$) and the four past input regressor ($n_b=4$), i.e.

Table 8.9 Parameters of SISO NARX models

Model parameters	SISO NARX model
Nonlinear subspace (P) matrix & Linear subspace matrix (Q)	$P = Q = \begin{bmatrix} 0.1276 & -2.0132 & -0.6882 & -0.3795 & 1.3535 & 13.2895 & -35.9536 & 37.6343 & 24.1571 \\ 0.0973 & -2.1296 & -1.0093 & -0.0027 & 0.7169 & 8.5022 & 10.3721 & -63.2216 & -65.1947 \\ 0.0689 & -2.1929 & -1.2830 & 0.2247 & -0.1168 & 1.1941 & 38.9912 & -2.9281 & 83.3336 \\ 0.0426 & -2.1937 & -1.5172 & 0.3691 & -0.8655 & -6.8742 & 15.5663 & 63.6563 & -63.3491 \\ 0.0192 & -2.1294 & -1.7186 & 0.4380 & -1.6306 & -13.7905 & -32.8414 & -34.4972 & 21.8677 \\ 0.9959 & 1.2437 & -5.2582 & -7.3901 & -5.1429 & 1.0373 & 0.3517 & 0.1251 & -0.1905 \\ 1.0393 & 0.6317 & -2.1063 & 7.2699 & 12.2621 & -1.3791 & -0.1453 & -0.0112 & 0.2706 \\ 1.0416 & -0.1725 & 2.4483 & 7.1016 & -12.3218 & 1.2461 & -0.3405 & 0.1863 & -0.1012 \\ 1.0025 & -0.9636 & 5.2342 & -7.5648 & 5.0326 & -2.9368 & 1.0130 & -0.8017 & -0.1871 \end{bmatrix}$
Linear coefficients	$L = \begin{bmatrix} 0.0254 \\ -0.0583 \\ 0.0082 \\ 0.0074 \\ 0.0004 \\ 0.0238 \\ -0.0127 \\ -0.0008 \\ 0.0078 \end{bmatrix}$

Table 8.9 Cont'd

Dilation	$b_n = 1 \times 10^3$ $\begin{bmatrix} -0.0139 & 6.2438 & 0.0014 & 0.0026 \\ 0.0229 & 5.5581 & -0.0957 & -0.0025 \\ -0.0095 & 4.0224 & 0.1936 & -0.0011 \\ -0.0044 & -0.4914 & 0.0055 & -0.0026 \\ -0.0004 & -1.6669 & -0.2226 & -0.0018 \\ 0.0032 & -1.3183 & 0.0171 & -0.0022 \\ -0.0077 & -1.8584 & 0.0003 & 0.0045 \\ 0.0097 & 5.1746 & -0.0002 & 0.0026 \\ 0.0267 & 2.2908 & 0.0001 & -0.0006 \end{bmatrix}$
Output coefficients	$a_n = [-0.0141 \quad -0.0119 \quad -0.0682 \quad 0.0199]$
Regressor mean	$r = [0.6067 \quad 0.6065 \quad 0.6062 \quad 0.6058 \quad 0.6052 \quad 0.6932 \quad 0.6926 \quad 0.6921 \quad 0.6916]$
Translation	$c_n = 1 \times 10^4 [0.0067 \quad -1.2068 \quad -0.0001 \quad 0.0011]$
Output offset	$d = 0.6425$

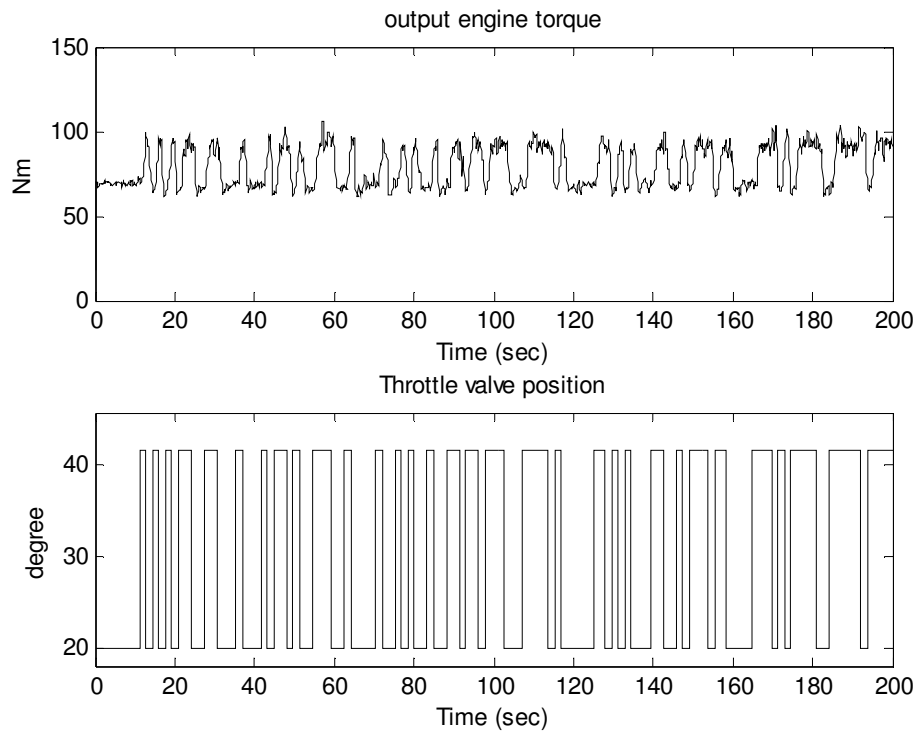


Figure 8.21 PRBS of the throttle valve position (bottom) and measured values of torque (top)

The regression vector

$x = [y(t-1), y(t-2), y(t-3), y(t-4), y(t-5), u(t-1), u(t-2), u(t-3), u(t-4)]$ where y and u are the output and the input of the system, respectively. Figure 8.22 gives the recorded response of the experimental set-up to the PRBS test signal together with the estimated response recorded during the iterative prediction-error minimization method. The parameters which give the minimum are then used in the nonlinear model. As seen in Figure 8.22, the two signals are close as expected. However, convergence of the estimated response to the real system output in an iterative prediction-error method does not guarantee the convergence of the parameter estimates to the true values. Consequently, minimizing the prediction error alone is not enough to show the success of the identification procedure. Obtained model should be validated using the estimated parameters to generate a new set of output data by simulation of the identified model.

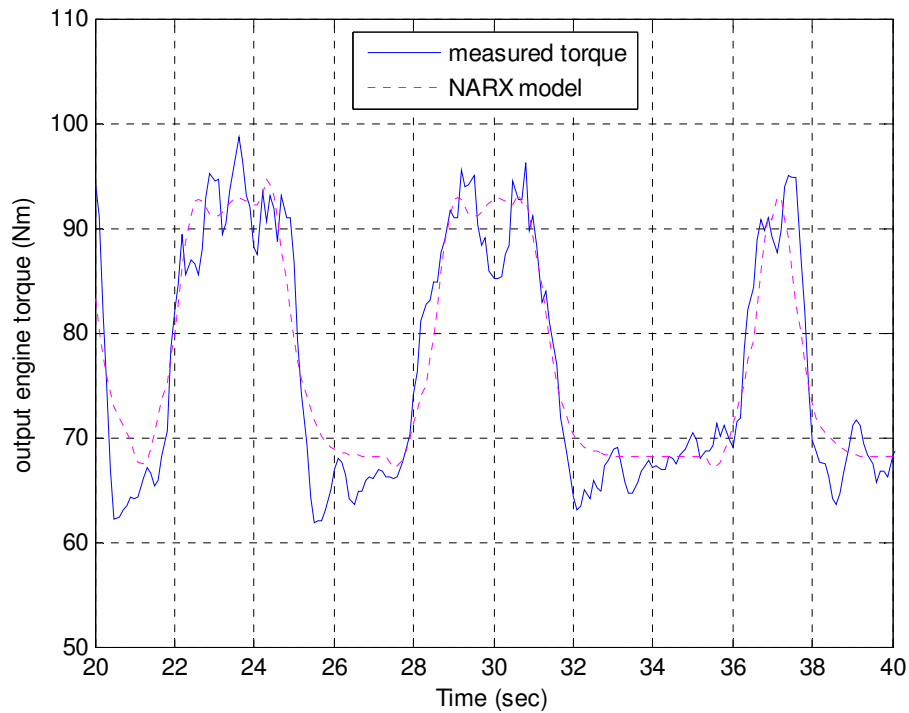


Figure 8.22 Results of the identification experiment. Torque response of the SI engine is given in solid line, and NARX model estimated torque is given in dotted line

8.2.4.4 NARX Model Validation

Model validation provides the way to assess the quality of a proposed model and also to find out the inadequacy of the model in explaining an observed system behavior [223]. The last step of the system identification procedure is the validation of the estimated model. After estimating, the model should be validated to determine whether the model can reproduce system behavior by estimating within acceptable bounds.

The selection of model structure and their orders is the main purpose. The selection of model structure depends on nonlinear effects in the system, system properties and prior knowledge of the system. The second purpose is selection of the model orders. The model orders were determined by trial and error method. After estimation the

best model by using the trial and error. In fact, another input data is given to the system and the model and their outputs are compared [223].

The NARX model obtained by identification of the engine is tested by simulating the model with PRBS input data set. The PRBS input signal applied to the process for identification. The simulated response is given in Figure 8.23 together with the real system response obtained by experiment.

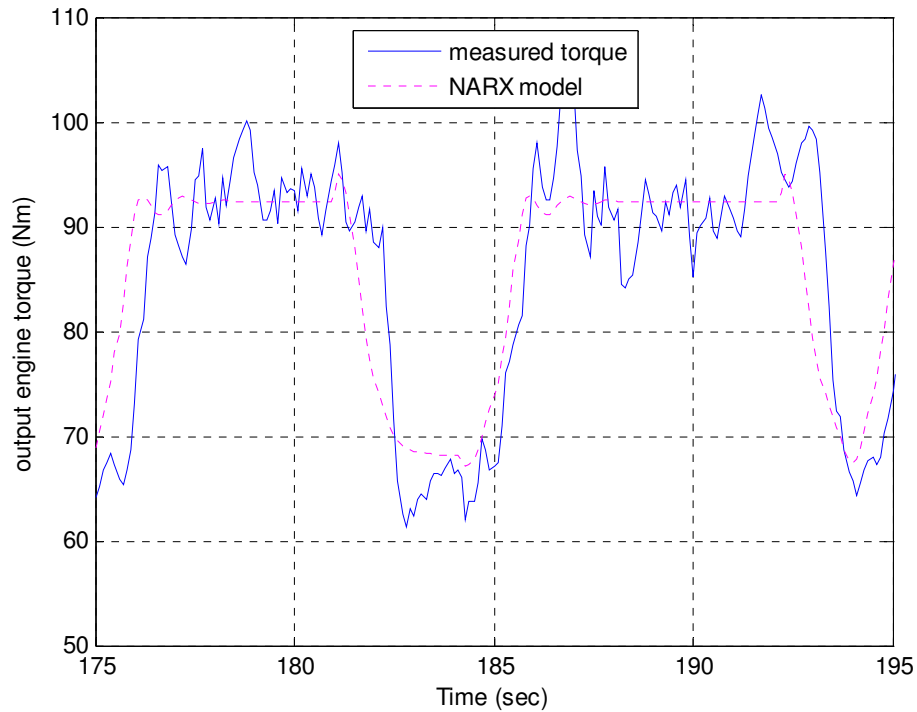


Figure 8.23 Validation of identification results. Torque response of the SI engine to PRBS input is given in solid line, and simulated response of the obtained NARX model is given in dotted line

Inspection of the identification results in Figure 8.22 reveals that the identification procedure generates a highly accurate estimated response to input variations even in fast transient phases and high frequency load effects. Although it does not guarantee that the identified model accurately represents the process behavior, this result gives useful information for online applications of control. Figure 8.23 gives plot of the model validation experiments. The identified model is tested using the set of data used in identification, and results in Figure 8.23 reveal the performance of the model in response to the PRBS test signal. Despite the fact that this model is too simple to

represent the highly nonlinear and complex thermodynamics, gas dynamics, and mechanics in the engine, the identified model response follows the true torque measurement with an acceptable degree of accuracy. However, it should be noted that the model is insufficient in representing the high frequency components that result from effects like measurement noise and mechanical vibrations in the process.

The mean square error (MSE) method given in Equation 8.16 is the most commonly used one for model testing purposes [28, 219]. The MSE values for the nonlinear identification experiments were calculated for different model orders, and the results are tabulated in Table 8.10.

Table 8.10 MSE values for nonlinear identification experiments

Model order	1	2	3	4	5	6	7
MSE	42.596	39.362	38.513	37.008	36.644	48.513	81.156

The nonlinear identification results, however, reveal definitely that the fifth order model gives the best result as far as the identification error is concerned. Further increase in the model order brought no significant improvement in the performance of the predicted models.

8.2.4.5 Conclusions

This case study deals with the problem of identifying of a spark ignition engine torque from input-output data. Nonlinear model was developed for the system. A nonlinear representation and identification approach using the sigmoid based nonlinear ARX model structure was used for the present system. A suitable experimental setup was built and tested using iterative prediction-error minimization method. The measured data obtained experimental setup is used by a software program that runs in Matlab environment to identify unknown system parameters. The nonlinear system identification with fifth order nonlinear dynamics gives the best result. The results are numerically and graphically demonstrated. Inspection of the identification results reveals that the identification procedure generates a highly accurate estimated response to input variations even in fast transient phases and high frequency load effects. The results of the present study are meant to constitute a

starting point for on going studies on identification of gasoline engine system by other nonlinear methods and adaptive control applications for nonlinear systems.

8.2.5 A comparative study of neural network structures in identification of gasoline engine torque

8.2.5.1 Introduction

System identification has become an important area of study because of the increasing needs in estimating the behavior of a system with partially known dynamics. Especially in the areas of control, pattern recognition and even in the realm of stock markets the system of interest needs to be known to some extent. A common property of real life systems is the fact that they have multiple variables, some of which are subjected to stochastic disturbances. Since a system may have a complicated dynamic behavior, the varying environmental changes make the identification process much more difficult than the cases in which those changes are modeled deterministically [14, 15].

Artificial neural network (ANN) opened a new horizon in identification and control of highly nonlinear and complex structured systems. These networks are implemented using massive connections among the neurons with variable strengths. Moreover, their parallel, distributed and fault tolerant processing properties make them powerful tools for both identification and control of nonlinear dynamical systems. Especially learning capabilities of these networks enable them to process the information adaptively [18, 19].

The use of ANN in system identification has been gaining more and attention in recent years. Neural networks have good general approximation capabilities for reasonable nonlinear systems [20, 21]. Nerandra and Parthasaraty [22] have demonstrated that artificial neural networks could be used successfully for the identification and control of nonlinear dynamic systems. A series of works performed by Chen and Billings and their coworkers have developed the foundation of using neural networks as a tool for nonlinear system identification [23-25].

The engine torque is one of the most important performance variables of an ICE and, for this reason; a torque control system can improve substantially the performance of the overall vehicle [7, 8]. Their modeling efforts were focused on an experimental method of system identification that captures the nonlinear engine torque characteristics for a large range of operating conditions [10]. Automotive engines are multivariable system with severe nonlinear dynamics, and their modeling and control are challenging tasks for control engineers [77].

Moreover, ANN has been proven to be useful for modeling and identification nonlinear dynamic systems. RNN have been used by many researchers. Some of which are used for simulating the air-fuel ratio (AFR) dynamics into the intake manifold of a spark ignition (SI) engine [75], for identify the nonlinear dynamic of the intake manifold and the throttle body processes in an automotive engine [1], for modeling air-fuel ratio in SI engine [81], for AFR identification and control in SI engines [76], for AFR identification in SI engine [105]. Different neural network structures like multilayer perceptron (MLP), pseudo linear radial basis function and local linear model tree networks for modeling variable valve timing [78] and torque [79] of a SI engine has been studied. An artificial neural networks approach to estimate the indicated torque of a single-cylinder diesel engine from crankshaft angular position and velocity measurements are presented in [86]. The dynamic multi layered perceptron and the generalized Hammerstein model are described and compared to the experimental identification of the charging process in diesel engines [89]. Hou et al. [91] provided a method of identifying AFR of a HL495Q gasoline engine based on elman neural network. A dynamic local neural network approach has been applied for modeling the NO_x emissions characteristics of a 1.9l direct injection diesel engine [85]. A neural approach has been applied for modeling and control of a turbocharged diesel engine speed with pollution constraints [92]. A different neural network approach has been used for fault diagnosis and identification in automotive engine [94]. Exhaust gas recirculation control in SI LPG engine has been proposed using RBF neural network approach. Autoregressive Neural network has been used for identification of locomotive diesel engine [101]. Neural network model has been presented for identification and control of the AFR of automotive engine [102].

Neural networks have been successfully used in wide range of automotive control applications. An adaptive RBF model based model predictive control to the air/fuel ratio control of automotive engines [77]. Wang et al. [2-4] presented an application of adaptive neural network modeling and model based predictive control for modeling the crankshaft speed, intake manifold pressure, manifold temperature [2], air fuel ratio [3] and engine speed [4]. A radial basis function (RBF) neural network was utilized for them. A fast neural network models for engine control design purposes are applied in [83, 84, 98, 99]. A nonlinear model based control has been proposed for an efficient control of the air actuators of a turbocharged SI engine using neural network [93]. SI engine idle speed control has been presented using ANN [100]. ANN has been used for adaptive AFR control in gasoline engines and for adaptive AFR control in SI engine [80]. Transient fueling control of SI engine has been presented using feed forward neural network [111, 112].

In this case study, different neural network structures are used to identify nonlinear dynamic models for the SI engine torque. Dynamic Levenberg-Marquardt algorithm is applied to the weight-estimation using the neural network toolbox version 7.0 in Matlab. Experimental results show that the neural network based models are more precise and generalized in performance than the Hammerstein and NARX models. Such models can be used for control system design, or in a model-based fault detection and diagnosis strategy.

8.2.5.2 Neural Network System Identification

The neural network based black-box method is used to model the SI engine torque dynamics taking into account the interaction between the input and output of the SISO system. The simplest linear discrete-time input-output model is the ARX model [17]. The optimal predictor of an m th order ARX model is

$$\hat{y}(t) = b_1 u(k-1) + \dots + b_m u(k-m) - a_1 y(k-1) - \dots - a_m y(k-m). \quad (8.21)$$

As we know, a wide class of nonlinear systems can be described by NARX (nonlinear ARX) model [224] in a straightforward manner by replacing the linear relationship in Equation (8.21) with unknown nonlinear function $f(\cdot)$, that is,

$$\hat{y}(k) = f(u(k-1), \dots, u(k-m), y(k-1), \dots, y(k-m)) \quad (8.22)$$

Identifying the nonlinear dynamic system using the neural network is to find a fit neural network structure to substitute for the nonlinear function $f(\cdot)$ under the known system model structure as shown in Equation 8.22. By readjusting the connection weight value of the neural network, the output of neural network is equal to the output of the plant. Identified model was obtained the as following

$$\hat{y}(k) = f_{NN}(u(k-1), \dots, u(k-n_u), y(k-1), \dots, y(k-n_y)) \quad (8.23)$$

where $y(k)$ denotes the output vector, $u(k)$ the input vector, n_y and n_u denoted the dynamic order of the model output and input respectively.

Thus, the NARX model is trained in series-parallel configuration, whose structure was shown in Figure 8.24. This model can be considered as a feedforward network model.

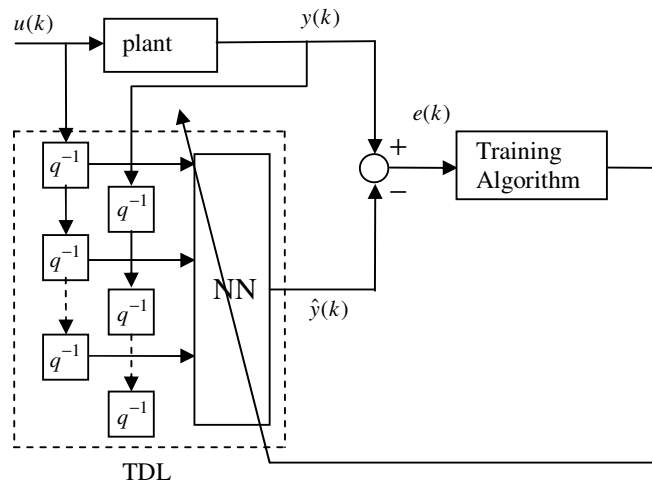


Figure 8.24 Series- parallel model for neural network identification

The number of past outputs and control inputs required to be fed for the system identification depends upon the order and the structure of the system. One drawback of models with output feedback is that the choice of the dynamic order m is crucial

for the performance and no really efficient methods for its determination are available. Often the user is left with a trial-and-error approach.

8.2.5.2.1 Feed Forward Neural Networks (FFNN) for System Identification

An identification procedure, in the most general sense, entails a matching between the system outputs and an identifier output. Artificial neural networks (ANNs) are massively parallel distributed structures and have ability to learn through experience [158]. ANNs due to their ability to act as universal approximators can very effectively be used for this purpose [14, 15]. Narandra and Parthasarathy [22] have reported an extensive study on the use of these networks for identification and control purposes.

Useful properties of ANNs such as nonlinearity, input/output mapping and adaptability have been exploited to model the dynamic of the SI engine torque. As one hidden layer with sufficient number of neurons is good enough to approximate any nonlinear function [158], only one hidden layer is used for the present work. Levenberg-Marquardt (LM) optimization algorithm is used to minimize the cost function defined by the mean square error (MSE) given by

$$MSE = \frac{1}{N} \sum_{j=1}^N (y_j(k) - \hat{y}_j(k))^2 \quad (8.24)$$

where N is the number of data points, and $y_j(k)$ and $\hat{y}_j(k)$ denote the desired and model output at the k th sample points. Actually, the desired $y_j(k)$ is the observation data in the experiments. The output of the network is computed by proceeding layer by layer through the network. The net internal activity level V_j^k for a neuron j in hidden layer k is given by

$$V_j^k(n) = \sum_{i=0}^p W_{ji}^k(n) Y_i^{k-1}(n) \quad (8.25)$$

where $Y_i^{k-1}(n)$ is the output of neuron i of the layer $k-1$, $W_{ji}^k(n)$ is the net weight of neuron j in the layer k connecting to the i_{th} neuron of layer $k-1$. the output of the neuron j in layer k is computed using the tan-hyperbolic activation function given by

$$Y_j^k(n) = 1 - \frac{2}{1 + \exp(2V_j^k(n))} \quad (8.26)$$

For neural network training using LM algorithm, the gradient vector can be calculated as

$$g(\theta) = J^T(\theta)e(\theta) \quad (8.27)$$

where $J(\theta)$ is the system Jacobian matrix, θ is the parameter vector and $e(\theta)$ is the error vector defined by

$$e(\theta) = [e_1, e_2, \dots, e_n]^T \quad (8.28)$$

The minimum is found by iteratively solving the equation

$$(J(\theta)^T J(\theta) + \mu I)\Delta\theta = -J(\theta)^T e(\theta) \quad (8.29)$$

where μ is a scalar quantity and I is an identity matrix.

SI engine identification experiments were performed using the set-up described in section 7.4. For identification of SI engine, the SISO neural network model is used throttle valve position u as the input vector and engine torque y as the output vector. The neural network training is performed off-line utilizing a previously generated training data set. The backpropagation, backpropagation with adaptive learning rate, backpropagation with momentum and Levenberg-Marquardt (LM) training algorithms of Matlab were tested. As mentioned in [225], the LM algorithm was found to be the fastest training algorithm, but requiring more memory with the same error convergence bound compared to the other algorithms.

The system identification problem requires a suitable excitation signal. Usually a signal, which is sufficiently rich and persistently exciting all the system modes, is selected. PRBS (pseudo random binary signal) well suited for identification. Imitates white noise in discrete time with a deterministic signal and thus excites all frequencies equally well [17]. To create the disturbances needed to perform identification of the process, PRBS were used [41, 95]. A PRBS was designed for throttle angle position to obtain a representative set of input-output data. A set of data samples, including throttle valve position and the torque was collected for the system identification. Each set contains 2000 data samples.

After training the network, the identification process is tested by using the Figure 8.24. The speed estimate $\hat{y}(k)$ of the so called identifier will be compared with the experimental and/or simulated output $y(k)$ to evaluate the performance of the identified NN reflecting the dynamics of SI engine.

Several neural networks with different structures were tried in order to find the optimal model. The data sequences are divided into two sections. One section is used for training and another section is used for testing. Table 8.11 shows the performance comparison. In Table 8.11, hn is defined as the number of the hidden neurons of the neural network model.

Based on the results of Table 8.11, it is seen that both the orders of the input variables and the number of the hidden neurons have an effect on the model performance. The results presented in Table 8.11 reveal clearly that the selection of the number of the hidden neurons is ten, while the orders of the input variables are, respectively $n_u = 4$ and $n_y = 4$.

A two-layer feedforward neural network with eight input neurons, ten neurons in the hidden layer and one output neuron, denoted as 8-10-1, has been used in the network. The proposed ANN model is given in Figure 8.25. The learning algorithm used in the study is Levenberg-Marquardt (LM); activation function is tan-sigmoid (tansig) transfer functions. The number of hidden neurons has been determined by trial-and-error. Using a larger number of hidden neurons can approximate the system

dynamics better with a time penalty for training. For the LM training algorithm, the data was normalized within the [-0.5, +0.5] range, which is a common practice for

Table 8.11 Performance comparison for neural models

Neural network structure	Correlation coefficient (R)
$n_u = 2, n_y = 2, hn = 7$	0.98403
$n_u = 2, n_y = 2, hn = 8$	0.98418
$n_u = 2, n_y = 2, hn = 9$	0.9841
$n_u = 2, n_y = 2, hn = 10$	0.98481
$n_u = 3, n_y = 3, hn = 7$	0.9851
$n_u = 3, n_y = 3, hn = 8$	0.9855
$n_u = 3, n_y = 3, hn = 9$	0.9856
$n_u = 3, n_y = 3, hn = 10$	0.9865
$n_u = 4, n_y = 4, hn = 7$	0.9854
$n_u = 4, n_y = 4, hn = 8$	0.9861
$n_u = 4, n_y = 4, hn = 9$	0.9868
$n_u = 4, n_y = 4, hn = 10$	0.9871

the neural network training using tan-sigmoid activation function. The algorithm itself selected the initial weights randomly. This induced the possibility of having slightly differing results at each training.

The identifier has been assessed using the following test signal shown in Figure 8.21. The real system response and the identifier outputs are shown in Figure 8.26. Obtained model should be validated using the estimated parameters to generate a new set of output data by simulation of the identified model. The simulated response is given in Figure 8.27 together with the real system response obtained by experiment.

Inspection of the identification results in Figure 8.26 reveals that the identification procedure generates a highly accurate estimated response to input variations even in fast transient phases and high frequency load effects. Although it does not guarantee that the identified model accurately represents the process behavior, this result gives useful information for online applications of control. Figure 8.27 give plots of the model validation experiments. The identified model is tested using the set of data used in identification, and results in Figure 8.27 reveal the performance of the model in response to the PRBS test signal.

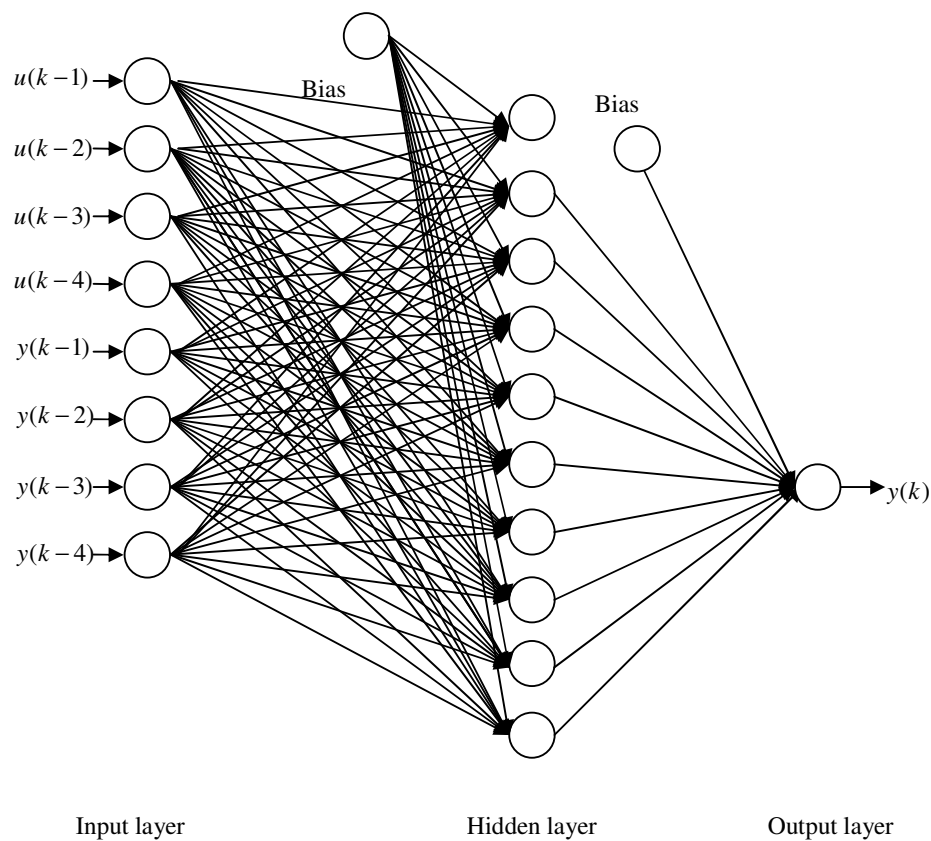


Figure 8.25 FFNN architecture

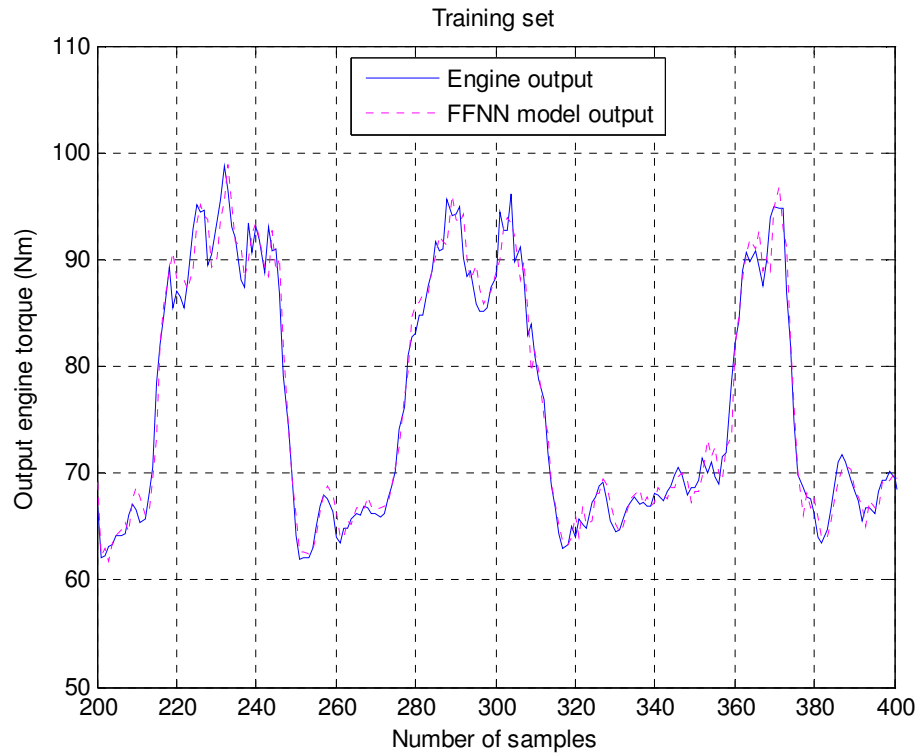


Figure 8.26 Modeling results of the FFNN model with identification experiment



Figure 8.27 Modeling results of the FFNN model with validation of identification results

8.2.5.2.2 Radial Basis Function (RBF) Neural Networks for System Identification

Feedforward neural networks trained with the backpropagation (BP) algorithm have been widely used in system identification and control. There are several drawbacks of such formulation, however, such as potentially pre-converging to a local minima, relatively slow convergence rate, and difficulties to determine an adequate architecture to obtain a minimum, etc., [226].

Another popular layered feedforward network is the radial-basis function (RBF) network which has important universal approximation properties [158]. Comparing with the feedforward neural networks and multi-layer perceptron neural networks, RBF neural networks has some better approximation properties [227], such as high accuracy of approximation, especially, the connection weights from the hidden layer to the output layer are linear (which implies that linear optimal algorithms can be used in RBF neural networks and guarantees the global convergence of the parameters). Moreover, while training RBF neural networks, only one part of the nodes will be affected by a given input, and only a portion of the model parameters may be need to be adjusted, thus reducing the training time and computational burden [226]. A RBF neural network has an input layer, a nonlinear hidden layer and a linear output layer. The nodes within each layer are fully connected to the previous layer nodes. The input variables are each assigned to nodes in the input layer and connected directly to the hidden layer without weights. The hidden layer nodes are RBF units. The nodes calculate the Euclidean distances between the centers and the network input vector, and pass the results through a nonlinear function [228]. The output layer nodes are weighted linear combinations of the RBF in hidden layer.

For a RBF neural network with m inputs nodes, p outputs nodes and N hidden nodes, the hidden unit can be expressed as a matrix

$$\psi = [\psi_1 \quad \psi_2 \quad \cdots \quad \psi_N] \quad (8.30)$$

and the neural networks weight $W = \{w_{ij}, i = 1, 2, \dots, N, j = 1, 2, \dots, p\}$, where, input $X(k) = (x_1(k), \dots, x_m(k))^T$, $\hat{Y}(k) = (\hat{y}_1(k), \dots, \hat{y}_p(k))^T$, $\psi_j(X(k))$ is a nonlinear function and it is chosen as a Gaussian activation function

$$\psi_j(X(k)) = \exp\left(-\frac{\|X(k) - C_j\|^2}{\lambda_j^2}\right) \quad (8.31)$$

where $C_j (j = 1, 2, \dots, N) \in R^N$ is the center of the j th hidden unit, and with the same dimension as the input vector $X(k)$, λ_j the width of the j th RBF hidden unit, $\|\cdot\|$ Euclidean norm.

Then i th RBF network output can be represented as a linearly weighted sum of N basis functions

$$\hat{y}_i(k) = w_{0,i} + \sum_{j=1}^N w_{ji} \psi_j(X(k)), \quad i = 1, 2, \dots, p \quad (8.32)$$

where w_{ji} and $w_{0,i}$ are the weights.

With the structure described above, the transformation from the input layer to the hidden layer is nonlinear, due to the use of Gaussian functions $\psi(\cdot)$ for RBF, and the connection of the hidden layer to the output layer is linear [228].

The objective of this case study is to use RBF neural networks to model the SI engine torque. According to identification structure of SI engine torque in Figure 8.22, where TDL is the tapped delay line that the output vector has for its elements delayed values of the input signal.

In Figure 8.24, the predictive error $e(k) = y(k) - \hat{y}(k)$, and $\hat{y}(k)$ is the predictive output of the neural networks. In this case study, the criterion of training a RBF neural networks is to minimize mean square errors (MSE) given in Equation (8.24).

The number of hidden units is previously determined by trial-error fashion. Based on satisfying the minimum MSE conditions in Equation (8.24) and shorter training time. A neural network is trained using all the available data set based on satisfying the condition of not greater than the objective MSE. The structure of a RBF neural networks with the orders of the input variables are, respectively $n_u = 4$ and $n_y = 4$ given in Figure 8.28.

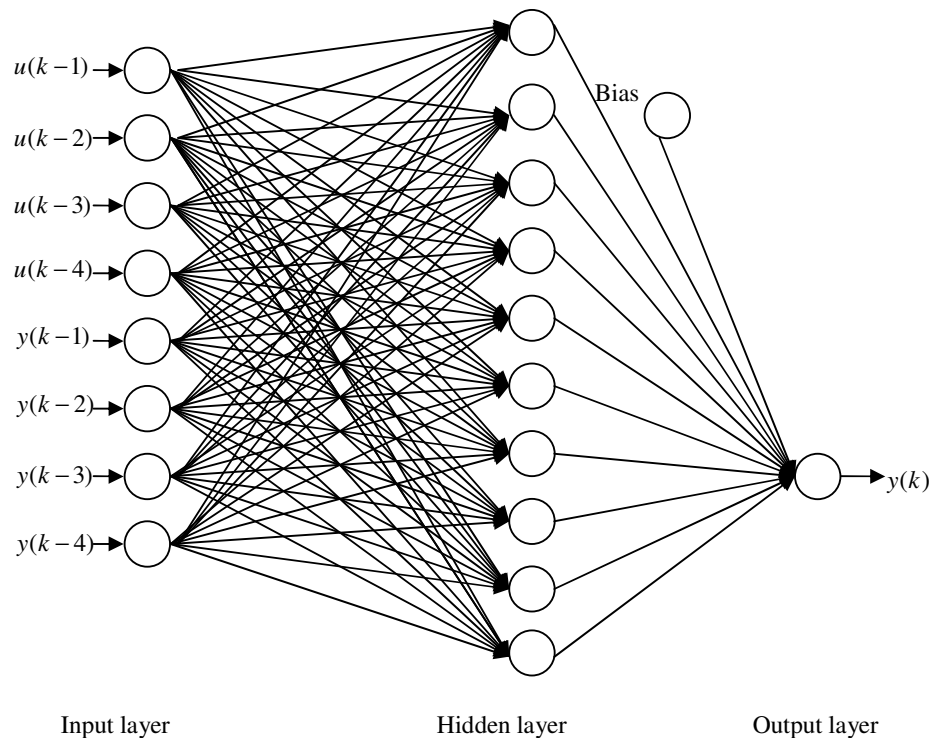


Figure 8.28 RBF neural network structure

The identifier has been assessed using the following test signal shown in Figure 8.19. The real system response and the identifier outputs are shown in Figure 8.29. Obtained model should be validated using the estimated parameters to generate a new set of output data by simulation of the identified model. The simulated response is given in Figure 8.30 together with the real system response obtained by experiment.

Inspection of the identification results in Figure 8.29 reveals that the identification procedure generates a highly accurate estimated response to input variations even in fast transient phases and high frequency load effects. Although it does not guarantee that the identified model accurately represents the process behavior, this result gives useful information for online applications of control. Figure 8.30 give plots of the model validation experiments. The identified model is tested using the set of data used in identification, and results in Figure 8.30 reveal the performance of the model in response to the PRBS test signal.

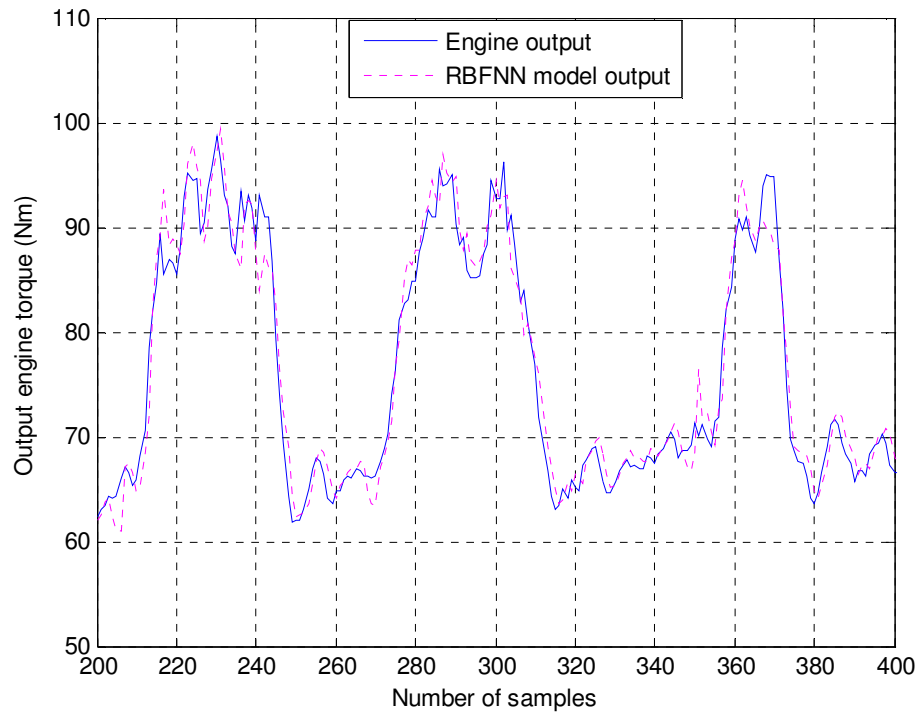


Figure 8.29 Modeling results of the RBF neural network model with identification experiment

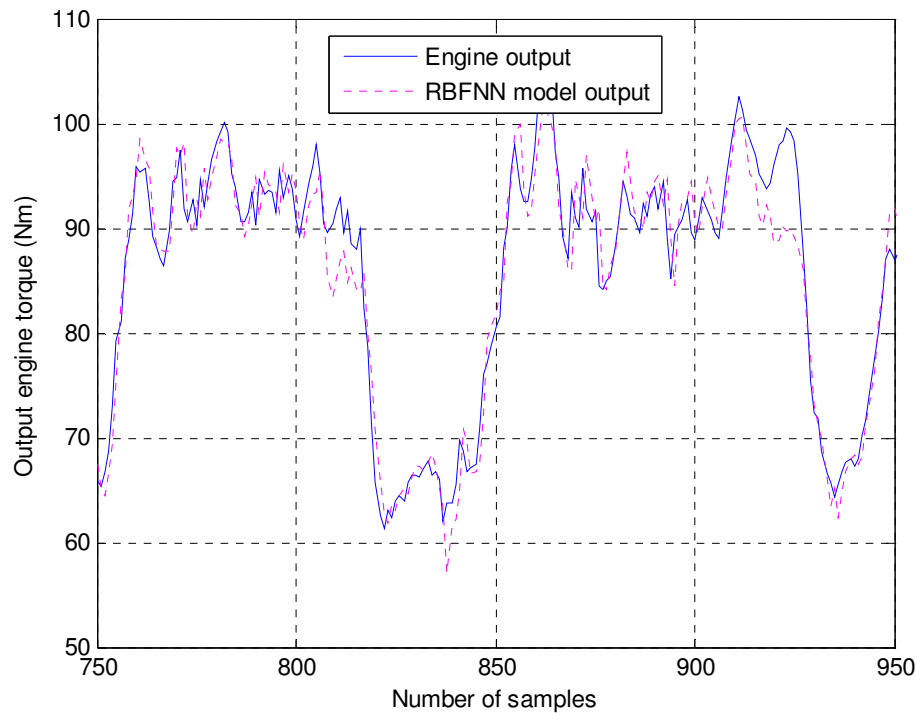


Figure 8.30 Modeling results of the RBF neural network model with validation of identification results

8.2.5.2.3 Recurrent Neural Networks (RNN) for System Identification

The recurrent neural network (RNN) that is a special type of the dynamic neural networks is derived from the multi layer perceptron feedforward neural networks (MLPNN) by considering feedback connections among the neurons. RNN has the advantage of detecting and identifying time-varying model. Elman neural network is a kind of recurrent network.

Elman neural network is a dynamic recurrent neural network with feedback layer which owns the dynamic characteristics and recurrent function [91]. The feedback connections in Elman recurrent neural network are from the outputs of neurons in the hidden layer to the context layer units that are called as context nodes. This part of input layer, namely, the context layer, plays a role in storing internal states in Elman neural networks [165].

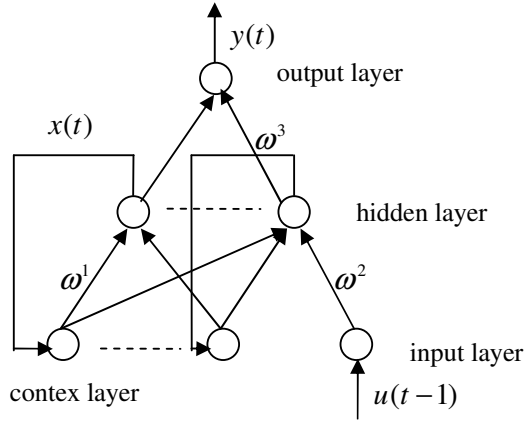


Figure 8.31 Structure of Elman neural network

The structure of the Elman neural network is illustrated in Figure 8.31. Where $\omega^1, \omega^2, \omega^3$ is the corresponding layer the weight matrix, $u(t-1)$ being input vector at $(t-1)$ time, $x(t)$ being output vector of context layer at t time, $y(t)$ being output vector of neural network at t time. The neural network is composed of the input layer, hidden layer, context layer and output layer. The context layer can memorize previous output of the hidden layer unit, therefore the network has the memory function. The neural network shown in Figure 8.29 has the following nonlinear state space expression.

$$x(t) = f(\omega^1 x^c(t) + \omega^2 u(t-1)) \quad (8.34)$$

$$x^c(t) = x(t-1) \quad (8.35)$$

$$y(t) = g(\omega^3 x(t)) \quad (8.36)$$

In the above formula, x^c is the context layer output and $f(\cdot)$ and $g(\cdot)$ are the activation functions of the output layer and hidden layer respectively.

To identify SI engine torque, the system was excited with a PRBS signal. The data set, comprising 2000 data points, was divided into two sets; half of the data set was used to train the network and the other half used to validate the model.

Several neural networks with different structures were tried in order to find the optimal model. Table 8.12 shows the performance comparison. Based on the results of Table 8.12, it is seen that both the orders of the input variables and the number of the hidden neurons have an effect on the model performance. The results presented in Table 8.12 reveal clearly that the selection of the number of the hidden neurons is ten, while the orders of the input variables are, respectively $n_u = 4$ and $n_y = 4$.

Table 8.12 Performance comparison for Elman neural network model

Neural network structure	Correlation coefficient (R)
$n_u = 2, n_y = 2, hn= 7$	0.98777
$n_u = 2, n_y = 2, hn= 8$	0.98843
$n_u = 2, n_y = 2, hn= 9$	0.98852
$n_u = 2, n_y = 2, hn= 10$	0.98942
$n_u = 3, n_y = 3, hn= 7$	0.98936
$n_u = 3, n_y = 3, hn= 8$	0.98958
$n_u = 3, n_y = 3, hn= 9$	0.98962
$n_u = 3, n_y = 3, hn= 10$	0.98981
$n_u = 4, n_y = 4, hn= 7$	0.99085
$n_u = 4, n_y = 4, hn= 8$	0.99143
$n_u = 4, n_y = 4, hn= 9$	0.99158
$n_u = 4, n_y = 4, hn= 10$	0.99172

Elman neural network is a two-layer BP neural network with a feedback from the outputs of hidden layer to inputs. Choosing Elman neural network with input layer eight neurons, hidden layer ten neurons and output layer one neuron, then the topology structure of Elman neural network of SI engine torque is 8-10-1, has been

used in the network. The number of hidden neurons has been determined by trial-and-error. The learning algorithm used in the study is Levenberg-Marquardt (LM); the activation function of hidden layer neurons is tan-sigmoid (tansig), while it is purelin of output layer. Elman neural network of SI engine torque identification was trained using Matlab neural network toolbox.

The SI engine torque actual values taken from the experimental set-up described in section 7.4 and the output values of Elman neural network model is shown in Figure 8.32. Obtained model should be validated using the estimated parameters to generate a new set of output data by simulation of the identified model. The simulated response is given in Figure 8.33 together with the real system response obtained by experiment.

Inspection of the identification results in Figure 8.32 reveals that the identification procedure generates a highly accurate estimated response to input variations even in fast transient phases and high frequency load effects. Although it does not guarantee that the identified model accurately represents the process behavior, this result gives useful information for online applications of control. Figure 8.33 give plots of the model validation experiments. The identified model is tested using the set of data used in identification, and results in Figure 8.33 reveal the performance of the model in response to the PRBS test signal.

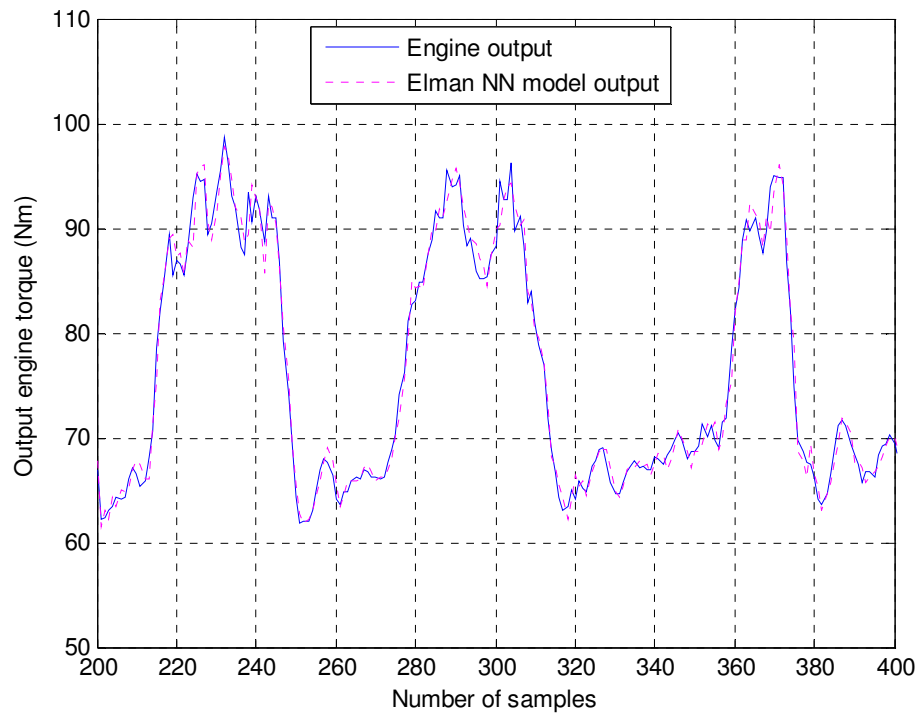


Figure 8.32 Modeling results of the Elman NN model with identification experiment

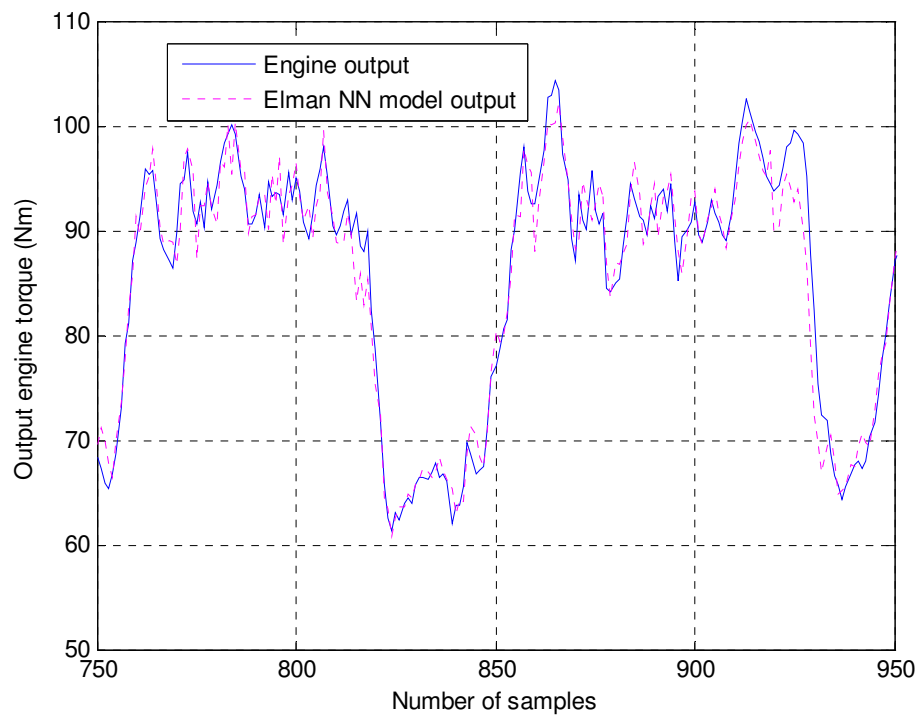


Figure 8.33 Modeling results of the Elman NN model with validation of identification results

8.2.5.3 Comparison of the Three Approaches

This case study has shown a procedure for using neural networks for identification of the nonlinear process, i.e. output torque in automotive SI engine. To evaluate the quality of the model identified from the process data, there are various means, among which the statistical information criteria are one, used to test the quality of the model. The correlation coefficient (R), the mean square error (MSE) and the mean absolute percentage error (MAPE) are some of the commonly employed criteria given by

$$R = \frac{\sum (y(k) - y')(\hat{y}(k) - \hat{y}')}{\sqrt{\sum (y(k) - y')^2 \sum (\hat{y}(k) - \hat{y}')^2}} \quad (8.37)$$

$$MAPE = \frac{1}{N} \left| \frac{y(k) - \hat{y}(k)}{\hat{y}(k)} \right| * 100 \quad (8.38)$$

where y' and \hat{y}' are the mean values of $y(k)$ and $\hat{y}(k)$, respectively N is the number of total number of data.

The statistical performance of three approaches is given in Table 8.13. It can be seen from the Table 8.13 that the neural network based model captures the dynamics very well and the method is suitable for modeling the SI engine torque. The Elman recurrent neural network slightly outperformed the feedforward network with a high correlation coefficient (R) and a low mean absolute percentage error (MAPE) and also a low mean square error (MSE). However all three approaches identified the SI engine torque dynamics well.

As seen in Table 8.13, a high correlation coefficient (R) and a low mean absolute percentage error (MAPE) were obtained for the training and testing data sets for the SI engine torque. The proposed Elman recurrent neural network model for the SI engine torque had correlation coefficients of 0.99172 and 0.97812 for training and testing data set, respectively. Moreover, MAPE of the engine torque was 1.3457 and

Table 8.13 Statistical performance of three approaches

NN structure	Set	MSE	MAPE	Corr. Coff. R
FFNN	Train	0.00019	1.6708	0.98742
	Test	0.00049	2.2111	0.97317
RBF neural network	Train	0.00036	2.3236	0.97846
	Test	0.00042	2.4624	0.97727
Elman neural network	Train	0.00013	1.3457	0.99172
	Test	0.00040	1.9483	0.97812

1.9483 for the training and testing set, respectively. Similarly, MSE of the engine was 0.00013 and 0.0004 for the training and testing set, respectively. As it is seen these statistical performance parameters are fairly reasonable.

8.2.5.4 Conclusions

This case study analyzes the performance of neural network methodologies from the point of system identification. In the assessment level, correlation coefficient, together with the mean square error is considered as the primary comparison measures. Numerous simulations are performed on a SI engine torque model.

All three approaches are tested for the same command signal. For the tracking error performance, Elman recurrent neural network showed the best performance. On the other hand, FFNN and RBF neural network are the simplest approaches in the sense of computational complexity.

The contribution of this case study is to show the identification performance of the neural network structures and to demonstrate the distinguished performance of the three approaches with off-line operation. Some results can be concluded in the following:

1. Neural network based models have simple structure and are not difficult to obtain based on measured input-output data.

2. Neural network based models can capture the inherent nonlinearities and the dynamics of the engine torque in automotive engines.
3. Neural network based models can be as good if not better in performance accuracy than the nonlinear model obtained according to polynomial models.

The experimental results presented in the case study show that the neural network based models are promising for modeling for the purpose of control of automotive engines. In addition, the obtained neural models show good performance in the form of generalization capability and robustness. However, additional work needs to be done to fully understand the capabilities of such techniques for modeling the entire engine.

CHAPTER 9

9. CONCLUSIONS

The study presented here is on the modeling and identification of a SI engine. The developed procedure and formulations are applied to a 1400 cc, four cylinder Fiat SI engine presented at the IC engines Laboratory of the University of Gaziantep. In this chapter, conclusions and recommendations for future study to succeed this work.

The contributions and achievements can be summarized as follows:

1. The dynamic formulations of a slider- crank mechanism have been successfully formulated with only one independent variable. These equations are the theoretical models of the system dynamics, but they are comprised of highly nonlinear differential equations and so, can not be used for on-line and on-duty applications. They are good for design purposes, but are not suitable to use in control. For on-line control, simpler models involving much less calculations are required. This is actually the scope of this thesis.
2. Steady-state experiments were carried out on a SI engine to model the engine torque and brake specific fuel consumption using soft computing techniques. Neural networks (NN) and Gene-Expression Programming (GEP) which is an extension of Genetic Programming (GP) are used for modeling the SI engine torque at steady-state conditions. The results of the proposed NN and GEP models show very good agreement with the experimental results. The performance of accuracies of proposed NN and GEP models are quite satisfactory. The results of the GEP model are compared to that of the NN model with which the results are found to be in excellent agreement. The present study verifies the robustness of soft computing techniques for the modeling and analysis of various engineering problems where it is difficult to obtain a mathematical model.

3. Dynamic experiments were carried out in SI engine to identify and model the system. The most common nonlinear black-box parametric models namely Hammerstein model and nonlinear auto-regressive with exogenous inputs (NARX) model were developed. And also different neural network structures are used to identify nonlinear dynamic models for the SI engine torque.

4. Nonlinear system modeling approaches with parametric representation are investigated. Volterra series, Hammerstein, Wiener, and NARMAX models are explained in detail. Identification of nonlinear systems using the above mentioned model structures are discussed. Algorithms for the identification processes are given.

5. The experimental study on nonlinear modeling and identification of a SI engine torque from input-output data is presented. The nonlinear model is developed for the system. A nonlinear representation and identification approach using the nonlinear Hammerstein system structure is used for the present system. A suitable experimental setup is built and tested using the RLS identification algorithm for the nonlinear case. The measured data obtained experimental setup is used by a computer program that runs in Matlab environment to identify unknown system parameters. The results are numerically and graphically demonstrated. Inspection of the identification results reveals that the identification procedure generates a highly accurate estimated response to input variations even in fast transient phases and high frequency load effects.

6. In this study, a nonlinear model of the SI engine torque is obtained. A procedure to provide the nonlinear model of the dynamics between the throttle valve command and torque of a gasoline engine, directly from raw data is presented. The nonlinear system model is built and a sigmoid based nonlinear ARX model is developed using the input and output data. The model parameters were estimated using an iterative prediction-error minimization method. The nonlinear system identification with fifth order nonlinear dynamics is found to give the best result. The model validation results concluded that the selected model order has the potential of capturing the nonlinearity of the process.

7. In this thesis, the artificial neural networks is considered from the identification perspective. It is well known that the concept of identification plays an important role in the systems and control area. This, mainly, stems from the fact that we generally want to obtain an approximate model of the system, such that the resulting model is mathematically tractable and closely matches the system dynamics. Neural networks were proven to be successful identifiers, because they can learn any kind of nonlinear mapping with any degree of accuracy. From this point of view, neural networks can identify a system so that the identification model could be used to devise a controller. Training range is another important point in the neural identification procedure. The backpropagation, backpropagation with adaptive learning rate, backpropagation with momentum and Levenberg-Marquardt (LM) training algorithms of Matlab were tested, the LM algorithm was found to be the fastest training algorithm, but requiring more memory with the same error convergence bound compared to the other algorithms.

8. In this study, different neural network structures are used to identify nonlinear dynamic models for the SI engine torque. System identification is done using the input-output test data. The test data must incorporate all the properties of the system. So the way system identification experiment is performed is very crucial. In this thesis, considering the engine as a single-input single-output (SISO) system, the basic input variable is the throttle valve position u , while the model output is the engine torque y . In engine data collection, the input-output data must be representative of engine behavior in order to identify the engine. This means that input and output signals should adequately cover the region in which the system is going to be modeled. A set of Pseudo Random Binary Signal (PRBS) signals are often very suitable as process inputs because they excite the process at a wide range of amplitudes and frequencies. To create the disturbances needed to perform identification of the process, PRBS's were used. A PRBS was designed for throttle angle position to obtain a representative set of input-output data. A set of data samples, including the throttle valve position and the torque was collected for the system identification. Each set contains 2000 data samples. The neural network training is performed off-line utilizing a previously generated training data set. The neural network based black-box method is used to model the SI engine torque dynamics taking into account the interaction between the input and output of the

SISO system. NARX model is used in this study because a wide class of nonlinear systems can be described by NARX.

9. The first type of neural network to be developed here is the feedforward neural network (FFNN) model. Feedforward networks with a range of hidden layer neurons were tested. A two-layer feedforward neural network with eight input neurons, ten neurons in the hidden layer and one output neuron, denoted as 8-10-1, has been used in the network. The learning algorithm used in the study is Levenberg-Marquardt (LM); activation function is tan-sigmoid (tansig) transfer functions. The feedforward networks modeled the SI engine torque well.

10. The second type of neural network to be developed is the Radial Basis Function (RBF) neural network model. The structure of a RBF neural network with the orders of the input variables is, respectively $n_u = 4$ and $n_y = 4$. Orthogonal Least Squares (OLS) method is adopted to determine RBF neural networks centers. The obtained results have shown that the modeling accuracy is high and it is feasible to setup the model of the nonlinear SI engine torque system based on RBF neural networks identification. The most important is that the modeling process avoids complicated dynamical modeling and avoids using complicated differential equation groups to model the torque of a SI engine, and the input-output performance can be achieved quickly by the neural network model.

11. Finally, Elman type recurrent neural network is developed for SI engine torque modeling. Choosing Elman neural network with input layer of eight neurons, hidden layer of ten neurons and output layer of one neuron, then the topology structure of Elman neural network of SI engine torque is 8-10-1, has been used in the network. The learning algorithm used in the study is Levenberg-Marquardt (LM); the activation function of hidden layer neurons is tan-sigmoid (tansig), while it is purelin of output layer. The obtained results have shown that the SI engine torque has been identified successfully. The extracted model has predicted the system behavior well. Identified models have been verified on a real system with equally accurate results.

12. Different neural network structures are used to analyze the performance of neural network methodologies from the point of system identification. The neural network based model captures the dynamics very well and the method is suitable for modeling the SI engine torque. The Elman recurrent neural network slightly outperformed the feedforward network with a high correlation coefficient (R) and a low mean absolute percentage error (MAPE), and also a low mean square error (MSE). However all three approaches identified the SI engine torque dynamics well. The experimental results presented in this thesis show that the neural network based models are promising for modeling for the purpose of control of automotive engines. In addition, the obtained neural models show good performance in the form of generalization capability and robustness.

9.1 Recommendations for Future Work

System identification is the process of developing a mathematical model of a dynamic system based on the input and output data from the actual process. This means it is possible to sample the input and output signals of a system and using this data to generate a mathematical model. An important stage in control systems design is the development of a mathematical model of the system to be controlled. In order to develop a controller, it must be possible to analyze the system to be controlled and this is done using a mathematical model. Another advantage of system identification is evident if the process is changed or modified. System identification allows the real system to be altered without having to derive the dynamical equations and measuring the model parameters again.

It is obvious that artificial intelligence techniques or specifically soft computing approaches such as Fuzzy logic, NNs, Genetic Algorithm and Genetic Programming, will have much more profound application areas in the future for nonlinear system identification and control area.

The following can be suggested for future studies:

1. The existing SI engine can be upgraded by adding measurement device to identify and model the other SI engine parameters such as, the inlet manifold

pressure and the temperature, the engine speed, the air/fuel ratio, the air mass flow rate, the fuel mass flow rate etc.

2. The developed nonlinear models can be used to predict the SI engine torque off-line which makes it possible to design an off-line controller for SI engine torque.
3. The dynamical systems contain nonlinear relations which are difficult to model with conventional techniques. In this study, the nonlinear modeling techniques such as Hammerstein model, NARX model and neural network model have been successfully applied to unknown nonlinear system identification and modeling. Other system identification methods have been applied for efficiently identification and modeling the SI engine dynamics and other nonlinear dynamic systems such as, genetic programming identification, Fuzzy logic and neuro-fuzzy systems (ANFIS).
4. The system identification problem requires a suitable excitation signal. Usually a signal, which is sufficiently rich and persistently exciting all the system modes, is selected. In this study, Pseudo Random Binary Signal (PRBS) was designed for throttle angle position to obtain a representative set of input-output data. And also, other signals such as random amplitude signals (RAS), random Gaussian signals (RGS) and etc. can be used as the training input signal.
5. ICE modeling is still an open field of research due to the antithetical needs of describing a very complex, nonlinear system and driving simple model structures suitable for the control synthesis or diagnosis phase.

REFERENCES

- [1] Tan, Y., Saif, M. (2000). Neural-networks-based nonlinear dynamic modeling for automotive engines. *Neurocomputing*, **30**, 129-142.
- [2] Wang, S.W., Yu, D.L., Gomm, J.B., Page, G.F., Douglas, S.S. (2006). Adaptive neural network model based predictive control of an internal combustion engine with a new optimization algorithm. *Proceedings of the Institution of Mechanical Engineers, Part D: Journal of Automobile Engineering*, **220 (2)**, 195-208.
- [3] Wang, S.W., Yu, D.L., Gomm, J.B., Page, G.F., Douglas, S.S. (2006). Adaptive neural network model based predictive control for air-fuel ratio of SI engines. *Engineering Applications of Artificial Intelligence*, **19**, 189-200.
- [4] Wang, S.W., Yu, D.L., Gomm, J.B., Beham, M., Page, G.F., Douglas, S.S. (July 2005). Adaptive modeling and predictive control of an IC engine. *In: 16th IFAC World Congress*, Prague.
- [5] DeNicolao, G., Scattolini, R., Siviero, C. (1996). Modeling the volumetric efficiency of IC engines: parametric, non-parametric and neural techniques. *Control Engineering Practice*, **4 (10)**, 1405-1415.
- [6] Rakotomamonjy, A., LeRiche, R., Gualandris, D., Harchaoui, Z. (2008). A comparison of statistical learning approaches for engine torque estimation. *Control Engineering Practice*, **16**, 43-55.
- [7] Falcone, P., Fiengo, G., Glielmo, L. (April 2004). Non-linear net engine torque estimator for internal combustion engine. *In: IFAC Symposium on Advances in Automotive Control*, Salerno, Italy.

- [8] Fritzsche, C., Dünow, H.P. (2008). New Approaches in Automation and Robotics. In H. Aschemann (Eds.), *Advanced torque control*.
- [9] Ali, A., Blath, J.P. (2006). Application of modern techniques to SI-engine torque control. In: *Proceedings of the IEEE International Conference on Control Applications*, Munich, Germany, October 4-6, 2405-2410.
- [10] Ingram, G.A., Franchek, M.A., Balakrishnan, V., Surnilla, G. (2003). Spark ignition engine torque management. In: *Proceedings of the American Control Conference*, 767-772.
- [11] Kapucu, S., Baysec, S. (1997). On the identification of linear mechanical systems. *Mechatronics*, **7** (3), 297-313.
- [12] Huyck, B., DeBrabanter, J., VanImpe, J., DeMoor, B. (2008) Identification and modeling of dynamical system. In: *Proceedings of the Third European Conference on the Use of Modern Information and Communication Technologies*, Gent, Belgium, 213-224.
- [13] Rahrooh, A., Shepard, S. (2009). Identification of nonlinear systems using NARMAX model. *Nonlinear Analysis: Theory, Methods & Applications*, **71** (12), 1198-1202.
- [14] Efe, M.O., Kaynak, O. (1999). A comparative study of neural network structures in identification of nonlinear systems. *Mechatronics*, **9**, 287-300.
- [15] Efe, M.O., Kaynak, O. (2000). A comparative study of soft-computing methodologies in identification of robotic manipulators. *Robotics and Autonomous Systems*, **30**, 221-230.
- [16] Weyer, E. (2000). Finite sample properties of system identification of ARX models under mixing conditions. *Automatica*, **36**, 1291-1299.

- [17] Nelles, O. (2001). *Nonlinear System Identification: from Classical Approaches to Neural Networks and Fuzzy Models*. Springer, Berlin, Germany.
- [18] Efe, M.O. (1996). *Identification and control of nonlinear dynamical systems using neural networks*, MSc Thesis, University of Boğaziçi.
- [19] Jovanović, O. (1997). Identification of dynamic system using neural network. *Facta Universitatis-Architecture and Civil Engineering*, 525-532.
- [20] Sjöberg, J., Hjalmarsson, H., Ljung, L. (1994). Neural networks in system identification. *Preprints of the 10th IFAC Symposium on Identification and System Parameter Estimation*, Copenhagen, Denmark, 49-71.
- [21] Sjöberg, J., Zhang, Q., Ljung, L., Benveniste, A., Deylon, B., Glorennec, P.Y., Hjalmarsson, H., Juditsky, A. (1995). Nonlinear black-box modeling in system identification: A unified overview. *Automatica*, **31(12)**, 1691-1724.
- [22] Narendra, K.S., Parthasarathy, K. (1990). Identification and control of dynamical systems using neural networks. *IEEE Transactions on Neural Networks*, **1(1)**, 4-27.
- [23] Chen, S., Billings, S.A., Grant, P.M. (1990). Non-linear system identification using neural networks. *International Journal of Control*, **51(6)**, 1191-1214.
- [24] Chen, S., Billings, S.A., Cowan, C.F.N., Grant, P.M. (1990). Practical identification of NARMAX models using radial basis functions. *International Journal of Control*, **52(6)**, 1327-1350.
- [25] Billings, S.A., Jamaluddin, H.B., Chen, S. (1992). Properties of neural networks with applications to modeling non-linear dynamical systems. *International Journal of Control*, **55(1)**, 193-224.
- [26] Ljung, L. (1987). *System identification: Theory for the user*. Englewood Cliffs, NJ, USA, Prentice Hall.

- [27] Söderström, T., Stoica, P. (1989). *System identification*, Cambridge, UK, Prentice Hall.
- [28] Kara, T., Eker, İ. (2004). Nonlinear modeling and identification of a DC motor for bidirectional operation with real time experiments. *Energy Conversion and Management*, **45**, 1087-1106.
- [29] Ni, X., Verhaegen, M., Krijgsman, A.J., Verbruggen, H.B. (1996). A new method for identification and control of nonlinear dynamic systems. *Engineering Applications of Artificial Intelligence*, **9 (3)**, 231-243.
- [30] Huang, C.C., Loh, C.H. (2001). Nonlinear identification of dynamic systems using neural networks. *Computer-Aided Civil and Infrastructure Engineering*, **16**, 28-41.
- [31] Pérez, E., Blasco, X., García-Nieto, S., Sanchis, J. (2006). Diesel engine identification and predictive control using Wiener and Hammerstein models. *In: Proceedings of the IEEE International Conference on Control Applications*, Munich, Germany, October 4-6, 2417-2423.
- [32] Scattolini, R., DeNicolao, G., Cittadini, M., Rossi, C., Siviero, C. (1997). Modelling internal combustion engines via NARX identification techniques. *In: Proceedings of the IEEE Mediterranean Control Conference*, Cyprus.
- [33] DeNicolao, G., Rossi, C., Scattolini, R., Suffritti, M. (1999). Identification and idle speed control of internal combustion engines. *Control Engineering Practice*, **7**, 1061-1069.
- [34] DeNicolao, G., Moro, O., Poggio, L., Rossi, C., Scattolini, R., Siviero, C. (1997). Identification of nonlinear IC engine models for idle speed control. *In: 4th European Control Conference*, Louvain (B).
- [35] Hrovat, D., Sun, J. (1997). Models and control methodologies for IC engine idle speed control design. *Control Engineering Practice*, **5 (8)**, 1093-1100.

- [36] Rachid, A., Liazid, A., Champoussin, J.C. (1994). Nonlinear modelling of a turbocharged diesel engine. *In: Proceedings of the 3rd IEEE Conference on Control Applications*, 1, August 24-26, 133-136.
- [37] Glass, J.W. (1999). NARMAX modelling and robust control of internal combustion engines. *International Journal of Control*, **72(4)**, 289-304.
- [38] Pfeiffer, R., Haraldsson, G., Olsson, J.O., Tunestål, P., Johansson, R., Johansson, B. (2004). System identification and LQG control of variable-compression HCCI engine dynamics. *In: Proceedings of the IEEE International Conference on Control Applications*, Taipei, Taiwan, September 2-4, 1442-1447.
- [39] Jones, V.K., Ault, B.A., Franklin, G.F., Powell, J.D. (1995). Identification and air-fuel ratio control of a spark ignition engine. *IEEE Transactions on Control Systems Technology*, **3(1)**, 14-21.
- [40] Souder, J.S., Hedrick, J.K. (2004). Adaptive sliding mode control of air-fuel ratio in internal combustion engines. *International Journal of Robust and Nonlinear Control*, **14**, 525-541.
- [41] Arsie, I., Pianese, C., Rizzo, G. (1997). Identification of emission models in a spark ignition engine for control applications. *In: Proceedings of the 5th IEEE Mediterranean Conference on Control Systems*, Paphos, Cyprus, July 21-23.
- [42] Luh, G.C., Rizzoni, G. (1994). Identification of a nonlinear MIMO IC engine model during I/M240 driving cycle for on-board diagnosis. *In: Proceedings of the American Control Conference*, Baltimore, Maryland, 1581-1584.
- [43] Falcone, P., De Gennaro, M.C., Fiengo, G., Glielmo, L., Santini, S., Langthaler, P. (December 2003). Torque generation model for diesel engine. *In: Proceedings of the 42nd IEEE Conference on Decision and Control*, Maui, Hawaii.

- [44] Khiar, D., Lauber, J., Floquet, T., Guerra, T.M. (2005). An observer design for the instantaneous torque estimation of an IC engine. *In: Proceedings of the IEEE Conference on Vehicle Power and Propulsion*, September 7-9, 391-395.
- [45] Franko, J., Franchek, M.A., Grigoriadis, K. (2008). Real-time brake torque estimation for internal combustion engines. *Mechanical Systems and Signal Processing*, **22**, 338-361.
- [46] Vong, C.M., Wong, P.K., Li, Y.P. (2006). Prediction of automotive engine power and torque using least squares support vector machines and Bayesian inference. *Engineering Applications of Artificial Intelligence*, **19**, 277-287.
- [47] Ali, A., Blath, J.P. (2006). Nonlinear torque control of a spark-ignited engine. *In: Proceedings of the American Control Conference*, Minneapolis, Minnesota, USA, June 14-16, 3266-3271.
- [48] Connolly, F.T., Yagle, A.E. (1993). Modeling and identification of the combustion pressure process in internal combustion engines. *IEEE Midwest Symposium on Circuits and System*, **1**, 204-207.
- [49] Connolly, F.T., Yagle, A.E. (1993). Modeling and identification of the combustion pressure process in internal combustion engines: ii-experimental results. *Journal of Engineering for Gas Turbines and Power*, **115 (4)**, 801-809.
- [50] Billings, S.A., Chen, S. (1989). The identification of linear and nonlinear models of a turbocharged automotive diesel engine. *Mechanical Systems and Signal Processing*, **3 (2)**, 123-142.
- [51] Rizzoni, G., Zhang, Y. (1994). Identification of a non-linear internal combustion engine model for on-line indicated torque estimation. *Mechanical Systems and Signal Processing*, **8(3)**, 275-287.

- [52] Polóni, T., Johansen, T.A., Rohal'-Ilkiv, B. (2008). Modeling of air-fuel ratio dynamics of gasoline combustion engine with ARX network. *Journal of Dynamic Systems Measurement and Control –Transactions of the ASME*, **130(6)**, 1009-1018.
- [53] Brahma, A., Upadhyay, D., Serrani, A., Rizzoni, G. (2004). Modeling, identification and state estimation of Diesel engine Torque and NOx dynamics in response to fuel quantity and timing excitations. *In: Proceedings of the American Control Conference*, Boston, Massachusetts, June 30-July 2, 2166-2171.
- [54] Bengtsson, J., Strandh, P., Johansson, R., Tunestål, P., Johansson, B. (2006). Model predictive control of homogenous charge compression ignition (HCCI) engine dynamics. *In: Proceedings of the IEEE International Conference on Control Applications*, Munich, Germany, October 4-6, 1675-1680.
- [55] Cook, J.A., Powell, B.K. (1988). Modeling of an internal combustion engine for control analysis. *IEEE Control Systems Magazine*, **8(4)**, 20-26.
- [56] Jankovic, M. (2002). Nonlinear control in automotive engine applications. *In: Proceedings of the fifteenth International Symposium on Mathematical Theory of Networks and Systems*, University of Notre Dame.
- [57] Zito, G., Landau, I.D. (2005). Narmax model identification of a variable geometry turbocharged diesel engine. *In: Proceedings of the American Control Conference*, Portland, USA, June 8-10, 1021-1026.
- [58] Weeks, R.W., Moskwa, J.J. (1995). Automotive engine modeling for real-time control using matlab/simulink. *SAE Paper 950417*.
- [59] Larimore, W.E., Javaherian, H. (2009). Identification and monitoring of automotive engines. *In: Proceedings of the American Control Conference*, St. Louis, USA, June 10-12, 1800-1807.
- [60] Ohata, A., Furuta, K., Nita, H. (2006). Identification of nonlinear ARX model with input and output dependent coefficients. *In: Proceedings of the IEEE*

International Conference on Control Applications, Munich, Germany, October 4-6, 2577-2582.

[61] Levin, A.U., Narendra, K.S. (1996). Control of nonlinear dynamical systems using neural networks-Part II: Observability, identification, and control. *IEEE Transactions on Neural Networks*, **7(1)**, 30-42.

[62] Levin, A.U., Narendra, K.S. (1993). Control of nonlinear dynamical systems using neural networks-controllability and stabilization. *IEEE Transactions on Neural Networks*, **4(2)**, 192-206.

[63] Martin, S., Kamwa, I., Marceau, R.J. (1995). Applications of artificial neural networks to the identification of dynamical systems. *IEEE Canadian Conference on Electrical and Computer Engineering*, **2**, 606-612.

[64] Todorović, N., Klán, P. (2006). State of the art in nonlinear dynamical system identification using artificial neural networks. In: *Proceedings of the 8th Seminar on Neural Network Applications in electrical Engineering, NEUREL-2006*, University of Belgrade, Serbia, September 25-27, 103-108.

[65] Liu, G.P., Kadiramanathan, V., Billings, S.A. (1998). Predictive control for non-linear systems using neural networks. *International Journal of Control*, **71 (6)**, 1119-1132.

[66] Chen, S., Billings, S.A. (1992). Neural networks for nonlinear dynamic system modeling and identification. *International Journal of Control*, **56 (2)**, 319-346.

[67] Billings, S. A., and Chen, S., 1992, Neural networks and system identification. In G.W. Irwin, K. Warwick and K.J. Hunt (Eds.), *Neural Networks for Systems and Control*, London: Peter Peregrinus, 181-205.

[68] Liu, G.P., Kadiramanathan, V., Billings, S.A. (1999). Variable neural networks for adaptive control of nonlinear systems. *IEEE Transactions on Systems, Man, and Cybernetics-Part C: Applications and Reviews*, **29 (1)**, 34-43.

- [69] Ahmed, R.S. (2001). Identification of nonlinear dynamic systems using a rapid neural network. *IECON'01: The 27th Annual Conference of the IEEE Industrial Electronics Society*, 3, 1734- 1739.
- [70] Abdollahi, F., Talebi, H.A., Patel, R.V. (2006). Stable identification of nonlinear systems using neural networks: theory and experiments. *IEEE/ASME Transactions on Mechatronics*, **11** (4), 488-495.
- [71] Nouri, K., Dhaouadi, R., Braiek, N.B. (2002). Identification of a nonlinear dynamic systems using recurrent multilayer neural networks. *IEEE International Conference on Systems, Man and Cybernetics*, 5.
- [72] Liu, Y., Zhu, J.J. (2008). Continuous-time nonlinear system identification using neural network. *In: Proceedings of the American Control Conference*, Washington, USA, June 11-13, 613-618.
- [73] Ren, X.M., Rad, A.B., Chan, P.T., Lo, W.L. (2003). Identification and control of continuous- time nonlinear systems via dynamic neural networks. *IEEE Transactions on Industrial Electronics*, **50** (3), 478-486.
- [74] Wang, C.H., Chen, P.C., Lin, P.Z., Lee, T.T. (2009). A dynamic neural network model for nonlinear system identification. *IEEE International Conference on Information Reuse & Integration*, 440-441.
- [75] Arsie, I., Pianese, C., Sorrentino, M. (2006). A procedure to enhance identification of recurrent neural networks for simulating air-fuel ratio dynamics in SI engines. *Engineering Applications of Artificial Intelligence*, **19**, 65-77.
- [76] Arsie, I., Di Iorio, S., Pianese, C., Rizzo, G., Sorrentino, M. (2008). Recurrent neural networks for air-fuel ratio estimation and control in spark-ignited engines. *In: Proceedings of the 17th IFAC World Congress*, Seoul, Korea, July 6-11.

- [77] Zhai, Y.J., Yu, D.L. (2009). Neural network model-based automotive engine air/fuel ratio control and robustness evaluation. *Engineering Applications of Artificial Intelligence*, **22**, 171-180.
- [78] Beham, M., Yu, D.L. (2004). Modelling a variable valve timing spark ignition engine using different neural networks. *Proceedings of the Institution of Mechanical Engineers, Part D: Journal of Automobile Engineering*, **218 (10)**, 1159-1171.
- [79] Yu, D.L., Beham, M. (2005). Comparative study on engine torque modeling using different neural networks. *Lecture Notes in Computer Science*, **3498**, 865-870.
- [80] Wang, S., Yu, D.L. (2008). Adaptive RBF network for parameter estimation and stable air-fuel ratio control. *Neural Networks*, **21**, 102-112.
- [81] Zhang, Y., Xi, L., Liu, J. (2007). Transient air-fuel ratio estimation in spark ignition engine using recurrent neural network. *Lecture Notes in Computer Science*, **4693**, 240-246.
- [82] Yin, X., Ge, A. (2001). A dynamic model of engine using neural network description. In: *Proceedings of the IEEE International Vehicle Electronics Conference*, 109-114.
- [83] Hafner, M., Schüler, M., Nelles, O., Isermann, R. (2000). Fast neural networks for diesel engine control design. *Control Engineering Practice*, **8**, 1211-1221.
- [84] Hafner, M., Schüler, M., Nelles, O. (1999). Dynamical identification and control of combustion engine exhaust. In: *Proceedings of the American control Conference*, San Diego, California, 222-226.
- [85] Isermann, R., Müller, N. (2003). Design of computer controlled combustion engines. *Mechatronics*, **13**, 1067-1089.
- [86] Zweiri, Y. (2006). Diesel engine indicated torque estimation based on artificial neural networks. *International Journal of Intelligent Technology*, **1 (1)**, 233-239.

- [87] Zweiri, Y.H., Whidborne, J.F., Seneviratne, L.D., Althoefer, K. (2002). A comparison of dynamic models of various complexity for diesel engines. *Mathematical and Computer Modelling of Dynamical Systems*, **8(3)**, 273-289.
- [88] Chamaillard, Y., Higelin, P., Charlet, A. (2004). A simple method for robust control design, application on a non-linear and delayed system: engine torque control. *Control Engineering Practice*, **12**, 417-429.
- [89] Ayoubi, M. (1998). Comparison between the dynamic multi-layered perceptron and the generalized Hammerstein model for experimental identification of the loading process in diesel engines. *Control Engineering Practice*, **6**, 271-279.
- [90] Yazdanpanah, M.J., Kalhor, A. (2003). Air/fuel ratio control in SI engines using a combined neural network and estimator. *In: Proceedings of the IEEE Conference on Control Applications*, 347-352.
- [91] Hou, Z., Sen, Q., Wu, Y. (2006). Air fuel ratio identification of gasoline engine during transient conditions based on elman neural networks. *In: Proceedings of the Sixth International Conference on Intelligent Systems Design and Applications (ISDA'06)*, Jinan, China, October 16-18, 32-36.
- [92] Ouladsine, M., Block, G., Dovifaaz, X. (2004). Neural modelling and control of a diesel engine with pollution constraints. *Journal of Intelligent and Robotic Systems*, **41**, 157-171.
- [93] Colin, G., Chamaillard, Y., Block, G., Corde, G. (2007). Neural control of fast nonlinear systems-application to a turbocharged SI engine with VCT. *IEEE Transactions on Neural Networks*, **18 (4)**, 1101-1114.
- [94] Sangha, M.S., Gomm, J.B., Yu, D.L., Page, G.F. (2005). Fault detection and identification of automotive engines using neural networks. *In: Proceedings of the 2005 IFAC World Congress*.

- [95] Cui, H. (2006). Exhaust gas recirculation control in a spark-ignition LPG engine using neural networks. *In: Proceedings of the 6th World Congress on Intelligent Control and Automation*, Dalian, China, 21-23 June, 6332-6335.
- [96] Li, X., Yu, W. (2002). Dynamic system identification via recurrent multilayer perceptrons. *Information Sciences*, **147**, 45-63.
- [97] Ayeb, M., Theuerkauf, H., Wilhelm, C., Winsel, T. (2006). Robust identification of nonlinear dynamic systems using design of experiment. *In: Proceedings of the IEEE Conference on Computer Aided Control Systems Design*, Munich, Germany, October 4-6, 2321-2326.
- [98] Isermann, R., Müller, N. (2001). Nonlinear identification and adaptive control of combustion engines. *In: IFAC-Workshop on Adaptation and Learning in Control and Signal Processing*, Como, Italy, August 29-31.
- [99] Hafner, M., Weber, M., Isermann R. (2002). Model-based control design for IC-engines on dynamometers: the toolbox ‘optimot’. *IFAC 15 th Triennial World Congress*, Barcelona, Spain.
- [100] Czarnigowski, J. (2010). A neural network model-based observer for idle speed control of ignition in SI engine. *Engineering Applications of Artificial Intelligence*, **23(1)**, 1-7.
- [101] Biao, L., Chun, L.Q., Hua, J.Z., Fang, N.S. (2009). System identification of locomotive diesel engines with autoregressive neural network. *4 th IEEE Conference on Industrial Electronics and applications*, 3417-3421.
- [102] Alippi, C., de Russis, C., Piuri, V. (2003). A neural-network based control solution to air-fuel ratio control for automotive fuel-injection systems. *IEEE Transactions on Systems, Man, and Cybernetics-Part C: Applications and Reviews*, **33(2)**, 259-268.

- [103] Alippi, C., de Russis, C., Piuri, V. (1998). A fine control of the air-to-fuel ratio with recurrent neural networks. *IEEE Instrumentation and Measurement Technology Conference*, Minnesota, USA, May 18-21, 924-929.
- [104] Frith, A.M., Gent, C.R., Beaumont, A.J. (1995). Adaptive control of gasoline engine air-fuel ratio using artificial neural networks. *Fourth International Conference on Artificial Neural Networks*, 274-278.
- [105] Saraswati, S., Chand, S. (2008). Application of neural network for air-fuel ratio identification in spark ignition engine. *International Journal of Computer Applications in Technology*, **32** (3), 206-215.
- [106] Wu, J.D., Huang, C.K., Chang, Y.W., Shiao, Y.J. (2010). Fault diagnosis for internal combustion engines using intake manifold pressure and artificial neural network. *Expert Systems with Applications*, **37**, 949-958.
- [107] Thompson, G.J., Atkinson, C.M., Clark, N.N., Long, T.W., Hanzevack, E. (2000). Neural network modelling of the emissions and performance of a heavy-duty diesel engine. *Proceedings of the Institution of Mechanical Engineers, Part D: Journal of Automobile Engineering*, **214** (2), 111-126.
- [108] García-Nieto, S., Martínez, M., Blasco, X., Sanchis, J. (2008). Nonlinear predictive control based on local modal networks for air management in diesel engines. *Control Engineering Practice*, **16**, 1399-1413.
- [109] Worden, K., Hickey, D., Haroon, M., Adams, D.E. (2009). Nonlinear system identification of automotive dampers: a time and frequency-domain analysis. *Mechanical Systems and Signal Processing*, **23**, 104-126.
- [110] Turin, R.C., Geering, H.P. (1993). On-line identification of air-to-fuel ratio dynamics in a sequentially injected SI engine. *SAE Special Publications*, **955**, 41-51.

- [111] Franchek, M.A., Mohrfeld, J., Osburn, A. (2006). Transient fueling controller identification for spark ignition engines. *Journal of Dynamic Systems Measurement and Control-Transactions of the ASME*, 128, 499-509.
- [112] Stroh, D.J., Franchek, M.A., Kerns, J.M. (2001). Fueling control of spark ignition engines, *Vehicle System Dynamics*, **36(4)**, 329-358.
- [113] Ye, Z. (2007). Modeling, identification, design, and implementation of nonlinear automotive idle speed control systems-an overview. *IEEE Transactions on Systems, Man, Cybernetics-Part C: Applications and Reviews*, **37 (6)**, 1137-1151.
- [114] Ortner, P., del Re, L. (2007). Predictive control of a diesel engine air path. *IEEE Transactions on Control Systems Technology*, **15 (3)**, 449-456.
- [115] Coelho L.S., Pessôa, M.W. (2009). Nonlinear model identification of an experimental ball-and-tube system using a genetic programming approach. *Mechanical Systems and Signal Processing*, **23**, 1434-1446.
- [116] Gray, G.J., Murray-Smith, D.J., Li, Y., Sharman, K.C., Weinbrenner, T. (1998). Nonlinear model structure identification using genetic programming. *Control Engineering Practice*, **6**, 1341-1352.
- [117] Madár, J., Abonyi, J., Szeifert, F. (2005). Genetic programming for the identification of nonlinear input-output models. *Industrial and Engineering Chemistry Research*, **44 (9)**, 3178-3186.
- [118] South, M., Bancroft, C., Willis, M.J., Tham, M.T. (1996). System identification via genetic programming. In: *Proceedings of the UKACC International Conference on Control'96*.
- [119] Iba, H., Sato, T., de Garis, H. (1994). System identification approach to genetic programming. In: *Proceedings of the First IEEE Conference on Evolutionary Computation*, 401-406.

- [120] Flores, J.J., Graff, M. (2005). System identification using genetic programming and gene expression programming. *Lecture Notes in Computer Science*, **3733**, 503-511.
- [121] Bai, Y., Zhu, Y., Jiang, Y. (2007). A new nonlinear system identification method using gene expression programming. *In: Proceedings of the IEEE International Conference on Mechatronics and Automation*, August 5-8, Harbin, China, 2951-2956.
- [122] Zhu, Y., Bai, Y., Jiang, Y. (2008). Study of nonlinear system identification based on gene expression programming. *Journal of System Simulation*, **20(7)**, 1842-1845.
- [123] Rodríguez-Vázquez, K., Fleming, P.J. (1998) Multiobjective genetic programming for gas turbine engine model identification. *In: Proceedings of the UKACC International Conference on Control*, September 1-4, 1385-1390.
- [124] Rodríguez-Vázquez, K., Fleming, P.J. (1998). Multi-objective genetic programming for nonlinear system identification. *Electronics Letters*, **34(9)**, 930-931.
- [125] Evans, C., Fleming, P.J., Hill, D.C., Norton, J.P., Pratt, I., Rees, D., Rodríguez-Vázquez, K. (2001). Application of system identification techniques to aircraft gas turbine engines. *Control Engineering Practice*, **9**, 135-148.
- [126] Arkov, V., Evans, C., Fleming, P.J., Hill, D.C., Norton, J.P., Pratt, I., Rees, D., Rodríguez-Vázquez, K. (2000). System identification strategies applied to aircraft gas turbine engines. *Annual Reviews in Control*, **24**, 67-81.
- [127] Ruano, A.E., Fleming, P.J., Teixeira, C., Rodríguez-Vázquez, K., Fonseca, C.M. (2003). Nonlinear identification of aircraft gas-turbine dynamics. *Neurocomputing*, **55**, 551-579.

- [128] Rodríguez-Vázquez, K., Fonseca, C.M., Fleming, P.J. (2004). Identifying the structure of nonlinear dynamic systems using multiobjective genetic programming. *IEEE Transactions on Systems, Man, and Cybernetics-Part A: Systems and Humans*, **34(4)**, 531-545.
- [129] Kiguchi, K., Jang, H.H., Fukuda, T. (1999). Identification of robot manipulators using neural networks and genetic programming. *IEEE International Conference on Systems, Man and Cybernetics*, 802-806.
- [130] Korenberger, G., Feilmayr, C., Kommenda, M., Winkler S., Affenzeller, M., Bürgler, T. (2009). System identification of blast furnace processes with genetic programming. *In: Proceedings of the IEEE 2nd International Conference on Logisitcs and Industrial Informatics*, 1-6.
- [131] Han, P., Zhou, S., Wang, D. (2006). A multi-objective genetic programming/NARMAX approach to chaotic systems identification. *In: Proceedings of the 6th World Congress on Intelligent Control and Automation*, Dalian, China, June 21-23, 1735-1739.
- [132] Beligiannis, G.N., Skarlas, L.V., Likothanassis, S.D., Perdikouri, K.G. (2005). Nonlinear model structure identification of complex biomedical data using a genetic programming-based technique. *IEEE Transactions on Instrumentation and Measurement*, **54 (6)**, 2184-2190.
- [133] Yang, Y.W., Wang, C., Soh, C.K. (2005). Force identification of dynamic systems using genetic programming. *International Journal for Numerical Methods in Engineering*, **63**, 1288-1312.
- [134] Hussian, A., Sheta, A., Kamel, M., Telbaney, M., Abdelwahab, A. (2000). Modeling of a winding machine using genetic programming. *In: Proceedings of the IEEE Congress on Evolutionary Computation*, 398-402.

- [135] Winkler, S., Affenzeller, M., Wagner, S. (2005). New methods for the identification of nonlinear model structures based upon genetic programming techniques. *Systems Science*, **31(1)**, 1-13.
- [136] Willis, M.J., Hiden, H., Hinchliffe, M., McKay, B., Barton, G.W. (1997). Systems modeling using genetic programming. *Computers and Chemical Engineering*, **21(1)**, 1161-1166.
- [137] McKay, B., Willis, M., Barton, G. (1997). Steady-state modelling of chemical process systems using genetic programming. *Computers and Chemical Engineering*, **21 (9)**, 981-996.
- [138] Grosman, B., Lewin D.R. (2004). Adaptive genetic programming for steady-state process modeling. *Computers and Chemical Engineering*, **28**, 2779-2790.
- [139] Hinchliffe, M.P., Willis, M.J. (2003). Dynamic systems modelling using genetic programming. *Computers and Chemical Engineering*, **27**, 1841-1854.
- [140] Witczak, M., Obuchowicz, A., Korbicz, J. (2002). Genetic programming based approaches to identification and fault diagnosis of non-linear dynamic systems. *International Journal of Control*, **75 (13)**, 1012-1031.
- [141] Lew, T.L., Spencer, A.B., Scarpa, F., Worden, K., Rytherford, A., Hemez, F. (2006). Identification of response surface models using genetic programming. *Mechanical Systems and Signal Processing*, **20**, 1819-1831.
- [142] Yuan, X.L., Bai, Y., Dong, L. (2008). Identification of linear time-invariant, nonlinear and time varying dynamic systems using genetic programming. *IEEE Congress on Computational Intelligence*, June 1-6, 56-61.
- [143] Grosman, B., Lewin, D.R. (2002). Automated nonlinear model predictive control using genetic programming. *Computers and Chemical Engineering*, **26**, 631-640.

- [144] Ha, J.L., Fung, R.F., Chen, K.Y., Hsien, S.C. (2006). Dynamic modeling and identification of a slider-crank mechanism. *Journal of Sound and Vibration*, **289**, 1019-1044.
- [145] Erkaya, S., Su, Ş., Uzmay, İ. (2007). Dynamic analysis of a slider-crank mechanism with eccentric connector and planetary gears. *Mechanism and Machine Theory*, **42**, 393-408.
- [146] Metallidis, P., Natsiavas, S. (2003). Linear and nonlinear dynamics of reciprocating engines. *International Journal of Non-Linear Mechanics*, **38**, 723-738.
- [147] www.qrg.northwestern.edu/papers/Files/qrg-workshops/QR97/DeNicolao_tutorial_1997_System_Identification_Problems_Perspectives.pdf
- [148] Hsia, T.C. (1977). *System Identification*. D. C. Heath and Co., USA.
- [149] Mizukami, Y., Wakasa, Y., Tanaka, K. (2006). A proposal of neural network architecture for nonlinear system modeling. *Electronics and Communications in Japan*, **89 (11)**, 40-49.
- [150] Kim, H., Fok, S., Fregene, K., Lee, D.H., Oh, T.S., Wang, D.W.L. (2004). Neural network-based system identification and controller synthesis for an industrial sewing machine. *International Journal of Control, Automation and Systems*, **2(1)**, 83-91.
- [151]. Nowak, R.D. (2002). Nonlinear system identification. *Circuits Systems Signal Processing*, **21(1)**, 109-122.
- [152] Kara, T. (2005). Adaptive control of nonlinear system with applications, PhD thesis, University of Gaziantep.
- [153] Norquay, S.J., Palazoglu, A., Romagnoli, J.A. (1998). Model predictive control based on Wiener models. *Chemical Engineering Science*, **53(1)**, 75-84.

- [154] Alonge, F., D'Ippolito, F., Raimondi, F.M., Tumminaro, S. (2003). Identification of nonlinear systems described by Hammerstein models. *In: Proceedings of the 42nd IEEE Conference on Decision and Control*, Maui, Hawaii USA, 3990-3995.
- [155] Leontaritis, I.J., & Billings, S.A. (1985). Input-output parametric models for nonlinear systems, Part1: Deterministic non-linear systems and Part2: Stochastic non-linear systems. *International Journal of Control*, **41(2)**, 303-328 and 329-344.
- [156] Kalogirou, S.A. (2003). Artificial intelligence for the modeling and control of combustion processes: a review. *Progress in Energy and Combustion Science*, **29**, 515-566.
- [157] Kalogirou, S.A., Bojic, M. (2000). Artificial neural networks for the prediction of the energy consumption of a passive solar building. *Energy*, **25**, 479-491.
- [158] Haykin, S. (1994). *Neural networks: a comprehensive foundation*. New York: Macmillan.
- [159] Rumelhart, D.E., Hinton, G.E. and Williams, R.J. (1986). Learning internal representation by error propagation *Parallel Distributed Processing: Exploration in the Microstructure of Cognition*, Vol. 1. MIT Press, Cambridge, MA, Chapter 8.
- [160] Bonala, S. (2009). *A study on neural network based system identification with application to heating, ventilating and air conditioning (HVAC) system*. MSc Thesis, National Institute of Technology, Department of Electrical Engineering, Rourkela.
- [161] Jain, A.K., Mao, J., Mohiuddin, K.M. (1996). Artificial neural networks: a tutorial. *IEEE Computer*, **29(3)**, 31-44.
- [162] Ahmad R., Jamaluddin, H. (2002). Radial basis function (RBF) for non-linear dynamic system identification. *Jurnal Teknologi*, **36(A)**, 39-54.

- [163] Hacib, T., Mekideche, M.R., Ferkha, N., Ikhlef, N., Bouridah, H. (2007). Application of a radial basis function neural network for the inverse electromagnetic problem of parameter identification. *In: Proceedings of the IEEE International Symposium on Industrial Electronics, ISIE 2007*, June 4-7, Spain, 347-352.
- [164]. Abraham, A. (2005). Handbook of Measuring System Design. In Peter H. Sydenham and R. Thorn (Eds.), *129: Artificial Neural Networks*.
- [165] Şeker, S., Ayaz, E., Türkcan, E. (2003). Elman's recurrent neural network applications to condition monitoring in nuclear power plant and rotating machinery. *Engineering Applications of Artificial Intelligence*, **16**, 647-656.
- [166] Efe, M.O., Kaynak, O. (2001). A novel optimization procedure for training of fuzzy inference systems by combining variable structure systems technique and Levenberg-Marquardt algorithm. *Fuzzy Sets and Systems*, **122**, 153-165.
- [167]. Gorp, J.V. (2000). Nonlinear identification with neural networks and fuzzy logic. A doctorate thesis, Dienst Algemene Elektriciteit & Instrumentatie (ELEC), Vrije Universiteit Brussel, Brussel, Belgium.
- [168] Cho, D., Hedrick, J.K. (1989). Automotive powertrain modeling for control. *ASME Journal of Dynamic Systems, Measurement and Control*, **111(4)**, 568-576.
- [169] Hendricks, E. Vesterholm, T. (1992). The analysis of mean value SI engine models. *SAE Technical Paper*, No.920682.
- [170] Hendricks, E. and Sorenson, S.C. (1990). Mean value modeling of spark ignition engines. *SAE Technical Paper*, No.900616.
- [171] Rajamani, R. (2006). *Vehicle Dynamics and Control*, Springer, New York.
- [172] Guzzella, L., Onder, C.H. (2004). *Introduction to modeling and control of internal combustion engine systems*, Berlin, New York, Springer.

- [173] Hendricks, E. (1997). Engine modeling for control applications: A critical survey. *Meccanica*, **32**, 387-396.
- [174] Karmiggelt, R. (1998). Mean value modeling of a s.i. engine. MSc. Thesis, Eindhoven University of Technology.
- [175] Ganguli, A. and Rajamani, R., (2004). Tractable model development and system identification for longitudinal vehicle dynamics. *Proceedings of the Institution of Mechanical Engineers, Part D: Journal of Automobile Engineering*, **218(10)**, 1077-1084.
- [176] Hendricks, E., Chevalier, A., Jensen, M., Sorenson, S.C., Trumpy, D., Asik, J. (1996). Modelling of the manifold filling dynamics. *SAE Technical Paper*, 960037.
- [177] Hendricks, E., Engler, D., Fam, M. (2000). A generic mean value engine model for spark ignition engines. *In: Proceedings of 41st Simulation Conference*, Denmark Technological University, Lyngby, Denmark.
- [178] Heywood, J.B. (1988). *Internal Combustion Engine Fundamentals*, Mc-Graw Hill, Inc.
- [179] Pulkrabek, W.W. (1997), *Internal Combustion Engine*, Prentice-Hall, Inc.
- [180] www.datatranslation.com/docs/specs/dt300_specs.pdf
- [181] Parlak, A., Islamoglu, Y., Yasar, H., Egrisogut, A. (2006). Application of artificial neural network to predict specific fuel consumption and exhaust temperature for a diesel engine. *Applied Thermal Engineering*, **26**, 824–828.
- [182] Yuanwang, D., Meilin, Z., Dong, X., Xiaobei, C. (2002). An analysis for effect of cetane number on exhaust emissions from engine with the neural network. *Fuel*, **81**, 1963–1970.

- [183] Lucas, A., Durán, A., Carmona, M., Lapuerta, M. (2001). Modeling diesel particulate emissions with neural networks. *Fuel*, **80**, 539–548.
- [184] Nasr, G.E., Badr, E.A., Joun, C. (2003). Backpropagation neural networks for modeling gasoline consumption. *Energy Conversion and Management*, **44**, 893–905.
- [185] Gölcü, M., Sekmen, Y., Erduranli, P., Salman, M.S. (2005). Artificial neural network based modeling of variable valve-timing in a spark ignition engine. *Applied Energy*, **81**, 187–197.
- [186] Arcaklioğlu, E., Çelikten, I. (2005). A diesel engine's performance and exhaust emissions. *Applied Energy*, **80**, 11–22.
- [187] Yücesu, H.S., Sozen, A., Topgül, T., Arcaklioğlu, E. (2007). Comparative study of mathematical and experimental analysis of spark ignition engine performance used ethanol-gasoline blend fuel. *Applied Thermal Engineering*, **27**, 358–368.
- [188] Sayin, C., Ertunc, H.M., Hosoz, M., Kilicaslan, I., Canakci, M. (2007). Performance and exhaust emissions of a gasoline engine using artificial neural network. *Applied Thermal Engineering*, **27**, 46–54.
- [189] Krijnsen, H.C., Kooten, W.E.J., Calis, H.P.A., Verbeek, R.P., Bleek, C.M. (1999). Prediction of NO_x emissions from a transiently operating diesel engine using an artificial neural network. *Chemical Engineering Technology*, **22(7)**, 601–607.
- [190] Alonso, J.M., Alvarruiz, F., Desantes, J.M., Hernández, L., Hernández, V., Moltó, G. (2007). Combining neural networks and genetic algorithms to predict and reduce diesel engine emission. *IEEE Transactions on Evolutionary Computation*, **11**, 46–55.
- [191] Kalogirou, S.A. (2000). Applications of artificial neural-networks for energy systems. *Applied Energy*, **67**, 17–35.

- [192] Akcayol, M.A., Cinar, C. (2005). Artificial neural network based modeling of heated catalytic converter performance. *Applied Thermal Engineering*, **25**, 2341–2350.
- [193] Massie, D.D. (2001). Neural-network fundamentals for scientists and engineers. In: *Efficiency, cost, optimization, simulation and environmental impact of energy systems ECOS'01*, Istanbul, Turkey, July 4–6, 123–131.
- [194] Holland, J.H. (1975). *Adaptation in natural and artificial systems*. Ann Arbor: University of Michigan Press.
- [195] Gen, M., Cheng, R. (1997). *Genetic algorithms and engineering design*. London: Wiley.
- [196] Kesgin, U. (2004). Genetic algorithm and artificial neural network for engine optimization of efficiency and NOX emission. *Fuel*, **83**, 885–895.
- [197] Atashkari, K., Nariman-Zadeh, N., Gölcü, M., Khalkhali, A., Jamali, A. (2007). Modelling and multi-objective optimization of a variable valve-timing spark-ignition engine using polynomial neural networks and evolutionary algorithms. *Energy Conversion and Management*, **48**, 1029–1041.
- [198] Yang, Z., Wang, L., Li, S. (2008). Investigation into the optimization control technique of hydrogen-fueled engines based on genetic algorithms. *International Journal of Hydrogen Energy*, **33**, 6780–6791.
- [199] Hiroyasu, T., Miki, M., Kamiura, J., Watanabe, S., Hiroyasu, H. (2002). Multi-objective optimization of diesel engine emissions and fuel economy using genetic algorithms and phenomenological model. *SAE paper*, No:01-2778.
- [200] Cai, G., Fang, J., Xu, X., Liu, M. (2007). Performance prediction and optimization for liquid rocket engine nozzle. *Aerospace Science and Technology*, **11**, 155–62.

- [201] Verma, R., Lakshminarayanan, P.A. (2006). A case study on the application of a genetic algorithm for optimization of engine parameters. *Proceedings of the Institution of Mechanical Engineers, Part D: Journal of Automobile Engineering*, **220(4)**, 471–479.
- [202] Tong, X.Y., Cai, G.B., Zheng, Y.T., Fang, J. (2006). Optimization of system parameters for gasgenerator engines. *Acta Astronautica*, **59**, 246–252.
- [203] Wang, J.J., Jing, Y.Y., Zhang, C.F. (2010). Optimization of capacity and operation for CCHP system by genetic algorithm. *Applied Energy*, **87**, 1325–1335.
- [204] Saerens, B., Vandersteen, J., Persoons, T., Swevers, J., Diehl, M., Bulk, E., et al. (2009). Minimization of the fuel consumption of a gasoline engine using dynamic optimization. *Applied Energy*, **86**, 1582–1588.
- [205] Al-Hinti, I., Samhouri, M., Al-Ghandoor, A., Sakhrieh, A. (2009). The effect of boost pressure on the performance characteristics of a diesel engine: a neuro-fuzzy approach. *Applied Energy*, **86**, 113–121.
- [206] Koza, J.R. (1992). *Genetic programming: on the programming of computers by means of natural selection*. Cambridge, MA: MIT Press.
- [207] Yang, W.X. (2006). Establishment of the mathematical model for diagnosing the engine valve faults by genetic programming. *Journal of Sound and Vibration*, **293**, 213–226.
- [208] Togun, N.K., Baysec, S. (2010). Prediction of torque and specific fuel consumption of a gasoline engine by using artificial neural networks. *Applied Energy*, **87**, 349–355.
- [209] Ferreira, C. (2001). Gene expression programming: a new adaptive algorithm for solving problems. *Complex Systems*, **13(2)**, 87–129.

- [210] Ferreira, C. (2001). Gene expression programming in problem solving. *In: Invited tutorial of the 6th Online World Conference on Soft Computing in Industrial Applications*.
- [211] Taghavi, N., Sadr, A. (2008). Piezoelectric transducer modeling: with system identification (SI) method. *In: Proceedings of World Academy of Science, Engineering and Technology*, 29, 296-301.
- [212] Soumelidis, M.I., Stobart, R.K. (2006). Dynamic modeling of three way catalysts using nonlinear identification techniques. *Proceedings of the Institution of Mechanical Engineers Part I-Journal of Systems and Control Engineering* **220 (7)**, 595-605.
- [213] Rizzoni, G., Connolly, F.T. (1993). Estimate of IC engine torque from measurement of crankshaft angular position. *In: Proceedings of the SAE Conference*, 1937-1947.
- [214] Krishnaswami, V. (1997). Determination of influencing inputs and their orders for nonlinear dynamic systems- application to IC engine modeling. *In: Proceedings of the American Control Conference*, Albuquerque, New Mexico, 299-303.
- [215] Daw, C.S., Kennel, M.B., Finney, C.E.A., Connolly, F.T. (1998). Observing and modeling nonlinear dynamics in an internal combustion engine, *Physical Review E*, **57(3)**, 2811-2819.
- [216] Petridis, A.P., Shenton, A.T. (2003). Inverse-NARMA: a robust control method applied to SI engine idle speed regulation. *Control Engineering Practice*, **11**, 279-290.
- [217] Scattolini, R., Siviero, C., Mazzucco, M., Ricci, S., Poggio, L., Rossi, C. (1997). Modeling and identification of an electromechanical internal combustion engine throttle body. *Control Engineering Practice*, **5(9)**, 1253-1259.

- [218] Orlov, Y., Kolmanovsky, I.V., Gomez, O. (2006). On-line identification of SISO linear time-delay systems from output measurements: theory and applications to engine transient fuel identification. *In: Proceedings of the American Control Conference*, Minneapolis, Minnesota, USA, June 14-16, 1179-1184.
- [219] Eker, İ. (2004). Open-loop and closed loop experimental on-line identification of a three mass electromechanical system. *Mechatronics*, **14**, 549-565.
- [220] Hong, X., Mitchell, R.J., Chen, S., Harris, C.J., Li, K., Irwin, G.W. (2008). Model selection approaches for non-linear system identification: a review. *International Journal of Systems Science*, **39(10)**, 925-946.
- [221] Ramesh, K., Aziz, N., Abd Shukor, S.R. (2008). Development of NARX model for distillation column and studies on effect of regressors. *Journal of Applied Science*, **8(7)**, 1214-1220.
- [222] Ramesh, K. (2009). Nonlinear model predictive control of a distillation column using Hammerstein model and nonlinear autoregressive model with exogenous input. PhD thesis, Universiti Sains Malaysia.
- [223] Shojaeefard, M.H., Goudarzi, K., Noorpoor, A.R., Fazelpour, M. (2008). A study of thermal contact using nonlinear system identification models. *American Journal of Engineering and Applied Sciences*, **1(1)**, 16-23.
- [224] Chen, S., Billings, S.A. (1989). Representation of nonlinear system: the NARMAX model. *Internal Journal of Control*, **49(3)**, 1013–1032.
- [225] Hagan, M.T., Menhaj, M.B. (1994). Training feedforward networks with the Marquardt algorithm. *IEEE Transactions on Neural Networks*, **5(6)**, 989-993.
- [226] Warwick, K., Craddock, R. (1996). An introduction to radial basis functions for system identification a comparison with other neural network models. *In: Proceedings of the IEEE 35th Conference on Decision and Control*, Kobe, Japan, 464-469.

[227] Abido, M.A., Abdel-Magid, Y.L. (1997). On-line identification of synchronous machines using radial basis function neural networks. *IEEE Transactions on Power Systems*, **12(4)**, 1500-1506.

[228] Shen, C., Cao, G.Y., Zhu, X.J. (2002). Nonlinear modeling of MCFC stack based on RBF neural networks identification. *Simulation Modelling Practice and Theory*, **10**, 109-119.

[229] Chen, S. Cowan, C.F.N., Grant, P.M. (1991). Orthogonal least squares learning algorithm for radial basis function Networks. *IEEE Transactions on Neural Networks*, **2(2)**, 302-309.

APPENDIX 1: IDENTIFICATION OF THE GENERAL NARMAX MODEL

The NARMAX representation of nonlinear systems includes both input and output nonlinearity. The output nonlinearity is assumed to be an invertible one, which considerably simplifies the procedure of identification. The method that will be discussed in this section for the identification of the NARMAX model is the nonlinear recursive extended least squares (NRELS) method [152].

The general NARMAX system given in Figure 4.7 is considered. The overall system input-output relationship is given by:

$$y_o(k) = F_o^{-1} \left(\frac{B(q^{-1})}{A(q^{-1})} F_i(u(k)) + \frac{C(q^{-1})}{A(q^{-1})} \xi(k) \right) \quad (\text{A.1})$$

Then,

$$\begin{aligned} A(q^{-1})F_o(y_o(k)) &= B(q^{-1})F_i(u(k)) + C(q^{-1})\xi(k) \\ A(q^{-1}) \left(y_o(k) + f_{02}y_o^2(k) + \dots + f_{0n_{f0}}y_o^{n_{f0}}(k) \right) &= B(q^{-1}) \left(u(k) + f_{i2}u^2(k) + \dots \right. \\ &\quad \left. \dots + f_{in_{fi}}u^{n_{fi}}(k) \right) + C(q^{-1})\xi(k) \end{aligned} \quad (\text{A.2})$$

The equation above can be written in the form below:

$$y_o(k) = \phi(k)\theta + \xi(k) \quad (\text{A.3})$$

where

$$\phi(k) = [-y_0(k-1), \dots, -y_0(k-n_a), -y_0^2(k), \dots, -y_0^2(k-n_a), \dots, -y_0^{n_{F0}}(k), \dots, -y_0^{n_{F0}}(k-n_a),$$

$$u(k), \dots, u(k-n_b), u^2(k), \dots, u^2(k-n_b), \dots, u^{n_{Fi}}(k), \dots, u^{n_{Fi}}(k-n_b), \xi(k-1), \dots, \xi(k-n_c)]$$

$$\theta^T = [a_1, \dots, a_{n_a}, f_{02}, a_1 \cdot f_{02}, \dots, a_{n_a} \cdot f_{02}, \dots, f_{0n_{F0}}, \dots, a_{n_a} \cdot f_{0n_{F0}},$$

$$b_0, b_1, \dots, b_{n_b}, b_0 \cdot f_{i2}, \dots, b_{n_b} \cdot f_{i2}, \dots, b_0 \cdot f_{in_{Fi}}, \dots, b_{n_b} \cdot f_{in_{Fi}}, c_1, \dots, c_{n_c}]$$

One can see that the linear regression model given in (A.3) allows the estimation of the parameters a_j , b_j , c_j , and f_{0j} , which explicitly appear in the parameter vector θ . However, the parameters of the input nonlinearity, f_{ij} , do not appear explicitly, but the products $b_m \cdot f_{ij}$ can be estimated. Consequently, the parameters f_{ij} can simply be estimated using ordinary least squares algorithm [152].

APPENDIX 2: SPECIFICATIONS OF THE DYNAMOMETER

Engine torque was measured with a dynamometer. Water brake dynamometer was used to measure engine torque at different speeds; by changing the water level in the dynamometer, the load applied to the engine could be varied. The specifications of the dynamometer are given in table below.

Table A.1 Specifications of Go Power System DA 516 model water brake dynamometer

Type of absorption	Water brake
Construction	High strength aluminum alloy
Loading capacity	100 HP
Maximum allowable speed	7400 rpm
Torque transducer system	Hydraulic load cell
Rotation direction	Clockwise or counterclockwise
Inlet water flow rate	2.2 l/s
Inlet water pressure	240 kPa
Water outlet	Gravity drain to atmosphere
Measuring device	Pressure transducer
Maximum torque capacity	1017 Nm
Weight	43 kg

APPENDIX 3: SPECIFICATIONS OF THE PRESURE TRANSDUCER

Pressure transducer was mounted on the hydraulic load cell of the dynamometer. The specifications of the Cole Parmer C-68075-50 pressure transducer are given in table below.

Table A.2 Cole Parmer C-68075-50 transducer specifications

Range	0 to 250 psig
Application	Torque measurement
Accuracy	±0.25 % full-scale
Output	0.5 to 5.5 V
Temperature range (compensated)	-4° to 176°F (-20° to 80°C)
Operating temperature	-40° to 260°F (-40° to 125°C)
Electrical connections	2-ft cable
Process connection	1/4" NPT(M)
Dimensions	2 3/4"L x 1 1/2" dia
Power	9 to 30 VDC
Wetted parts	17-4 PH stainless steel



Figure B.1 Cole Parmer C-68075-50 transducer

APPENDIX 4: TECHNICAL SPECIFICATIONS OF THE SERVO MOTOR

Throttle valve position is controlled by servo motor which has a 0.75 kW and 3000 rpm. The specifications of the used servo motor are given in table below.

Table A.3 Specifications of the ECMA-C30807GS servo motor

Rated output power	750 W
Rated torque	2.39 Nm
Rated speed	3000 rpm
Rated current	5.1 A
Armature resistance	0.42 Ohm
Armature inductance	3.53 mH
Insulation resistance	>100 M Ω , DC 500V
Insulation strength	1500 V AC, 60 seconds
Operating temperature	0°C to 40°C (32°F to 104°F)
Storage temperature	-10°C to 80°C (-14°F to 176°F)

APPENDIX 5: SPECIFICATIONS OF THE DATA ACQUISITION CARD

DT 304 is a family of low cost multi function data acquisition board and is connected at PCI bus of computer. The specifications of the used data acquisition card are given in table below.

Table A.4 Specifications of the DT 304 Data acquisition card

Dimensions	8.5 inches (length) by 4.2 inches (width)
Operating temperature range	0°C to 70 °C
Storage temperature range	-25°C to 85°C
Accessories	STP 300 Screw Terminal panel and EP 305 cable
Resolution	12 bits
Analog input	
Number of analog input channels	16 single ended, 8 differential
Input ranges	± 10 , ± 5 , ± 2.5 , ± 1.25 V bipolar 0-10, 5, 2.5, 1.25 V unipolar
Sampling rate	400 kS/s@0.03% accuracy
Maximum input voltage	± 40 V (protection)
Analog output	
Number of analog output channels	2 (Voltage output)
Output range	± 10 V or ± 5 V 0 to 10, 5 V
Sampling rate	10 kS/s
Digital I/O	
Number of lines	8 bidirectional
High level input voltage	2 V minimum
Output driver high voltage	2.4 V minimum
Number of counter/timer channels	4

CURRICULUM VITAE

PERSONAL INFORMATION

Surname, Name: TOĞUN, Necla KARA
Nationality: Turkish (TC)
Date and Place of Birth: 1 November 1978, Gebze
Marital Status: Married
Phone: +90 342 317 25 34
Fax: +90 342 360 11 04
email: nkara@gantep.edu.tr

EDUCATION

Degree	Institution	Year of Graduation
MS	Gaziantep University, Graduate School of Naturel and Applied Sciences	2004
BS	Gaziantep University Department of Mechanical Engineering	2001
High School	Yenimahalle Alparslan Lisesi (Ankara)	1995

WORK EXPERIENCE

Year	Place	Enrollment
2002- Present	Gaziantep University Department of Mechanical Engineering	Research Assistant

FOREIGN LANGUAGES

English

PUBLICATIONS

International Journal Papers

1. Togun, N.K., Baysec, S. (2010). Prediction of torque and specific fuel consumption of a gasoline engine by using artificial neural Networks. *Applied Energy*, 87(1), 349-355.
2. Togun, N., BAYSEC, S. (2010). Genetic programming approach to predict torque and brake specific fuel consumption of a gasoline engine. *Applied Energy*, 87(11), 3401-3408.
3. Togun, N., Kose, A., Gunay, N., Tarakcioglu, M., Demiryurek, A.T. (2010). Formulation of effects of atropine, pralidoxime and magnesium sulfate on cardiac tissue levels of nitric oxide, malondialdehyde and glutathione in organophosphate poisoning using artificial neural network. *Computers in Biology and Medicine*, 40, 29-36.

4. Togun, N., Baysec, S., Kara, T. (2010). Nonlinear modeling and identification of a spark ignition engine torque. *Mechanical systems and signal processing*. (under review).
5. Togun, N., Baysec, S. (2010). Nonlinear modeling and identification of a spark ignition engine torque using nonlinear ARX model. *ISA Transactions*. (under review).

National Conference Papers

1. Kara, N., Öz, H.R., Yıldırım, C.A. (2005). Yumuşak doku - kemik sisteminde ezilme hasarı”, *UMTS 2005, 12. Ulusal Makine Teorisi Sempozyumu*, 09-11 Haziran 2005, s. 615-622, Erciyes Üniversitesi, Kayseri.
2. Kara, N., Öz, H.R., Yıldırım, C.A. (2004). Bir deprem senaryosunda Maxwell tipi yumuşak doku - kemik sisteminde ezilme hasarı-in vitro modelleme”, 7. *TÜRKİYE Acil Tıp Sempozyumu ve 3. Acil Hemşireliği ve Paramedik Sempozyum* 24-27 Kasım 2004, s. 221, Gaziantep.
3. Kara, N., Öz, H.R., Yıldırım, C.A., Kaplan, M. (2006). Viskoelastik Yumuşak doku-kemik sisteminde ezilme hasarı. *Biomekanik 2006, 3. Ulusal Biomekanik Kongresi, 01-02 Aralık 2006*, s.187-198, İstanbul Teknik Üniversitesi, İstanbul.
4. Kara, N., Öz, H.R., Bayram, N. (2006). Solunum yolları sesleri ile akciğer hastalıklarının sınıflandırılması. *Biomekanik 2006, 3. Ulusal Biomekanik Kongresi, 01-02 Aralık 2006*, s.275-288, İstanbul Teknik Üniversitesi, İstanbul.
5. Kara, N., Öz, H.R., Bayram, N. (2007). Hırıltı (Wheezing) sesi üzerine bir literatür araştırması. *UMTS 2007, 12. Ulusal Makine Teorisi Sempozyumu*, 07-09 Haziran 2007, s. 563-571, Cumhuriyet Üniversitesi, Sivas.
6. Togun, N.K., Bayseç, S. (2009). Benzinli bir motor torkunun genetik programlama kullanarak modellenmesi ve formülasyonu. *UMTS 2009, 14. Ulusal Makine Teorisi Sempozyumu*, 02-04 Temmuz 2009, s. 307-312, ODTÜ Kuzey Kıbrıs Kampüsü, Güzelyurt/Kıbrıs.
7. Togun, N.K., Bayseç, S. (2009). Benzinli bir motor torkunun yapay sinir ağları kullanarak modellenmesi ve formülasyonu. *UMTS 2009, 14. Ulusal Makine Teorisi Sempozyumu*, 02-04 Temmuz 2009, s. 313-318, ODTÜ Kuzey Kıbrıs Kampüsü, Güzelyurt/Kıbrıs.

HOBBIES

Computer, reading, travelling, cooking.

